U.PORTO

DOUTORAMENTO
NEUROCIÊNCIAS CLÍNICAS, NEUROPSIQUIATRIA E SAÚDE MENTAL

DEVELOPMENTAL VENOUS ANOMALIES, CEREBRAL CAVERNOUS MALFORMATIONS AND BEYOND: NEUROIMAGING INSIGHT INTO PEDIATRIC CEREBROVENOUS VASCULAR MALFORMATIONS

Ana Filipa Geraldo da Silva Couceiro

D

2023

To my daughters

Article 48, third paragraph 3: The Faculty is not responsible for the doctrines expounded in the thesis dissertation (Regulation of the Faculty of Medicine of Porto – Decree-Law No. 19337, 29th January 1931).

SUPERVISOR

Sofia Cristina Pereira Reimão, MD MSc PhD
Neurological imaging department, Centro Hospitalar Lisboa Norte-Hospital de Santa Maria, Lisbon, Portugal
Imaging University Clinic, Faculty of Medicine of the University of Lisbon, Lisbon, Portugal
Institute of Molecular Medicine (IMM) João Lobo Antunes, Lisbon, Portugal

CO-SUPERVISORS

Joana Guimarães, MD PhD
Neurology department, Centro Hospitalar e Universitário São João, Porto, Portugal
Department of Clinical Neurosciences and Mental Health, Faculty of Medicine of the University of Porto, Porto, Portugal

Mariasavina Severino, MD
Neuroradiology Unit, IRCCS Istituto Giannina Gaslini, Genoa, Italy

JURY OF THE PhD THESIS

Pursuant to the provisions of paragraph 2 of article 18 of the Regulation of the Third Cycles of Studies of the University of Porto, the jury of the PhD in Neurosciences – Branch of Clinical Neurosciences, Neuropsychiatry and Mental Health, named by vice-rectoral order of 15.05.2023.

President:

Lia Paula Nogueira Sousa Fernandes, MD PhD
Faculty of Medicine of the University of Porto, Porto, Portugal

Other members of the Jury:

Cláudia Maria Coelho de Faria, MD PhD

Faculty of Medicine of the University of Lisbon, Lisbon, Portugal

Tiago Gil Oliveira, MD PhD

Faculty of Medicine of the University of Braga, Braga, Portugal

Sofia Pereira Coutinho, MD MSc PhD

Faculty of Medicine of the University of Lisbon, Lisbon, Portugal

Paulo Miguel da Silva Pereira, MD PhD

Faculty of Medicine of the University of Porto, Porto, Portugal

Célia da Conceição Duarte Cruz, PhD

Faculty of Medicine of the University of Porto, Porto, Portugal

CONTENTS

ACKNOWLEDGMENTS

Any journey starts with a simple step. Although the initial motivation usually lies within us, we only reach the desired destination when we are surrounded by the right people.

I would like to express my gratitude to all who directly or indirectly made this work possible, with a very special recognition to my PhD mentor Professor Dr. Sofia Reimão - brilliant neuroradiologist and a friend - for her role model, honest guidance, wise and motivational words as well as permanent support given to the concretization of this work. She never doubted that I would make it, even in the darkest hours.

I would also like to thank my co-mentors Dr. Mariasavina Severino and Professor Dr. Joana Guimarães, highly recognized doctors in the field of Neuroradiology and Neurology, respectively, for their inestimable advice, fruitful scientific discussions, and leading female example.

I am also grateful to the multidisciplinary team that collaborated in the different steps of the research work as well as in the organization of the current thesis. A special word of recognition to Professor Dr. Andrea Rossi, head of department of UOC Neuroradiology of the Giannina Gaslini Pediatric Hospital (Genoa, Italy), and all his staff for receiving me in his department with arms wide open and making me feel at home there since 2012.

My gratitude also goes to Dr. Kjitish Mankad, Dr. Erin Schwartz, and Professor Dr. Rui Vaz, heads of the Neuroradiology Department of Great Ormond Street (London, UK), the Neuroradiology Department of Philadelphia Children Hospital (Philadelphia, USA), and the Neurosurgery Department of Centro Hospitalar e Universitário São João (Porto, Portugal), respectively, for accepting immediately and without reserves the collaborative work between institutions and for the critical appraisal of the scientific manuscripts.

I would like to acknowledge Dr. César Alves and Dr. Aysha Luis, rising stars in the field of Neuroradiology and caring colleagues, for their participation in imaging analysis and for their commitment to this project and all the developed work.

I also would like to thank Dr. Pedro Sousa, head of Imaging Department at Centro Hospitalar Vila Nova de Gaia/Espinho (CHVNG/E), as well as Dr. Rui Guimarães, chairman of the board of the directors of CHVNG/E, for believing in me and supporting my dreams at an institutional level.

Another word of appreciation goes to Iva Paiva, who was always available for timely and clear explanation of bureaucratic administrative issues related with the PhD program and the Faculty of Medicine of the University of Porto.

The road would have been way more difficult without my good friends and colleagues, including old ones and some new that I have made along the way. A simple, supportive conversation on the telephone or around a coffee table can make all the difference in difficult days.

I can´t finalize without expressing my deep love, admiration and recognition to my mother, father and sister, as well as the beautiful new family that I am creating for myself: Carlos, Laura and little Clara. This nuclear team, together with other close family members that I cherish, gave me a loving environment as well as everyday incentive and support from the beginning to the end of this long journey and without them this work and many other life achievements would not have been possible.

ABBREVIATIONS

3D - Three dimensional

ADC - Apparent diffusion coefficient

AED - Anti-epileptic drug

ASL - Arterial spin labelling

AVM - Arteriovenous malformation

BMP - Bone morphogenetic protein

BOLD - Blood-oxygen level dependent

BRBNS - Blue rubber bleb nevus syndrome

CASH - Cavernoma-associated symptomatic hemorrhage

CCM - Cerebral cavernous malformation

c-DVA - Complicated developmental venous anomaly

CI - Confidence interval

CM - Cavernous malformation

CMMRDS - Constitutional mismatch repair deficiency syndrome

CNS - Central nervous system

CRE - Cavernoma-related epilepsy

CT - Computed tomography

cUS - Cerebral ultrasound

CVM - Cerebrovenous vascular malformation

CVMS - Cerebrofacial venous metameric syndrome

dAVF - Dural arteriovenous fistula

DCEQP - Dynamic contrast-enhanced quantitative perfusion

DDL4 - Delta-like protein 4

DNA - Deoxyribonucleic acid

DSA - Digital subtraction angiography

DTI - Diffusion-tensor imaging

DTT - Diffusion-tensor tractography

DVA - Developmental venous anomaly

DWI - Diffusion weighted imaging

EndMT - Endothelial-to-mesenchymal transition

EphB4 - Ephrin receptor B4

ERK - Extracellular-signal-regulated kinase

FCCM - Familial cerebral cavernous malformation syndrome

FLAIR - Fluid attenuated inversion recovery

fMRI - Functional magnetic resonance imaging

GRE - Gradient recovery echo

HASTE - T2 Half-Fourier Acquisition Single-shot Turbo spin Echo imaging

HRQOL - Health-related quality of life

ICH - Intracranial hemorrhage

ILAE - International league against epilepsy

IRB - Institutional review board

ISVM - Intraspinal venous malformations

KLF - Krüppel-like factor

LITT - Laser interstitial thermal therapy

MAP3K3/MEKK3 - Mitogen-activated protein kinase kinase kinase 3

MAPK - Mitogen-activated protein kinase

MEDIC - T2 multi-echo data image combination

MR - Magnetic resonance

MRA - Magnetic resonance angiography

MRI - Magnetic resonance imaging

MRV - Magnetic resonance venography

MS - Multiple sclerosis

mTOR - Mammalian target of rapamycin

PIK - Phosphatidylinositol kinase

PIK3CA - Phosphatidylinositol-4,5-bisphosphate 3-kinase, catalytic subunit alpha

PRHTS - PTEN-related hamartoma tumor syndrome

PROS - PIK3CA-related overgrowth syndromes

PTEN - Phosphatase and tensin homolog

QSM - Quantitative susceptibility mapping

RNA - Ribonucleic acid

ROCK - RhoA/Rho kinase

SCCM - Spinal cord cavernous malformation

SRS - Stereotactic radiosurgery

SWI - Susceptibility-weighted imaging

T - Tesla

TEK - TEK receptor tyrosine kinase

TGF-β - Transform growth factor β

TLR4 - Toll-like receptor 4

TVA - Transitional venous anomaly

u-DVA - Uncomplicated developmental venous anomaly

US - Ultrasound

WI - Weighted-imaging

WM - White matter

SUMMARY

Background

Pediatric cerebrovenous vascular malformations (CVM) are a group of non-shunting slow-flow pathologies mainly involving the intracranial venous/capillary venous systems that are discovered *in utero* or during childhood. Neuroimaging plays a pivotal role in the diagnosis of CVM as well as in the assessment of potentially associated complications and/or syndromes. Developmental venous anomalies (DVA) and cavernous malformations (CM), although being the two most common subtypes of CVM regardless of the age group, remain largely underreported in children. Indeed, research studies focusing on these two subtypes of CVM in pediatric only cohorts are still scarce and the information regarding their origin (congenital vs postnatal), prevalence, neuroimaging features and natural history remains limited in this age group.

Aims

The general aim of the investigation that embodies this doctoral thesis was to use magnetic resonance imaging (MRI) to investigate and characterize CVM presenting in the pediatric age (anytime from fetal to adolescent life), mainly focusing on DVA and CM. The research work has been subsequently centered in two main areas: neonatal DVA and pediatric familial cerebral cavernous syndrome (FCCM).

Materials and methods

Firstly, we have undertaken a comprehensive narrative review focusing on the imaging characteristics of DVA and CM, with special emphasis on the pediatric age, with an additional case report published by our group as a *Letter to the Editor* of a DVA detected *in utero* using fetal MRI that was confirmed post-natally.

Secondly, we have developed a monocenter retrospective cohort study including all neonates that have performed at least one brain MRI up to 28 days of corrected age in one tertiary pediatric center (Istituto Giannina Gaslini, Genoa, Italy) and in whom the imaging report contained the term "*developmental venous anomaly*".

Thirdly, we have performed a multicenter retrospective cohort study involving three tertiary pediatric centers (Istituto Giannina Gaslini, Genoa, Italy; Children´s Hospital of Philadelphia,

Philadelphia, United States of America and Great Ormond Street Hospital, London, United Kingdom) including all consecutive patients with a diagnosis of FCCM during childhood (≤ 18 years) between January 2010 and August 2021 and with at least one complete spine MRI available for review.

Lastly, we have conducted a multicenter retrospective cohort study involving four tertiary pediatric institutions (Istituto Giannina Gaslini, Genoa, Italy; Children´s Hospital of Philadelphia, Philadelphia, United States of America; Great Ormond Street Hospital, London, United Kingdom and Centro Hospitalar e Universitário São João, Porto, Portugal) including all consecutive subjects with a diagnosis of FCCM during childhood (≤ 18 years) between January 2010 and September 2021, and with at least the initial brain MRI available for review.

Results

The initial clinical study that focused on neonatal DVA included n = 41 subjects and demonstrated a real-world MRI-detection of DVA in this population of 1.9%, with 36.6% of all DVA being complicated by parenchymal abnormalities (most commonly white matter signal changes). Complications were significantly more common in patients with multiple DVA (P = 0.002) and in lesions drained by multiple and larger collectors (P = 0.008 and P < 0.001, respectively), although neuroimaging and neurologic outcomes were favorable in most cases. In addition, *in utero* detection of these lesions was possible in 27.3% of cases that previouslyunderwent fetal MRI.

The subsequent clinical study evaluated spinal findings in a cohort of n = 31 children with FCCM and showed that although rarely symptomatic, spinal cord CM can be detected in up to 16% of pediatric FCCM patients using diverse spine MRI protocols and may also appear *de novo*. Opposingly, intraspinal venous malformations were absent in our population.

Finally, the third clinical study analyzed the natural history of CM in a cohort of n = 43 children with FCCM and demonstrated that the 5-year annual hemorrhagic risk and the cumulative symptomatic hemorrhagic risk were 17.1% and 5.0% per person-year, respectively. Furthermore, the number of brainstem (adjusted HR = 1.37, P = 0.005) and posterior fossa (adjusted HR = 1.64, P = 0.004) CM at first brain MRI were significant independent predictors of prospective symptomatic hemorrhage in our cohort.

Discussion/conclusion:

Our research points to the hypothesis that there is a higher risk of flow-related complications in DVA during the neonatal period than in other phases of life although with overall good outcomes, a risk that is significantly associated with lesions´ multiplicity as well as intrinsic angioarchitectural factors. In addition, results obtained from the developed work seem to support the theory that DVA are indeed congenital lesions in many cases that can be detected already *in utero*.

On the other side, our data suggest that children with FCCM treated according to the current best clinical practice have a 5-year risk for symptomatic hemorrhage similar to the one described in the literature for children and adults with all types of cerebral CM and that their imaging features at first brain MRI may help to predict this risk. Furthermore, given the relative commonality of asymptomatic spinal cord CM, serial screening spine MRI should be considered in FCCM starting in childhood.

Importantly, the investigation culminating in the current thesis was developed, in most cases, as a multicenter international collaboration, allowing inclusion of large samples of children when compared with historical cohorts harboring the same pathologies in equivalent age groups, therefore allowing more reliable results. From our work, it also emerges a recommendation of imaging protocol to investigate pediatric CM, namely in the setting of FCCM.

The novel findings presented in the current thesis provide valuable data to the current body of evidence and can be used for more precise prognostication and individual counselling in both neonatal DVA and pediatric FCCM. These may be incorporated in health policies and future clinical trials, namely evaluating novel disease-modifying medical therapies in the latter disorder, eventually with an impact in clinical practice and patient's management.

However, there is the need for additional prospective multi-modal neuroimaging studies in children with CVM for validation and expansion of our results, aiming for a better comprehension of the angioarchitecture, pathophysiology, natural history and complications of these disorders in this age group. In an era of ever-increasing patient-centered care, it is of the utmost importance to give voice to children and their families and focus the research on the needs and specificities of this often-neglected age group.

Keywords: *developmental venous anomaly, cavernous malformation, familial cavernous malformation syndrome, pediatric, neuroimaging, magnetic resonance imaging*

RESUMO

Introdução:

As malformações vasculares cerebrovenosas (CVM) pediátricas são um grupo de lesões vasculares de baixo fluxo envolvendo principalmente as veias e os capilares venosos intracranianos e que se manifestam entre o período intra-uterino e a adolescência. A neuroimagem desempenha um papel fundamental no diagnóstico das CVM, bem como na avaliação de complicações e/ou síndromes potencialmente associadas a estas entidades.

As anomalias venosas do desenvolvimento (DVA) e as malformações cavernosas (CM), embora constituam os subtipos mais comuns de CVM em todos os grupos etários, permanecem relativamente pouco estudadas na idade pediátrica. De facto, os estudos dirigidos a estas duas malformações venosas em coortes exclusivamente pediátricas são escassos e os dados sobre sua origem (congénita vs pós-natal), prevalência, características de neuroimagem e história natual permanecem limitados.

Objectivos:

O objetivo geral da investigação efectuada no âmbito da presente tese de doutoral foi aplicar a imagem por ressonância magnética (RM) para investigar e caracterizar as CVM que se apresentam durante a idade pediátrica (desde o período fetal até à adolescência), com particular enfoque nas DVA e nas CM. O trabalho de investigação foi posteriormente dividido em duas áreas principais: DVA neonatais e síndrome cavernosa cerebral familiar (FCCM) pediátrica.

Materiais e métodos:

Em primeiro lugar, levámos a cabo uma revisão do estado da arte das CVM, centrada nas características de neuroimagem das DVA e dos CM, em especial na idade pediátrica. Neste contexto, publicámos ainda sob a forma de uma carta ao editor o relato de um caso clínico de uma DVA detectada *in utero* através de RM fetal e posteriormente confirmada em estudo de RM cerebral pós-natal.

De seguida, realizámos um estudo de coorte retrospectivo monocêntrico incluindo todos os recém-nascidos que realizaram pelo menos uma RM cerebral até aos 28 dias de idade corrigida

num centro pediátrico terciário (Istituto Giannina Gaslini, Génova, Itália) e nos quais o respectivo relatório continha o termo "*anomalia venosa do desenvolvimento"*.

Posteriormente, efectuámos um estudo de coorte retrospectivo multicêntrico envolvendo três centros pediátricos terciários (Istituto Giannina Gaslini, Génova, Itália; Children's Hospital of Philadelphia, Filadélfia, Estados Unidos da América e Great Ormond Street Hospital, Londres, Reino Unido) incluindo todas as crianças (idade ≤ 18 anos) com diagnóstico de FCCM durante a idade pediátrica entre janeiro de 2010 e agosto de 2021 e com pelo menos uma RM do ráquis disponível para revisão.

Por fim, desenvolvemos um estudo de coorte retrospectivo multicêntrico envolvendo quatro instituições pediátricas terciárias (Istituto Giannina Gaslini, Génova, Itália; Children's Hospital of Philadelphia, Filadélfia, Estados Unidos da América; Great Ormond Street Hospital, Londres, Reino Unido e Centro Hospitalar e Universitário São João, Porto, Portugal) incluindo todas as crianças (idade ≤ 18 anos) com diagnóstico de FCCM entre janeiro de 2010 e setembro de 2021, e com pelo menos a RM cerebral de base disponível para revisão.

Resultados:

O trabalho de investigação dirigido às DVA neonatais incluiu n = 41 recém-nascidos, e revelou uma taxa de de detecção de 1,9% destas lesões através de estudos de RM cerebral, sendo que em 36,6% dos casos estas lesões se associavam complicações imagiológicas no respectivo território de drenagem (mais frequentemente alterações de sinal da substância branca). As complicações foram significativamente mais frequentes em pacientes com múltiplas DVA (P = 0,002) e em lesões drenadas por coletores múltiplos e com maior calibre (P = 0,008 e P < 0,001, respectivamente). A evolução dos achados de neuroimagem e dos *outcomes* neurológicos a longo-prazo foi favorável na maioria dos casos. Adiconalmente, a detecção *in utero* das DVA foi possível em 27,3% dos casos com RM fetal prévia disponível para revisão.

Por outro lado, o estudo clínico centrado nos achados raquidianos numa coorte de n = 31 crianças com FCCM demonstrou que, embora raramente sintomáticos, as CM medulares são detectadas em até 16% dos casos utilizando diversos protocolos de RM do ráquis, podendo inclusivamente surgir *de novo*. Ao invés, nenhuma malformação venosa intra-vertebral foi identificada nas crianças incluídas no estudo.

Finalmente, o estudo clínico que analisou a história natural das CM numa coorte de n = 43 crianças com FCCM revelou um risco anual de hemorragia sintomática e um risco cumulativo de

hemorragia sintomática aos 5 anos de 17,1% e de 5,0% por pessoa-ano, respectivamente. Por outro lado, o número de CM no tronco cerebral (HR ajustado = 1,37; P = 0,005) e na fossa posterior (HR ajustado = 1,64; P = 0,004) presentes na primeira RM cerebral foram preditores independentes significativos de hemorragia sintomática subsequente na nossa coorte.

Discussão/Conclusão:

Os dados obtidos através do nosso estudo dirigido às DVA neonatais sugerem um risco acrescido de complicações secundárias a estas lesões vasculares nessa etapa do desenvolvimento quando comparado com os valores descritos em populações de outros grupos etários, e que esse risco se associa de forma significativa com a presença de múltiplas DVA e com fatores angioarquitectónicos lesionais. Além disso, os resultados da avaliação retrospectiva das RM fetais dos doentes com DVA neonatal suportam a hipótese da origem congénita destas malformações vasculares.

Por outro lado, os resultados dos estudos centrados em crianças com FCCM tratadas de acordo com a melhor prática clínica atual indicam um risco cumulativo de hemorragia sintomática aos 5 anos semelhante ao descrito na literatura para crianças e adultos com todos os tipos de CM cerebral e indicam que a primeira ressonância magnética cerebral pode ser preditiva de hemorragia sintomática aos 5 anos de seguimento. Adicionalmente, dada a considerável prevalência de CM medulares assintomáticos nesta população, estudos seriados de RM do ráquis devem ser considerados desde a infância em doentes com diagnóstico de FCCM.

Os dados obtidos através da nossa investigação clínica acrescentam valor ao conhecimento actual sobre as CVM pediátricas e podem ser utilizados para melhor prognosticação e aconselhamento mais individualizado de crianças que se apresentam com DVA no período neonatal ou que são diagnosticadas com FCCM. Os nossos resultados poderão também ser incorporados em futuras políticas de saúde bem como em novos ensaios clínicos que testem novas terapias médicas modificadoras de doença em crianças com estas patologias, o que por sua vez pode determinar impacto na prática clínica e na orientação destes pacientes e dos seus familiares. Do nosso trabalho resulta ainda uma recomendação de protocolo de abordagem de neuroimagem das CM pediátricas, incluindo em contexto de FCCM.

É importante ressaltar que a investigação que culminou na presente tese envolveu na maioria dos estudos uma colaboração internacional multicêntrica, permitindo a inclusão de grandes amostras comparativamente às coortes históricas de caraterísticas semelhantes, permitindo

assim resultados mais confiáveis. No entanto, há necessidade de desenhar e desenvolver estudos prospectivos de neuroimagem multimodal em crianças com CVM para validação e expansão dos nossos resultados, visando uma maior e melhor compreensão da angioarquitectura, fisiopatologia, história natural e complicações destas patologias na idade pediátrica.

Numa era de cuidados cada vez mais centrados no doente, é essencial dar voz às crianças e às suas famílias e focar a investigação clínica nas necessidades e especificidades deste grupo etário, ainda muitas vezes negligenciado.

Palavras-chave: anomalia venosa do desenvolvimento, malformação cavernosa, síndrome de malformação cavernosa familiar, pediatria, neuroimagem, ressonância magnética

INTRODUCTION

Pediatric cerebrovenous vascular malformations (CVM) are a group of non-shunting slow-flow pathologies mainly involving the intracranial venous/capillary venous system that are discovered during the period that ranges from fetal to adolescent life and include the following entities: 1) developmental venous anomalies (DVA), 2) cerebral cavernous malformations (CCM), 3) *sinus pericranii* and 4) dural sinus malformations without arteriovenous shunting [1–3].

Manifestations of pediatric CVM are highly heterogeneous and depend not only on the individual malformation and its location and size but also on the specific age of presentation, ranging from asymptomatic, incidentally encountered focal lesions to variable degrees of neurological disability and even death [1–3]. On the other side, children with CVM including CCM and DVA have a reported higher frequency of other vascular disorders and/or systemic conditions as it will discussed below, many of these with a genetic background [4–6].

Neuroimaging plays a pivotal role in the diagnosis, characterization, follow-up and/or surgical planning of CVM at all age groups, including in children and fetuses. There is a wide spectrum of imaging techniques available for the postnatal study of these vascular lesions, such as transfontanellar cerebral ultrasound (cUS), computed tomography (CT) with or without angiography (CTA)/venography (CTV), magnetic resonance imaging (MRI) with or without angiography (MRA)/venography (MRV), and digital subtraction angiography (DSA) [7–10]. Moreover, whenever a brain and/or spine MRI is performed, different advanced MRI techniques may also be added to the imaging protocol for either clinical and/or research purposes [11, 12]. On the other side, imaging evaluation of fetuses can be also made using prenatal US including color-coded Doppler imaging, fetal MRI and fetal postmortem MRI [9, 13, 14]. The optimal imaging method to access these malformations should be tailored to the specific clinical situation and depends on individual variables, including patient's age, type and location of the lesion, clinical presentation, degree of cooperation as well as availability and physical properties of the imaging methods [7, 8].

Although the prevalence of each CVM subtype is variably reported in the literature due to the methodologic heterogeneity of the published studies (namely concerning the type of design, method of identification of the neurovascular lesion, specific pediatric subgroup as well as clinical indication for neuroimaging), there is a large consensus that DVA and CCM represent the two most frequent subtypes of CVM in both children and adults. Despite this, DVA and cavernous malformations (CM) remain surprisingly underreported in children. Indeed, although DVA and CM have been frequently reported in adults and mixed age populations, research

studies focusing on these lesions in pediatric only cohorts are still scarce. Therefore, their origin (congenital vs postnatal), prevalence, neuroimaging features and associated complications in this age group remain largely unknown, more so in neonates and/or in associated syndromes, such as the familial cavernous malformation syndrome (FCCM). In addition, they may differ from their adult counterparts, as some authors [15–17] but not all [18–20] report a more aggressive and/or dynamic course of these subtypes of CVM during childhood.

Importantly, *"children are not small adults"* and their brains exhibit specific anatomic and physiologic characteristics as well as increased remodeling capacity and recovery potential, challenging the diagnosis as well as potentially influencing clinical manifestations and prognosis of this group of vascular malformations [1]. Indeed, dynamic changes in the intracranial venous system have been reported during the entire human lifetime span, under both physiological and pathological conditions, but are more striking during early life years [3, 21–24]. In addition, differently from arteries, the brain veins have no muscular tissue in their thin walls, possess no valves and are highly prone to anatomical variants [22, 23], factors that contribute to the high variability of the clinical and imaging picture of affected patients and may lead to potential neuroimaging pitfalls. Conversely, some CVM have also the potential to locally disrupt the normal development of the central nervous system (CNS) during fetal life and childhood [1]. On the other side, pediatric neuroimaging is characterized by increased complexity due to variable imaging appearances related to the different phases of normal development [9, 25]. Finally, safety and radioprotection issues are of particular concern in children, including potential effects of ionizing radiation and use of contrast media and sedation in this age group, requiring adoption of the "*as low as reasonably achievable"* concept and utilization whenever possible of imaging strategies aiming to reduce the need for sedation in pediatric CT and/or MRI, such as fast brain MRI protocols and the *feed and wrap* technique [9, 26].

The longitudinal, non-invasive MRI study of pediatric DVA and CM is of importance as it will allow a better characterization of their angioarchitectural features and potentially associated imaging abnormalities, adding relevant information to the further understanding of these entities. In turn, the gathered knowledge has the potential to be used in the future in affected children with similar ages to estimate individual risks of symptomatic and asymptomatic hemorrhage and/or other possible complications as well as long-term outcomes, thereby supporting a more individualized treatment approach as well as a better prognostic counseling. Results from such investigations may also be potentially used by healthcare decision makers, namely in the establishment of formal recommendations for management of DVA and CM in children, including standardized neuroimaging assessments for initial evaluation and follow-up of these entities.

Finally, as disease-modifying pharmacologic therapies aiming to stabilize or prevent CM development (namely propranolol and atorvastatin) are already being investigated in adults [27–29], epidemiological, clinical and neuroimaging data obtained by research on this topic can potentially be used to estimate sample sizes, evaluate disease progression and/or constitute surrogate biomarkers for disease severity in future clinical trials including also affected children.

AIMS

Although most CVM have been frequently studied in adult and mixed age populations, they remain largely undescribed in children. The general aim of this work was to apply MRI to investigate and characterize CVM presenting in the pediatric age (anytime from fetal to adolescent life), using structural conventional sequences as well as advanced and angiographic MRI techniques. We choose to subdivide the approach to the CVM subject in two main divergent topics: neonates with DVA and children with FCCM.

Primary objective:

1. To describe the prevalence, the neuroimaging features and associated complications of CVM in the pediatric population, with special emphasis in postnatal MRI studies of children diagnosed with neonatal DVA or FCCM.

Secondary objectives:

1. To perform a narrative review of CVM, focusing on the neuroimaging/angioarchitectural features of DVA and CM as well as their distinctive features in the pediatric age;
2. To correlate the neuroimaging findings of neonatal DVA and pediatric FCCM at diagnosis with the neurological phenotype, genetic background (if appropriate) and clinical outcome;
3. To compare epidemiological, clinical and neuroimaging features of neonatal DVA as well as brain and spinal CM in children with FCCM among specific pediatric sub-groups as well as adults;
4. To retrospectively assess neuroimaging changes along time of neonatal DVA as well as brain and spinal CM in pediatric FCCM patients;
5. To study the natural history of CCM in pediatric patients with FCCM, with an emphasis on symptomatic hemorrhagic events and associated risk factors;
6. To describe the accuracy of fetal MRI in the identification of DVA in neonates with confirmed disease and to assess any imaging modifications in this subtype of vascular malformation between prenatal and postnatal studies;

7. To evaluate the neuroimaging characteristics of neonatal DVA and brain and spinal CM pediatric FCCM in gradient recovery echo (GRE)/ susceptibility-weighted imaging (SWI) sequences, whenever available.

We hypothesize that pediatric DVA and FCCM have different epidemiological and clinical features, neuroimaging/angioarchitectural characteristics, complication rates and natural history compared to what is usually described in the general population/adults and that these features also vary within specific pediatric sub-groups.

MATERIALS & METHODS

Institutional review board (IRB) approval was obtained for the postdoctoral project. Written informed consent was waived because of the retrospective nature of the studies. All procedures related with the investigation were performed in accordance with the ethical standards of 1964 Helsinki Declaration and its later amendments or comparable ethical standards, including Good Clinical Practice.

Firstly, a narrative review of the literature focusing on the neuroimaging features of pediatric CVM was performed including a case report from our group published as *Letter to the Editor*.

Subsequently, three different although related research studies on this field were developed.

We started with a monocenter retrospective cohort study in a tertiary pediatric center (IRCCS Istituto Giannina Gaslini, Genoa, Italy) including all neonates that have performed at least one brain MRI up to 28 days of corrected age during a 12-year period (January 2008 to December 2019) and in whom the imaging report contained the term “developmental venous anomaly”. Patients were searched using the radiology information system and the DVA diagnosis was confirmed after independent analysis by two neuroradiologists. Available prenatal and longitudinal postnatal brain imaging were reviewed and clinical data collected.

Afterwards, we have performed a multicenter retrospective cohort study involving three tertiary pediatric centers (IRCCS Istituto Giannina Gaslini, Genoa, Italy; Children´s Hospital of Philadelphia, Philadelphia, United States of America and Great Ormond Street Hospital, London, United Kingdom) including all consecutive patients with a diagnosis of pediatric FCCM (≤ 18 years) between January 2010 and August 2021 and with at least with one complete spine MRI available for review. Available longitudinal spine and brain imaging were reviewed, and clinical and genetic data collected.

Lastly, we have conducted a multicenter retrospective cohort study involving four tertiary pediatric institutions (IRCCS Istituto Giannina Gaslini, Genoa, Italy; Children´s Hospital of Philadelphia, Philadelphia, United States of America; Great Ormond Street Hospital, London, United Kingdom and Centro Hospitalar e Universitário São João, Porto, Portugal) including all consecutive subjects with a pediatric diagnosis of FCCM (≤ 18 years) between January 2010 and September 2021, and with at least the initial brain MRI available for review. Available longitudinal brain and spine imaging were reviewed and clinical and genetic data collected.

Statistical analyses were performed by using Stata, v14.0 (StataCorp, College Station, Texas) or SPSS Statistics software, v24.0 (IBM, Armonk, NY).

Quantitative data were presented as median and interquartile range, and categorical data as frequencies and percentages. Student´s t/Mann–Whitney or Pearson's $\chi 2$ /Fisher exact tests were used to compare categorical and continuous variables, respectively, as appropriate. In the third clinical study, additional statistical analysis was performed, including calculation of the annual risk and cumulative rates of symptomatic hemorrhage. The latter were illustrated using the Kaplan–Meier method, and the curves were compared by the log-rank test. Survival analysis and univariable and multivariable Cox regression survival analyses were also performed.

In all studies the significance level was set at P = 0.05 (2-sided).

PUBLICATIONS LIST

Geraldo AF, Melo M, Monteiro D, Valente F, Nunes J. **Developmental venous anomaly depicted incidentally in fetal MRI and confirmed in post-natal MRI**. Neuroradiology. 2018 Oct;60(10):993-994. doi: 10.1007/s00234-018-2089-y.

Impact factor: **3.112**; Q2 Journal

Geraldo AF, Messina SS, Tortora D, Parodi A, Malova M, Morana G, Gandolfo C, D'Amico A, Herkert E, Govaert P, Ramenghi LA, Rossi A, Severino M. **Neonatal Developmental Venous Anomalies: Clinicoradiologic Characterization and Follow-Up**. AJNR Am J Neuroradiol. 2020 Dec;41(12):2370-2376. doi: 10.3174/ajnr.A6829.

Impact factor: **3.825**; Q1 Journal

Geraldo AF, Luis A, Alves CAPF, Tortora D, Guimarães J, Reimão S, Pavanello M, de Marco P, Scala M, Capra V, Rossi A, Schwartz ES, Mankad K, Severino M. **Spinal involvement in pediatric familial cavernous malformation syndrome.** Neuroradiology. 2022 Aug;64(8):1671-1679. doi: 10.1007/s00234-022-02958-1.

Impact factor: **3.112**; Q2 Journal

Geraldo AF, Alves CAPF, Luis A, Tortora D, Guimarães J, Abreu D, Reimão S, Pavanello M, de Marco P, Scala M, Capra V, Vaz R, Rossi A, Schwartz ES, Mankad K, Severino M. **Natural history of familial cerebral cavernous malformation syndrome in children: a multicenter cohort study**. Neuroradiology. 2022 Oct 6; 65(2):401-414. doi: 10.1007/s00234-022-03056-y.

Impact factor: **3.112**; Q2 Journal

PART I- NEUROIMAGING CHARACTERISTICS OF CEREBROVENOUS MALFORMATIONS: STATE OF THE ART

1.1. PROLOGUE

We started our work with a narrative literature review on the topic of pediatric CVM, mainly focusing on the neuroimaging findings of the two most common subtypes (DVA and CM) and associated lesions and/or syndromes. In addition, we provide one additional case report that was published by our group as *Letter to the Editor* describing for the first time a DVA detected *in utero* with fetal MRI and subsequently confirmed in post-natal brain MRI.

1.2. BACKGROUND

Pediatric CVM are a large and heterogeneous group of non-proliferative entities that affect (solely or not) the intracranial vascular system and that present during fetal life or childhood [1–3, 30]. The normal development of the intracranial vascular system starts during the 5-6th weeks of gestation with the formation of the *meninx primitiva* at the surface of the early brain and progresses along the whole intrauterine period as well as in the post-natal phase [22].

Regardless of their location and age of presentation, vascular lesions are overall classified by the International Society for the Study of Vascular Anomalies in vascular tumors and vascular malformations [2]. In turn, the latter have also been subdivided in simple malformations, combined malformations, malformations of major named vessels or malformations associated with other anomalies [2].

However, in the particular case of simple vascular malformations involving the cerebrovascular system in children, there is currently no uniform classification system [1–3]. Despite this, most of the available classifications subdivide these lesions in1to main subgroups based on their major vascular component (or target of the insult), as presented in a simplified form in **Table 1.2.1** [1–3].

Table 1.2.1. Simplified classification of simple pediatric cerebrovascular malformations based on the main involved vessel.

Main involved vessel/Target	Subtype of cerebrovascular malformation
Capillaries	Capillary telangiectasia
AV unit	Arteriovenous malformation Dural arteriovenous fistula Vein of Galen malformation Dural sinus malformation (with associated AV shunts)
Venous capillaries/Veins	Developmental venous anomaly Cavernous malformation *Sinus pericranii* Dural sinus malformation (without associated AV shunts)

Legend: AV- arteriovenous. Adapted from [1–3].

Therefore, and as referred in the introductory chapter, CVM are a subgroup of simple, slow-flow cerebrovascular malformations characterized by predominant involvement of the neural venous/capillary venous structures [1–3].

Among the wide available armamentarium of neuroimaging techniques available for the diagnosis and characterization of adult and pediatric CVM, selection of the best diagnostic method depends on multiple variables, including the specific subtype of CVM, patient-related factors as well as available commodities and infrastructures [7–9]. Our comprehensive narrative review and subsequent clinical research will focus on the two most common CVM, ie DVA and CM, with special emphasis in their neuroimaging assessment as well as aspects specific to the pediatric age presentation.

1.3. DEVELOPMENTAL VENOUS ANOMALIES

Introduction

DVA, a term first coined by Lasjaunias *et al* in 1986 [31], corresponds to the most common subtype of CVM in all age groups.

These lesions are characterized by a cluster of radially oriented parenchymal veins converging centripetally into one (or rarely more) dilated venous collector(s) that in turn drain(s) towards the superficial and/or deep venous system [31–34].

DVA are more commonly identified in the supratentorial compartment, especially in the frontal lobes. They can also be present in the posterior fossa, including the cerebellum and the brainstem (the latter location corresponding to 2-5% of all DVA) [17, 34–37].

They are usually single lesions, but multiple DVA are present in a single patient in about 7-16% of cases [17, 33, 34, 36].

Although these vascular anomalies were once considered *benign anatomic variants* discovered incidentally on neuroimaging [31], they represent in fact areas of venous fragility that can be occasionally associated with adjacent imaging abnormalities including other vascular malformations and may even complicate and become symptomatic [36, 38–40]. Indeed, DVA provide the solely draining route to the surrounding brain parenchyma, the drained territory is relatively larger than normal and usually depends on a single collector and a single drainage route, and these features determine a less robust venous pathway commonly leading to hemodynamical changes [40].

In addition, recent studies have demonstrated that DVA, especially whenever multiple, can be associated with multiple systemic disorders and their presence may even support or suggest the subjacent diagnosis, as it will be further explored below.

Epidemiology

Estimates of DVA prevalence in the general population in contemporary neuroimaging studies range from roughly 5 to 10% [36, 37]. These values are higher than previously reported, probably due to increased availability and technical advances in both CT and MRI examinations in the last 20 years [33, 52, 53].

There is large consensus that the prevalence of DVA is roughly equal between genders [37]. Inversely, the influence of age in the prevalence of DVA remains controversial [37, 54].

Pathology

Histologically, DVA are composed of distended, thin-walled venous radicles with a fan-shaped spread distributed along the cerebral parenchyma and draining into one or multiple large caliber vein(s) with a thicker wall but without a smooth muscle layer nor elastic lamina [55–57]. In case of high venous pressure, progression of vessel wall thickening and microvascular hyalination within the lesion may occur [58].

Genetics and pathophysiology

The pathogenesis of these vascular anomalies is still incompletely understood, including the timing of development. The classic, neurovascular theory hypothesizes that DVA arise secondarily to a hemodynamic need due to arrest of normal venous development caused by a nonspecific insult during the first trimester of gestation. This will lead to retention of primitive medullary veins, followed by recruitment of transhemispheric anastomotic drainage pathways, and eventual maturation into a typical DVA [31, 34]. Therefore, they have been considered extreme variations of the normal cerebral venous angioarchitecture that form to provide compensatory drainage to brain areas whose typical venous drainage patterns have been disrupted due to hypoplasia, aplasia, or an early occlusion, leading however to a less robust venous drainage pathway [31, 59].

More recently, a seminal paper by Snellings *et al* first described the presence of gain-of-function pathogenic variants involving the phosphatidylinositol-4,5-bisphosphate 3-kinase, catalytic subunit alpha (*PIK3CA*) gene in DVA associated with CCM [60] and suggested that DVA are intermediate lesions that act as a genetic precursors of sporadic CCM [60]. Other acquired mutations in different genes are then need for full sporadic CCM development, as it will be deeply explained in the chapter dedicated to CCM [60].

DVA are already known to be associated with other *PIK3CA*-related disorders (PROS) (See DVA-associated anomalies and/or syndromes section), therefore supporting these initial results, that will certainly open new avenues in the understanding of DVA.

Clinical presentation and natural history

In most cases, DVA are asymptomatic lesions incidentally encountered in neuroimaging studies performed in both children and adults for other unrelated reasons and therefore of no clinical significance [52, 58, 59, 61].

However, a subset of these lesions may become symptomatic due to complications related with a coexistent sporadic CCM [38, 39]. More rarely, patients with a DVA may also present with

refractory seizures caused by adjacent structural cortical abnormalities in the context of a shared insult or a common genetic background [3, 62, 63].

Alternatively, a DVA itself may become complicated through multiple different mechanisms that have been categorized in three subtypes: one related with mechanical compression and the other two with flow imbalance [38–40]. Such mechanisms and the corresponding clinical manifestations are summarized in **Table 1.3.1** and will be reviewed subsequently in more detail. In a small percentage of patients with DVA no definitive cause for the presenting neurologic symptoms is identified and the manifestations are considered idiopathic [38].

Table 1.3.1. Pathogenic mechanisms and clinical manifestations of symptomatic developmental venous anomalies.

Mechanism	**Symptomatic manifestation**
Mechanical compression due to mass effect	
● Neurovascular conflict (+++V, VII and VIII cranial nerves)	Cranial nerve compressive neuropathy: trigeminal neuralgia, hemifacial spasm, hearing loss/tinnitus
● Blockage of ventricular outflow pathways (+++Monro foramen and Sylvius aqueduct)	Obstructive hydrocephalus
Abnormal flow Reduced outflow ● Anatomic obstacles (stenosis and/or thrombus) ● Functional (distant high flow shunt) Increased inflow ● AV microshunt within the DVA (TVA) ● AVM draining towards a DVA ⇩ Increased pressure within the venous anomaly venous hypertension/stasis/infarction and/or acute hemorrhage	Seizures FND Headaches Altered mental status Unilateral movement disorders

Legend: AV- Arteriovenous, AVM- Arteriovenous malformation, DVA- Developmental venous anomaly, FND- Focal neurologic deficit, TVA- Transitional venous anomaly. Adapted from [38, 39].

Mechanical compression

In some rare instances, DVA (most often the venous collector) can cause local mass effect on adjacent brain structures due to their specific location, configuration and/or size.

In particular, these venous anomalies may lead to neurovascular conflict and associated compressive neuropathy, more often affecting the trajectory (especially the root entry zone) of the V, VII and VIII cranial nerves [38, 64–66].

Moreover, DVA can also cause obstructive hydrocephalus, usually due to an obstruction/compression at the level of the Sylvius aqueduct or the foramen of Monro [38, 67–70]. Importantly, DVA-related mechanical compression tends to occur more often in younger patients, namely children [39].

Flow-related mechanisms

More often, DVA manifest with flow-related complications, either due to a decreased outflow or an increased inflow, ultimately leading to an increased pressure within the venous anomaly [38, 39].

In particular, **decreased venous outflow** may occur due to anatomic obstacles (including thrombosis or stenosis of the venous collector with or without associated systemic procoagulating factor or state) or functional conditions (such as a coexistence of a remote arteriovenous shunt not draining directly into the DVA but causing venous hypertension and therefore limiting DVA drainage) [38, 39].

On the other side, **increased venous inflow** within a DVA may be caused by presence of rare arteriovenous microshunts directly at the DVA (corresponding to the so-called transitional venous anomalie*s* (TVA) that will be analyzed in more detail subsequently) or alternatively a typical nidal-type arteriovenous malformation (AVM) draining through the DVA [38, 39, 71].

In both situations, presenting symptoms include focal neurological deficits (FND), seizures, headaches and altered mental status or more rarely unilateral movement disorders due to chronic venous hypertension/congestion with or without associated mineralization, ischemia and/or infarction as well as intracranial hemorrhage (ICH) [38, 39, 72]. Importantly, and as previously mentioned, seizures may be also cause by coexistence of malformations of cortical development in the draining territory of a DVA [3, 62, 63] and such cortical abnormalities should be always actively searched for.

DVA with special features: Transitional venous anomalies

TVA (also known as arterialized DVA) are rare vascular lesions situated in a *continuum* between DVA and AVM and characterized by presence of microarteriovenous shunting between the radicles of the DVA but without a distinct parenchymal nidus [71, 73–75].

TVA are probably underrecognized and underreported as they resemble regular DVA on conventional cross-sectional imaging and are usually only distinguished with DSA due to presence of early venous filling. More recently, arterial spin labelling (ASL) has been proposed as a non-invasive alternative MRI technique to detect and monitor TVA, therefore obviating the need for DSA at least in asymptomatic cases [75]. Indeed, according to a recent study, increased ASL signal in the parenchyma surrounding a DVA, as well as in the main venous collector and/or in a distal draining vein or dural venous sinus can provide useful diagnostic information about a subjacent arteriovenous shunting and therefore identify a TVA [75].

The origin of TVA is still under debated but according to current knowledge these intermediate lesions seem to form in consequence of thrombosis-related outflow obstruction of a DVA that in turn promotes proximal arterialization, in a mechanism similar to a dural arteriovenous fistula (dAVF). Supporting this concept, the great majority of TVA cases have been reported in adults (reviewed in [71]).

The natural history of TVA is also relatively unknown, but it is estimated that these present an AVM-like behaviour. Indeed, they appear associated with a higher incidence of hemorrhagic and non-hemorrhagic manifestations than typical DVA [71].

Association with pathologies and/or syndromes

Intracranial and cervico-facial slow-flow vascular lesions

As already mentioned, DVA may coexist with other intracranial and extracranial vascular malformations, in most instances with a **sporadic CCM** [76]. Indeed, together they represent the most common combination of mixed vascular malformations. By contrast, familial CCM have not been associated with a DVA.

The percentage of DVA with a concurrent sporadic CCM is varied in the literature reports and depends on numerous factors, namely the used imaging technique and the clinical and epidemiological characteristics of the cohorts, but it is estimated to range between 4-11% for the general population [17, 36, 37, 77]. DVA associated with CCM have a higher risk of

hemorrhage than isolated lesions. Inversely, it is still debatable if a CCM associated with DVA presents an increased risk of hemorrhage when compared with an isolated CCM [83, 84].

Interestingly, multiple case reports have described *de novo* formation of CCM in the drainage territory of a DVA over time and not the opposite [78–80]. It has also been shown that the prevalence of CCM associated with a DVA increases with age [37, 81] and the sum of these findings lead to the concept that DVA play a role in the development and growth of sporadic CCM. Accordingly, it has been classically hypothesized that chronic elevation of pressure within a DVA, as well as chronic venous congestion and venous ischemia in its draining territory due to poor venous outflow leads to endothelial proliferation and subsequent formation of fragile vessels between the venous radicles that are prone to microhemorrhages and that subsequently result in CM formation through the process of *hemorrhagic angiogenic proliferation* [76]. However, as presented above, a recent seminal paper by Snellings *et al* suggests that DVA develop as the result of a pathogenic variants in the *PIK3CA* gene, being a genetic primer for subsequent sporadic CCM formation following acquisition of an additional somatic mutations [60].

Besides age, additional putative risk factors for the development of DVA-associated sporadic CCM include infratentorial location of the DVA [77], depiction of tortuosity, multiplicity, kinking, outflow stenosis and/or deep drainage of the collector vein(s), presence of multiple DVA [77] and history of comorbid inflammatory disorders [82].

Capillary telangiectasias, corresponding to multiple dilated thin-walled capillaries without smooth muscle/elastic fibers and interspersed within normal brain parenchyma are also commonly reported in association with DVA [85–88]. Opposingly to CCM, capillary telangiectasias associated with DVA do not increase the hemorrhagic risk of the latter lesions. Alternatively, a mixed vascular malformation characterized by the combination of DVA with both CCM and capillary telangiectasia may also occur, corresponding to the so-called **neurovascular triad** [89–92].

In some instances, simple dilatations of a vein known as **secondary cerebral venous varices** can be identified in the draining territory of a DVA in both children and adults [93, 94]. The former possibly form due to congenital weakness of the vessel wall combined with DVA-related increased regional flow volume or increased pressure.

Finally, it has been demonstrated that DVA are also more common in patients with **cervicofacial venous malformations** and/or intracranial **dural sinus ectasia**, probably as part of the spectrum of the Cerebrofacial Venous Metameric syndrome (CVMS), a disorder that is currently included in the PROS umbrella, as it will be addressed below [95–97]. In such cases, DVA are usually located ipsilateral to the facial vascular lesions and share the same metameric location [95–97].

Blue rubber bleb nevus syndrome

BRBNS, also known as Bean syndrome, is a rare, multiorgan syndrome caused by activating double (cis) somatic mutations in *TEK Receptor Tyrosine Kinase* (*TEK)* gene, either acquired *de novo* or in an autosomal dominant fashion [42, 98, 99]. This gene encodes TIE2, a receptor for the angiopoietins, that in turn causes constitutive activation of the *PIK3CA*-mammalian target of rapamycin (mTOR) signaling pathway [42, 98, 99]. This disorder is characterized by the classic triad of multiple venous malformations, iron deficiency anemia (due to recurrent occult or frank gastrointestinal bleeding) and localized intravascular coagulopathy [42, 99]. The CNS is involved in about 13% of BRBNS cases, and patients usually present with multiple DVA and CCM ipsilaterally to scalp venous malformations [41, 43–45]. Orbital venous abnormalities may also coexist [100, 101]. More rarely, intracracranial arterial or arteriovenous lesions, such as aneurysms, dAVF or vein of Galen malformations have also been described in affected patients [100].

Constitutional mismatch repair deficiency syndrome

Constitutional mismatch repair deficiency syndrome (CMMRDS) is a rare autosomal recessive inherited cancer-predisposition syndrome with a very high penetrance caused by pathogenic variants in one of the mismatch repair genes [102–106]. Affected patients usually present during childhood or adolescence with a spectrum of malignant and benign tumors from multiple organs (most commonly high-grade gliomas) as well as *café-au-lait* macules and other neurofibromatosis-like features [102–106]. In addition, it has been recently reported a very high incidence of DVA in these patients, that are usually multiple and not associated with CCM [49–51]. Therefore, the combination of high-grade gliomas and multiple DVA in a pediatric or young adult patient should prompt the neuroradiologist to suggest an underlying diagnosis of CMMRD, with implications in the diagnosis, prognosis and follow-up of affected patients [49–51].

PIK3CA-related overgrowth syndromes

In recent years, somatic activating mutations in the *PIK3CA* gene that encodes a protein involved in the PIK3CA-mTOR pathway were identified as the genetic cause underlying a great subset of

conditions with overlapping features characterized by segmental overgrowth accompanied by vascular, cutaneous, subcutaneous, and bone anomalies. These disorders tend to present in the pediatric age group and are currently grouped under the umbrella term of PIK3CA-related overgrowth syndromes (PROS) [107–110]. The number of disorders recognized as belonging to the PROS family has been growing over time and CVMS has just been recently added to this list [111]. The latter is a rare complex disorder characterized by a spectrum of low-flow vascular lesions (including veno-lymphatic malformations, DVA, CCM, dural sinus ectasia and cavernous sinus cavernous malformation) located in the skin/soft tissues, bone and CNS along a given craniofacial metamere [95, 111]. Some of other PROS entities, including Klippel-Trenaunay syndrome, are also known to be associated with DVA and other intracranial and spinal low-flow vascular malformations [112, 113].

The association of DVA with PROS is supported by the fact that, as already addressed, pathogenic variants in *PIK3CA* have been recently detected within DVA with sporadic CM in their vicinity [60].

PTEN-related hamartoma tumor syndrome

The term *PTEN*-related hamartoma tumor syndrome *(*PRHTS) encompasses a group of pathologies with overlapping features caused by germline pathogenic variants in the *phosphatase and tensin homolog* (*PTEN)* tumor suppression gene that is also involved in the mTOR pathway, including Bannayan-Riley-Ruvalcaba syndrome, Cowden syndrome, adult Lhermitte-Duclos disease, and autism spectrum disorder with macrocephaly [114–116]. All PRHTS phenotypes are characterized by aberrant tissue growth (including hamartomas and propensity for cancers) and may be associated with intracranial and spinal vascular anomalies, including multiple DVA with or without associated CCM [46–48, 115, 117–121]. However, Bannayan-Riley-Ruvalcaba syndrome and autism spectrum disorder with macrocephaly are usually identified in the pediatric age group due to cognitive or neurobehavioral problems, while Cowden syndrome is generally diagnosed in early adulthood in the context of early-onset cancer or polyposis [114–116].

Sporadic primary CNS tumors

Some authors have described a higher prevalence of DVA in both adult and pediatric patients with sporadic primary CNS tumors when compared with healthy subjects or patients with other subtypes of intracranial tumors (namely craniopharyngiomas or metastasis) [122–124]. As pathogenic variants in *PIK3CA* can be observed in a subset of adult and pediatric primary gliomas and *PIK3CA* mutations have been also detected in DVA and other venous malformations, it has

been suggested that DVA could be an imaging biomarker of *PIK3CA*-mutated gliomas [125], although further research is needed on the topic.

Multiple sclerosis

Demyelinating plaques may occur around a pre-existing DVA [126, 127] and a few neuroimaging studies have reported a significantly higher prevalence of DVA in adult patients with multiple sclerosis (MS) than in the general population [128–131]. However, these results have not been confirmed by other authors [132, 133] and therefore the putative association between the two conditions remains elusive and not well-understood. Some authors have proposed that the impaired venous hemodynamics caused by a DVA increase the vulnerability of these structures to surrounding demyelination in a patient with MS [126, 127]. Nevertheless, as there is long-time controversy regarding the role for disrupted venous vasculature and flow within MS lesions (reviewed in [134]), this topic should be further investigated in larger samples, as well as in children with MS and other neuroinflammatory disorders.

Conventional neuroimaging

Prenatal imaging

Prenatal identification of a DVA has only been recently reported and our group was indeed the first to describe a DVA incidentally diagnosed *in utero* using fetal MRI and subsequently confirmed with postnatal imaging [135] (See full article below).

On prenatal US images, DVA has been described as a persistent, solitary parenchymal echogenic lesion with a collector presenting venous flow running from it depicted on high resolution Doppler imaging and without clastic or structural changes [136]. On fetal MRI, DVA present as linear hypointense signal(s) on T2 Half-Fourier Acquisition Single-shot Turbo spin Echo imaging (HASTE) with corresponding *blooming effect* on GRE images, as we and other authors have described [135, 136].

DEVELOPMENTAL VENOUS ANOMALY DEPICTED INCIDENTALLY AND CONFIRMED IN POST-NATAL MRI

Ana Filipa Geraldo,[1] Mónica Melo MD,[2] David Monteiro,[1] Francisco Valente,[2] Joana Nunes[1]

[1] Department of Medical Imaging, Neuroradiology unit, CHVNG/E- Centro Hospitalar Vila Nova de Gaia/Espinho, Portugal

[2] Department of Gynecology-Obstetrics, Prenatal Diagnosis unit, CHVNG/E- Centro Hospitalar Vila Nova de Gaia/Espinho, Portugal.

Cerebral DVA are the most common subtype of congenital brain vascular malformation. They are widely reported in the adult population and less frequently within the pediatric age group [19, 34]. Interestingly, their depiction and characterization *in utero* using US with Doppler and/or fetal brain MRI has only recently been described in a small case series, although post-natal images were not provided in that paper [136].

We herein report a case of 2 gravida 0 para mother with chronic hypertension referred to our pediatric imaging unit at 33 weeks´ gestation following the detection of apparently isolated ventricular enlargement in fetal ultrasound. Fetal brain MRI was performed at the same gestational age, confirming mild left ventriculomegaly. In addition, a linear hypointense signal on T2 HASTE and GRE images was incidentally depicted in the left parietal region, extending from the enlarged ventricular surface up to the cortex **(Fig.1.3.1)**. No other anomalies in the CNS were identified and the diagnosis of DVA was assumed. In light of the above, fetal ultrasound with high-definition Doppler was repeated at 34 weeks´ gestation showing venous flow in the corresponding area, although no associated changes in the echogenicity of the adjacent parenchyma could still be appreciated. The infant was born prematurely at 35 weeks´ gestation by vaginal vacuum delivery. Post-natal MRI was undertaken at 1 month of age (corresponding to 39 weeks´ corrected age) due to progressive enlargement of the left lateral ventricle in consecutive transcranial cerebral ultrasounds performed in the neonatal unit. The prenatal diagnosis of a left parietal DVA was then confirmed **(Fig. 1.3.2)**. No associated cavernous malformation or signal abnormality in the adjacent parenchyma could be detected.

DVAs consist of dilated venules disposed with a radial configuration between normal neural parenchyma and converging centripetally into a large collector vein; this collector in turn drains into ependymal veins, cortical veins, or rarely into a combination of both. Complex DVA may also occur, with multiple collectors draining a single DVA or multiple DVA draining into the same collector. The etiology of DVAs is not clearly understood, but the most accepted theory states

that they represent a compensatory mechanism secondary to any phenomenon disturbing the normal development of the transmedullary veins [19, 34, 136]. They have been classically regarded as normal variants, but their ability to become symptomatic either spontaneously or by mechanical/flow-related factors has also been addressed in the literature [38]. Interestingly, in this specific case, the DVA was ipsilateral to the unilaterally enlarged lateral ventricle. This can be regarded as a matter of coincidence, but also allows us to hypothesize that the enlargement could be secondary to a small intraventricular hemorrhagic complication of this lesion. We favor this second theory as a focal area of hypointensity on GRE could be depicted in the ependymal surface of the left occipital horn in the post-natal MRI, although we can´t completely rule out traumatic birth-related hemorrhage. Other possibilities include chronic ischemia secondary to venous hypertension leading to parenchymal volume loss with ex vacuo dilatation of the ipsilateral lateral ventricle or a single developmental insult causing both the DVA and the adjacent parenchymal atrophy.

This case report further supports the concept that DVA are congenital lesions that can actually be diagnosed in utero, as described by Krajden Haratz *et al* [136]. In addition, it suggests that fetal MRI including GRE sequences has the ability to identify and characterize these lesions in utero even when they are not associated with changes in the normal echogenicity of the cerebral parenchyma in fetal ultrasound.

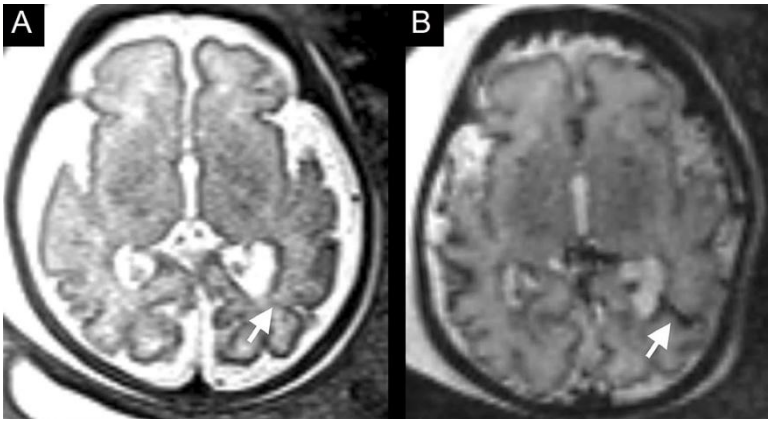

Fig. 1.3.1. Pre-natal brain MRI of the child at 33 weeks´ gestational age. Axial T2 HASTE (A) and T2 gradient echo (B) showing a linear hypointense image in the left parietal region extending from the atrium of the lateral ventricle up to the cortex (*arrows*), compatible with a developmental venous anomaly. Unilateral mild ventriculomegaly is also present.

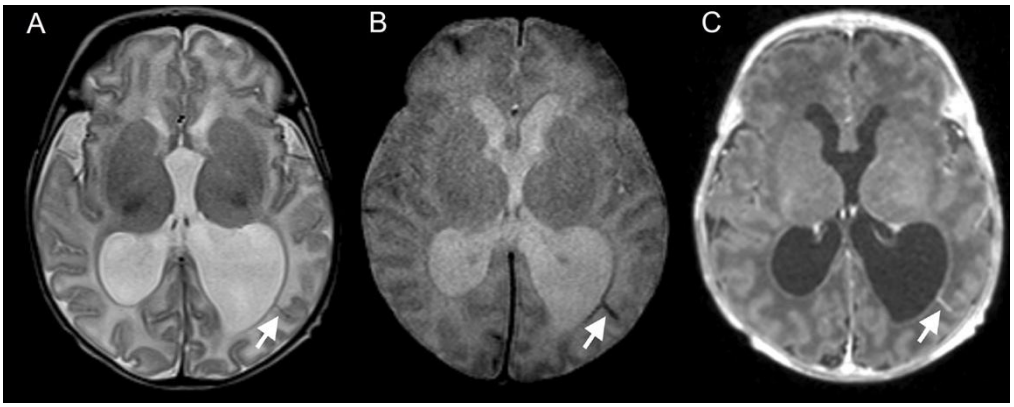

Fig 1.3.2. Post-natal brain MRI of the same child presented in Fig. 1.3.1 at 4 weeks of age (corresponding to 39 weeks´ corrected age). Axial T2-weighted (A), gradient echo (B) and axial T1 contrast-enhanced (C) images showing the linear structure with vascular flow-void and enhancement in the left parietal region compatible with a subependymal developmental venous anomaly with cortical drainage (*white arrows*).

Postnatal imaging

Initial assessment

cUS

Reports of DVA identified with postnatal cUS in neonates and young infants are also exceptional in the literature and identify them as areas of increased echogenicity with variable intensity and initially difficult to distinguish from arterial or venous infarction [19]. However, Doppler US can show in most of cases the presence of blood flow in the collector vein, that is usually located at the centre of the hyperechogenicity [19].

CT

In unenhanced head CT, DVA are usually isodense but associated imaging findings such as adjacent calcifications and/or parenchymal atrophy can be often identified, likely resulting from chronic cerebral ischemia and/or venous hypertension [58, 137] **(Fig. 1.3.3 A-B and 1.3.4 A-B)**. In particular, mineralization can occur within the walls of the DVA or in the surrounding brain parenchyma, and is particularly common when the DVA is located in the region of the deep grey matter nuclei [39, 72, 137, 138]. Therefore, DVA should be included in the differential diagnosis of unilateral calcification of the basal ganglia/thalami [72, 138]. Associated CCM, signs of acute ICH and/or DVA thrombosis (namely spontaneous hyperdensity within the collecting vein) may also be occasionally depicted with this imaging technique [58].

After injection of iodinated contrast (and/or CTA/CTV), DVA usually become easily appreciated due to enhancement of the venous radicles and main collector, giving the typical *umbrella*, fan or *caput medusae*-like appearance of these lesions [34, 58] **(Fig. 1.3.3 C-F and 1.3.4 A-C).**

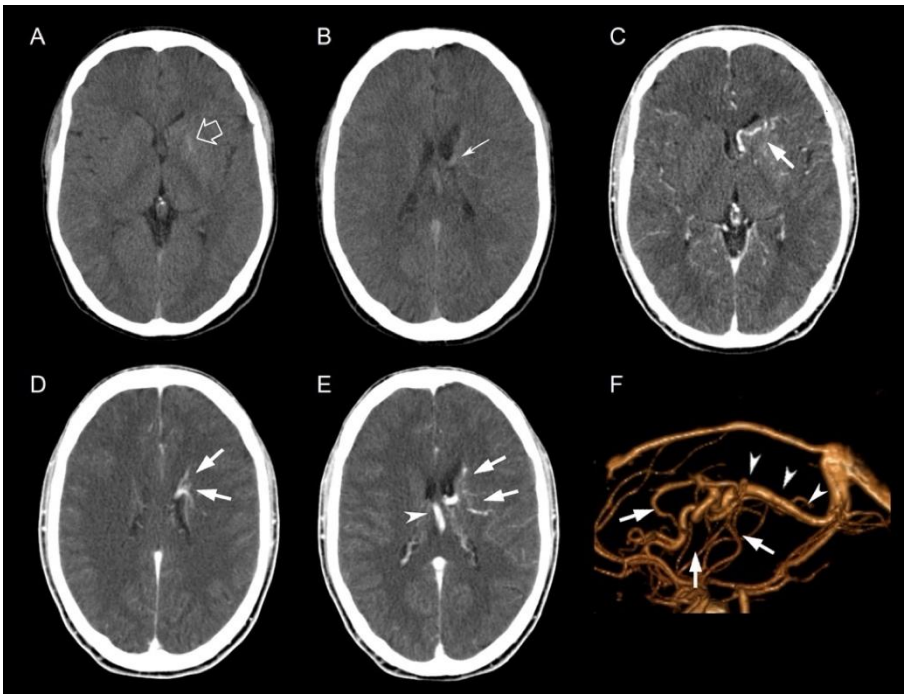

Fig. 1.3.3. Axial unenhanced head CT scan (A-B) obtained in a male teenager presenting with headaches demonstrates a subtle focal calcification in the left lenticular nucleus (o*pen white arrow*) as well as a small tubular structure projecting towards the left lateral ventricle (*thin white arrow*), suspected of a developmental venous anomaly (DVA). Axial CT venography (CTV) (C-E) confirms a lesion compatible with a DVA, characterized by presence of multiple venous channels in the left nucleo-capsular region and corona radiata with a *fan* or *caput medusa-like* shape (*white arrows*) converging towards a single, tortuous and dilated venous collector (*open white arrows*), that in turn drains into the deep venous system. Three-dimensional reformats of the CTV (F) better depict the angioarchitecture of the DVA.

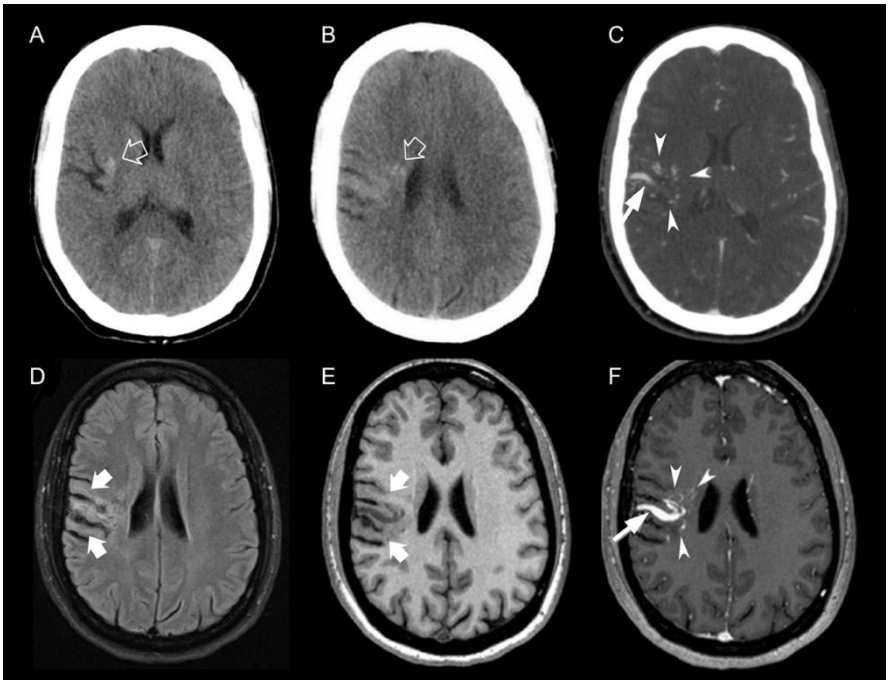

Fig. 1.3.4. Axial unenhanced (A,B) and contrast-enhanced (C) head CT scan as well as brain MRI including axial FLAIR (D), T1WI (E) and contrast-enhanced T1WI (F) brain MRI images obtained in a young female adult presenting with seizures reveal a focal area of calcification in the right external capsule and *corona radiata* (*open white arrows*) as well as multiple small tubular structures (*white arrowheads*) in the vicinity, draining towards a venous collector that appears to have a focal area of stenosis (*thin white arrows*), compatible with a developmental venous anomaly (DVA). There is also cortico-subcortical atrophy in the draining territory of the DVA with corresponding enlargement of the adjacent sulci and body of the right lateral ventricle as well as adjacent white matter FLAIR hyperintensity (*thick white arrows*).

MRI

Brain MRI is the primary non-invasive imaging method for DVA diagnosis and lesions are better recognized on postcontrast T1 weighted-imaging (WI), especially when 3 dimensional (3D) sequences are used [34, 36, 139] **(Fig 1.3.4 F and 1.3.5 A-D)**. The vast majority of DVA present medium to small size and drain a minor volume of the adjacent intracranial parenchyma. However, some patients present very large DVA, that may inclusively drain near an entire brain hemisphere in some rare instances [140–142]. Very tiny DVA can also occur and may be overlooked even on contrast-enhanced sequences if images are not examined carefully. In addition, DVA and/or associated CCM may be hidden or compressed by an adjacent acute ICH and a high index of suspicion should be present in those cases, especially in normotensive patients and atypical hematoma location.

Although the typical DVA features may also be detected on routine unenhanced T1WI and T2WI, the sensitivity of these sequences to this regard is overall low, especially if the lesions are not large [36, 139]. DVA are usually more conspicuous on GRE and SWI magnitude images than on T1WI and T2WI, due to presence of high amount of deoxyhemoglobin in the abnormal and slow flowing medullary and draining veins leading to associated *blooming effect* [139, 143] **(Fig 1.3.5 E-H)**. However, SWI-negative cases have been reported, some of these probably related with general anesthesia-related changes in brain hemodynamics [139, 143–145]. Overall, the sensitivity of SWI for DVA detection in pediatric cases has been estimated to be approximately 86% [139] and therefore this sequence has the potential to become a valid non-contrast alternative sequence for the diagnostic work up of DVA, especially when contrast injection is contraindicated. In addition to application of T2*WI techniques, higher field scanners including ultra-high-field MRI also improve the diagnosis of DVA [146, 147].

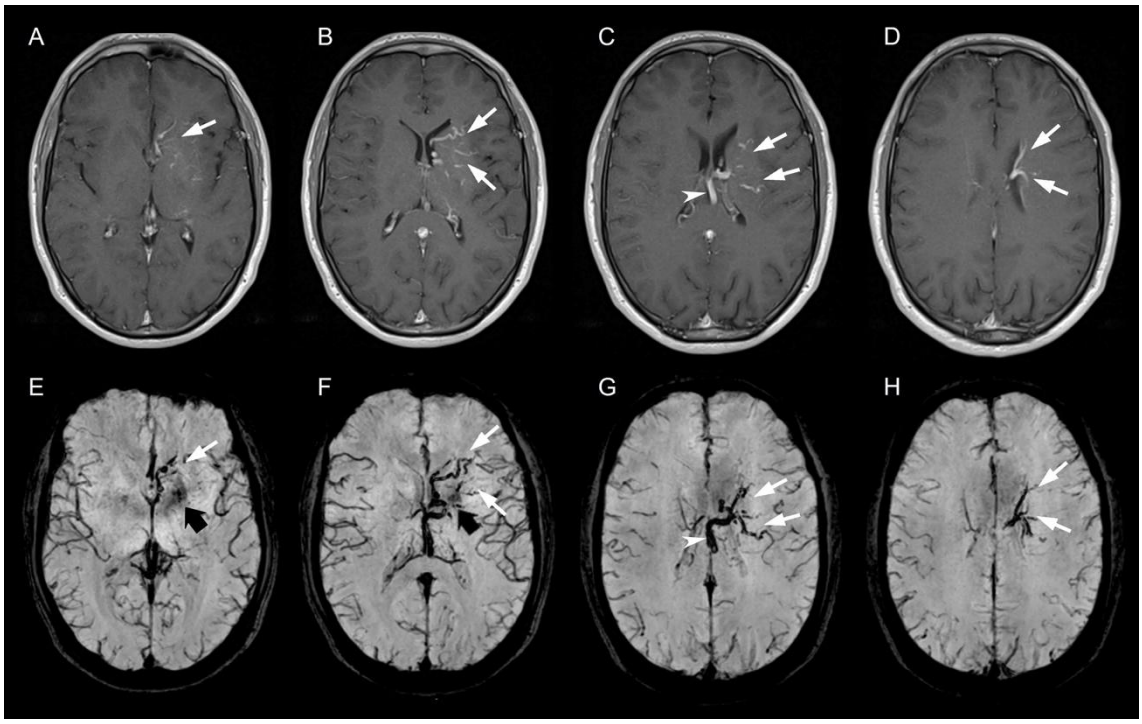

Fig. 1.3.5. Brain MRI including contrast-enhanced axial T1WI (A-D) images show the venous radicles (*white arrows*) and the venous collector (*white arrowhead*) of the developmental venous anomaly (DVA) previous presented on **Fig. 1.3.3**. The lesion is also well-defined in axial SWImagnitude images (E-H) (*white arrows* and *white arrowheads*). Note the small foci of susceptibility effect in the left globus pallidus (*thick black arrows*), corresponding to the area of calcification also demonstrated in the axial unenhanced CT images of **Fig. 1.3.3**.

According to the location of the convergence of the radicles with the collector vein, DVA can be classified as juxtacortical, subcortical and periventricular [34]. In turn, the collecting vein crosses a variable length of cerebral or cerebellar parenchyma to join either the deep or, more often, the superficial venous system, in some instances through an associated venous varix. Presence of multiple (≥ 2) collectors draining a single DVA can be detected in up to 10% of cases, occasionally with concurrent drainage into both the superficial and deep venous systems, although usually with predominance of one of the drainage pathways [33, 36, 137]. In some studies, multiple collectors have been associated with larger lesions and infratentorial location [36, 137]. Alternatively, multiple DVA may also drain into the same collector and a DVA can also drain arteriovenous lesions, including AVM or dAVF [38, 71].

In the setting of a DVA, radiologists should actively sought for an associated sporadic CCM (that can appear *de novo* over time as discussed above) within its draining territory especially in GRE/SWI sequences, as the latter are also highly sensitive for detection of these lesions in both adults and children [139]. As already discussed, identification of an adjacent CM is of importance as it increases the risk of a future hemorrhagic complication when compared to an isolated DVA [38, 148]. Although the imaging features of CCM will be extensively addressed in a subsequent

dedicated section, it is important to note that small foci of susceptibility effect in magnitude SWI images adjacent to the venous radicles of a DVA and not visible in other MRI sequences nor after gadolinium injection pose the differential diagnosis between CM Zabramski type IV, microhemorrhages and calcifications, and all of them may occur as a complication of DVA [139, 149]. Nevertheless, the latter can be usually distinguished from the remainder as foci of hyperintensity on SWI phase images in right-handed MR imaging systems or as hyperdense foci in head CT scans [11]. As previously presented, capillary telangiectasias can also be detected in adjacent to DVA, in some instances in the context of a neurovascular triad, and are usually characterized on MRI by isointensity on T1WI and T2WI, increased susceptibility effect on GRE/SWI and a mild *brush* or *stipple-like* enhancement between normal brain parenchyma on postcontrast T1WI [85–88] **(Fig. 1.3.6)**.

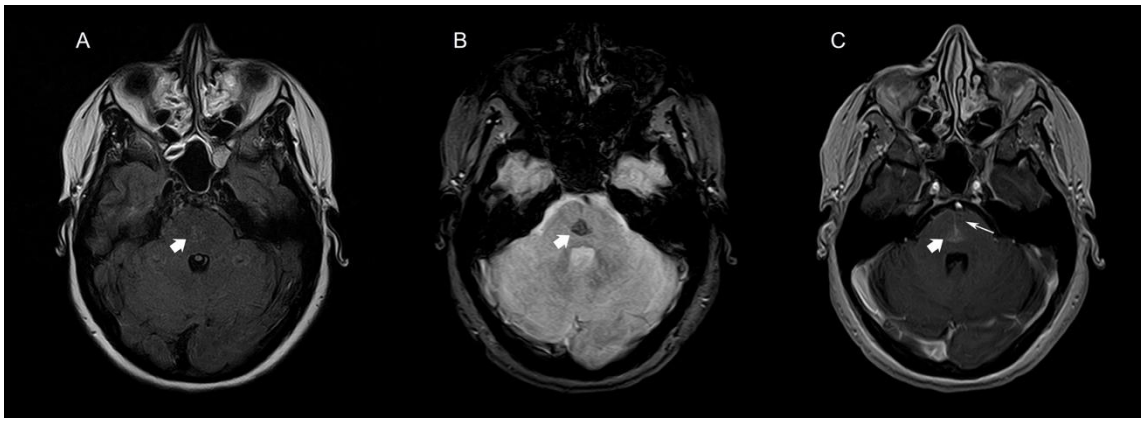

Fig. 1.3.6. Brain MRI including axial FLAIR (A), SWI (B) and contrast-enhanced T1WI (C) images obtained in a male teenager depicts a very subtle area of FLAIR hyperintensity within the pons, with marked susceptibility effect and faint enhancement after gadolinium injection (*thick white arrows*), compatible with a capillary telangiectasia. Also note an adjacent venous collector draining anteriorly, corresponding to an associated developmental venous anomaly (*thin white arrow*).

Interestingly, white matter (WM) signal abnormalities characterized by high T2WI/Fluid-attenuated inversion recovery (FLAIR) signal intensity have also been reported in some patients in the vicinity of a DVA [19, 20, 37, 137, 149–152] **(Fig. 1.3.4 D-E)**. Their prevalence is variably reported in the literature (ranging from 5% to near 50% of cases), with an apparent bimodal distribution peaking in younger children and older adults [19, 20, 37, 137, 149–152]. In addition, WM signal changes have been more commonly described in deeply localized DVA [150] as well as in patients with associated hypointense foci on GRE/SWI sequences [149]. Moreover, one study reported that WM signal changes occur more frequently in DVA with higher susceptibility values in the respective draining veins identified using Quantitative Susceptibility Mapping

(QSM), indicating an increased oxygen extraction fraction and therefore venous stasis/hypertension in those lesions [152]. The pathologic substract of DVA-related WM signal abnormalities is still a matter of debate and may include edema, delayed demyelination, demyelination, loss of oligodendrocytes, and gliosis or any combination of them [19, 20, 37, 137, 149–152].

High-resolution conventional MRI (especially isotropic 3D T1 sequences) should be scrutinized aiming to detect cortical abnormalities (most commonly polymicrogyria) in the draining territory of a DVA, especially in patients presenting with both DVA and refractory seizures [3, 62, 63]. In addition, subtle, focal parenchymal atrophy in the vicinity of a DVA can also be better appreciated in this high-resolution sequences.

In case of subjects with suspected or confirmed CVMS and/or other systemic syndrome known to be associated with DVA (see above), a special effort to identify these lesions on neuroimaging should be made. Conversely, if multiple DVA are detected in one patient, careful review of the remainder parenchyma, intracranial dural and cavernous sinuses as well as head and neck compartments is warranted, in order to try to depict any associated anomaly that can support the diagnosis of the subjacent disorder [95–97]. In particular, if multiple DVA are detected in a child together with a remote infiltrative lesion, the diagnosis of CMMRDS should be considered [49–51].

Angiographic techniques

Although DSA remains the *gold standard* for the diagnosis of DVA, it is generally accepted that angiographic techniques are not required for the study of DVA with characteristic morphology on structural imaging and without associated complications. Opposingly, whenever atypical DVA imaging findings or associated clinical and/or imaging abnormalities are detected (especially in the context of an ICH, angiographic studies including DSA can add diagnostic information, namely confirming the DVA and ruling out possible causes of increased inflow or reduced outflow [38, 39, 75]. Indeed, in normal circumstances, DVA opacify at the same time as the normal veins and dural venous sinuses, being easily identified in the early and mid-venous phase of angiograms due to the already mentioned characteristic *caput medusae* angioarchitecture. However, pathological signs of venous outflow obstruction or thrombosis may be detected in acutely complicated DVA cases, including prolonged transition and venous stasis and missing central venous collector, respectively [153]. In addition, signs of arteriovenous shunting within the radicles of the DVA itself (corresponding to the previously discussed TVA) with early DVA venous filling or as a separated lesion with a nidal configuration eventually draining towards the DVA may also be identified [39, 75]. Nevertheless, as the flow is lower in TVA than in AVM,

venous opacification in the former is not detected until the capillary phase and signs of high-flow arteriopathy are typically absent [71].

Follow-up imaging

The role of follow-up MRI evaluation of children or adults with DVA is currently not established but in case of a single, incidentally detected DVA without associated CCM, routine longitudinal neuroimaging evaluation is generally not recommended. Nevertheless, genesis of a new CM **(Fig. 1.3.7)** and/or progressive changes in the adjacent parenchymal may occur over time in a subset of patients harbouring these lesions, as previously referred.

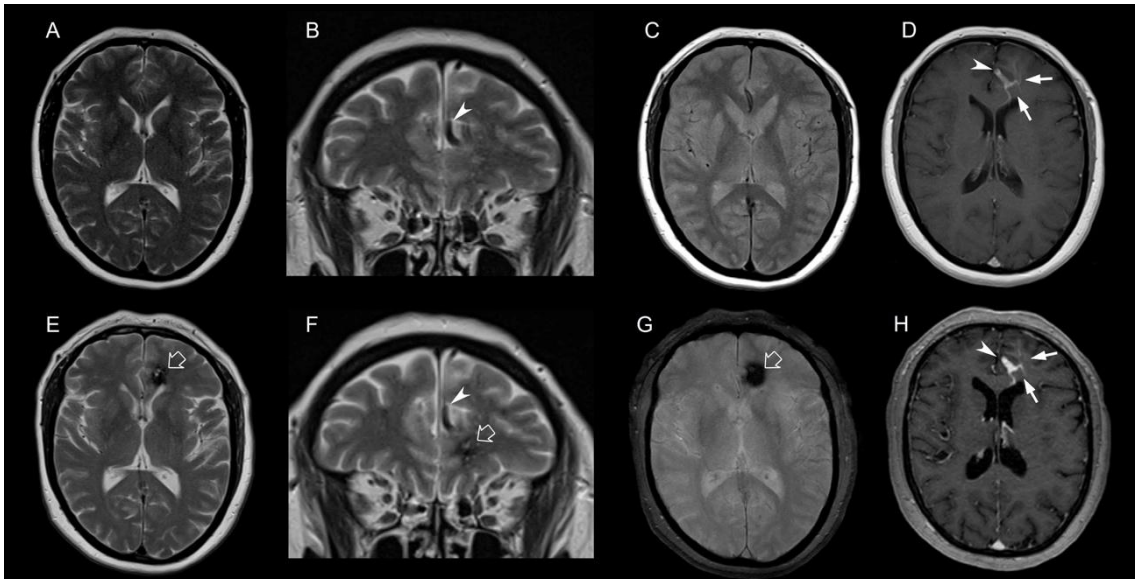

Fig. 1.3.7. Brain MRI including axial (A) and coronal (B) T2WI, axial T2* (C) and axial contrast-enhanced T1WI (D) images obtained in a middle-aged female patient presenting with headaches reveals multiple venous channels with a fan-like morphology in the left frontal region (white arrows) draining towards a venous collector (*white arrowheads*), compatible with a developmental venous anomaly (DVA). Follow-up brain MRI of the same patient performed 10 years later including axial (E) and coronal (F) T2WI, axial T2* (G) and axial contrast-enhanced T1WI (H) images depicts *de novo* formation of a sporadic cavernous malformation (*white open arrow*) in the draining territory of the already known DVA (*white arrows* and *arrowheads*), that in turn maintains similar imaging features.

On the other side, in case of a DVA with symptomatic presentation and/or development of new neurological manifestations over time, neuroimaging follow-up should be considered, aiming to detect further complications and the subjacent pathomechanism.

Finally, although *de novo* formation of a DVA has never been reported, it is important to be aware that these lesions may show subtle longitudinal imaging changes especially in the early

years of life, probably due to progressive maturation of the vascular system and the CNS [154, 155].

Advanced imaging techniques

Hemodynamic changes (including increased cerebral blood flow and volume, mean transit time, and maximum time to peak), have been widely reported in the intracranial parenchyma drained by a DVA in both CT and MR perfusion techniques, even without associated imaging changes on conventional MRI and/or clinical manifestations [75, 156–160]. Adjacent parenchymal metabolic abnormalities have been also found in most DVA using Fluorodeoxyglucose-Positron Emission Tomography Imaging, being more commonly represented by hypometabolism [161, 162].

On the other side, DVA can display very similar features to neural signal patterns in resting state functional MRI (fMRI) and constitute a potential source of bias in this technique, especially when superficially located [163]. Therefore, awareness of their presence and potential influence in resting state fMRI signal is important for the correct interpretation of results obtained with this technique.

Clinical management and treatment

As previously mentioned, most DVA follow a benign clinical course and do not require specific surgical or medical treatment [35]. In particular, the risk of hemorrhage after the first presentation appears to be very low, ranging from 0% to 1.28% per year [35].

In the rare occasions in which children or adults present with neurological signs and symptoms potentially attributable to flow imbalance within a DVA (due to venous outflow obstruction/stenosis or presence of microshunts) and/or to coexistence of an adjacent vascular lesion such as a CCM, conservative management is still recommended as an initial strategy [39].

In the particular setting of a thrombosed DVA, most authors suggest that it should be managed as cortical or dural venous sinus thrombosis, with anti-coagulation and eventually steroids, although presence of an adjacent CCM may increase the risk of bleeding (reviewed in [164]). On the other side, in case of DVA-related seizures, images should be carefully evaluated aiming to identify the exact epileptogenic mechanism and patients treated with antiepileptic drugs (AED) and/or other appropriate treatment dedicated to the subjacent cause [39].

Only in case of persistent and/or serious manifestations, a more interventive approach should be attempted, tailored according to the specific signs and/or symptoms and the subjacent pathomechanism. If microsurgical management of a DVA-related complication is required, namely due to a compressive ICH or edema, particular care must be taken to save the DVA

collecting vein aiming to preserve normal venous outflow pathways and avoid a venous infarction. The same principle applies to the treatment of TVA, CCM associated with a DVA or an AVM draining towards a DVA, as the latter are considered *"no touch lesions"* [38, 39, 71]. More recently, it has been described an innovative rescue endovascular approach through transvenous stenting to treat stenosis of the venous collector in an adult with a symptomatic DVA that did not respond to medical treatment [165].

Lastly, surgical options for mechanical compression related to a DVA are more consensual, such as microvascular decompression or percutaneous rhizotomy in case of cranial neuropathy or conventional cerebrospinal fluid diversion (including endoscopic third ventriculostomy or ventricular shunting) in case of obstructive hydrocephalus [38, 39].

1.4. CAVERNOUS MALFORMATIONS

Introduction

CM are non-shunting, low-flow venous malformations with heterogeneous clinical presentations and imaging phenotypes as well as diverse progression over time [1]. Importantly, the term *cavernous hemangioma* should not be used since hemangiomas are true proliferating vascular neoplasms, while CM are not [1].

This subtype of CVM usually occurs sporadically as a solitary lesion, but it may also have a familial trait, most commonly under the form of multiple lesions with a scattered distribution in the brain parenchyma and/or other tissues. Moreover, CM may also be caused by effects of radiation therapy [166, 167], but in this review we will focus in the other two most common subtypes.

CM may be located anywhere along the neuroaxis, including the intracranial parenchyma and the spinal cord (SCCM) [168] and their relative distribution is proportional to the overall tissue volume. More specifically, supratentorial lesions occur in 65–80% of cases, mainly within the cerebral hemispheres, but also in the nucleocapsular and thalamic region. On the other side, infratentorial lesions may involve either the brainstem (especially the pons) or the cerebellum [169], with the former being associated with the worst outcomes as it will be described in more detail below. A variable percentage of patients with SCCM may harbor a similar intracranial lesion [170–172]. Less commonly, the inverse phenomenon may also occur, especially in the setting of multiple CCM, and both cases are more frequently seen in the familial form of the disease [173]. Apart from the brain and spinal cord location, CM may also be present in other tissues, such as the ventricular system, cranial nerves, cavernous sinuses, orbit/retina, skin, bones and solid organs, also predominantly in familial forms [174–176].

Importantly, although CM may remain stable over time, they are considered dynamic lesions and often grow or reduce size (and even disappear) in longitudinal assessments and formation of new lesions may also occur [177].

Epidemiology

The exact prevalence of CCM and SCCM is unknown as many patients are asymptomatic and MRI and/or biopsy are required for the diagnosis. In recent years, due to more widespread availability of MRI and improvement of technical aspects, both lesions have been more commonly identified in clinical practice and consequently more often reported in the literature [178].

Available works estimate that CCM constitute the second most common subtype of CVM after DVA (about 10%-20% of all cases), occurring in 0.5-1% of the general population [179, 180].

The prevalence of SCCM remains more controversial. Indeed, these lesions have been historically considered exceptionally rare although recent data suggest that they are more common than previously considered, representing up to 5% of neural CM [173].

Both CCM and SCCM have been described in all race and ethnicities. However, familial cases are more frequently reported in Hispanic-Americans of south western regions of the United States of America as well as in Ashkenazi Jewish due to founder mutations in two of the causative genes, more specifically in *CCM1* (also known as *Common Hispanic Mutation*) and *CCM2* genes, respectively [181, 182]. Another less common founder CCM1 mutation has been detected in probands of Sardinian lineage [183].

On the other side, although CM may be detected at any age and even pre-prenatally, most cases present in adults between the third and fourth decades of life [168]. Overall, it is estimated that ~25% of all CM are identified during childhood, accounting for 5-10% of all causes of acute intracranial hemorrhage in children [39]. In pediatric age, median age at diagnosis occurs at approximately 10 years of age [184], with onset usually earlier in children FCCM than in those with the sporadic form of the disease [185].

Finally, most research studies have failed to demonstrate a significant difference between sexes in the prevalence of CM.

Pathology and immunohistochemistry

CM are *mulberry-like* malformations of the microvasculature composed of abnormally enlarged, multilobulated, and leaky blood-filled sinusoidal spaces devoid of mature vascular walls included in a dense collagen matrix and without intervening neural tissue [186–188].

In particular, CM have thin, single-layered and dysregulated endothelial walls that lack pericytes, elastic tissue and vascular smooth muscle cells [186–188]. Indeed, they present defective endothelial tight and adherent cell-cell junctions as well as dysfunctional blood–brain barrier leading to chronic deposition of blood breakdown products, including hemosiderin and non-heme, often with gliotic changes and/or edema in the surrounding brain tissue [187–189]. Moreover, CM are characterized by intralesional thrombi of varying ages as well as areas of calcification and recanalization [186, 188].

On the other side, there is often an associated immune response characterized by inflammatory cell infiltration, selective synthesis of IgG, and deposition of immune complexes and complement proteins [190, 191].

Genetics

As previously mentioned, CM may be sporadic or familial, with the latter subtype representing up to 20% of cases [185] and recent breakthroughs suggest that they tend to present distinct genetic trajectories [60, 192–197].

Indeed, according to the Knudsonian two-hit hypothesis, the pathogenesis of both familial and sporadic CCM formation begins with an inherited or somatic mutation, respectively, followed by somatic mutations resulting in lesion genesis and growth [60, 198, 199]. This means that loss of one allele in an endothelial cell due to a germline or somatic mutation in one given culprit gene (first hit) needs to be followed by the occurrence of a somatic mutation in the other allele of the same gene (second hit). Nevertheless, most FCCM cases are thought to be caused by a germline loss-of-function mutation in one of the *CCM1-3* genes, followed by a somatic mutation in the same gene at a local level resulting in bi-allelic loss-of-function of *CM*. These second mutations may occur in different anatomical locations, leading to multiple CM typical of FCCM [60, 193]. On the other side, the main genetic pathway leading to formation of sporadic CCM appears to be the acquisition of two somatic gain-of-function mutations in the *mitogen-activated protein kinase kinase kinase 3* (*MAP3K3)* gene [60, 193].

Despite these diverse preferential genetic trajectories, in a small percentage of cases sporadic CM develop due to acquisition of two somatic loss-of-function mutations in the *CCM1-3* genes involved in FCCM and, conversely, FCCM can also be rarely caused by two gain-of-function mutations involving the *MAP3K3* gene [60, 193]. Taken together, these findings suggest that both gain-of-function pathogenic variants in *MAP3K3* and loss-of-function pathogenic variants in *CCM1-3* genes can initiate CM formation and therefore have similar functional roles. This observation is supported by the fact that the heterotrimeric CCM complex is a direct inhibitor of the MAP3K3 kinase. A recent study by Huo *et al* including children and adults with sporadic CCM has shown that lesions harboring somatic *MAP3K3* mutations were associated with a lower risk of symptomatic hemorrhagic events, less pronounced destruction of the blood-brain barrier, as well as reduced concentrations of local anticoagulant molecule in the endothelium when compared to lesions with somatic *CCM1-3* mutations [192].

Interestingly, it appears that in both familial and sporadic CM cases, the mutually exclusive biallelic mutations on either *MAP3K3* or *CCM1-3* genes are only able to cause quiescent lesions. Indeed, recent data suggests that all CM subtypes require additional somatic gain-of-function mutation(s) (acquired either before or after the *CCM1-3* or *MAP3K3* mutations) in the *PIK3CA* gene in order to grow and become symptomatic [60, 193]. Moreover, as addressed in the DVA section of the present thesis, *PIKC3A* but not *MAP3K3* mutations are also found in DVA adjacent

to sporadic CM [60, 193]. Therefore, DVA may function as intermediate lesions, being a genetic primer for CM [60, 193].

Pathophysiology

The mechanisms that lead to CM development are complex and not yet fully elucidated, although significant multidisciplinary research progress on this subject has been made in the last decade. Indeed, diverse recent studies have shed some light into the cellular events and molecular signal cascades controlled by the proteins encoded by the *CCM1-3* genes (whether acting as a trimeric complex or as single effectors) and the biological consequences of their impairment in affected endothelial cells and adjacent environment (reviewed in [200, 201]). Importantly, the growing knowledge of the underlying processes involved in CM formation provides new options for the development of novel patient-tailored pharmacological therapies targeting CM (reviewed in [202]).

Although a comprehensive review of each of the involved pathobiological mechanisms goes beyond the scope of this clinically oriented thesis, an overview of the main events is important for the understanding of CM. More specifically, it has been shown that CM pathogenesis is associated with endothelial-to-mesenchymal transition (EndMT) [203, 204], angiogenesis [205–207], impaired autophagy [208], altered reactive oxygen species homeostasis and enhanced sensitivity to oxidative stress [209–211], increased exocytosis [212], abnormal inflammatory and immune responses [210, 213–215] and dysregulated hemostasis and immunothrombosis [216]. An abnormal crosstalk between the CM endothelium and the surrounding pericytes and astrocytes also appears to contribute to the neurovascular dysfunction during lesion development [206, 213, 217]. Moreover, some research papers have also suggested a *gut-brain axis* in the genesis of CM, influenced by the microbiome and disruption of the gut barrier [218–221].

There are multiple dysregulated intracellular signaling cascades subjacent to the above mentioned pathological phenomena, including increased activation of the 1) RhoA/Rho kinase (ROCK), 2) MAP3K3/p38 mitogen-activated protein kinase (MAPK), 3) extracellular-signal-regulated kinase (ERK)/Krüppel-like factor 2 and 4 (KLF2/KLF4), 4) transform growth factor β (TGF-β)/bone morphogenetic protein (BMP), 5) Wnt/β-catenin, 6) delta-like protein 4 (DDL4)/notch and 7) ephrin receptor B4 (EphB4) pathways (reviewed in [193, 200, 222]). In turn, the MAP3K3 signaling can be upregulated by lipopolysaccharide derived from gram negative bacteria in the gut microbiome through the Toll-like Receptor 4 (TLR4) [193, 200, 222]. More recently, it has also been shown that CCM also present impaired retinoid acid signaling [223].

There is also increasing evidence that dysregulation of micro ribonucleic acids (micro-RNA, ie, small strands of non-coding RNA of around 20 nucleotides that regulate gene expression by binding completely or partially to their respective complementary sequences) involved in angiogenesis may also have a role in the CM pathogenesis, namely contributing to genesis, maturation and/or acute symptomatic hemorrhage [224–227]. More specifically, Kar *et al* identified numerous dysregulated micro-RNA in the brainstem of CCM patients, five of which being more significant (namely let-7b-5p, miR-361-5p, miR-370-3p, miR-181a-2-3p, and miR-95-3p) [224]. In addition, differentially expressed plasma circulating micro-RNA, in isolation or combined with others can be also detected in CM patients and may become a potential diagnostic and/or prognostic biomarkers of this disorder [226, 227].

Numerous other plasma molecules as well as polymorphisms in response gene pathways (namely involved in dysregulated angiogenesis, endothelial permeability, inflammatory/immune processes) have been mechanistically linked to CM and also constitute biomarker candidates in this disorder [226, 228–231], but their exact role in both children and adults with sporadic or familial disease, needs to be further explored.

Clinical presentation and natural history

CCM

Overview

Up to 50% of CCM cases are asymptomatic and discovered incidentally in imaging studies performed for unrelated reasons. This rate has increased in the last decades due to a more widespread use of MRI for various neurological symptoms. Silent CCM may be also identified in the context of dedicated imaging screening due to a confirmed or suspected case of FCCM in the individual or in a first degree relative [232].

When neurological manifestations occur, they are closely related to the location and size of the lesion(s), and usually include epileptic seizures, FND, impaired consciousness and/or headaches in both children and adults [233, 234]. Occasionally, patients can present with movement disorders (dystonia, hemichorea, hemiparkinsonism, hemichorea-hemiballism), torticollis or neuralgia [235–238]. In young children with giant CCM or CCM-associated hydrocephalus, bulging fontanelles and/or increased head circumference as well as irritability, progressive lethargy and gaze palsy may also occur [239]. These neurologic manifestations may in turn be associated or not with signs of acute ICH, as defined by consensus criteria published in 2008 by a group of investigators from the previous *Angioma Alliance Scientific Advisory Board* and that will be addressed subsequently in more detail [240].

After presentation, the clinical behavior of individual CCM lesions remains widely variable and unpredictable in both children and adults, ranging from a benign clinical course due to lesion regression or overall stability to a progressive clinical evolution with repetitive hemorrhages and neurological deterioration [241]. Nevertheless, decreased quality of life is common in adult patients with CCM [244, 245] and may be even present without associated functional impairment or neurological symptoms [246]. Unfortunately, there are no available studies in the literature addressing patient reported outcomes in pediatric-only cohorts with CCM treated either conservatively or surgically, including health-related measures of quality of life (HRQOL).

CCM presenting with symptomatic hemorrhage

According to the 2008 definitions and reporting standards of hemorrhage from CCM published by a group of investigators from the *Angioma Alliance Scientific Advisory Board*, in order to consider a neurological event as a CCM-related symptomatic hemorrhage, the signs and/or symptoms need to be anatomically related with a CCM and the acute hemorrhage confirmed by radiological, pathological, surgical, or rarely only cerebrospinal fluid evidence [240]. These guidelines not only standardize the definition of symptomatic ICH, but also the appropriate type and timing of the necessary investigations in the setting of new neurological symptoms in patients with CCM (see Imaging section) [240].

Early CCM natural history studies calculating ICH rates have reported a wide range of frequencies, partly due to differences in hemorrhage definitions prior to 2008, but also diverse study designs and populations, different statistical methods of risk calculation (lifetime hemorrhage rate vs prospective hemorrhage rate) as well as mixed analysis of combined, first, or recurrent ICH [233, 242].

Since 2008, numerous contemporary studies have been published on the topic as well as two meta-analysis (one including aggregate data and the other individual patient data), confirming that among CCM cases identified incidentally in the general population, the risk of first symptomatic hemorrhage is overall low, especially in non-brainstem locations [232, 233, 242–245]. Nevertheless, initial CCM presentation with symptomatic hemorrhage is one of the major risk factors for a subsequent hemorrhage in both children and adults [184, 233, 242, 246]. Indeed, the re-hemorrhage rate is consistently greater than the risk of a first event especially within 2-3 years after the index hemorrhage and declining thereafter [184, 233, 242, 244, 247], and this phenomenon has been named *temporal clustering* [248].

In addition, CCM location in the brainstem is also a well-known independent risk factor for symptomatic rehemorrhage in all age groups [83, 233, 242]. However, it remains unclear if brainstem CCM are indeed biologically more prone to repetitive bleeding events or if

hemorrhage in these lesions is more likely to become symptomatic than in supratentorial lesions due to the densely packed, complex and highly eloquent nature of the brainstem.

Some authors have reported an increased symptomatic bleeding rate in children with CCM when compared to adults [18, 249], but these findings were not confirmed in other studies [15, 16]. Other possible risk factors for hemorrhage include female sex, multiplicity/familial history [250], Zabramski type [247, 251, 252], associated DVA [83, 84, 184, 253, 254] and coexistence of cardiovascular risk factors (namely obesity) [255, 256].

Finally, mortality after a first symptomatic CCM bleeding is estimated to be ~2% [242, 257] while reports of overall morbidity rate are more heterogeneous, ranging from 26% to 61% [242, 257].

As disease-specific scales are yet to be developed for patients with CCM, utilization of other well-known scales to measure impairment or HRQOL have been recommended, namely the National Institute of Health Stroke Scale, the modified Rankin Scale or the Short Form 12, the Short Form 36 (www.sf-36.org) and the EQ-5D (www. euroqol.org) [243].

CCM presenting with epilepsy and/or focal neurologic deficit

In most published cohorts, epileptic seizures represent one of the most common clinical presentations of both children and adults with CCM (ranging between 20.8-70% of cases). In addition, approximately up to 40% of CCM patients develop medically refractory epilepsy at follow-up [258]. Inversely, it is estimated that approximately 4% of all medically refractory epilepsies are related to a subjacent CCM [259].

Although the occurrence of ICH itself may lead to epileptic seizures, CCM can cause seizures without acute or prior symptomatic ICH [260] and CCM even appear to be amongst the most epileptogenic mass lesions [261]. The mechanism of CCM-induced epilepsy is still not fully understood. Nevertheless, as CCM do not contain neuronal tissue they cannot themselves be the ictal-onset zone or epileptogenic zone, and the latter is probably represented by the peripheral gliosis stained with blood degradation products [262].

According to a consensus paper released by the International League Against Epilepsy (ILAE), whenever epilepsy occurs in a patient with at least one CCM, it may be classified as definitive cavernoma-related epilepsy (CRE), probable CRE or epilepsy unrelated to the CCM [262], as systematized in **Table 1.4.1**.

Table 1.4.1. Definition of cavernoma-related epilepsy according to the International League Against Epilepsy.

Term	Definition
Definite CRE	≥ 1 CCM + epilepsy with evidence of a seizure onset zone in the vicinity of the CCM
Probable CRE	≥ 1 CCM + focal epilepsy ipsilateral as the CCM but not necessarily in its immediate vicinity + exclusion of other causes of epilepsy
CCM unrelated to epilepsy	≥ 1 CCM + epilepsy not causally related

Legend: CCM- Cerebral cavernous malformation, CRE- Cavernoma related epilepsy. Adapted from [253].

CRE is of particular concern in pediatric patients due to the known negative effect of refractory seizures in the developing brain [263] and therefore expedited management is recommended [234].

Several risk factors have been reported for CRE, with location being the most consensual one. Indeed, supratentorial and cortical-based CCM, especially whenever located in the temporal lobe, are more commonly associated with CRE than lesions in other locations [262, 264–266].

The association between total lesion burden and CRE is also consistently identified in contemporary studies [260, 265, 266]. Accordingly, both adult and pediatric individuals with FCCM have been shown to have a particularly high seizure frequency, reaching a cumulative incidence during childhood and by age 80 years of ~20% and ~60%, respectively [267]. Moreover, in cohorts including only familial cases, patients with increased lesion counts also appear to be at a higher risk of seizures [267]. On the other side, pathogenic variants in CCM3 were also more commonly associated with seizures [267] probably because patients harboring mutations in this gene also present a significantly higher number of CCM lesions when compared with other FCCM genes [268–271].

Finally, other less established putative risk factors for CRE include size of the lesion and presence of hemosiderin rim [262].

A risk stratification scoring system (BLED2 score) has been recently developed for adults presenting with seizures or FND, with higher values predicting a higher risk of prospective neurological events [272]. Importantly, after a first seizure occurs in a general patient harboring a CCM, the risk of developing a second episode/epilepsy within the next five years is very high, reaching 94% [260]. In addition, although CCM patients with other type of clinical presentation may also develop seizures during follow-up, the probability is relatively low, with an overall 5-year risk to develop a first-ever seizure of 4% and 6% in case of incidental detection or presentation with ICH or FND, respectively [260].

SCCM

In a similar fashion to their intracranial counterparts, SCCM can be detected incidentally or present with associated signs and symptoms. Sensory or motor disturbances are the most frequently reported neurological abnormalities (~60% of cases) followed by pain (30%) and bladder/bowl dysfunction (20%) or a combination of these [172, 273]. When considering clinical presentation and progression over time, SCCM are commonly divided according to the Ogilvy *et al* classification scheme [274], that includes 5 subtypes (denominated A-E) as presented in **Table 1.4.2.**

Table 1.4.2. Ogilvy classification of presentation and natural history of spinal cord cavernous malformations.

Type of SCCM	Definition
A	Discrete episodes of neurological deterioration with varying degrees of recovery between episodes
B	Slow progression of neurological decline
C	Acute onset of symptoms with rapid decline
D	Acute onset of mild symptoms with subsequent gradual decline lasting weeks to months
E	Asymptomatic incidentally detected lesions

Legend: SCCM- Spinal cord cavernous malformation. Adapted from [274].

The natural history of untreated SCCM remains relatively unclear, because of the relative rarity of these lesions, scarce information concerning long-term clinical outcomes, heterogeneity of definition of hemorrhage as well as diverse methodologies for calculation of risk estimates after initial diagnosis. However, recent studies including meta-analysis confirms that the prognosis of SCCM tends to be poor and clinically progressive [273]. This more aggressive behavior is probably related to the intrinsic anatomy and size of the spinal cord, leading to greater susceptibility of the tightly compacted eloquent cord structures to mass effect/small hemorrhages.

Initial studies using lifetime risk estimates reported annual hemorrhagic rates of SCCM ranging from 1.4% to 6.8% per person-year (reviewed in [275]). Nevertheless, this statistical approach does not incorporate the previously described *temporal clustering pattern* of CM-related hemorrhage, probably leading to an underestimation of results [275]. Indeed, more contemporary studies point towards values higher than the previously reported range, reaching up to 8.5% per person-year [275]. In addition, SCCM in the pediatric population appear to be more aggressive than in adults, with several authors reporting higher annual symptomatic hemorrhage and rehemorrhage rates of SCCM during childhood than in the adult life [275–277].

Importantly, prior hemorrhage is also the strongest risk factor of subsequent hemorrhage in cohorts of patients with SCCM [171, 275]. On the other side, new SCCM-related symptomatic hemorrhagic events during follow-up are significantly associated with unfavorable functional outcomes [275] and the probability of full recovery declines with each SCCM-related bleeding event [278]. Presence of Zabramski type I lesions, large size lesion, sub-arachnoid hemorrhage, and extent hemosiderin involvement in the initial spine MRI as well as presentation with motor dysfunction also appear to predict hemorrhagic events during follow-up and/or bad outcome in affected patients [275, 279].

Association with pathologies and/or syndromes

Familial cerebral cavernous malformation syndrome

FCCM belongs to the group of rare diseases, with an estimated prevalence of 1/3000 to 1/3800 persons in screening exome sequencing databases [280]. It is currently considered a progressive systemic disease characterized by the presence of multiple CM in diverse tissues, caused initially by germline, autosomal dominantly inherited loss-of-function heterozygous pathogenic variants in one of three protein-encoding genes that form a heterotrimeric complex (the CCM signaling complex) involved in maintenance of endothelial integrity: *CCM1* (KRIT1, OMIM * 604214), *CCM2* (*Malcavernin*, OMIM * 607929), and *CCM3* (*PDCD10*, OMIM* 609118) (reviewed in [60, 193, 200, 201]). In addition, as previously mentioned, each gene product is a multi-domain adaptor protein, which interacts with numerous binding molecules, scaffolding proteins, and kinases and therefore participates in several different signaling pathways, through which regulates numerous cellular processes. Importantly, FCCM presents variable expressivity, including high inter- and intrafamilial phenotypic variability and therefore different types of manifestations with variable degrees of severity are common, even in members of the same family. Moreover, clinical penetrance is incomplete, with values as low as 63% for *CCM3* (reviewed in [200, 201]). Therefore, genetic variants and environmental factors are likely important modifiers of CM pathogenesis [229]. A summary of the main features of the responsible genes and associated proteins of FCCM are presented in **Table 1.4.3.**

Table 1.4.3. Familial cavernous malformation syndrome: genes and related proteins.

Gene	Locus	Protein	Penetrance	Pathogenic variants
CCM1	7q21.2	KRIT1 736aa 84 kDa	88%	>300 mutations +++ frameshift, nonsense, missense, and splice site sequence variants Rare insertions and deletions
CCM2	7p13	Malcavernin 444 aa 48 kDa	70% (previously described as 100%)	>90 mutations +++ missense, nonsense, frameshift, and splice site variants Deletions and insertions not uncommon
CCM3	3q26.1	PDCD10 212 aa 25 kDa	63%	>70 mutations

Legend: aa- aminoacids, kDA- kilodaltons, KRIT1- Krev interaction trapped protein 1, PDCD10- Programmed cell death 10.

The diagnosis of FCCM is usually made based on the presence of ≥ 1 CCM or SCCM associated with a positive family history (defined as presence of ≥ 1 known first or second-degree relative with a proven CM or a confirmed *CCM1-3* pathogenic variant) and/or identification of a pathogenic variant in one of the *CCM1-3* genes in the proband [281]. Adequate inclusion criteria for a diagnostic molecular genetic testing of *CCM* carriers include either positive family history or presence of multiple CCM without associated DVA nor prior history of brain radiation [234]. Genetic screening should include the analysis of all coding exons and exon/intron junctions followed by sequencing and deletion/duplication testing through sequencing and copy number analysis of the three target genes of germline deoxyribonucleic acid (DNA) extracted from blood and complementary DNA analysis, in order to assure high diagnostic accuracy [201, 280]. When stringent criteria are used together with appropriate genetic testing, detection rate is reported to be >75% (usually reaching ~90% of cases) [282], with more than 300 different *CCM1-3* pathogenic variants identified to date including point mutations, deletions, and duplications [201, 283]. However, the exact type of mutation within the same *CCM1-3* gene does not have a significant impact on disease severity [193].

The existence of a possible fourth gene harboring germline mutations in FCCM patients that lack any identifiable mutation in *CCM1-3* remains controversial, but so far it appears unlikely as no new genes have been confirmed since 2005 [280]. More probably, those apparently negative mutation patients present pathogenic variants in one of the three known *CCM* genes that remain undetected using common genetic diagnostic methods (including variants outside the screened exonic regions as well as deep intron variants, genomic inversions, or copy number neutral

genomic rearrangements). Accordingly, the mutation detection rate may reach near 100% if more extensive molecular genetic analyses are also performed, including whole exome or whole genome sequencing [201, 280, 284, 285].

Interestingly, a recent study has shown that a combination of plasma levels of micro-RNA and circulating proteins improves the diagnostic accuracy of FCCM in human subjects to 95% and may become a translatable circulating biomarker of this genetic disorder [227].

In mixed-age cohorts, pathogenic variants in *CCM1*, *CCM2*, and *CCM3* represent 60–65%, 20%, and 10% of FCCM cases, respectively. However, the percentage of *CCM3* mutations in pediatric only cohorts is usually higher, reaching 15-20% of cases. Indeed, the few phenotype-genotype correlations published so far support an earlier and more severe disease presentation (including higher lesion burden) in patients harboring pathogenic variants in *CCM3* compared to other genotypes, probably due to the exclusive role of *CCM3* in the gut endothelium, as described above [219, 268–271]. In addition, *CCM3* genotype has been associated with intracranial extra-axial expansile lesions that resemble meningiomas as well as scoliosis [268–271], while cutaneous CM are more often described in patients with pathogenic variants in *CCM1* [286].

On the other side, *CCM3* appears to be more prone to *de novo* mutations than *CCM1* and *CCM2* and therefore absence of positive family history is more common in patients with pathogenic variants involving this gene (reviewed in [200, 201]).

As already mentioned, extra-cranial CM are commonly present in FCCM, and may be distributed in the spinal cord, the skin/subcutaneous tissues, retina, solid organs and bone structures [174, 176, 185]. In addition, small focal calcifications in the adrenal gland(s) are also frequently detected in patients with FCCM (probably also corresponding to CM), and show a positive correlation with patient age and number of intracranial lesions [175].

Further details of this syndrome will be subsequently addressed in dedicated sections, whenever relevant.

7p contiguous deletion syndrome

In very rare cases, combined features of FCCM and Greig cephalopolysyndactyly syndrome may be seen in the setting of a 7p contiguous deletion syndrome, involving deletion of *CCM2* and multiple adjacent genes including GLI3 (the gene responsible for Greig cephalopolysyndactyly syndrome and that is located 2.8 megabase pairs from the former) [287]. Affected patients usually present in the pediatric age with polydactyly, macrocephaly, hypertelorism, and developmental delay as well as multiple CCM [287]. Whenever this constellation of features is detected in a single patient this syndrome should be suggested, helping to direct the genetic screening towards a probable *CCM2* deletion.

Other lesions and/or syndromes

As addressed in above, CM can occur in association with other intracranial, craniofacial or spinal vascular lesions, including DVA and/or telangiectasias as well as other venous/venolymphatic malformations. In some instances, these different subtypes of low-flow vascular lesions coexist in the setting of a subjacent systemuc syndrome, including the previously discussed PROS (such as CVMS and Klippel-Trenaunay syndrome) [95, 111–113], BRBNS [41–45] and the PRHTS [46–48].

Conventional imaging

Prenatal imaging

As far as we are concerned, there are no case reports in the literature describing prenatal detection of SCCM. Opposingly, a few papers have been published identifying CCM using cUS, fetal MRI or both techniques with subsequent diagnostic confirmation through fetal autopsy, postnatal MR and/or surgical biopsy [288–292].

CCM-related imaging abnormalities are usually identified in the context of routine prenatal US, with changes detected as early as 21 gestational weeks [288–292]. However, a dedicated examination may also be ordered as a screening method in case of suspected or confirmed FCCM [292]. On cUS, CCM are usually described as hyperechogenic lesions of variable size, in some instances with associated cysts, and with corresponding moderate vascularization and low impedance blood flow on Doppler. Mass effect may be present with or without associated hydrocephalus and macrocephaly. In addition, focal clastic lesions or hypoplasia/atrophy of the involved anatomical region as well as presence of acute blood products may also be detected due to associated hemorrhage [288–292].

Fetal MRI is usually performed as an adjunctive imaging tool of prenatal US whenever anomalies are detected in order to confirm the US findings, add diagnostic information and provide relevant information that can guide perinatal care [13]. Through this technique, CCM may be detected on T1WI and/or T2WI and whenever visible, can present as homogeneous or heterogeneous lesions, with dimensions ranging from only one millimeter to a few centimeters. T2*WI sequences (including GE and echo planar imaging) are particularly sensitive to these lesions also in fetal MRI, due to its high content in deoxyhemoglobin and/or hemosiderin [14, 292] and should be routinely added to the protocol. Nevertheless, prenatal imaging features of CCM are often unspecific and not uncommonly the macroscopic hemorrhage masquerades the

subjacent lesion. Therefore, the differential diagnosis of these lesions in fetuses includes congenital tumors, teratomas or other vascular lesions.

Postnatal imaging

Initial assessment

CT

Head CT has poor sensitivity and specificity to make a diagnosis of CCM in both children in adults, especially if the lesion is small. In addition, as previously discussed, this technique uses ionizing radiation and therefore its utilization is of particular concern in pediatric patients. Nevertheless, it may identify associated calcifications **(Fig 1.4.1 A)** and/or signs of acute intra and/or extralesional hemorrhage as well as potential complications (including adjacent vasogenic edema, loco-regional mass effect, hematic ventricular inundation and/or hydrocephalus), and therefore it is commonly performed in acute situations due to its wide availability and fast acquisition time.

As *per consensus* definition, acute hemorrhage related to a CCM should have a Hounsfield value consistent with acute blood in a head CT scan performed within one week of the neurological event or should resolve on a follow-up CT performed at least 2 weeks later [240]. In addition, if any previous CT scans are available, the high density should be new [240].

On the other side, CT of the spine has no role in the diagnosis of SCCM regardless of the clinical presentation due to its limited ability to evaluate the spinal cord.

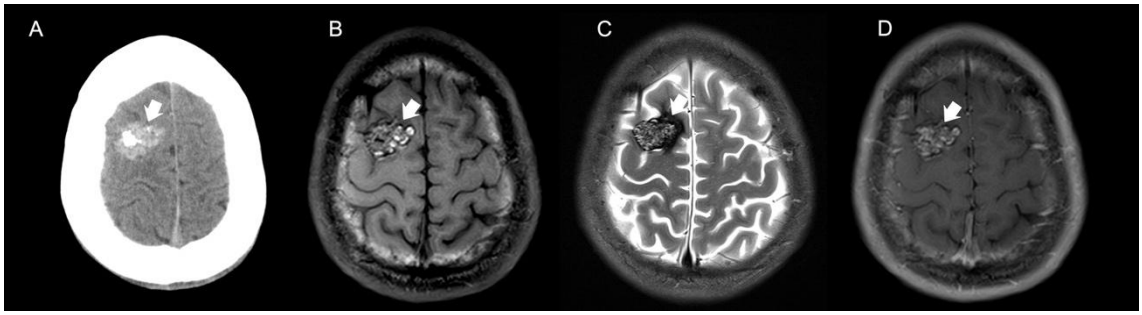

Fig. 1.4.1. Axial unenhanced head CT scan (A) obtained in a young boy presenting with seizures reveals a well-defined, spontaneously hyperdense intra-axial lesion in the right frontal lobe with associated calcifications (*thick white arrow*), but without perilesional edema and only minor mass effect. Brain MRI including axial T1WI (B), T2WI (C) and contrast-enhanced T1WI (D) demonstrates a mixed-signal lesional core, a complete hemosiderin rim as well as absence of marked enhancement, in keeping with a cavernous malformation Zabramski type III (*thick white arrows*).

MRI

MRI is the test of choice for diagnosis and characterization of both CCM and SCCM at all age groups (class I level B evidence) [234].

However, it is important to note that the sensitivity of CM detection depends on the field strength of the MR units. Indeed, as 3.0-T magnets provide higher spatial and contrast resolution as well as increased susceptibility artifacts, they are preferable over 1.5-T whenever available for detection of such lesions [293]. Utilization of ultra-high field (7.0-T) MR systems in CCM identification is promising, as initial studies suggest additional detection of small lesions when compared with standard MR systems and are also more sensitive for DVA identification [146, 294]. In any case, information concerning the magnetic field strength, pulse sequences of the examination and eventual gadolinium injection should be always discriminated in the imaging report in order to inform the reader regarding the sensitivity of the study for blood products and therefore CM [234].

CCM

Although no definitive standard brain MRI protocol has been recommended in the current consensus guidelines for clinical management of CCM [234], all studies performed in this setting should include at least one T2*WI sequence, ideally SWI (class I level B evidence) [146, 234, 293, 295–297]. These sequences are sensitive to the paramagnetic effects caused by the iron-rich blood breakdown by-products that are characteristically present in CCM, and greatly enhance lesion detection especially in case of small and/or multiple CCM [146, 293, 295–297] **(Fig 1.4.2)**.

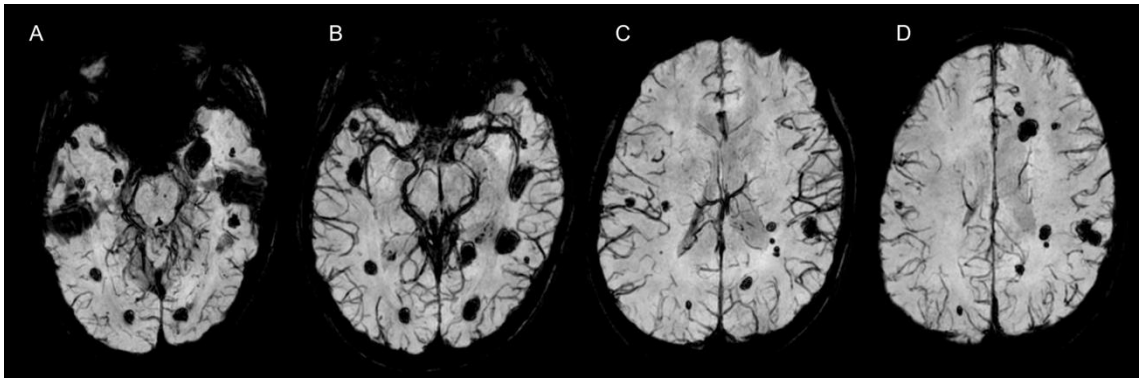

Fig. 1.4.2. Brain MR including axial magnitude SWI images (A-D) in multiple levels acquired in a child with familial cerebral cavernous malformation syndrome due to a proven pathogenic variant in the *CCM3* gene demonstrates multiple supra and infratentorial lesions of variable sizes with *blooming effect* compatible with cerebral cavernous malformations.

Brain MRI assessment should also include at least T1WI (especially 3D sequences, as they better delineate the relation of CCM with adjacent structures), T2WI and FLAIR images [262, 298]. On

the other side, gadolinium injection is not routinely needed for the diagnosis of CCM, especially when the classical imaging features are present. However, postcontrast T1WI better depict a potential adjacent DVA or capillary telangiectasia, may support the diagnosis of a neoplasm in case of dubious initial imaging phenotypes and may be necessary as part of presurgical neuronavigation MRI protocols [178, 234, 299]. Moreover, some case series have described an association of *CCM3* pathogenic variants with intracranial neoplasms, corresponding to putative meningiomas and gadolinium administration may be helpful in this specific setting [271, 300]. Whatever the case, the use of gadolinium should be carefully weighed against the risks in both children and adults and whenever needed administered according to available guidelines [301, 302]. In case of contrast injection, CCM have variable enhancement, from none to moderate [169, 178, 299] **(Fig 1.4.1 B,D)**.

CCM can be located anywhere within the intracranial parenchyma **(Fig 1.4.1 B-D)** and more rarely in the extra-axial space and usually present as discrete, well-circumscribed, round, oval or lobular lesions [234].

When CCM are multiple, the numbers can greatly vary (from 2 to uncountable) [246, 251, 295, 296]. Small numbers of CCM should be described in detail, including their exact location and relationship with important eloquent areas as well as nerve/vascular structures for correlation with clinical manifestations as well as potential presurgical assessment and planning [169, 234]. In case of a high lesion burden, at least overall number estimates together with exact number and discriminated topography of lesions located in eloquent regions (especially the brainstem) should be provided in the report [234].

As a rule, single lesions are usually detected in sporadic cases while familial cases tend to present with multiple, scattered CCM [185, 246, 295, 296] **(Fig. 1.4.2)**. However, multiple lesions may be detected even in sporadic cases (namely clustered in the vicinity of a DVA), while a single CCM can occasionally be identified at initial diagnosis in patients with FCCM [185]. Depiction of a DVA adjacent to a CCM has been shown to help establishing the differential diagnosis between the two CCM subtypes, favoring the diagnosis of sporadic over a familial disease whenever noted [146, 303, 304].

Excluding the multiplicity and adjacent DVA, individual sporadic or familial CCM are otherwise morphologically undistinguishable on neuroimaging [169]. Their signal features are diverse and usually categorized in IV subtypes according to the Zabramski classification system (Zabramski type I-IV), that incorporates signal characteristics of CCM on T1WI, T2WI and GRE/SWI [305]. More recently, an additional category (CCM type V) has been added to the original classification scheme, corresponding to a CCM with acute hemorrhage with overt extralesional spread [252].

Details of this imaging-based classification system and the corresponding pathological features are presented in **Table 1.4.4** and **Fig. 1.4.3.**

Table 1.4.4. Revised Zabramski classification of cerebral cavernous malformations by MRI and histology.

Zabramski type	**T1WI**	**T2WI**	**GRE/SWI**	**Histology**
I	Hyperintense core	Hyper or Hypointense core Hypointense rim	Complete rim with *blooming effect*	Acute/subacute hemorrhage surrounded by a rim of hemosiderin-stained macrophages and gliotic changes
II (*popcorn-like lesion*)	Mixed signal intensity core	Mixed signal intensity core Hypointense rim	Complete rim with *blooming effect*	Loculated areas of hemorrhage and thrombosis of varying ages, surrounded by a rim of hemosiderin-stained macrophages and gliotic changes as well as calcifications
III	Hypo or isointense core	Hypointense core and rim	Complete rim with *blooming effect*	Chronic resolved hemorrhage with hemosiderin staining in and around lesion
IV	Not seen/difficult to identify	Not seen/ difficult to identify	Punctate lesions with *blooming effect*	
V	Similar to type I lesions, but with signs of extracapsular spread of the hematoma			

Legend: GRE- Gradient recovery echo, WI- weighted-imaging, SWI- Susceptibility weighted imaging. Adapted from [252, 305].

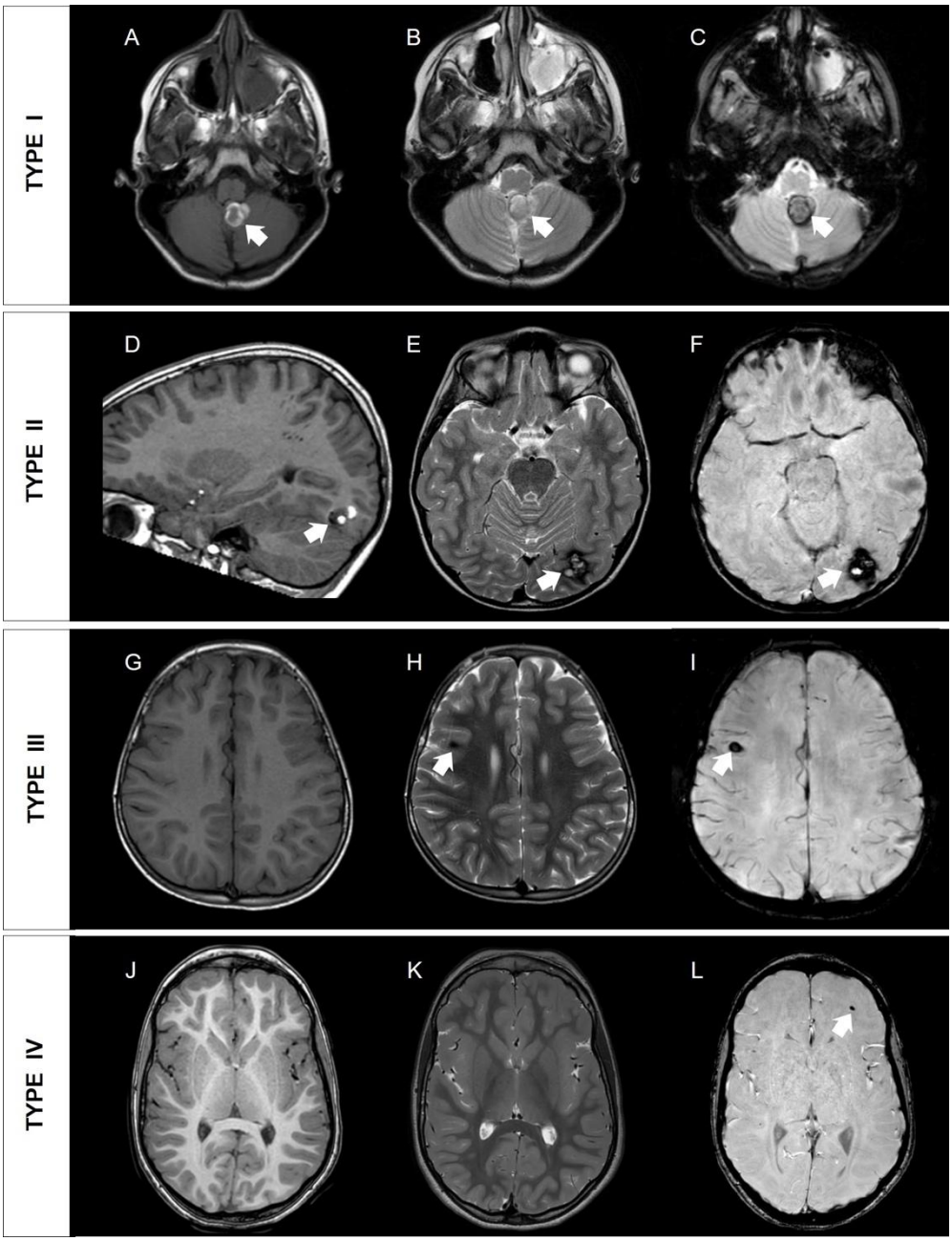

Fig. 1.4.3. Examples of MRI classification of Zabramski types of cerebral cavernous malformations (CCM). Axial T1WI (A), T2WI (B) and magnitude SWI (C) images reveal a Zabramski type I CCM in the left cerebellar tonsil (*thick white arrows*), in keeping with subacute intralesional hemorrhage. Sagittal T1WI (D), T2WI (E) and magnitude SWI (F) images depict a Zabramski type II CCM in the left occipital region (*thick white arrows*), with the typical *popcorn-like* appearance. Axial T1WI (G), T2WI (H) and magnitude SWI (I) images show a Zabramski type III CCM in the right frontal lobe (*thick white arrows*), compatible with chronic hemorrhage. Axial T1WI (J), T2WI (K) and magnitude SWI (L) images demonstrate a Zabramski type IV CCM (also known as *dot-like* CCM) in the left frontal lobe (*thick white arrow*), with *blooming effect* on SWI and barely visible in other sequences.

The most typical lesion corresponds to a Zabramski type II CCM, being characterized by an inner core with multiple chambers and a reticulated appearance, showing mixed T1 and T2WI signal

with or without fluid-fluid levels as well as a complete hypointense peripheral T2WI halo with blooming effect on T2*WI, therefore resembling a *popcorn* [305] **(Fig. 1.4.1 B-D and 1.4.3 D-F).** The other Zabramski subtypes, especially when isolated, are less characteristic and pose differential diagnosis in both children and adults, that should be correlated with patient´s age and clinical information [11, 143] **(Table 1.4.5)**. However, presence of at least one classic Zabramski type II CCM together with any other lesion type(s) favors the diagnostic of multiple CCM.

Table 1.4.5. Differential diagnosis of cerebral cavernous malformations on brain MRI.

Zabramski type	Differential diagnosis
I/III/V	Hemorrhagic and/or calcified metastatic lesion(s) Hemorrhagic and/or calcified primary brain tumor(s) Other vascular lesions and malformations (AVM, dAVF, thrombosed aneurysm or thrombosed venous varix) Granulomas
II (*popcorn-like lesion*)	Usually pathognomonic
IV	Microbleeds (eg. cerebral amyloid angiopathy/ABRA, chronic hypertensive angiopathy, diffuse traumatic axonal injury, vasculitis, critical illness microbleeds) Calcifications (eg. neurocysticercosis) Fat cerebral emboli Radiation-related capillary telangiectasia and/or CM Metallic particles (ECMO-related foci of susceptibility)

Legend: ABRA- Amyloid Beta-related angiitis, AVM- Arteriovenous malformation, dAVF- Dural arteriovenous fistula, CM- Cavernous malformation, ECMO- Extracorporeal membrane oxigenation, ICH- Intracranial hemorrhage. Adapted from [298, 299].

Although this classification system does not directly correlate with indications for surgery or clinical outcomes, some studies have shown that Zabramski type I and type II subtypes are more prone to subsequent symptomatic and/or asymptomatic ICH when compared to type III and type IV lesions [251, 252]. Nevertheless, the later are not purely benign lesions [251] and the Zabramski subtypes are neither static and may progress from one type to another over time (see follow-up section) [306].

In some instances, a CCM may be partially or totally obscured by a recent intraparenchymal hemorrhage and may mimic other causes of ICH [178, 240, 299]. In such cases, presence of a T1 hyperintense perilesional sign can support the correct diagnosis with high specificity and moderate sensitivity [307] **(Fig. 1.4.4)**. Nevertheless, it is important to be aware that this sign may also be evident in other lesions, such as hemorrhagic metastasis, especially from melanoma [308]. Therefore, a follow-up brain MRI following resorption of blood products is recommended

to confirm the diagnosis [240], ideally within 3 months in the absence of new clinical events [299, 306].

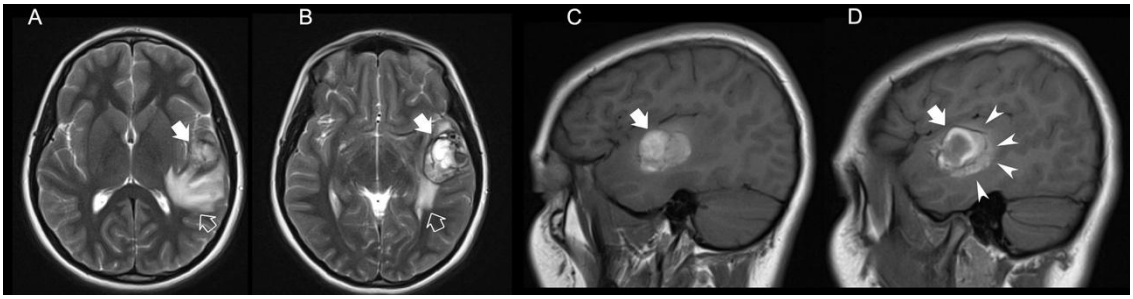

Fig. 1.4.4. Brain MRI including axial T2WI (A,B) and sagittal T1WI (C,D) in a young girl presenting with an acute neurologic deficit reveals an intra-axial expansile mass located in the left temporo-opercular region with a hiper-isointense core in both pulse sequences (*thick white arrows*), in keeping with an acute hemorrhagic lesion. There are signs of perilesional edema (*open white arrows*) as well as moderate loco-regional mass effect. Also note presence of a hyperintense T1WI perilesional sign (*white arrowheads*), supporting the diagnosis of a cerebral cavernous malformation Zabramski type I.

As suggested by the current guidelines, the single largest measurement or the orthogonal measurements should be provided for symmetric and asymmetric CCM, respectively, except for type IV lesions [234]. Measurements of individual CCM should be made based on spin echo (or fast- or turbo-spin echo) sequences and not in GRE/SWI, avoiding the *blooming* that causes them to appear larger than their real size in the brain in the latter sequences [234, 293].

Although most CCM lesions remain relatively small, in rare instances they become very large and are therefore classified as *giant CCM* [239, 309, 310]. The cut off diameter of these *giant* lesions has been arbitrarily defined, varying between 4 to 6 cm according to different authors [309, 310]. Interestingly, giant CCM have been described predominantly in the pediatric population, especially during the first 3 years of age [239, 309, 310]. On brain MRI, two different imaging appearances of *giant* CCM have been reported, denominated *multicystic* and *reticulated* subtypes [310] **(Fig. 1.4.5)**.

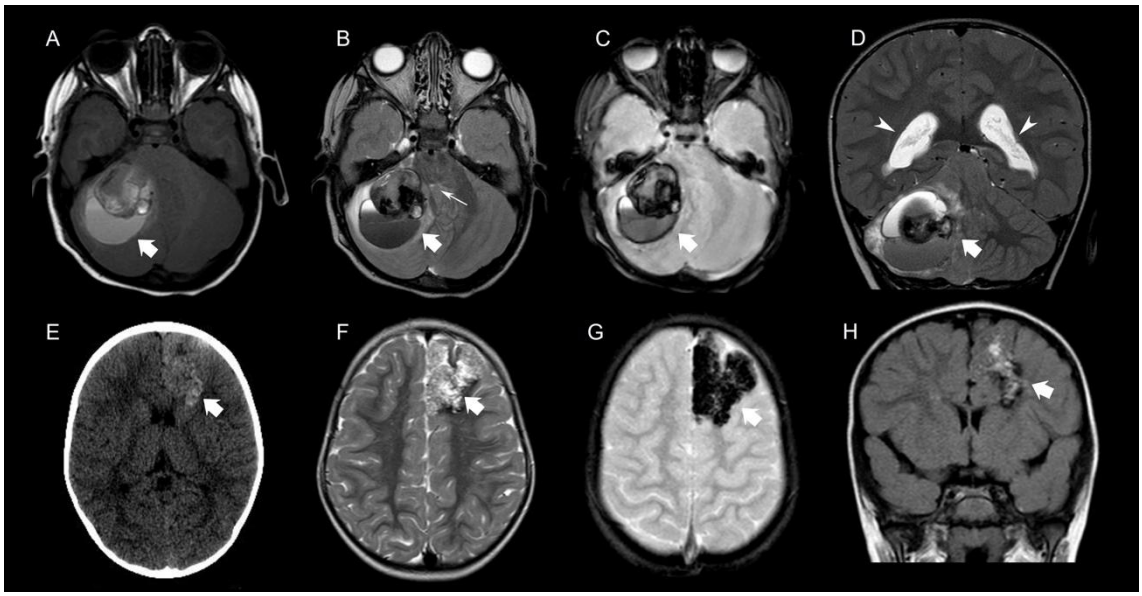

Fig. 1.4.5. Brain MR in a child presenting with ataxia including axial T1WI (A), T2WI (B) and magnitude SWI (C) images as well as coronal T2WI (D) image reveals a very large, multilobular, expansile lesion in the right cerebellar hemisphere, with a hemosiderin rim and multiple areas of hemorrhage of different ages including inner blood-levels, compatible with a multicystic type of giant cerebral cavernous malformation (CCM) (*thick white arrows*). Note the small area of peripheral edema as well as the associated mass effect, including severe compression of the IV ventricle (*very thin white arrow*) and mild dilatation of the occipital horns of the lateral ventricles associated with, in keeping with supratentorial obstructive hydrocephalus (*white arrowheads*). Axial unenhanced head CT image (A) and brain MR including axial T2WI (B) and magnitude SWI (C) and coronal FLAIR (D) images obtained in another child demonstrate a very large intra-axial lesion in the left frontal lobe, partially calcified, and with associated blooming effect compatible with reticulated type of giant CCM (*thick white arrows*). There is no associated vasogenic edema nor significant mass effect.

The former variant is more common and is characterized by a "*bubbles of blood"* appearance, caused by relatively large-sized, multiple blood-filled cavities with hemosiderin ring and fluid-fluid levels and accompanying edema and mass effect **(Fig. 1.4.5 A-D)**, while the latter presents instead a "*salt-and-pepper"* appearance [239, 309–312] **(Fig. 1.4.5 E-H)**. In both subtypes there may be punctate calcifications or, more rarely, an associated DVA [239, 309–312]. Giant CCM may also coexist with other smaller CCM in the context of FCCM, but are usually identified as isolated lesions, and not uncommonly misdiagnosed preoperatively as neoplasms or other type of vascular lesions [309, 310]. Nevertheless, the possibility of a giant CCM should be considered as a differential diagnosis of large supratentorial or cerebellar hemorrhagic masses with the aforementioned imaging characteristics, namely in infants/young children. Occasionally, especially in the pediatric age group, CCM lesions also present with a large cystic component with an associated nodule that also may mimic other conditions [313, 314].

After excluding possible differential diagnosis, assessing the number, location, size and Zabramski subtype as well as any associated lesions such as DVA, neuroradiologists should help determining if any CCM presents with signs of *symptomatic hemorrhage*, the most frequently reported outcome measure in CCM studies [240]. To this regard, brain MRI should ideally be performed within 2 weeks of the onset of an acute clinical event in order to demonstrate signal changes that are compatible with recent ICH (either intralesional or extending beyond the lesion) according to the expected MR time course of intraparenchymal hemorrhage [315], as presented in **Table 1.4.6**.

Table 1.4.6. Expected time course of intraparenchymal hemorrhage on brain MRI.

Stage	Time	Phase of blood	T1WI	T2WI	GRE/SWI
Hyperacute	< 12 hours	Oxyhemoglobin	Hypo or isointense	Hyperintense	Hypointense +++
Acute	12-48 hours	Deoxyhemoglobin	Hypo or isointense core Hyperintense rim	Hypointense core Hyperintense rim	Hypointense +++
Early Subacute	48-72 hours	Methemoglobin intracellular	Hyperintense	Hypointense	Hypointense
Late Subacute	3-20 days	Methemoglobin extracellular	Hyperintense	Hyperintense	Hypointense
Chronic	>3 weeks	Hemosiderin and ferritin	Hypointense	Hypointense	Hyper or isointense core Hypointense rim

Legend: GRE- Gradient recovery echo; SWI- Susceptibility weighted imaging, WI- Weighted-imaging. Adapted from [315].

Moreover, these signal changes should be new when compared to previous MRI, or, alternatively, should resolve on a follow-up MRI performed ≥ 2 months after the initial study [240]. Importantly, according to the current criteria, existence of a hemosiderin halo, or signs of lesion growth without other evidence of recent hemorrhage, do not fulfill criteria for acute hemorrhage [240]. Imaging findings need to be correlated with clinical information and neurological assessment, and the final diagnosis ideally decided in a multidisciplinary team. In addition, according to the aforementioned 2008 consensus criteria,

When a timely MRI and other methods fail to demonstrate acute blood products, the clinical event referable to the anatomical CCM location, but not due to migraine or epileptic seizure, is classified as a non-hemorrhagic FND. , when brain MRI is not performed at all nor at the correct

time, the term FND "*not otherwise specified"* should be used [240], as schematically presented in **Fig. 1.4.6**.

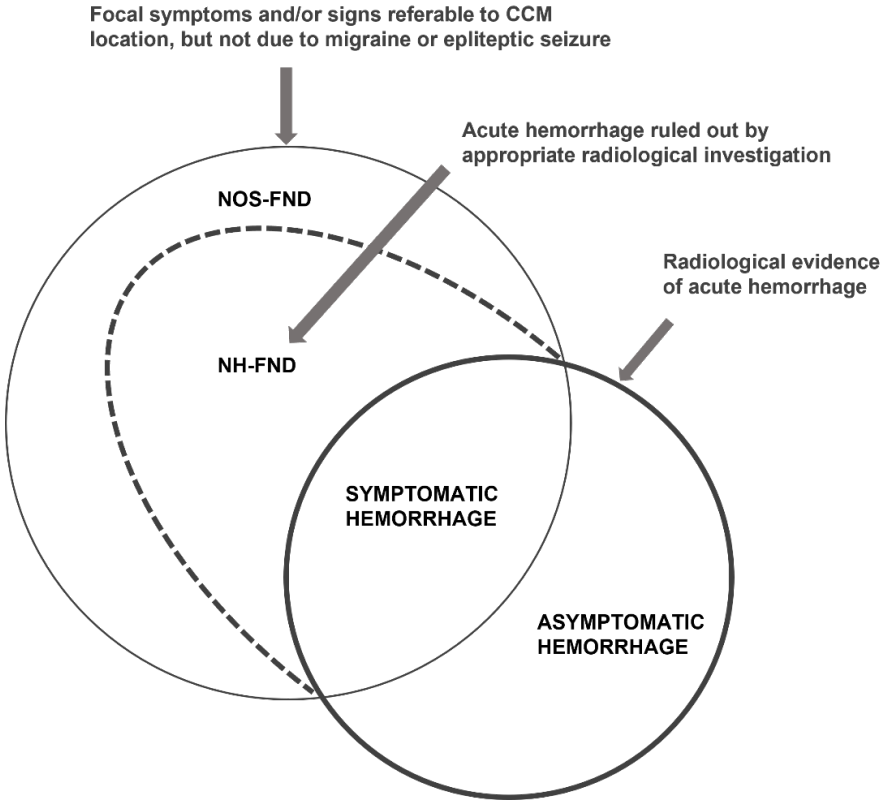

Fig. 1.4.6. Schematic presentation the cerebral cavernous malformations (CCM)-related focal neurological event concepts. **Legend:** FND- Focal neurologic deficit, NH- Non-hemorrhagic; NOS- Not otherwise specified. Adapted from [240].

In patients with suspected or confirmed FCCM, a spine MRI with optimal technique can be added as in a recent study including both children and adults with a confirmed pathogenic variant in *CCM1* due to the *Common Hispanic Mutation*, coexistent SCCM were detected in screening spinal studies in ~72% of patients [173]. In such cases, evaluation of all available imaging studies dedicated to other body segments may be also useful in order to depict potential additional systemic CM, namely calcifications in the suprarenal glands [175].

Finally, in all CCM patients and especially in children, it is also important to try identify any additional imaging feature that may point towards another systemic syndrome associated with CCM, including the previously discussed PRHTS [46–48], PROS (such as the Klippel-Trenaunay syndrome or the CVMS) [95, 111–113], BRNS [41–45] or 7p deletion continuous syndrome [287]. More specifically, neuroradiologists should evaluate presence of any intracranial or extracranial venous malformations or other vascular lesions, abnormal corpus callosum and/or megalencephaly [41–48, 95, 111–113].

SCCM and other spinal cavernous malformations

At spine MRI, SCCM tend to be small (< 1cm in length) expansile lesions, with eccentric axial location extending towards the cord surface and showing minimal enhancement and/or associated edema [316, 317]. Interestingly, the classic imaging features of CCM (including popcorn morphology, complete hemosiderin ring and inner blood-fluid levels) are frequently absent in SCCM [316, 317]. On the other side, presence of adjacent intramedullary hemorrhage separated from the hemosiderin ring, usually bidirectional and eccentric, is often detected in SCCM [316, 317], and may be a key-clue helping differentiate these lesions from other entities with overlap features, namely intramedullary tumors (especially hemorrhagic ependymomas and hemangioblastomas) as well as other spinal vascular malformations, including AVM or dAVF [316]. Although there are currently no specific definitions and reporting standards for symptomatic hemorrhage due to SCCM, adaptation of the available guidelines for CCM [240] is usually performed.

Dedicated spine MRI protocols should include sagittal T1WI and T2WI as well as gradient-based 3D T2 multi-echo data image combination (MEDIC) sequences, as the latter were found to be more sensitive to the detection of SCCM than conventional images [173]. Differently from brain MRI, the role of SWI is limited in the spine due to technical artifacts [173]. In case a SCCM is suspected on the sagittal images, axial T1WI, T2WI and GRE sequences should also be obtained in the suspected level.

A complementary brain MRI may also help establishing the final diagnosis, as SCCM are often reported in association with CCM in mixed-age populations [170, 273, 318]. Moreover, presence of additional CCM in the context of a SCCM also changes the presumptive diagnosis from sporadic to familial disease, allowing for appropriate clinical and genetic counselling.

On the other side, whenever a spine MRI is performed in patients with SCCM and/or CCM, especially if multiple and/or within the context of suspected or proven FCCM, careful evaluation of vertebral bodies is also suggested, aiming to detect intraspinal vertebral malformation (ISVM), especially with atypical features. Indeed, an association between ISVM and FCCM has been recently described in case reports, small case series and case-control studies, with most cases being described in adults [173, 319–322]. Contrary to typical ISVM (commonly designated as vertebral hemangiomas), atypical ISVM show T1-hypointensity and T2-hyperintensity, are often multiple and larger and present a more aggressive course, including associated pathologic fractures [322].

Finally, an association between *CCM3*-related FCCM and scoliosis has been described, reaching up to 40% of those patients and often showing progressive features over time [271]. Although additional studies are required to confirm and better characterize this possible association,

particular attention to abnormal spinal alignments in the three planes including inclusion of a coronal T2WI of the spine to the protocol may be adequate, especially in FCCM cases.

Angiographic techniques

CTA/CTV, MRA/MRV and DSA have no role in the diagnosis of CCM or SCCM, as they are *angiographically occult* and therefore not visible using these techniques. Accordingly, these angiographic techniques should only be performed in the setting of atypical imaging features, namely to exclude a differential diagnosis of CCM and/or an associated vascular lesion (class III, level C evidence) or for pre-surgical planning [234].

Follow-up imaging

CCM and SCCM

Neuromaging evaluation in patients with one or multiple known CM and any new/aggravated neurological symptoms/deficits or modifications of epilepsy characteristics should be promptly performed, ideally within 2 weeks after the symptom onset [234, 240, 262]. In such cases, either CT or MRI may be obtained for brain imaging within the first week after neurological changes, but afterwards only MRI should be performed (Class I, level C) [234]. As previously mentioned, for spinal imaging, MRI is always the preferred choice due to the limitations of spinal CT for evaluation of the spinal cord. The remainder considerations of the consensus definition of CCM-associated symptomatic hemorrhage previously discussed also apply for clinical events detected at follow-up [240].

Routine longitudinal neuroimaging assessment of stable adult or pediatric patients with CCM and/or SCCM submitted or not to surgical treatment is currently not well established, including indication, optimal timing, and imaging protocol. Therefore, follow-up imaging surveillance in these cases is still primarily based on clinical judgment, as well as upon insurance and patient/parent´s preferences.

In patients with previously symptomatic lesions conservatively treated, a routine follow-up imaging after 3-6 months of the event and thereafter at yearly intervals has been previously suggested by a task force of the ILAE commission [262]. In case of no interval rebleed, there is a characteristic pattern of signal evolution, with CM lesions evolving from Zabramski type I/V lesions at baseline towards Zabramski type II or III subtypes and showing regression of adjacent vasogenic edema and mass effect [306]. These expected imaging changes over time are useful in distinguishing true CM from mimics [306].

In asymptomatic, incidentally discovered CM the role of longitudinal neuroimaging studies is more controversial, especially in young children requiring sedation for neuroimaging [323, 324]. Nevertheless, even in such cases follow-up imaging is commonly performed, especially in familial cases.

Comparative imaging studies, either performed routinely or in the emergency setting, should be ideally performed using standardized imaging technique, with similar MRI scanners and protocols. However, variations are common in clinical practice and whenever the case, it is important to account for potential technical differences when evaluating putative changes in CM, including field strength, slice thickness, orientation and interslice gap [234].

Progressive imaging changes in both CM and SCCM include symptomatic hemorrhage, asymptomatic/subclinical hemorrhage as well as lesion growth [177, 252, 325], while *regressive* changes are represented by size reduction and, more rarely, lesion disappearance [252]. In the specific case of SCCM, increased spreading over time of the adjacent *flame-like* hemorrhage is another common longitudinal finding [316].

Besides careful evaluation of all previously detected CM aiming to identify any possible imaging variation over time, neuroradiologists should detect presence of any *de novo* lesion. Importantly, the new appearance should be shown on comparable or technically inferior consecutive MRI studies. Although *de novo* CM formation has been occasionally described in sporadic cases (usually in the draining territory of a DVA or adjacent to other vascular malformation) [78–80] **(Fig. 1.3.7)**, it predominantly occurs in patients with FCCM [177, 185, 252, 254] **(Fig. 1.4.7)**.

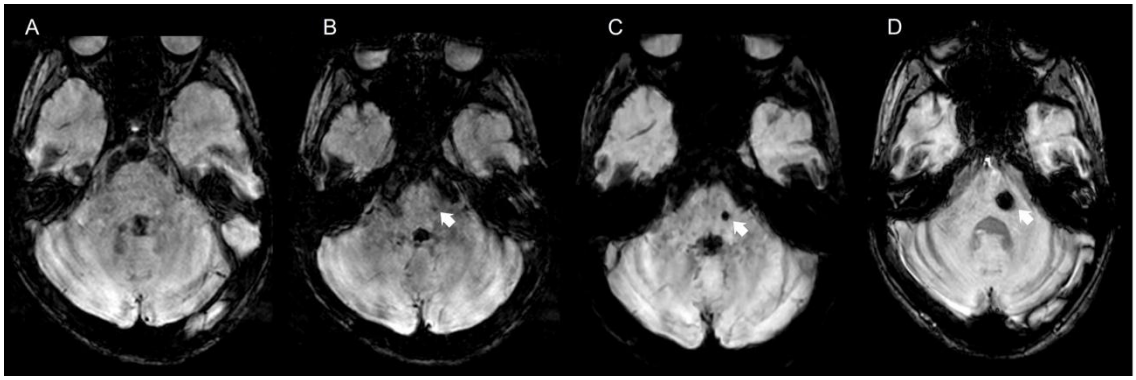

Fig. 1.4.7. Longitudinal brain MRI including axial magnitude SWI images (A-D) at the same level, performed in a child with familial cerebral cavernous malformation syndrome due to a proven pathogenic variant in the *CCM*1 gene demonstrates *de novo* appearance and progressive growth over time of a cerebral cavernous malformation in the left hemipons (*thick white arrows*).

The genesis of new lesions happens in an age-dependent fashion in both sporadic and familial forms [185, 326], and therefore the overall number of CM in affected FCCM adult patients may be so high that manual counting of all lesions in these patients is frequently arduous and time-consuming and associated with high intra- and inter-rater variability. An automated counting algorithm for Zabramski type IV CCM has been previous developed and tested, showing internal consistency and reducing reporting time and therefore potentially facilitating lesion quantification and tracking, namely in clinical research studies [327].

The role of *progressive* subclinical radiological changes and *de novo* lesion formation in the clinical management of CCM and SCCM in both sporadic and familial cases is still not established and remains a matter of debate, requiring further research. However, some studies have shown that such asymptomatic imahing changes in CM (growth and/or hemorrhage and new lesion formation) occur more commonly than symptomatic changes over time during follow-up and are more frequently detected in patients with prior symptomatic hemorrhage [177, 325]. Therefore, given their potential predictive role, *progressive* subclinical radiological changes have been recently included in a recent grading system for surgical decision making of CCM [328] that has been subsequently validated [329].

In patients that underwent CM resection, at least one postoperative brain and/or spine MRI is commonly requested, usually in the subacute/early chronic phase (from 1 to 3-6 months follow-up). This evaluation aims to detect residual CM components and/or CM recurrence as well as completeness of removal of the hemosiderin rim in CRE cases, after the blood has been resorbed and the tissues have healed [254, 330–334]. Nevertheless, it remains difficult to assess tiny remnants even at that time point and subsequent follow-up studies have been recommended by some authors [254, 331]. In particular, a close postsurgical imaging follow-up up to 18 years of age has been suggested for pediatric patients [241, 254] due to a highest probability of residual/recurrent CM in this age group, reaching an annual recurrence rate of 0.7% [254, 335, 336]. Long time follow-up is also necessary for any child or adult with familial disease/multiple CM even after one of their lesions has been surgically removed, aiming to evaluate the longitudinal behavior of the remainder lesions [254]. On the other side, imaging surveillance in adults and low-risk children with a single CM and signs of complete resection may be spaced in time and eventually discontinued [254]. Recently, an earlier postsurgical MRI (within 72 hours after surgery) has also been advocated by some authors for confirmation of surgery completeness in both children and adults [254, 331, 334] and patients with obvious positive imaging findings may return to the operating room to complete the resection [331]. In addition, early brain MRI can also provide additional information when compared to routine immediate

postoperative head CT scan in case of new or aggravated neurological impairment after CM surgery, namely regarding the etiopathology of the deficits as well as the expected functional outcome [332]. However, it is often hard at that time point to distinguish between a very small residuum of a CM and postoperative changes, including tissue edema, hemostatic agents, and pooled blood and therefore false positives may occur leading to a low positive predictive value at early assessment [331, 332].

Imaging screening in subjects with suspected or confirmed FCCM syndrome and close relatives

Currently there is no international consensus regarding the appropriateness, initial age and periodicity for routine brain and/or spinal MRI screening spinal MRI in patients with proven or suspected FCCM and their family members, although at least one baseline neuroimaging study is often requested [234].

Advanced imaging techniques

Advanced neuroimaging techniques may be also added to conventional MRI protocols to provide supplementary information in patients with CCM, namely for surgical planning of lesions located in/near eloquent areas (such as diffusion tensor imaging (DTI) and fMRI) as well as for quantitative assessment of their angioarchitectural and/or hemodynamic abnormalities (namely using QSM and dynamic contrast-enhanced quantitative perfusion (DCEPQ)). A brief overview of the basic principles and potential applications of these techniques in patients with CCM will be provided.

Diffusion tensor imaging

DTI is a non-invasive MRI technique that gives provides qualitative and quantitative information regarding WM microarchitecture, including course and connectivity. It is based in the analysis of water molecules diffusivity, using a mathematical tensor model to characterize diffusion in the 3D space, which has a variable degree according to the molecular characteristics of the tissue. Different quantitative parameters can be extracted from this technique (including fractional anisotropy, mean diffusivity, axial diffusivity and radial diffusivity and apparent diffusion coefficient (ADC)) using multiple approaches, either locally with region of interest analysis or globally with voxel-based analysis or tract-based spatial statistics. In addition, diffusion tensor tractography (DTT) can be obtained from DTI images through application of predefined algorithms that perform extraction of nervous tracts that follow the pathways of maximum coherence of diffusion, allowing *in vivo* 3D visualization of selected WM tracts in the brain [337–339].

Both DTI and DTT have multiple applications in children and adults with neurological disorders [337–339]. In the specific setting of CCM, a few studies have evaluated the utility of these techniques for decision making, mainly for lesions located in the brainstem (reviewed in [340]) but also supratentorially [341–344]. Indeed, DTI and DTT have the potential to better demonstrate the anatomical spatial relationship between CCM and perilesional vital WM bundles, as well as presence and extent of adjacent fiber tract involvement [341]. In addition, preoperative quantitative DTI changes may help predict post-interventional neurological outcomes. Importantly, DTI appears to be relatively unaffected by CCM–related artifacts related with their hemosiderin content and therefore remains a reliable imaging technique near these lesions [344]. Indeed, despite the scarcity of literature, a recent meta-analysis focusing on the clinical significance of DTI/DTT in management of brainstem CCM supported the benefit of these adjunctive techniques in the development of an individually-tailored operative plan including selection of brainstem safe entry zones and surgical trajectories in order to minimize morbidity as well as a prognostic tool for postoperative functional outcome (reviewed in [340]). These conclusions seem to also apply to supratentorial lesions [341–344]. However, limitations of available DTI/DTT studies in this topic should be taken into account, including lack of harmonized technical protocols and repeatable quantitative analysis of DTI alterations in most investigations as well as known susceptibility of DTI indices to partial volume effects leading to their underestimation in areas with multiple crossing fibers [337–339]. In addition, currently available studies evaluating the role of DTI in CCM include either adults [341, 345–348] or mixed-age populations [342, 343, 349–354] and future large prospective studies in pediatric only cohorts are necessary to better define the extent of DTI utility and reliability in the management of children with CCM.

functional MRI

In addition to DTI/DTT, fMRI (a noninvasive MR technique that evaluates blood oxygen level–dependent (BOLD) changes in the brain), has also been widely used for surgical planning of lesions located in eloquent regions in patients from all ages. Nevertheless, the relevance of this technique in CCM management remains residual [344, 355–359]. Moreover, concerns regarding the impact of the blood degradation products typically present within CCM lesions in the BOLD signal have been raised [344, 357]. In particular, a recent work by Colasurdo *et al* has shown that CCM can indeed lead to artifactual depression of fMRI signals in their vicinity and therefore authors suggest that this technique should be interpreted with caution near CCM [344]. Nevertheless, and in contrary to AVM, CCM appear to have minimal potential for language cortex reorganization as assessed using this technique [359, 360].

Quantitative Susceptibility Mapping and Dynamic Contrast-enhanced Quantitative Perfusion

As iron deposition, perfusion abnormalities and vascular permeability changes are pivotal events in the pathophysiology of CM [361], there has been an increasing interest in the *in vivo* investigation of quantitative descriptors of these biological phenomena derived from neuroimaging techniques in these lesions, especially using QSM and DCEQP magnetic resonance imaging. In turn, these two quantitative MRI-techniques (alone, combined or even weighted with other biochemical parameters) are potential biomarkers to objectively detect lesional hemorrhage, measure disease severity, monitor the course of the disease and the effect of the novel therapies as well as to predict CM symptomatic bleed and/or growth. Therefore, a brief explanation of DCEPQ and QSM techniques as well as the main results published in the literature concerning their application in patients with CM will follow.

DCEQP is a 2D T1WI-based gadolinium-dependent technique used to measure hemodynamic parameters. After image acquisition, data can be postprocessed into multiple maps (including permeability and perfusion maps), and from these multiple descriptors can be extracted using dedicated pipelines [362–364]. Recently, Girard *et al* demonstrated that mean background brain permeability measured by DCEQP is overall higher in FCCM cases (irrespectively of the genotype) as compared with sporadic CCM subjects or non-CCM controls and that mean lesional permeability increases significantly during follow-up studies within CCM with signs of bleeding or growth [365]. Moreover, FCCM subjects that developed *de novo* lesions over time showed increased background permeability as well as higher regional permeability in areas that later develop a new CCM as compared with the homologous contralateral brain region [365]. Other reports focusing on DCEQP-related perfusion on CCM have demonstrated that these lesions present inhomogeneous and dysregulated perfusion [366] and that hypoperfusion associated with hyperpermeability predicts a future symptomatic hemorrhage and/or asymptomatic bleed or growth [367].

On the other side, QSM is an MRI technique that allows precise quantitative measurements of spatial biodistribution of local magnetic susceptibility sources (such as iron) within biological tissues and therefore it can be used to assess iron deposition in the brain, including individual CM lesions [368, 369]. QSM measurements have shown close correlation with phantoms with varying iron concentration in different molecular states as well as the actual iron content within surgically excised CM as validated by mass spectroscopy [368]. In addition, it has been

demonstrated an excellent interobserver agreement of QSM evaluation, further supporting the utility of this neuroimaging technique [369].

Results published so far using this technique indicate that mean or maximum lesional iron content is higher in CCM with known prior symptomatic hemorrhagic events or with signs of hemorrhage at baseline MRI as well as in older patients [369–372]. In addition, during longitudinal imaging follow-up, CCM with interval symptomatic hemorrhage or growth demonstrated a significant increment in their mean QSM values [365, 369, 371].

Importantly, as QSM appears to have great sensitivity to hemorrhagic lesional activity due to its ability to detect subclinical changes [371], the application of this technique in CCM clinical trials may allow increased efficiency by reducing the sample size required to test a potential effect of novel therapies [371]. Moreover, a pilot study suggested that maximum QSM values at baseline MRI might abe used to predict 1-year outcome in adult FCCM patients [372].

In CCM studies where both DCEPQ and QSM techniques were performed, it has been reported a strong positive correlation between CCM permeability measured by DCEQP and iron burden measured by QSM. Indeed, CM with greater permeability tend to to show a significantly higher mean lesional iron content. This finding suggest that the phenomena of vascular leakage and iron deposition, although representing distinct physiopathological features of CCM, are probably biologically interrelated [373]. More specifically, it has been hypothesized that permeability reflects current leaking, whereas mean iron deposition is the result of the overall past leaking process within the lesion [373].

It is also important to note that the weighted combination of QSM and DCEQP techniques as biomarkers showed improved accuracy in predicting lesion instability than either technique alone [365, 367]. In addition, incorporation of additional biochemical biomarkers, such as circulating plasma proteins also enhances diagnostic and prognostic performances [365, 367] probably reflecting subjacent complementary biological mechanisms.

Recently, a phantom validation study of QSM and DCEQP MRI sequences across instruments and institutions demonstrated accurate and consistent measurements, supporting these techniques as potential diagnostic and prognostic imaging biomarkers in CCM [374]. Moreover, the neuroimaging assessment using both techniques according to harmonized protocols has already been incorporated as a secondary outcome variable in two ongoing clinical trials (Trial Readiness in cavernous angiomas with symptomatic hemorrhage (CASH) and AT CASH EPOC Trial) aiming to confirm their feasibility, accuracy, precision, and reproducibility at multiple sites [375]. Initial results of the CASH Readiness Trial reveal baseline QSM and permeability values of CASH lesions identical to historical CASH cases and consistent across sites [376]. Results from another recent

pilot clinical trial further support the feasibility of using DCEQP to evaluate permeability of CCM and in the background brain [377].

Nevertheless, it is important to note that QSM and/or DCEQP techniques have been applied only in adults or more commonly mixed-age populations with CCM with underrepresentation of children [365, 370, 373] and therefore future studies applying these techniques in pediatric only cohorts with CM/FCCM are warranted.

Clinical management and treatment

A multidisciplinary evaluation of affected patients by an experienced clinicians, including neurologists, epileptologists, neurosurgeons, geneticists, (neuro)radiologists as well as other dedicated healthcare professionals whenever needed is beneficial, especially in FCCM and/or pediatric cases [378].

Currently, there is no approved medical treatment to alter the course of either CCM or SCCM and management of adults and children with CM includes a conservative approach or an interventive treatment with either surgery, stereotactic radiosurgery (SRS) and/or magnetic resonance-guided laser interstitial thermal therapy (LITT). Although consensus guidelines on the topic have been published in 2017 [234], they present low classes and levels of evidence as the quality of the underlying studies is limited. In addition, most available data arises from specialized centers, and hence results may not necessarily be generalized to community settings without equivalent experience. Moreover, specific guidelines for pediatric patients and patients with FCCM are still lacking. Therefore, indications for more interventive CM treatments remain significantly center- and surgeon-dependent and are also influenced by the patient's (and/or parents) wishes, as well as available facilities and resources. Of note, a pilot clinical trial (Cavernomas A Randomised Effectiveness (CARE)) comparing medical management to either surgery or SRS for symptomatic CCM is already planned, aiming to solve this common clinical dilemma. In the meantime, an algorithm to guide clinical decision-making in the treatment of affected pediatric patients has been recently proposed by Hirschmann *et al* [379].

Finally, potential disease-modifying medical therapies for CM are also under investigation, some of them already being tested in clinical trials.

Both standard treatment modalities and more innovative therapies will be discussed below in more detail.

Conservative approach

Conservative management of CM includes medical treatment of related signs and symptoms, rehabilitation of possible neurological deficits, counselling on natural history of the disease,

decisions regarding the need and periodicity of imaging surveillance and eventual imaging screening of other organs and system as well as discussion of possible lifestyle modifications [234, 378].

In the specific case of definite or probable CRE, it is common in clinical practice to start with one AED immediately after the first seizure episode, as the risk of developing epilepsy subsequently is known to be very high, as already addressed above [244, 260, 380, 381]. In case poor seizure control is achieved by the first drug regimen (as expected in 40-50% of cases), referral to epileptic centers for individual risk-benefit assessment and optimal presurgical evaluation of the epileptogenic network may be appropriate for both children and adults, as high rates of postsurgical seizure freedom are reported in most studies [262, 263, 266, 381–384]. Alternative approaches to surgery in CRE include SRS or LTTS, as it will be addressed subsequently [383]. Opposingly, in patients with CM presenting incidentally or with ICH or FND, the risks of a first seizure do not appear to justify the prescription of prophylactic AED, that are also associated with undesirable side-effects [244, 260, 380].

Last, preconception genetic counseling and testing should be offered to all individual patients with familial or multifocal CM and their family members (class I, level C) and discussion should include family planning, potential risks to offspring, and reproductive options [234, 385].

Surgery

CCM

According to current treatment guidelines published in 2017, surgical resection is generally not recommended for asymptomatic, incidentally detected CCM either being single or multiple (class III, level B and level C, respectively) [234]. Surgical treatment of symptomatic CCM remains a more consensual option, especially when affected patients present with medically refractory epilepsy as it has been previously mentioned, even if only a probable relationship between CCM and epileptogenicity has been established (class IIa, level B) [234]. For other type of symptoms, including a single prior symptomatic hemorrhage, surgery may also be considered for both superficial and deep supratentorial CCM. However, for CCM located in the brainstem surgery should only be offered after repetitive symptomatic bleeding (Class IIb, level B) [234].

In terms of the surgical technique itself, as addressed in the previous section, it should be avoided dissection of any adjacent DVA, aiming to prevent associated complications, namely venous infarcts with or without hemorrhagic component [262, 386]. In addition, complete resection of the hemosiderin rim is also recommended in all DRE cases [262, 263, 333, 387].

The risk of death, ICH, or FND after CCM excision ranges between 4.3 and 7% [388–392], being higher for brainstem than supratentorial lesions as well as for CCM that have previously presented with ICH [384, 392, 393].

Several adjunctive tools including preoperative DTI/DTT and/or fMRI [340–344], intraoperative neuromonitoring [394], neuronavigation as well as electrocorticography and functional mapping via navigated transcranial magnetic stimulation [395] may be implemented in CCM-related microsurgery to minimize intervention-related morbidity and mortality, depending on the individual situation [293]. Special neurosurgical techniques including endoscope-assisted resection may also be used [396, 397], although further studies are needed in order to establish their role in CCM surgery. However, according to a recent meta-analysis, overall surgical risks have not significantly changed in recent years even with advances in microsurgical and other operative techniques [392].

Gross complete resection of CCM can be achieved in the great majority (~90%) of cases [391], and it represents the only method to avoid subsequent (re)hemorrhages. Recent studies have suggested that intraoperative MRI can be beneficial in CCM surgery, allowing immediate second-look revisions whenever needed and therefore reducing the frequency of residual lesion and/or hemosiderin ring components [398, 399].

A scarce number of research works have addressed the surgical experience with pediatric-only cohorts of patients with CCM. In addition, literature concerning this age group often considers only specific locations of CCM (namely brainstem vs cerebellar vs basal ganglia vs other supratentorial lesions) and/or presenting signs or symptoms (CRE vs hemorrhage). Results so far support the efficacy and safety profile of surgical intervention in children with CCM even in cases of multiple lesions [249, 263, 382, 400, 401]. Some authors consider that given the greater life expectancy leading to higher risk for repetitive symptomatic hemorrhage over time and the known higher brain plasticity allowing superior functional recovery in children, surgical treatment should be always considered earlier in children than in adults [241, 382]. On the other side, as previously mentioned, pediatric patients with CCM tend to have higher rates of recurrence/residual lesions following a surgical resection [335] and should have a more closed and long-term imaging follow-up [254].

SCCM

The optimal management of SCCM remains controversial, including indications for surgery. However, according to most recent studies including two systematic reviews, for patients with symptomatic lesions outcomes are significantly better in those that undergo SCCM resection

than for those who are treated conservatively. Whenever feasible, proactive early intervention might be particularly appropriate in SCCM with a prior hemorrhage and/or a Zabramski type I appearance as well as in pediatric patients and familial forms [171, 275–277, 402]. Overall, gross total resection can be achieved in ~95% of cases [172] and is associated with improved neurological outcomes after surgical intervention at all age groups [171, 273, 276, 402]. Surgery within 3 months of symptom onset, hemilaminectomy approach and post-operative symptom improvement are additional variables associated with favorable outcome [273].

Finally, neurophysiological monitoring as well as special surgical techniques may be used for deeply located lesions aiming to prevent iatrogenic injury to spinal cord fiber tracts or nerve roots [403].

Stereotactic Radiosurgery

According to current expert-based treatment guidelines, SRS is contraindicated in FCCM, due to concerns over the increased risk of new lesion formation in these cases due to radiation effects [234]. On the other side, it may be considered in in both adults and children with solitary CCM with previous symptomatic hemorrhage(s) that are located in eloquent areas and carry high surgical risk or are even inoperable (class IIb, level B) [234].

Nevertheless, there are still conflicting results regarding the efficacy of this treatment modality in CCM, especially within the first 2 years after treatment [404–406]. Indeed, it remains unclear if the risk reduction of neurologic events over time in patients treated with SRS is simply due to the natural history of the disease.

On the other side, despite the fact that the mortality and morbidity associated with SRS is reportedly low, it is important to note that the negative side effects of radiation, including new transient or permanent neurologic signs or symptoms, cyst formation, and radiation- induced signal changes/perilesional edema are not neglectable [404, 406].

In addition, although SRS has been already applied in numerous pediatric CCM cases (representing up to one quarter of all patients treated with this technique according to Poorthuis *et al* [405]), most studies include both adults and children and outcomes have been rarely explicitly reported in this subgroup. However, results from a recent paper by Samanci *et al* [407] including 46 children with CCM managed with SRS show low annual hemorrhage rates with no radiation-induced toxicity, supporting SRS as an alternative treatment modality for pediatric CCM.

Other treatment options

Magnetic Resonance Thermometry-Guided Stereotactic Laser Ablation

LITT is a minimally invasive procedure that uses 50-90 degrees Celsius heat to ablate diverse lesions or target brain structures to be disconnected [408]. It was first applied in patients with CCM in 2016 and since then a few more cases were reported, including two pediatric patients [409–414]. Pooled results from two meta-analysis on the topic support the efficacy, safety profile and technical feasibility of LITT for CCM, even in lesions located in deep and eloquent areas [415, 416]. Indeed, no deaths or new CCM-related hemorrhages were reported in association with this treatment and other complications were transient and resolved subsequently, except for one case in which cystic degeneration developed in the ablation site over time [409, 415, 416]. Imaging follow-up may show perilesional edema in the immediate post-operative acquisition but subsequent studies reveal involution and reduction in the size of the CCM in most cases [415, 416]. Further studies with larger cohorts including higher numbers of pediatric cases as well as longer follow-up times are necessary to obtain robust data concerning long-term efficacy and risks of this treatment modality.

Innovative medical treatments under investigation

As previously mentioned, numerous drugs are currently under investigation in either preclinical or clinical studies and the most relevant ones will be described below in more detail, including the respective targeted pathways.

1) ROCK inhibitors

As already mentioned, *CCM1-3* encoded proteins normally inhibit the ROCK cascade, thereby regulating endothelial barrier maintenance, cell polarity, and cytoskeletal contractility (reviewed in [201]). As expected, loss of any of the components of the CCM complex leads to increased activation of ROCK signaling pathway, with associated destabilization of the junctional integrity and elevation of actin stress fibers, as identified in CCM lesions [417–419]. Both *in vitro* and *in vivo* studies have demonstrated that increased ROCK-mediated endothelial permeability can be rescued by ROCK inhibition and this approach is a current line of investigation in pharmacological intervention in CM [418, 419].

Indeed, previous preclinical works demonstrated that ROCK inhibitors (such as fasudil and BA-1049) decrease lesion burden (including CCM number and size) in murine CM models that recapitulate human disease when compared to placebo [191, 420–422]. In addition, they also prevented maturation of CCM, including signs of hemorrhage, inflammation, and endothelial proliferation as well as iron deposition [191, 420–422].

A similar although less efficacious effect has also been detected in animal models treated with statins [421, 423], opening a second line of research using this class of drugs. Indeed, although statins are widely used and well-tolerated in humans as cholesterol lowering drugs due to inhibition of the HMG-CoA reductase, they present pleiotropic effects, including weak ROCK inhibitor properties. Importantly, the potential of repurposed use of statins (more specifically atorvastatin at 40 or 80 mg/day) in stabilizing CM in adult patients is already being evaluated in the AT CASH EPOC trial, a phase I-IIa randomized, placebo-controlled, double-blinded, and single-site clinical trial (clinicaltrials.gov: NCT02603328) [185]. In the meanwhile, a small pilot randomized controlled clinical trial using simvastatin in CM patients did not encounter any adverse events [29].

On the other side, a few population-based studies in patients with sporadic and/or familial CM treated with statins (associated or not with other medical therapies) for unrelated medical reasons have been published, with contradictory results concerning the hemorrhage risk of these drugs [424–426] and further results regarding the efficacy of ROCK inhibitors in CM in both children and adults are expected in the following years.

2) Propanolol

Propranolol, a pleiotropic, nonselective β-adrenergic receptor antagonist, is a safe, tolerable, low-cost and wide available drug initially developed in the 60s, and since then mainly used for treatment of some cardiovascular disorders as well as anxiety and tremors.

In 2015, results from a randomized controlled trial have shown that propranolol has also great benefit and a good safety profile in the treatment of infantile hemangioma at a dose of 3 mg *per* kilogram per day for 6 months and since then it became the frontline therapy for complicated forms of such lesions [427]. As infantile hemangiomas are benign vascular tumors of the skin that present many structural analogies with CM (also being formed by abnormal dilated capillary vessels with disorganized endothelial cells and pericytes), it has been suggested a repurposed utilization of propranolol for the treatment of CM [428]. In the meanwhile, a few anecdotal but favorable clinical reports have been published supporting the efficacy of this drug in both adults [429] and children with CCM [430–432]. In the same line, one *in vitro* study using *CCM2*-deficient cells cultures identified pindolol, another non-selective β-adrenergic receptor antagonist, as one of the top 10 drugs that was effective [433]. Moreover, recent research investigations using animal models have shown that propranolol reduces and stabilizes CM, supporting its utilization as a pharmaceutical treatment for this subtype of vascular lesion [434, 435]. On the other side, a few retrospective studies investigating patients with sporadic and/or familial CM on β-blocker for other medical reasons have shown conflicting results. Indeed, some authors have reported

a statistically significant association between the use of this medication and a decreased risk of ICH or FND [425] while others not [426, 436].

The mechanism of action of propranolol in infantile hemangiomas and/or CM is not clearly understood but current hypothesis include pathways both related and unrelated to its β-adrenergic function, including anti-angiogenic properties [437].

The results of a multicenter randomized controlled phase 2 pilot trial (Treat_CCM; clinicaltrials.gov: NCT03589014) comparing propranolol treatment plus standard care alone to standard care alone in adults with FCCM have been recently released, supporting safety and tolerance of propranolol in this disorder and showing signs of efficacy, thereby justifying a definitive phase 3 trial [27, 377]. According to the ClinicalTrials.gov, two additional randomized clinical trials evaluating propranolol in patients with CCM are ongoing (NCT03523650 and NCT03474614), one of them including pediatric patients.

PART II - NEONATAL DEVELOPMENTAL VENOUS ANOMALIES: CLINICAL RADIOLOGICAL CHARACTERIZATION AND FOLLOW-UP

Ana Filipa Geraldo,[1,2] Simona S Messina,[3] Domenico Tortora,[2] Alessandro Parodi,[4] Mariya Malova,[4] Giovanni Morana,[2] Carlo Gandolfo,[5] Alessandra D'Amico,[6] Ellen Herkert,[7] Paul Govaert,[7] Luca A Ramenghi,[4] Andrea Rossi,[2] Mariasavina Severino[2]

[1] Neuroradiology Unit, Centro Hospitalar de Vila Nova de Gaia/Espinho, Vila Nova de Gaia, Portugal

[2] Neuroradiology Unit, IRCCS Istituto Giannina Gaslini, Genova, Italy

[3] Radiology Unit, Casa di Cura Regina Pacis, Palermo, Italy

[4] Neonatal Intensive Care Unit, IRCCS Istituto Giannina Gaslini, Genova, Italy

[5] Interventional Unit, IRCCS Istituto Giannina Gaslini, Genova, Italy

[6] Dipartimento di Scienze Biomediche Avanzate, Universita' Federico II Napoli, Italy

[7] Division of Neonatology, Department of Paediatrics, Erasmus University Medical Centre, Rotterdam, The Netherlands

Abstract

Background and Purpose: Although developmental venous anomalies have been frequently studied in adults and occasionally in children, data regarding these entities are scarce in neonates. We aim to characterize clinical and neuroimaging features of neonatal developmental venous anomalies, and to evaluate any association between MR abnormalities in their drainage territory and corresponding angioarchitectural features.

Methods: We reviewed associated parenchymal abnormalities and angioarchitecture features of 41 newborns with developmental venous anomaly (20 males; mean corrected age 39.9 weeks) selected through radiology report text search from 2135 newborns who underwent brain MRI between 2008-2019. Fetal and longitudinal MRI were also reviewed. Neurological outcomes were collected. Statistics were performed using $\chi 2$, Fisher exact, Mann-Whitney or t-tests corrected for multiple comparisons.

Results: Developmental venous anomalies were detected in 1.9% of neonatal scans. These were complicated by parenchymal/ventricular abnormalities in 15/41 cases (36.6%), improving at last follow-up in 8/10 (80%), with normal neurological outcome in 9/14 (64.2%). Multiple collectors ($P=0.008$), and larger collector(s) caliber ($P<0.001$) were significantly more frequent in complicated developmental venous anomalies. At a patient level, multiplicity ($P=0.002$) was significantly associated with presence of ≥1 complicated developmental venous anomaly.

Retrospective fetal detection was possible in 3/11 subjects (27.2%).

Conclusion: One third of neonatal developmental venous anomalies may be complicated by parenchymal abnormalities, especially if with multiple and larger collector(s). Neuroimaging and neurological outcomes were favorable in the majority of cases, suggesting a benign, self-limit**ed** nature of these vascular anomalies**.** A congenital origin could be confirmed in one quarter of cases with available fetal MRI.

List of abbreviations: CCM- cerebral cavernous malformation, c-DVA- complicated developmental venous anomaly, cUS- cerebral ultrasound, CVMS- cerebrofacial venous metameric syndrome, DVA- developmental venous anomaly, u-DVA- uncomplicated developmental venous anomaly, T2*WI- T2*-weighted imaging

Background

Developmental venous anomalies (DVA) are the most frequently diagnosed intracranial vascular malformation, often encountered as incidental neuroimaging findings [35, 438]. On MRI, DVA are recognized on postcontrast T1WI as radially oriented veins with a *caput medusae* pattern converging into one (or rarely more) dilated venous collector [33, 36]. These features may be also detected on pre-contrast MR images [33, 36, 139], especially if T2*-weighted sequences (T2*WI), such as high-resolution SWI, are included in the protocol [139]. In addition, DVA may be occasionally recognized *in utero* using fetal MRI [135].

DVA are usually considered benign anatomical variants [31]. However, they represent areas of venous fragility that can become symptomatic through diverse pathomechanisms [38, 39]. Indeed, DVA-associated brain abnormalities are frequently depicted, including but not limited to sporadic cerebral cavernous malformations (CCM) [20, 38, 39, 137, 149–151, 158, 439]. Moreover, a higher prevalence of DVA has been described in patients with different pathologies and/or genetic conditions [49, 95, 122, 123, 129].

Although DVA are widely described and characterized in adults, they remain under-reported in the pediatric population. Indeed, there are noticeably less studies focusing exclusively on DVA in this age group, especially in the neonatal period [17, 19, 34, 49, 122, 123]. In particular, the largest case series of neonatal DVA described so far included 14 newborns, mostly detected using ultrasound during routine scanning for other reasons [19], with limited information on prevalence and perinatal characteristics of these vascular abnormalities, including complications and longitudinal evolution. Moreover, additional data on neonatal and fetal DVA would be of great interest as there is an ongoing debate regarding their congenital or postnatal etiology [54].

In this study, we aimed to describe the pre and post-natal appearance of DVA and associated brain anomalies in a relatively large single-center group of neonates, providing information on their imaging and clinical follow-up. In addition, we tested a possible association between parenchymal and/or ventricular abnormalities in the drainage territory of neonatal DVAs and their angioarchitectural features.

Materials and methods

Population

After IRB approval, one pediatric neuroradiologist (MS) searched in the Radiology Information System of a tertiary pediatric institution for reports of brain MRI studies performed in subjects up to 28 days of corrected age containing the term *developmental venous anomaly,* over a 12-year period (January 2008 - December 2019). During this period, 2135 neonatal patients

underwent brain MRI. Written informed consent was waived because of the retrospective nature of the study.

MR technique and image analysis

Neonates were scanned on 1.5-T or 3.0-T MR units with different imaging protocols, all including at least T1WI, T2WI, DWI and T2*WI (either GRE or SWI) sequences. Gadolinium-based contrast agents were injected only if clinically indicated. Neonates were fed before MRI examination in order to achieve spontaneous sleep, with mild oral midazolam sedation (0.1mg/kg) in case of head movements, and were breathing spontaneously during examination.

Brain MRI studies were reviewed by two pediatric neuroradiologists (MS and AFG with 10 and 5 years of experience, respectively), who confirmed the diagnosis and evaluated the presence of DVA-related mechanical compression of adjacent structures, draining vein thrombosis, and/or parenchymal abnormalities within the drainage territory. The latter included any of the following: increased T2 signal of surrounding WM, foci of restricted diffusion, hemorrhage, CCM [305], malformations of cortical development, or calcifications (defined as focal areas of hyperintensity on SWI phase images in right-handed MR systems or hyperdensity at head CT scans). Microhemorrhages were distinguished from type IV CCM based on their evolution on imaging. Indeed, vessels of CCM have a tendency to leak and bleed, thus frequently increasing or stabilizing in size over time, while microhemorrhages typically present a regular evolution of hemoglobin degradation with faster reduction in size and/or complete regression.

Subjects with ≥1 associated abnormality were considered to have *complicated* DVA (c-DVA group), and the remainder *uncomplicated* DVA (u-DVA group).

Additionally, we registered the number of DVA *per patient* as well as the corresponding angioarchitecture features [33, 150]: direction of drainage, number of collector vein(s), and mean collector caliber (defined as the caliber of the collector vein in case of a single collector or the mean of all collector calibers in case of multiple collectors, measured on axial T2*WI). Multiple collectors were defined as ≥ 2 draining veins. Fetal MRI, neonatal cerebral ultrasound (cUS), DSA, and follow-up MRI were reviewed when available.

Imaging findings at last MRI follow-up were classified as interval improvement, progression, stability, or mixed evolution.

Discrepancies were resolved by a third pediatric neuroradiologist (AR, 25 years of experience).

Clinical data

Data on gender, pregnancy history, gestational age at birth, cause of prematurity, type of delivery, Apgar scores, corrected age at first MRI, and imaging indications were obtained from

electronic clinical records. For c-DVA newborns, additional data including treatment, age at last clinical assessment, and neurological outcome (graded as normal, mild, moderate or severe impairment) were also registered.

Statistical analysis

Quantitative data were presented as median and interquartile range and categorical data as frequencies and percentages. Fisher exact, Chi-Square and independent sample student t-tests were used to compare clinical characteristics between c-DVA and u-DVA patient groups. Fisher exact, Chi-Square and Mann-Whitney tests were used to compare angioarchitectural characteristics and associated parenchymal/ventricular abnormalities between individual complicated and uncomplicated DVA. All results were corrected for multiple-comparison testing by using the Bonferroni correction method. Statistical significance was reached if the P value was < 0.05/k, where k = number of tests, resulting in thresholds for statistical significance of P<0.0045 and 0.0083 for patient and DVA levels of comparison, respectively. Statistical analyses were performed by using SPSS Statistics software, v24.0 (IBM, Armonk, NY).

Results

Neonatal imaging features

Forty-one neonates with DVA were retrieved by report search and confirmed by image review (20 males; mean corrected age at first MRI 39.9 weeks, range: 33-44), corresponding to a real-world MR DVA detection of 1.9% (41/2135) in a tertiary pediatric center. Preterm neonates were 46.3% (n=19). Brain MRI was obtained on a 3T scanner in 22 cases (53.7%). SWI and post-contrast T1WI were acquired in 38 (92.7%) and 7 cases (17.1%), respectively.

Fifteen patients (36.6%) had at least one DVA (range 1-6) associated with parenchymal abnormalities and/or CSF obstruction (c-DVA group) (**Fig. 2.1-2.3**). Two of these neonates were affected by cerebrofacial venous metameric syndrome (CVMS). **Online Table 2.1** summarizes clinico-radiological associations. In particular, at term birth (P=0.02), higher gestational age (P=0.05) and imaging indication other than *preterm screening* (P=0.005) were significantly more frequent in the c-DVA group but did not reach statistical significance after adjusting for multiple comparisons. Moreover, multiple DVA as well as additional craniofacial vascular lesions, were also more common in c-DVA patients (P=0.002 and P=0.02, respectively), but only multiplicity remained significant after multiple comparisons correction. Neonatal seizures likely attributable to a symptomatic DVA were detected in 2/15 c-DVA patients. One additional c-DVA patient developed probable DVA-related seizures at 11 months. A direct causal relationship between DVA and neonatal seizures was not identified in 2 u-DVA patients presenting with this symptom.

Overall, 58 DVA were identified, comprising multiple DVA in 9 cases. DVA location and angioarchitecture features are presented in **Table 2.1**. Multiple collectors and larger collector calibers were significantly more frequent in complicated DVA (P=0.008 and P<0.001, respectively), even after adjusting for multiple comparisons.

DSA was performed in 4 c-DVA patients: no signs of arteriovenous shunting through the DVA with or without an associated classic nidus were identified, while a subject with CVMS had an intraorbital AVF.

Fetal MRI and postnatal cUS

Fetal MRI was performed in 11 cases (26.8%), of which 6 belonged to the c-DVA group (21 examinations in total, 1-4 studies per patient, acquired between 20 and 38 gestational weeks). Retrospective analysis of single-shot FSE, b0 and/or T2*WI images identified a DVA and/or an abnormally enlarged draining pathway in 3 fetuses (27.3%). In another case, a DVA-associated cerebellar hemorrhage was detected but precluded the identification of the subjacent DVA. Of the remaining 7 fetuses in which the DVA was not visible, 3 presented craniofacial vascular lesions.

Postnatal cUS was available in 36 newborns: in 3 cases the DVA was suspected before the MRI examination due to presence of parenchymal linear hyperechogenic focus.

Management and clinical-radiological outcome of cDVA neonates

Of 15 c-DVA neonates, 13 were conservatively managed, with a wait-and-see approach in 10 cases, anticoagulation treatment in 2, and antiepileptic drugs in 1. Endoscopic third ventriculostomy was performed in one newborn with DVA-related obstructive hydrocephalus. Multiple interventional procedures were carried out in the child with CVMS and AVF.

Table 2.2 reports clinical-radiological outcome of c-DVA subjects. Longitudinal MR imaging was available in 10/15 patients (median follow-up 39.1 months, range: 2-97; age at last follow-up 2.5months - 8.2years). Eight patients (80%) showed imaging signs of improvement, while stability (n=1) or mixed evolution (n=1) were detected in the remaining cases.

Follow-up neurological evaluation was available in 14 c-DVA newborns (median follow-up 27.5 months, range: 11-97) and judged normal in 9 cases (64.2%), while minor or moderate psychomotor impairment was detected in 4 (28.5%) and 1 (7.1%) patients, respectively.

A brief description of a few illustrative cases of neonatal c-DVA is presented as **Online material**.

Discussion

In this study we identified 41 newborns with DVA, for a total of 58 DVA, from a population of 2135 neonates performing brain MRI for diverse clinical reasons and with different imaging techniques, corresponding to a real-world detection in a tertiary pediatric center of 1.9%. These findings are similar to a recent retrospective study by Brinjikji *et al*, describing prevalence of 1.5% in the 0-12 months age group [54]. Interestingly, both percentages are inferior to those reported in studies including older children, adults or mixed populations (5 to 10%) [17, 36, 54]. As the pathogenesis of DVA remains controversial, including their cause and timing of development, some authors have attributed these age-related prevalence differences to a postnatal origin [54]. However, caution is advised due to methodological discrepancies between studies in terms of selection criteria and imaging protocols. In addition, DVA may potentially be more difficult to detect in neonates due to small head size, uncomplete myelination, short imaging protocols, and motion artifacts. On the other side, statistically significant associations between DVA and both primary brain tumors and multiple sclerosis have been previously described [122, 129]. As these disorders are frequent MR indications in adults but very uncommon in the neonatal setting and infancy, clinical indication itself may act as a confounder in the relationship between age and DVA. Prospective neuroimaging studies in the health population at different ages using standardized imaging protocols are needed to better understand the relationship between age and DVA. Of note, we retrospectively identified DVA and/or related enlarged drainage pathways in 27.2% of cases with available fetal MRI, confirming a congenital origin of these vascular abnormalities in those patients [135, 440]. Conversely, we could not depict new DVA at follow-up studies, but considered this limited population, we can not exclude that some DVA can actually develop *de novo* postnatally.

In our cohort, greater than one third of newborns presented at least one type of vascular complication directly linked to DVA. Similarly, Horsch *et al* found a high percentage (42.9%) of abnormalities surrounding neonatal DVA [19], while variable frequencies have been described in studies including adults and/or older children [20, 137, 149–151]. Of note, initial differences regarding corrected age at first MRI, prematurity and imaging indication between newborns with cDVA and uDVA likely represent a detection bias related to the neuroimaging screening program of preterm neonates with birth weight < 1,500 g performed in our institution or even by chance alone as these values did not reach statistically significance after multiple-comparison correction.

In detail, associated WM signal abnormalities were present in 17.1% of our newborns and were even more frequent in the series published by Horsch *et al* (21.4%) [19]. Previous studies have suggested that DVA-related WM changes present a bimodal distribution, peaking in younger

children and older adults [20, 150]. However, the underlying mechanisms of these signal changes remain poorly understood. In younger children, delayed myelination in the draining territory of the DVA has been proposed as a potential explanation [20]. Alternatively, these signal alterations may represent venous congestion edema in the DVA territory due to imbalance of the in- and outflow of blood in the DVA system, raising the pressure in the DVA [38]. Of note, the latter mechanisms can also explain the relatively high frequency of associated hemorrhages and/or ischemic changes identified in our sample (19.5% and 9.8% of cases, respectively). In the general population, the risk of DVA-related hemorrhage is considered to be low (<1%/year) and usually attributed to adjacent CCM bleeding [35]. However, we detected CCM only in a small percentage of cases (4.9%), in keeping with the theory that non-familial CCM are acquired lesions related with DVA through the process of hemorrhagic angiogenic proliferation [81, 304]. Taken together, our findings suggest that in the neonatal period there is a higher risk of flow-related complications in DVA, potentially leading to venous hypertension and associated venous congestion, hemorrhage, and/or infarction. Putative neonatal risk factors of hemodynamic decompensation include mechanical distortion during vaginal birth and immaturity of the venous, immune and hemostatic systems as well as hypercoagulability, which may be potentiated by maternal factors or inflammation [82, 441, 442]. Finally, angioarchitectural factors yet unexplored in the neonatal setting, including angulation and stenosis of draining veins or tortuosity of medullary veins, could contribute to the development of ischemic or hemorrhagic complications [137, 443].

Interestingly, presence of multiple DVA (i.e. multiplicity) was significantly more common in c-DVA newborns even after multiple comparisons correction, suggesting that more severe and widespread venous pathology may correspond to a more fragile venous outflow system and/or higher propensity for thrombotic DVA events. Of note, two of these neonates presented clinical-neuroradiological features consistent with CVMS, a rare craniofacial vascular malformation disorder characterized by a wide spectrum of slow-flow vascular lesions distributed along one or more of the 3 craniofacial metameres, further supporting this theory [95]. Remarkably, one also presented a superior orbital fissure AVF, suggesting that this complex disorder may actually be a *continuum* potentially affecting more than one vessel type.

Our study also revealed focal polymicrogyria in the draining region of DVA in two newborns (4.9%). DVA and/or other venous drainage abnormalities have already been described adjacent to dysplastic cortical areas using conventional and ultra-high field MRI [3, 62, 444, 445]. As polymicrogyria is frequently associated with *in utero* disruptive events, coexistence of these two lesions suggest a causative effect of DVA in the formation of this cortical malformation or, more probably, a shared pathomechanism related to early failure, abnormal development, or

intrauterine occlusion of normal cerebral vessels [62, 444, 446]. Finally, in one neonate we observed obstructive hydrocephalus related to another type of DVA complication, i.e. mechanical compression of the cerebral aqueduct [38]. As in our patient, CSF diversion techniques usually lead to a good outcome in these rare cases [70].

As previously described, in our neonatal cohort DVA were more commonly located supratentorially and in the frontal lobe (41.4%) [82, 137]. Other common locations included the parieto-occipital (27.7%) and temporal (13.8%) lobes, while basal ganglia/thalamus were involved in only 8.6% of cases. Of note, differently from a previous neonatal case-series, we identified infratentorial DVA in 8.4% of cases, thus confirming a potential selection bias related to the use of cUS to depict posterior fossa DVA [19].

Regarding angioarchitecture features, we noticed a higher prevalence of multiple DVA collectors that, together with larger caliber collectors, were significantly associated with DVA-related parenchymal abnormalities. These features may be related to the DVA size and, ultimately, to the volume of parenchyma under hemodynamic stress, i.e. with reduced venous drainage capacity. Larger collectors may also be theoretically more prone to abnormal venous flow, with increased stasis and thrombosis. However, other studies performed in adults did not show statistically significant differences between parenchymal abnormalities and collecting vein diameters [150]; therefore the relationship between these neuroimaging features requires more detailed study. Similarly, in the present study posterior fossa location was not a risk factor for complicated DVA. Methodological issues in terms of population of interest and type of complication may justify this variability [17, 82, 439], and further studies are needed to also address this topic.

Serial imaging of a subgroup of c-DVA newborns revealed that DVA and adjacent MR abnormalities frequently present a dynamic evolution during the early years of life. These findings are in line with previous studies and probably reflect progressive brain and vascular maturation during early infancy [19, 154]. Indeed, neuroimaging follow-up demonstrated overall improvement in most c-DVA cases. More specifically, WM abnormalities were reduced in size or even completely resolved. Furthermore, ischemic and hemorrhagic foci also tended to subside, without signs of intracranial re-hemorrhage. Of note, clinical outcome of c-DVA patients was concordant with their favorable MRI evolution, with normal neurological examination in the great majority of cases. Good clinical and neurological outcomes were also reported by Horsch *et al* [19], and are probably related to intrinsic brain plasticity as well as normalization of potential risk factors present in the neonatal phase.

Limitations

This study presents some limitations. Firstly, case selection was based on a retrospective single-center search of radiological reports. Therefore, although DVA are routinely described in our institution by all staff members, the true DVA prevalence might be underestimated. Similarly, a relevant number of neonates was scanned on a 1.5-T system and gadolinium-based contrast media were only occasionally used, potentially leading to lower DVA detection [33, 36, 139]. However, SWI was performed in almost all neonates (92.7%), and has a high diagnostic sensitivity for DVA in children, especially when sedation is performed without propofol and sevoflurane [139]. Secondly, this study was performed in a tertiary pediatric institution leading to potential selection bias towards inclusion of more severe DVA cases and limiting generalizability towards a different setting. Moreover, DVA collectors were measured on axial T2*WI and this sequence can be influenced by the level of blood oxygenation and the magnetic field strength. However, none of the newborns was examined under general anesthesia, and complicated DVA were actually less frequent in the group of subjects scanned using a 3.0-T magnet. Therefore, if there were any bias related with the examination technique in terms of DVA collector size and MR complications, it would actually exerting its influence towards the null hypothesis. Finally, longitudinal data were missing in some patients and clinical evaluation at follow-up was obtained from clinical records, although formal neurological evaluation was performed in all assessed cases.

Conclusions

Real world DVA detection in this population of newborns with a clinically-indicated brain MRI reached 1.9%, which is inferior to studies including older children and adults and might be an underestimation of the true prevalence. Of all newborns with a detected DVA, around 1/3 presented DVA-related complications. The latter group had a significant tendency towards multiplicity and additional vascular malformations but usually presented favorable neuroimaging and neurological evolution at follow-up. DVA could be retrospectively diagnosed *in utero* in one quarter of newborns with fetal MR, confirming at least in these cases a congenital origin.

Tables and Legends

Table 2.1. Location and angioarchitecture characteristics of developmental venous anomalies.

	Total N=58	**Complicated DVA N=21 (36.2%)**	**Uncomplicated DVA N=37 (63.2%)**	**P value[a]**
Location (%)				0.44
Frontal	24 (41.4)	9 (42.9)	15 (40.5)	
Parieto-occipital	16 (27.7)	6 (28.6)	10 (27)	
Temporal	8 (13.8)	3 (14.3)	5 (13.5)	
Basal ganglia/thalami	5 (8.6)	0 (0)	5 (13.5)	
Brainstem	2 (3.4)	1 (4.8)	1(2.7)	
Cerebellum	3 (5.2)	2 (9.5)	1 (2.7)	
Infratentorial (%)	5 (8.6)	3 (14.3)	2 (5.4)	0.34
Right side (%)	33 (56.9)	13 (61.9)	20 (54.1)	0.59
Multiple collectors (%)	9 (15.5)	7 (33.3)	2 (5.4%)	0.008*
Main collector caliber (mm), median (IQR)	1.6 (1.18-2.10)	2.1 (1.95-2.30)	1.2 (1-1.6)	<0.001*
Drainage (%)				0.70
Deep	31 (53.4)	11 (52.4)	20 (54.1)	
Superficial	19 (32.8)	6 (28.6)	13 (35.1)	
Both	8 (13.8)	4 (19)	4 (10.8)	

Legend: IQR- interquartile range

[a] P values for group comparisons were determined by Chi-Square of Fisher exact tests for categoric variables or by Mann-Whitney test for continuous variables, as appropriate

*Value statistically significant (Statistical significance was set at *P<0.0083* after Bonferroni correction for multiple comparisons)

Table 2.2. Neuroimaging abnormalities associated with developmental venous anomalies.

MR abnormalities	**Neonatal period[a] N=15**	**Last follow-up[a] N=10**
WM T2-signal abnormalities	7	Reduced 2/5 Stable 1/5
		Complete regression 2/5
Restricted diffusion foci	4	Total regression 2/2
Hemorrhagic foci	8	Gliosis with or without hemosiderin deposits 3/3
Multiple CCM	2[b]	Stable 1/2
		Growth 1/2
PMG	2	Stable 2/2
Calcifications	2	Stable 2/2
Triventricular hydrocephalus	1	Resolution 1/1[c]
Draining venous varix thrombosis	1	Recanalization 1/1

Legend: CCM- Cerebral Cavernous Malformations, PMG- Polymicrogyria, WM-white matter
[a] Some patients presented ≥1 DVA-related complication
[b] Includes 1 newborn with Cerebral Venous Metameric Syndrome
[c] Post-endoscopic third-ventriculostomy

Supplemental Table 2.1. Global and subgroup baseline clinical characteristics.

	All cases N=41	c-DVA newborns N=15 (36.6%)	u-DVA newborns N=26 (63.7%)	P Value[c]
Male gender (%)	20 (48.8)	6 (40)	14 (53.8)	0.52
Gestational age (weeks), median (IQR)	38 (30.8-39.1)	39 (38-39)	33.9 (30.1-39)	0.05*
Prematurity (%)	19 (46.3)	3 (20)	16 (61)	0.02*
Corrected age first MRI (weeks), mean (SD)	39.9 (2.2)	39.6 (2.3)	40.1 (2.1)	0.44
Cesarean section (%)	22 (53.7)	5 (33)	17 (65.4)	0.06
Twin pregnancy (%)	6 (14.6)	0 (0)	6 (23.1)	0.07
Apgar score 1' (%)[a]				0.75
<7	16 (40)	5 (33.3)	11 (42.3)	
7-10	24 (60)	9 (66.6)	15 (57.7)	
Apgar score 5' (%)[a]				1
<7	3 (7.5)	1 (7.1)	2 (7.7)	
7-10	37 (92.5)	13 (92.9)	24 (92.3)	
Imaging indication (%)				0.005*
Prenatal imaging abnormalities	11 (26.8)	7 (46.7)	4 (15.4)	
Neonatal complications	10 (24.4)	6 (40)	4 (15.4)	
Preterm screening	18 (43.9)	2 (13.3)	16 (61.5)	
Congenital CMV infection	2 (4.9)	0 (0)	2 (7.7)	
Multiple DVA (%)	8 (19.5)	7 (46.7)	1 (3.8)	0.002*
Craniofacial vascular lesions (%)	5	4[b]	1[b]	0.02*

Legend: c-DVA: Complicated DVA, u-DVA Uncomplicated DVA; DVA: Developmental Venous Anomaly, IQR: Interquartile range, SD- Standard deviation

[a]Apgar score is missing in 1 newborn

[b] Including one patient with diagnosis of Cerebrofacial Metameric Venous Syndrome

[c] P values for group comparisons were determined by Chi-Square of Fisher exact tests (as appropriate) for categoric variables and by independent sample t test for continuous variables

*Value statistically significant (P<0.05)

Figures and Legends

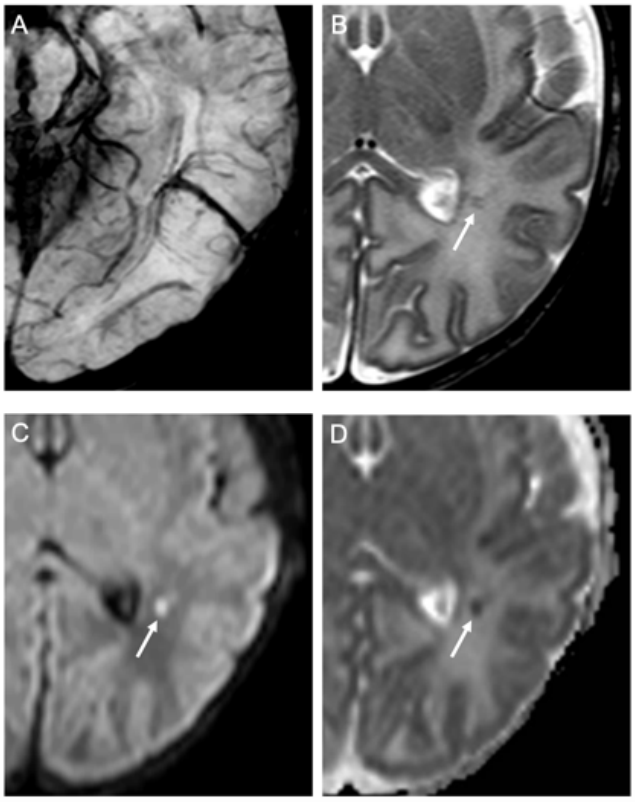

Figure 2.1. Neonatal developmental venous anomaly complicated by focal areas of venous ischemia. A) Axial SWI image shows a left parietal developmental venous anomaly with superficial drainage. B) Axial T2WI reveals small linear hypointense lesions in the surrounding white matter (*arrow*), with corresponding hyperintensity on b1000 images (C, *arrow*) and low apparent diffusion coefficient (ADC) values on ADC map (D, *arrow*).

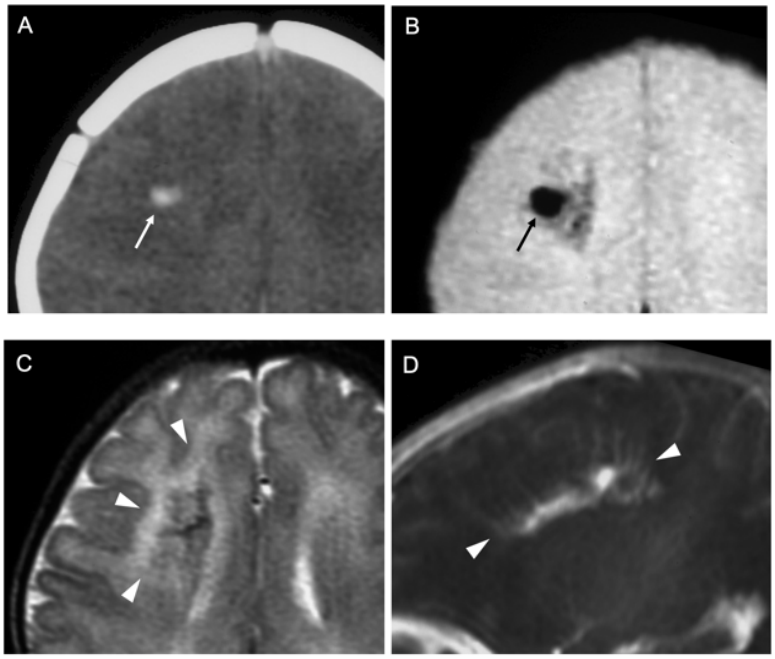

Figure 2.2. Neonatal developmental venous anomaly complicated by focal hemorrhage and diffuse WM signal abnormalities likely related to venous congestion. A) Unenhanced head CT scan demonstrates a focal area of spontaneous hyperdensity (*white arrow*) in the right frontal region, suggestive of recent hemorrhage. Corresponding axial gradient echo T2*-weighted image (B) and T2WI (C) show a blooming artifact (*black arrow*) in the region corresponding to the hemorrhage, that subsequently regressed (not shown), and diffuse hyperintensity of the surrounding WM (*arrowheads*) in keeping with venous congestion. D) Sagittal contrast-enhanced T1WI reveals a large developmental venous anomaly characterized by several radially-oriented dilated veins with a *caput medusae* morphology and deep venous drainage (*arrowheads*).

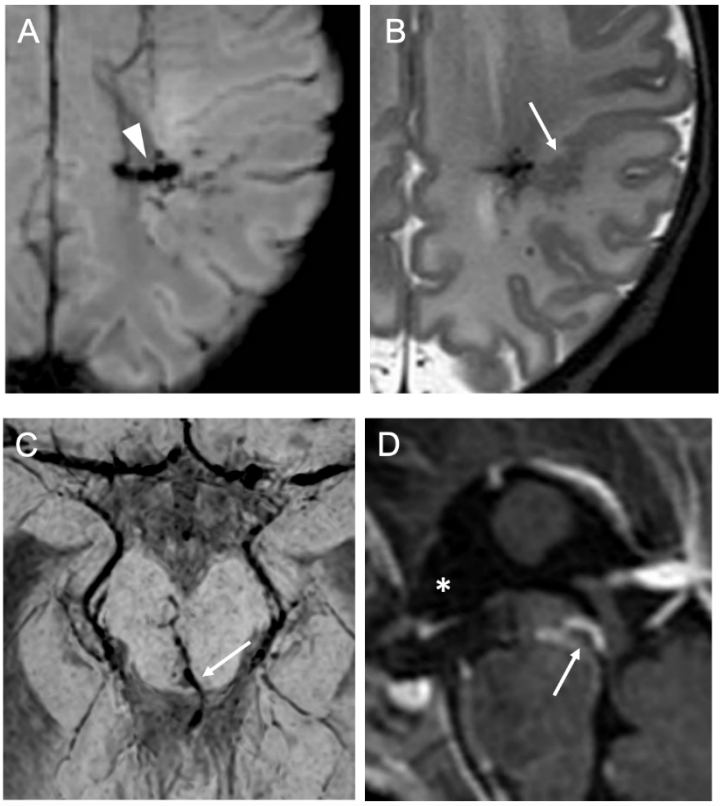

Figure 2.3. Neonatal developmental venous anomalies associated with focal polymicrogyria (A-B) and supratentorial hydrocephalus (C-D) in two different patients. Axial SWI (A) and T2WI (B) depict a developmental venous anomaly with deep venous drainage (*arrowhead*) and an adjacent area of cortical abnormality consistent with focal polymicrogyria (*arrow*). C) Axial SWI and D) sagittal post-gadolinium T1WI demonstrate a mesencephalic developmental venous anomaly with the venous collector (*arrows*) causing focal compression of the inferior third of the cerebral aqueduct and consequent dilatation of the anterior recesses of the III ventricle (*asterisks*) in keeping with supratentorial obstructive hydrocephalus (see also **Supplemental Figure 2.8**).

Case series

 # Case 1

Male term newborn with prenatal detection of an interhemispheric venous varix with signs of thrombosis **(Supplemental Fig. 2.1)**. A large right frontal DVA draining into this secondary partially thrombosed venous varix was diagnosed on postnatal MRI performed at 38.6 weeks corrected age **(Supplemental Fig. 2.2 A-E)**. DSA confirmed the characteristic appearance of a *caput medusae* in the corresponding region without associated arteriovenous shunting, draining into the inferior sagittal sinus through the venous varix **(Supplemental Fig.2.2 F,G)**. Long-term anticoagulation was initiated. White matter signal abnormalities in the draining territory of the DVA were more evident around the age of 2 months **(Supplemental Fig. 2.3 A-C)** and gradually decreased on follow-up MRI scans. At last brain MRI performed at 7.2 years the patient showed complete resolution of parenchymal signal changes **(Supplemental Fig. 2.3 D-F)** with normal ASL signal in that region **(Supplemental Fig. 2.3 H)**. Total recanalization of the interhemispheric venous varix was also depicted, with corresponding reduction in caliber **(Supplemental Fig. 2.3 D,G,I).** Neurological examination performed at last clinical follow-up was normal.

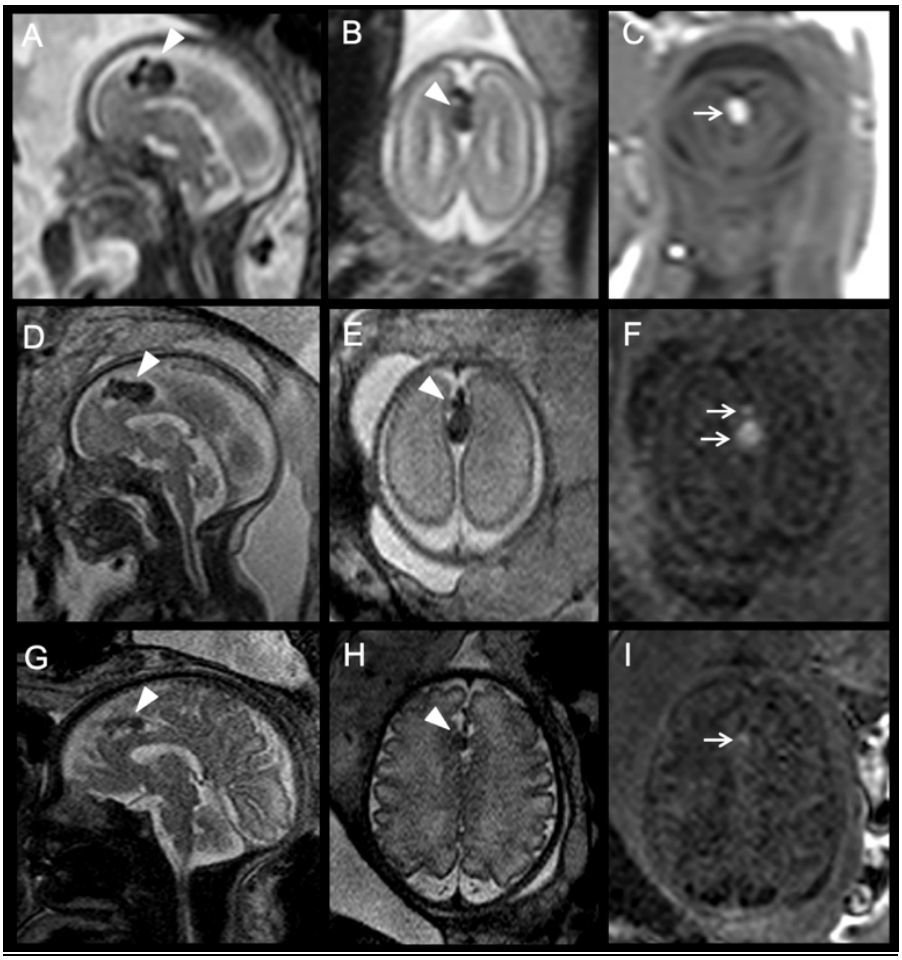

Supplemental Figure 2.1. Fetal MRI of patient #1 performed at 20 (A-C), 24 (D-F) and 32 (G-I) weeks of gestational age. Single-shot FSE T2WI (A,B,D,E,G,H) and T1WI (C,F,I) demonstrate a dilated vascular structure in the anterior interhemispheric fissure, compatible with a venous varyx (*arrowheads*), with signs of thrombosis that progressively reduced in size over time (*arrows*).

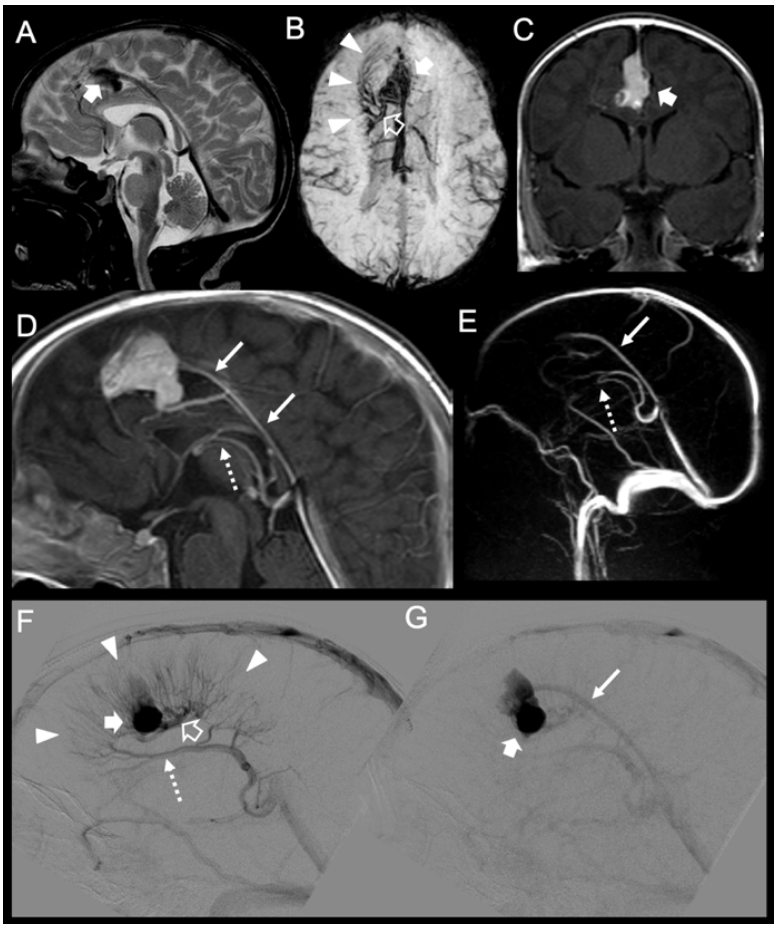

Supplemental Figure 2.2. Post-natal brain MRI and DSA of patient #1. A) Sagittal T2WI, B) axial SWI, C) coronal and D) sagittal contrast-enhanced T1WI, E) MRV, and F,G) DSA, sagittal angiograms in the venous phase. There are multiple dilated veins with a caput medusae morphology (*arrowheads*) in the right frontal lobe radially converging into a large transmedullary collector vein (*empty arrows*), that in turn drains towards a partially thrombosed median varyx (*thick arrows*) and then to the inferior sagittal sinus (*arrows*). Note an additional venous collector draining into the right internal cerebral vein (*dotted arrows*).

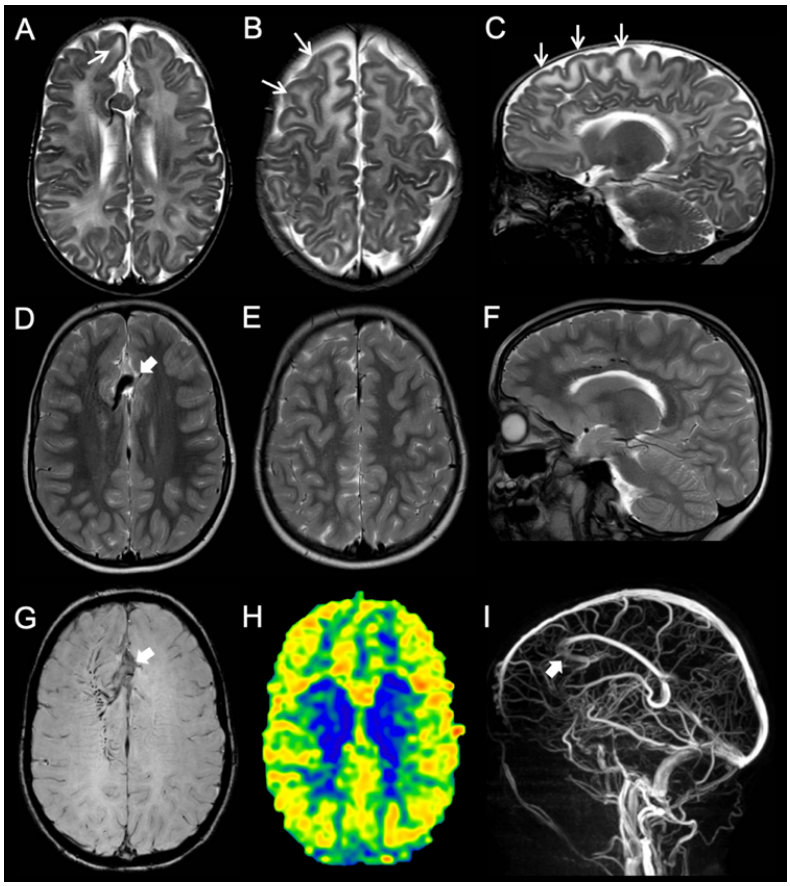

Supplemental Figure 2.3. Follow-up brain MRI of patient #1 performed at 2 months (A-C) and 7 years of age (D-I). A,B) Axial and C) sagittal T2WI demonstrate increased signal in the WM surrounding the right frontal developmental venous anomaly when compared with the remainder cerebral parenchyma (*arrows*). Corresponding axial T2WI (D,E), sagittal T2WI (F) and SWI (G) images performed at 7 years of age show complete resolution of WM signal abnormalities and progressive reduction in size of the interhemispheric venous varyx (*thick arrows*). H) Axial 3D pseudo-continuous arterial spin labeling map depicts symmetric perfusion of the frontal parenchyma. I) MRV, sagittal view, reveals venous flow signal in the draining varix, confirming almost complete resolution of the venous thrombosis (*thick arrow*).

 # Case 2

Male term newborn with respiratory distress after birth. Postnatal US identified a linear hyperechogenic focus in the left parietal region suggestive of DVA **(Supplemental Fig. 2.4 A,B)**. Brain MRI performed at 38.7 weeks corrected age confirmed the diagnosed and depicted foci of restricted diffusion and small hemorrhages in the surrounding parenchyma. A focal area of polymicrogyria was also noted in the DVA cortical drainage territory **(Supplemental Fig. 2.4 C-H)**. Follow-up brain MRI after 2 months demonstrated resolution of the areas of restricted diffusion. Neurological examination at 2.5 years was normal and no seizures were reported.

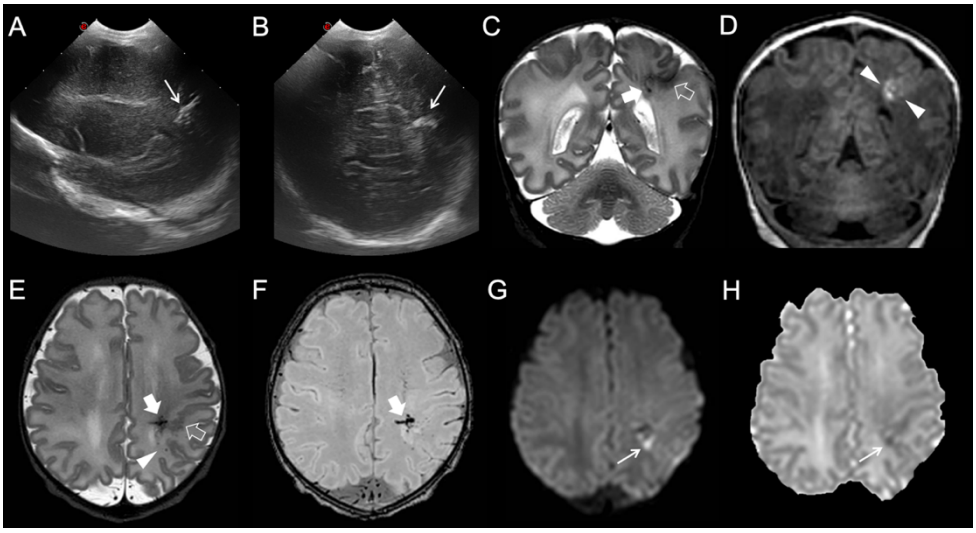

Supplemental Figure 2.4. Neonatal cerebral US (A,B) and brain MRI (C-H) of patient #2. A) Sagittal and B) coronal cerebral ultrasonograms identify a linear hyperechogenicity in the left parietal region (*thin arrows*) raising the suspicion of a developmental venous anomaly. Coronal T2WI (C) and T1WI (D) and axial T2WI (E) and SWI (F) images confirm a developmental venous anomaly with deep drainage (*thick arrow*) and adjacent focal polymicrogyria (*empty arrow*). Note the presence of punctate hemorrhages, hyperintense on T1WI and hypointense on T2WI, in the same region (*arrowheads*). Axial DWI (G) and ADC map (H) show additional foci of restricted diffusion in the draining territory of the developmental venous anomaly (*thin arrows*).

 # Case 3

Female term newborn with prenatal detection of hemorrhage involving the vermis and right cerebellar region (**Supplemental Fig. 2.5 A-D**), which was confirmed on postnatal MRI performed at 39.9 weeks corrected age (**Supplemental Fig. 2.5 E-J**). Neuroimaging follow-up during the first months of life revealed progressive resorption of the hemorrhagic component, with identification of a subjacent diffuse left cerebellar developmental venous anomaly and adjacent dystrophic calcifications **(Supplemental Fig. 2.5 K)**. Multiple CCMs were also detected in the cerebellum and brainstem. DSA confirmed presence of contrast medium staining in the venous phase in the vermis and left cerebellar hemisphere in keeping with a diffuse cerebellar DVA draining into both the superficial and deep venous system **(Supplemental Fig. 2.5 L)**. At 3 months of age, brain MRI showed the presence of a new vascular mass-like lesion at the level of the superior vermis, characterized by small hemorrhages and inhomogeneous contrast enhancement **(Supplemental Fig. 2.6)**, that slowly spontaneously regressed over the following months. Last follow-up MRI performed at 3 years of age showed further signs of interval improvement both regarding cerebellar hemorrhages and vermian vascular lesion, with only mild gliotic cerebellar changes, stable dystrophic calcifications and CCMs **(Supplemental Fig. 2.7)**. Clinical follow-up at the same age revealed mild neurological impairment (broad based gait).

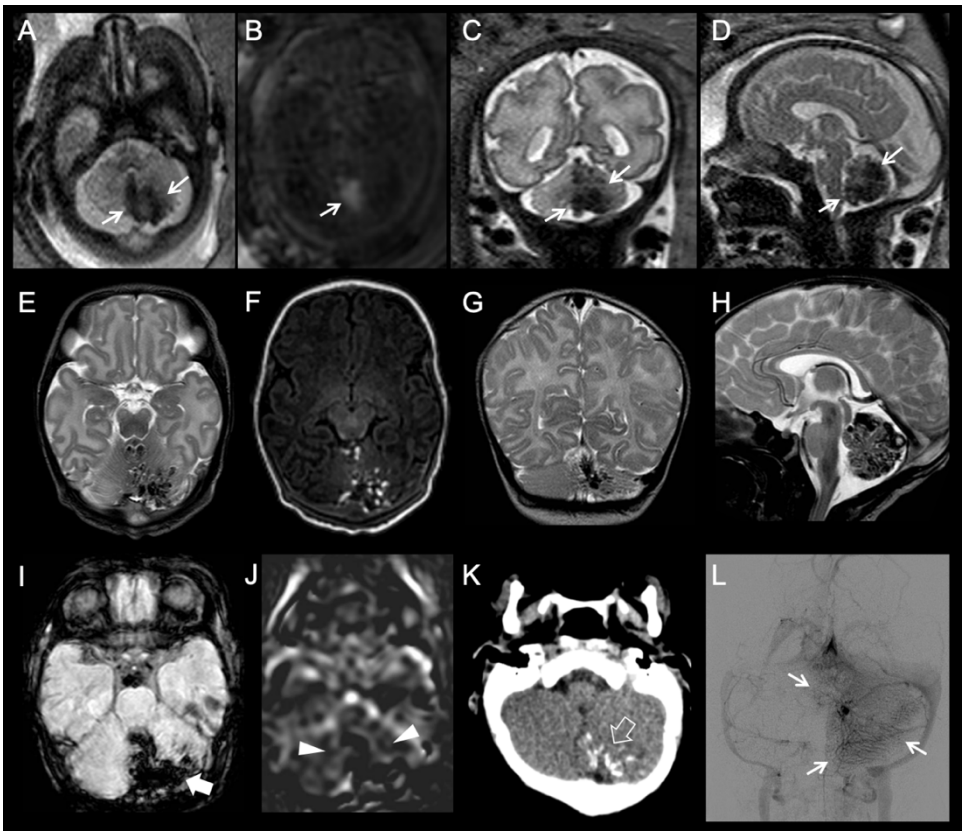

Supplemental Figure 2.5. Fetal MRI of patient #3 performed at 31 weeks of gestation (A-D); axial single-shot FSE T2WI (A), axial T1WI (B), coronal (C) and sagittal (D) single-shot FSE T2WI. There is a lobulated T2-hypointense and T1-hyperintense lesion in the vermis and left cerebellar hemisphere suggestive of parenchymal hemorrhage (*arrows*). **Postnatal brain MRI performed at 6 days of age (E-J);** axial T2WI (E), T1WI (F), coronal (G) and sagittal (H) T2WI, axial SWI (I), and 3D pseudo-continuous arterial spin labeling (J). Several confluent T2-hypointense and T1-hyperintense hemorrhagic lesions with a *salt and pepper* pattern are better appreciated in the cerebellum. There is an extensive blooming artifact on SWI (*thick arrow*), without increased ASL signal (*arrowheads*). K) Unenhanced head CT scan demonstrates multiple calcifications in the inferomedial left cerebellar region (*empty arrow*). L) Coronal DSA in the late venous phase depicts persistent staining in the left cerebellar region, compatible with an underlying large diffuse developmental venous anomaly (*arrows*).

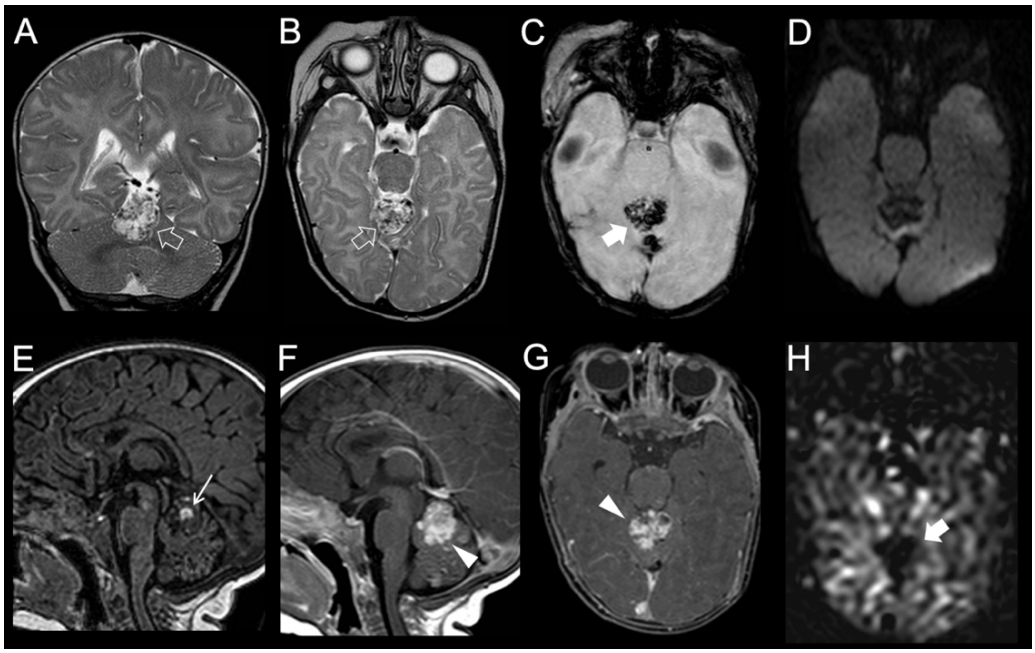

Supplemental Figure 2.6. Follow-up brain MRI of patient #3 performed at 3-months of age. Coronal (A) and axial (B) T2WI identify a new, heterogeneous expansive lesion in the superior vermis (*empty arrows*) with associated blooming artifact on axial SWI (C, *thick arrow*). This mass does not present hyperintensity of DWI b1000 images (D), but a focal inner area of spontaneous hyperintensity is detected on sagittal T1-weighted images (E, *arrow*). Post-gadolinium sagittal (F) and axial (G) T1WI show intense enhancement of this likely vascular pseudo-mass (*arrowheads*). H) 3D Pseudo-continuous ASL reveal reduced signal within the superior vermian lesion (*thick arrow*) and no areas of increased signal in the surrounding cerebellar parenchyma.

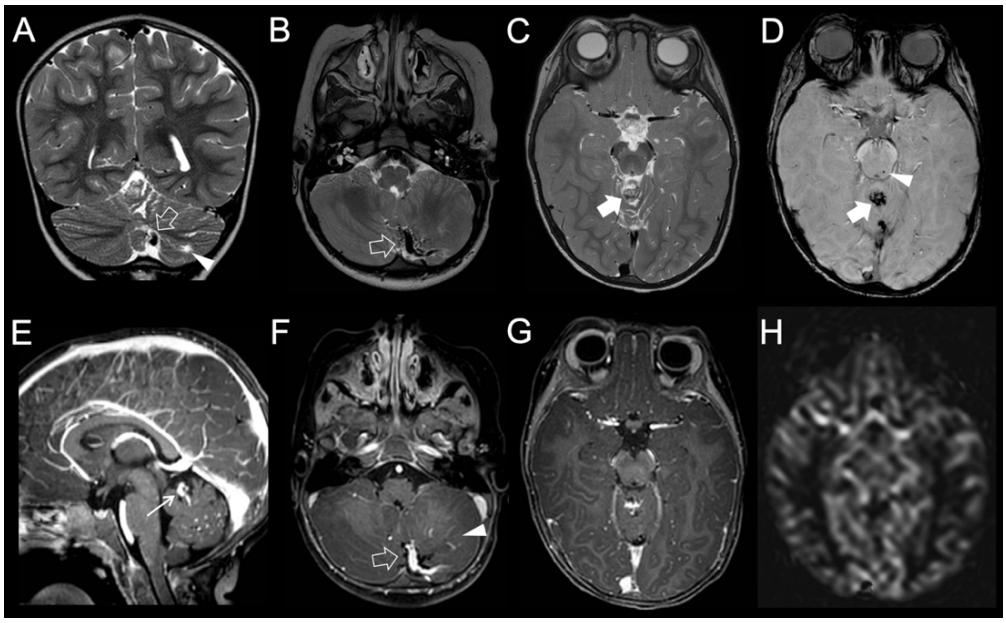

Supplemental Figure 2.7. Last brain MRI of patient #3 performed at 3-years of age. Coronal (A) and axial (B) T2WI demonstrate complete regression of the multiple cerebellar hemorrhagic lesions with residual gliotic changes in the left cerebellar hemisphere (*arrowhead*). A large DVA venous collector is now visible (*empty arrows*). Axial T2WI (C) and SWI (D) at a higher level and contrast-enhanced sagittal T1WI (E) reveal spontaneous subtotal regression of the vascular pseudo-mass with a small residual nodular lesion characterized by hemosiderin deposits (*thick arrow*) and contrast enhancement (*arrow*). Note the small cavernoma in the left posterior midbrain (*arrowhead*). F, G) After gadolinium injection, the left cerebellar venous radicles (*arrowheads*) and major collector (*empty arrow*) of this developmental venous anomaly draining to the left transverse sinus are better depicted. H) 3D pseudo-continuous ASL confirms no increased signal at the level of the residual superior vermian mass-like lesion.

Case #4

Female term baby with prenatal detection of ventriculomegaly. Postnatal US revealed progressive triventricular hydrocephalus. Brain MRI performed at 42 weeks corrected age identified a mesencephalic DVA with deep drainage as the obstructive cause of the sylvian aqueduct **(Supplemental Fig. 2.8 A-F)**, without other associated abnormalities. Endoscopic third ventriculostomy was performed and longitudinal follow-up at 3.7 years revealed normalization of the ventricular size **(Supplemental Fig. 2.8 G-I)** and normal neurological examination.

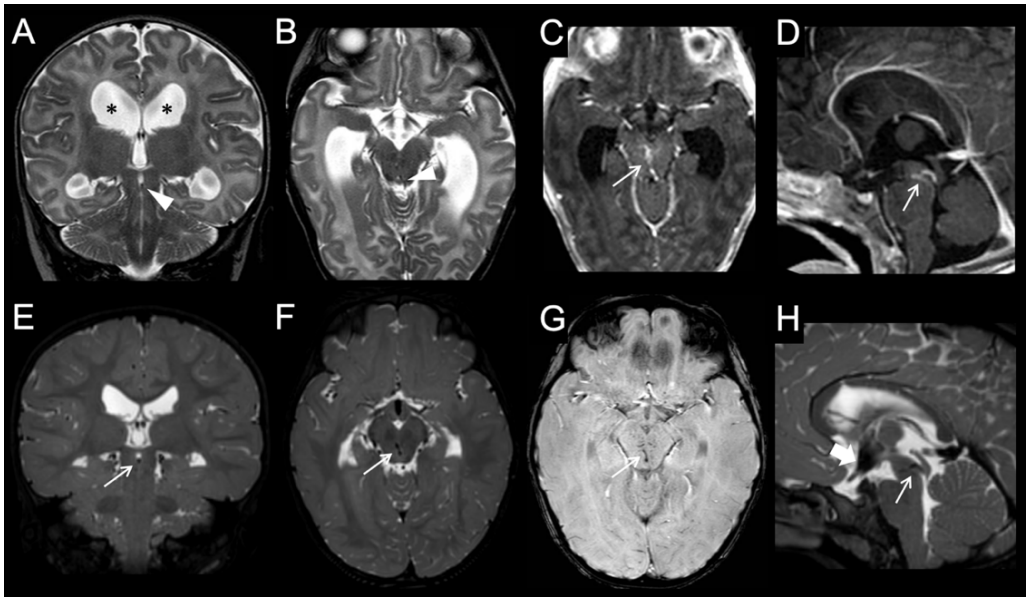

Supplemental Figure 2.8. Neonatal brain MRI of patient #4 (A-D). Coronal (A) and axial (B) T2WI depicts diffuse enlargement of the supratentorial ventricular system (*asterisks*), in keeping with obstructive hydrocephalus. There is also absence of the normal CSF flow signal within the cerebral aqueduct, with a small vascular flow void in the inferior aqueduct (*arrowheads*). C-D) On post contrast T1WI small venous radicles and a slightly more dilated venous collector are depicted in the mesencephalon (*arrows*), in keeping with a DVA causing focal aqueductal obstruction. **Post endoscopic third-ventriculostomy brain MRI performed at 3.7 years of age (E-H).** Coronal (E), axial (F) and sagittal (H) 3D T2WI reformats and axial SWI (G) confirm the presence of the mesencephalic developmental venous anomaly (*arrows*), and show interval resolution of the supratentorial hydrocephalus. A prominent CSF flow void is evident in the III ventricle floor in keeping with patency of the third-ventriculostomy (*thick arrow*).

 # Case 5

Female term newborn with prenatal detection of a dural sinus malformation without associated signs of thrombosis **(Supplemental Fig. 2.9 A-D)**. At birth, a right facial and orbital venous malformation was noted. Postnatal MRI performed at 42 weeks corrected age and follow-up MRI studies confirmed the presence of dural sinus malformation, that spontaneously regressed

over the months, and revealed additional venous lesions with a segmental distribution, including DVA (distributed in the cerebral hemispheres bilaterally and in the right cerebellar hemisphere) with venous congestion in the right temporal lobe and CCM **(Supplemental Fig. 2.9 E-H)**. Based on the type and segmental distribution of the vascular lesions, the diagnosis of CVMS type 2 was assumed. At the age of 2.5 years, the orbital venous malformation was complicated by massive hemorrhage and there was a suspicion of an associated high-low AVM on MRA **(Supplemental Fig. 2.10)**. DSA confirmed the presence of a right superior orbital fissure AVF **(Supplemental Fig. 2.10)**, that was treated with multiple embolization procedures as well as the facial venous malformation with several sessions of sclerotherapy. Longitudinal neuroimaging assessment at 8.2 years showed mixed evolution of brain DVA complications, including interval reduction of WM abnormalities with residual small focal gliosis in the right temporal lobe and interval growth of supratentorial CCM (**Supplemental Fig. 2.11**). Neurological examination at that age was normal.

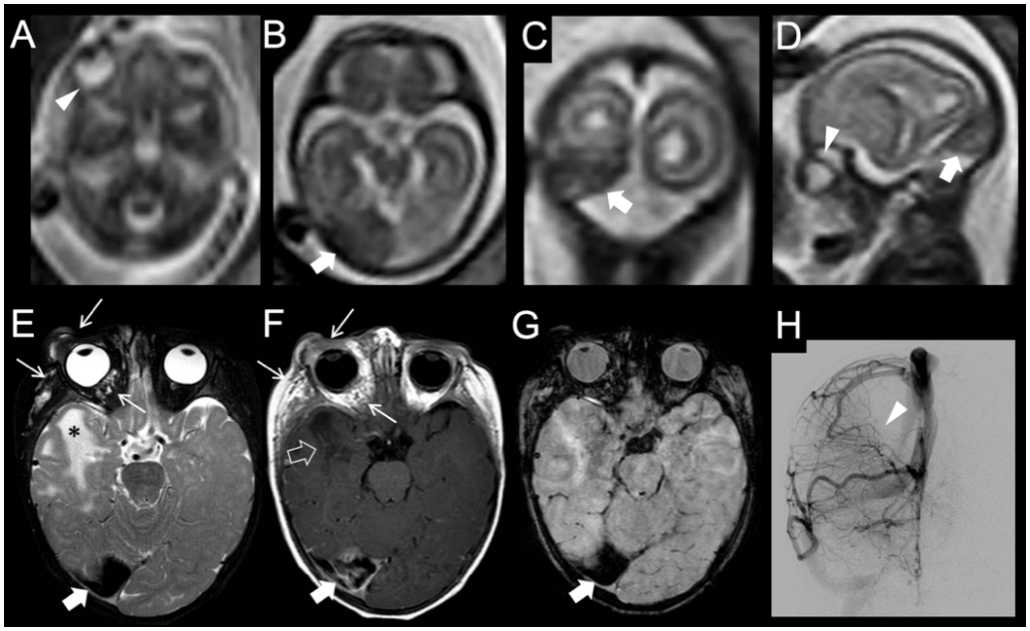

Supplemental Figure 2.9. Fetal MRI of patient #5 performed at 20 weeks of gestational age (A-D). Axial (A-B), coronal (C) and sagittal single-shot FSE T2WI identify a markedly enlarged right transverse sinus in keeping with a dural sinus malformation (*thick arrows*), without features suggestive of intraluminal thrombosis. Note the mild right proptosis (*arrowheads*). **Neonatal brain MRI of the same patient (E-H).** Axial T2WI (E), contrast-enhanced T1WI (F) and SWI (G) images show marked reduction of the dural sinus malformation (*thick arrows*) and additionally demonstrate venous malformations in the right intra-orbital, periorbital and masticatory spaces (*arrows)*. Increased T2 hyperintensity in the right temporal white matter is also depicted (*asterisks*) associated with small dilated veins corresponding to the *caput medusae* (*empty arrow*). H) DSA in the venous phase, coronal view, demonstrates patency of the enlarged right transverse sinus as well as persistent staining in the right parietal region consisting of radially oriented veins converging into a single collector draining into the deep venous system compatible with a developmental venous anomaly (*arrowhead*).

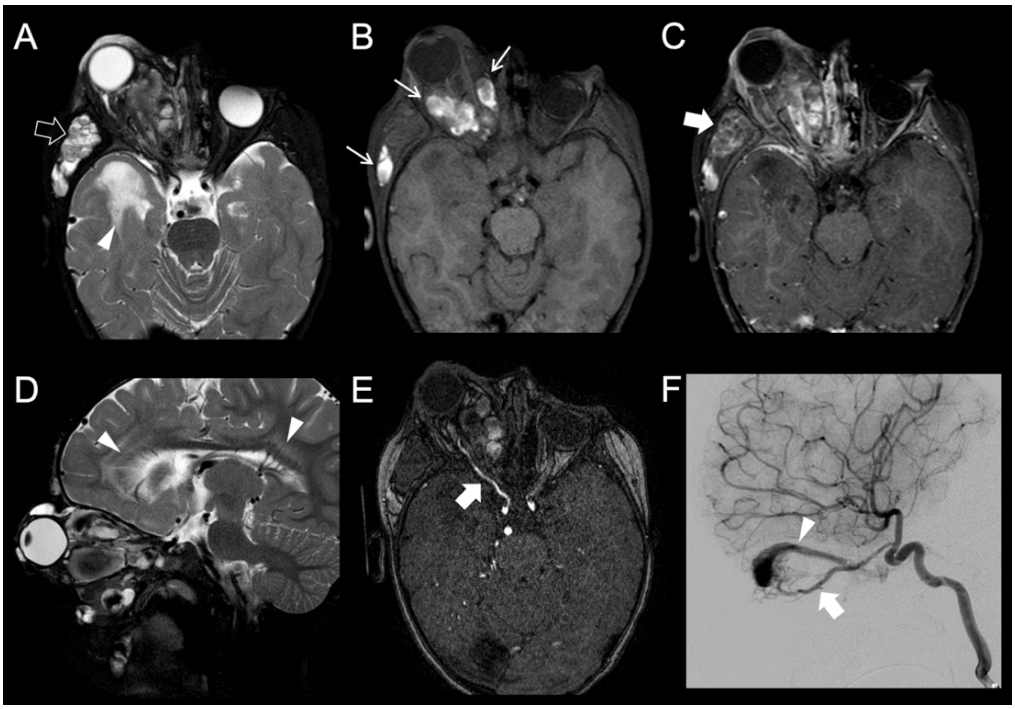

Supplemental Figure 2.10. Follow-up brain MRI of patient #5 performed at 2.5 years of age. Axial T2WI (A) as well as fat-saturated pre (B) and post-contrast (C) T1WI demonstrate marked enlargement of the facial/orbital venous-lymphatic malformations, leading to grade III right proptosis, mostly due to hemorrhagic evolution, with components characterized by multiple fluid-fluid levels (*empty arrow*), spontaneous T1-hyperintensity (*arrow*s), and inhomogeneous contrast enhancement (*thick arrow*). Note the persistence of T2-hyperintensity in the right temporal WM and periventricular fronto-parietal regions (*arrowheads*). E) Time-of-flight MRA reveals enlargement of the right ophthalmic artery indicative of an intraorbital arteriovenous shunt. F) DSA in the arterial phase, sagittal view, confirms dilatation of the right ophthalmic artery (*arrowhead*) with early filling of an intraorbital venous varyx and ophthalmic vein (*thick arrow*) into the ipsilateral cavernous sinus.

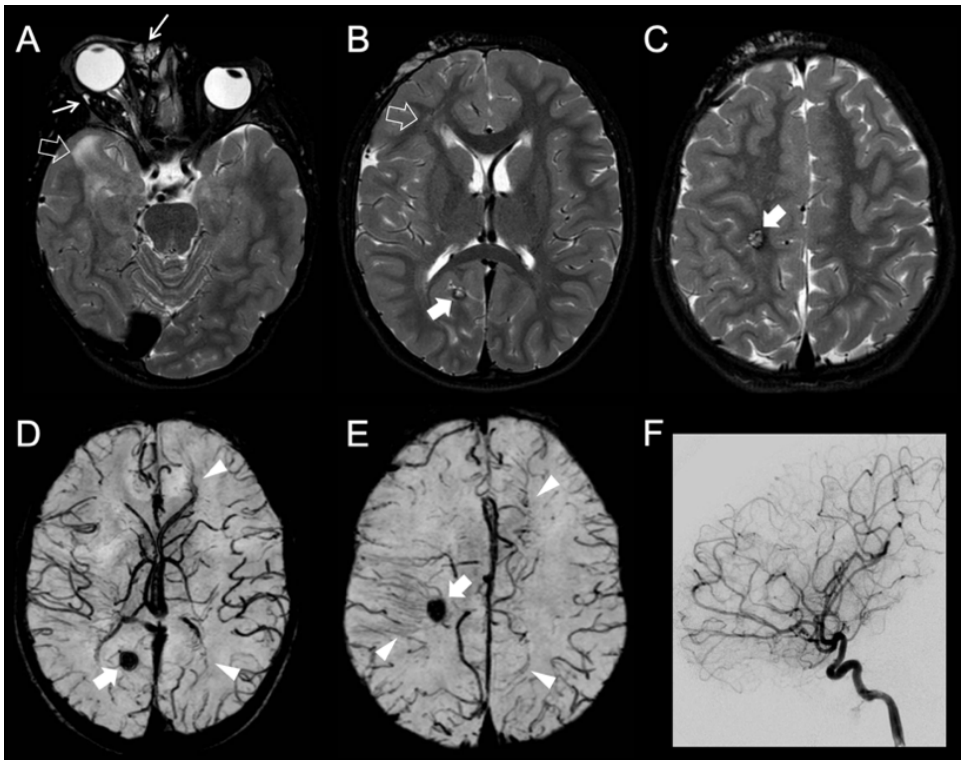

Supplemental Figure 2.11. Last brain MRI of patient #5 performed at 8 years of age, after multiple endovascular and percutaneous procedures; axial fat-saturated T2WI (A-C) and SWI (D, E). There is marked interval reduction in size of the right facial/orbital venous malformations (*arrows*) and right proptosis. The WM signal abnormalities have also partially regressed (*empty arrows*). Cerebral cavernous malformations are depicted in the right occipital and parietal regions (*arrows*). Multiple areas of dilated veins with a caput medusae morphology are detected in the right fronto-parietal region and left mesial frontal and parietal regions (*arrowheads*), corresponding to multiple bilateral hemispheric developmental venous anomalies. F) DSA in the arterial phase, sagittal view, reveal complete occlusion of the arteriovenous fistula.

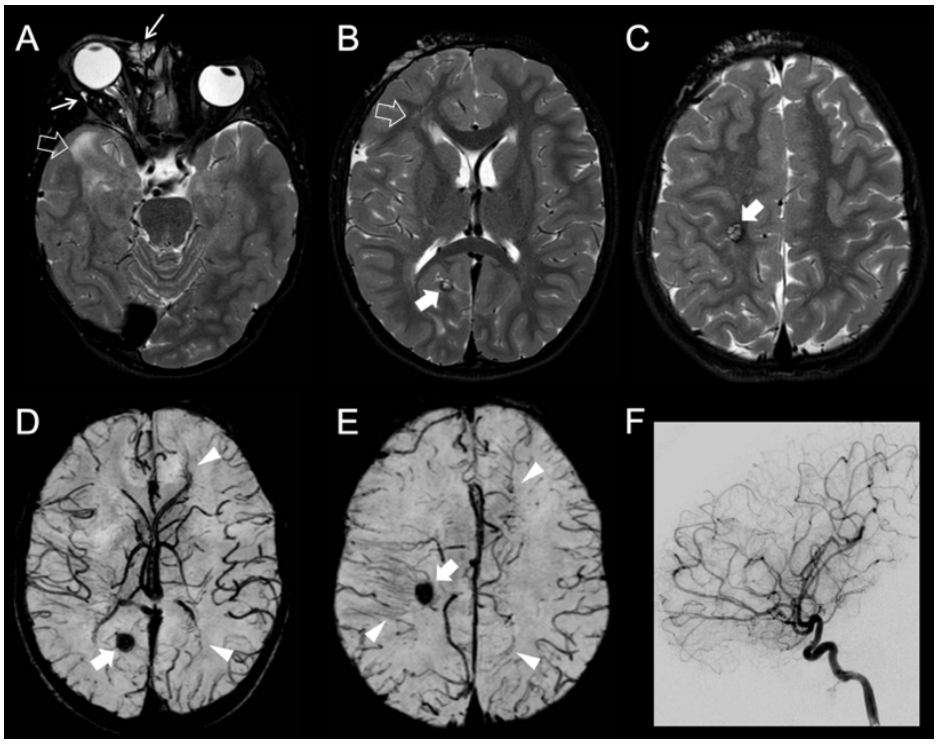

Supplemental Figure 2.12. Last brain MRI of patient #5 performed at 8 years of age, after multiple endovascular and percutaneous procedures; axial fat-saturated T2WI (A-C) and SWI (D, E). There is marked interval reduction in size of the right facial/orbital venous malformations (*arrows*) and right proptosis. The WM signal abnormalities have also partially regressed (*empty arrows*). Cerebral cavernous malformations are depicted in the right occipital and parietal regions (*arrows*). Multiple areas of dilated veins with a caput medusae morphology are detected in the right fronto-parietal region and left mesial frontal and parietal regions (*arrowheads*), corresponding to multiple bilateral hemispheric developmental venous anomalies. F) DSA in the arterial phase, sagittal view, reveal complete occlusion of the arteriovenous fistula.

 # Case 6

Female term newborn with mild signs of hypoxic-ischemic encephalopathy. Brain MRI and head CT performed at 39 weeks corrected age revealed cerebral bi-hemispheric DVA with diffuse T2* hypointensity and hyperdensity of the right fronto-parietal and left parietal WM (**Supplemental Fig,13 A-D).** Follow-up brain MRI and head CT performed at 11 months demonstrated almost complete regression of the T2* signal alterations with bilateral scattered areas of WM gliosis in the cerebral hemispheres, without associated calcifications **(Supplemental Fig,13 E-H)**. Neurological examination revealed moderate developmental delay.

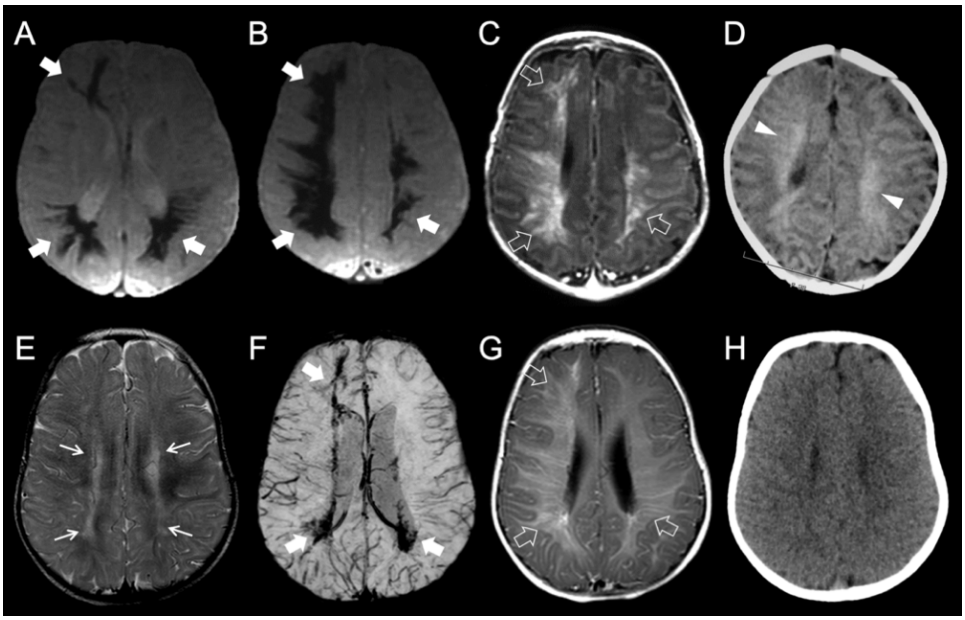

Supplemental Figure 2.13. Brain MRI and CT scan of patient #6 at diagnosis (A-D) and at 11 months of age (E-H). Axial gradient echo T2*WI (A,B) and contrast-enhanced T1WI (C) reveal multiple large developmental venous anomalies, diffusively involving the right cerebral hemisphere and the left parietal region with corresponding contrast enhancement (*empty arrows*) and extensive T2* hypointensity (*thick arrows*) in the cerebral white matter. D) Unenhanced head CT scan demonstrates bilateral cerebral white matter hyperdensity (*arrowheads*). E-G) Follow-up MRI at 11 months of age shows faint areas of increased periventricular and deep white-matter T2 hyperintensity (*arrows*), compatible with residual gliosis. There is also marked reduction of blooming artifact and contrast-enhancement depicted on SWI (F, *thick arrows*) and post-gadolinium T1WI (G, *empty arrows*), respectively. H) Unenhanced head CT scan depicts normalization of cerebral WM density, without evident calcifications.

 # Case 7

Female born preterm at 28 weeks gestational age due to premature rupture of the membranes (<12 hours) from vaginal birth. Pregnancy was not expected, with a history of smoking, alcohol consumption, use of ibuprofen, ketoprofen and anticonception pill. Brain MRI was performed at 33 weeks corrected age due to postnatal detection of right parietal linear hyperechogenic focus in keeping with DVA on cUS, and confirmed the presence of a parietal DVA with associated venous ischemic WM lesions and polymicrogyria. Other focal areas of polymicrogyria were also noted as well as open-lips schizencephaly bordered by hemosiderin and partial septum pellucidum agenesis **(Supplemental Fig. 2.14)**.

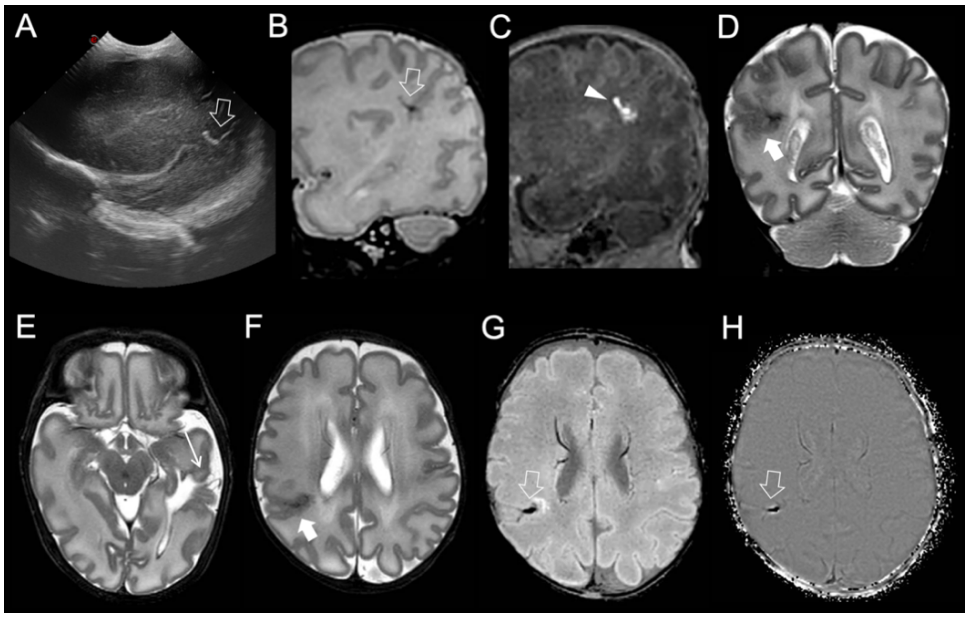

Supplemental Figure 2.14. Cerebral ultrasound (A) and brain MRI (B-H) of patient #7. A) Sagittal cerebral ultrasonogram performed shortly after birth identifies a linear hyperechogenicity in the right parietal region (*empty arrow*), raising the suspicion of a DVA. Sagittal T2WI (A) and T1WI (B) confirm the presence of a DVA with superficial venous drainage (*empty arrow*), as well as adjacent foci of microhemorrhage (*arrowhead*). Coronal (D) and axial (E, F) T2WI reveal a focal area of polymicrogyria at the same level (*thick arrows*), associated with an open-lip schizencephaly in the left temporal region (*arrow*). Axial SWI (G) and phase map (H) show the dilated DVA draining collector (*empty arrows*), without associated calcifications.

PART III- SPINAL INVOLVEMENT IN PEDIATRIC FAMILIAL CAVERNOUS MALFORMATION SYNDROME

Ana Filipa Geraldo[1,2], Aysha Luis[3,4], Cesar Augusto P. F. Alves[5], Domenico Tortora[6], Joana Guimarães[7,8], Sofia Reimão[2,9,10], Marco Pavanello[11], Patrizia de Marco[12], Marcello Scala[13,14], Valeria Capra[12], Andrea Rossi[6,15], Erin Simon Schwartz[5], Kshitij Mankad[3], Mariasavina Severino[6]

[1] Diagnostic Neuroradiology Unit, Department of Radiology, Centro Hospitalar Vila Nova de Gaia/Espinho (CHVNG/E), Vila Nova de Gaia, Portugal
[2] Clínica Universitária de Imagiologia, Faculty of Medicine of the University of Lisbon, Portugal
[3] Department of Radiology, Great Ormond Street Hospital for Children NHS Foundation Trust, London, UK
[4] Department of Radiology, King´s College London, London, UK
[5] Department of Radiology, Children's Hospital of Philadelphia, Philadelphia, PA, USA
[6] Neuroradiology Unit, IRCCS Istituto Giannina Gaslini, Genova, Italy
[7] Department of Neurology, Centro Hospitalar Universitário de São João, Porto, Portugal
[8] Department of Clinical Neusosciences and Mental Health, Faculty of Medicine of the University of Porto, Portugal
[9] Neurological Imaging Department, Hospital de Santa Maria, Lisbon, Portugal
[10] Laboratory of Clinical Pharmacology and Therapeutics, Instituto de Medicina Molecular, Faculty of Medicine of the University of Lisbon, Portugal
[11] Neurosurgery Unit, IRCCS Istituto Giannina Gaslini, Genova, Italy
[12] Medical Genetics Unit, IRCCS Istituto Giannina Gaslini, Genova, Italy
[13] Department of Neurosciences, Rehabilitation, Ophthalmology, Genetics, Maternal and Child Health, Università Degli Studi di Genova, Genoa, Italy.
[14] Pediatric Neurology and Muscular Diseases Unit, IRCCS Istituto Giannina Gaslini, Genoa, Italy
[15] Department of Health Sciences (DISSAL), University of Genoa, Genoa, Italy

Abstract

Purpose: The aim of the study was to assess the prevalence and characteristics of spinal cord cavernous malformations (SCCM) and intraosseous spinal vascular malformations (ISVM) in a pediatric familial cerebral cavernous malformation (FCCM) cohort and evaluate clinico-radiological differences between children with (SCCM+) and without (SCCM-) SCCM.

Methods: All patients with a pediatric diagnosis of FCCM evaluated at three tertiary pediatric hospitals between January 2010 and August 2021 with ≥1 whole spine MR available were included. Brain and spine MR studies were retrospectively evaluated, and clinical and genetic data collected. Comparisons between SCCM+ and SCCM- groups were performed using student-t/Mann-Whitney or Fisher exact tests, as appropriate.

Results: Thirty-one children (55% boys) were included. Baseline spine MR was performed (mean age= 9.7 years) following clinical manifestations in one subject (3%) and as a screening strategy

in the remainder. Six SCCM were detected in five patients (16%), in the cervico-medullary junction (n=1), cervical (n=3), and high thoracic (n=2) regions, with one appearing during follow-up. A tendency towards an older age at first spine MR (P=0.14) and ≥1 posterior fossa lesion (P=0.13) was observed in SCCM+ patients, lacking statistical significance. No subject demonstrated ISVM.

Conclusion: Although rarely symptomatic, SCCM can be detected in up to 16% of FCCM patients using diverse spine MR protocols and may appear *de novo*. ISVM were instead absent in our cohort. Given the relative commonality of asymptomatic SCCM, serial screening spine MR should be considered in FCCM starting in childhood.

Abbreviations: CM- cavernous malformation, FCCM- familial cerebral cavernous malformation syndrome, ISVM- intraosseous spinal vascular malformations, SCCM- spinal cord cavernous malformation

Introduction

Familial cerebral cavernous malformation syndrome (FCCM) is an autosomal dominant inherited disorder with incomplete penetrance and high intra- and inter-familial phenotypical variability, caused by heterozygous germline loss-of-function pathogenic variants in either one of three genes complexes involved in the maintenance of endothelial integrity: *CCM1* (*KRIT1,* OMIM * 604214), *CCM2* (Malcavernin, OMIM * 607929), and *CCM3* (*PDCD10,* OMIM * 609118) [28]. Although this entity has been classically defined by the association of multiple cerebral cavernous malformations (CM) and a positive family history, it is now recognized as a multisystem, progressive disorder, with development of CM in multiple locations over time [185, 447]. In particular, spinal cord cavernous malformations (SCCM) are being increasingly reported in the setting of FCCM [175, 176, 185] most likely due to the combination of increasingly widespread MRI availability, improved imaging techniques, and a higher awareness of their possible occurrence. Similarly, it has been shown that a high percentage of patients of all ages (15-40%) presenting with a SCCM may harbor at least one similar intracranial lesion, supporting their association [173, 320, 448]. The spinal vascular lesions are histologically identical to their intracranial counterparts, and also have a propensity to enlarge and/or hemorrhage over time. However, their clinical and imaging features have been less thoroughly established in the literature, likely due to their rarity [170, 273, 318].

In addition to SCCM, vertebral intraosseous spinal vascular malformations (ISVM) have also been associated with FCCM in case reports and small case series [318], and recently in case-control and prospective studies [319–321].

Studies focusing on SCCM and other spinal abnormalities including ISVM in cohorts of pediatric-only FCCM patients are currently lacking, and previous evidence suggests that pediatric presentation and familiarity have the potential to influence the natural history of both cerebral CM and SCCM [173, 322]. Additional clinical and imaging data on these lesions would thus be valuable for the assessment of the prognosis of affected individuals and the development of potential imaging screening programs and imaging endpoints in future clinical trials, since medical therapies are already being investigated for CM [276, 277, 282]. Pharmacological agents are particularly appealing for children with FCCM, as preliminary data suggest that these compounds not only stabilize CM but also prevent their formation, which is known to be age-dependent [27, 29, 435].

The aim of our study was to assess the prevalence and characteristics of SCCM and ISVM in a

pediatric cohort of FCCM and to evaluate any clinico-radiological differences between patients with (SCCM+) and without (SCCM-) SCCM. We hypothesized that SCCM are common and already present during the pediatric age in FCCM, and that SCCM+ patients have a higher number of intracranial and extra-CNS CM.

Material and Methods

Population

We performed a multicenter retrospective study involving three tertiary pediatric centers. All consecutive patients with a diagnosis of FCCM during the childhood (<19 years) evaluated at least once in the participating hospitals between January 2010 and August 2021 and with at least one complete spine MRI available were identified. The diagnosis of FCCM was based on: 1) presence of ≥1 cerebral CM or SCCM associated with a positive family history (defined as presence of ≥1 known first or second-degree relative with a proven CM) and/or 2) a confirmed pathogenic variant in *CCM1-3* in the affected patient or in a first-degree relative [27, 29, 435]. Exclusion criteria included 1) history of prior radiation and 2) poor-quality spine MR images. IRB approval was obtained and written informed consent was waived because of the retrospective nature of the study. An overall outline of the study is displayed in **Figure 1**.

MRI technique and image analysis

We retrospectively reviewed all available spine MR of the included subjects. Images were acquired at either 1.5 or 3.0 Tesla using local imaging protocols, including some with images following administration of gadolinium-based contrast agents.

A structured list of SCCM imaging features (including size, location, and signal intensity with subsequent Zabramski type classification [173, 281], along with adjacent intramedullary hemorrhage, blood-fluid levels and spinal cord edema) was scored according to previously published criteria [305] in the first spine MR available for each subject. Presence, location and size of potential lesions compatible with ISVM was also searched as part of our methodologic strategy [317].

Evaluation of available longitudinal spinal MR was retrospectively performed to analyze for changes in any previously identified lesions as well as for development of new lesions. Lesions were regarded as *de novo* only if their new appearance could be demonstrated employing magnets of similar or lower field strength and with identical protocols.

The first available brain MR for each patient was also reviewed (assessing total number and location of cerebral CM on gradient recalled echo (GRE) T2* or SWI images) as well as any available body MR and/or CT scans. Symptomatic cerebral CM hemorrhage was defined according to previous guidelines [322] and a similar approach was used for SCCM.

At each of the three involved hospitals, imaging studies were initially analyzed by one rater (for a total of three raters with 1, 7 and 7 years of experience in pediatric neuroradiology, respectively), blinded to the clinical and genetic information. Subsequently, anonymized MR studies with questionable evaluation and spine MR images of SCCM+ patients were decided by final consensus of all three readers during scheduled monthly meetings.

Clinical data

Data on demographics, method, and age at clinical presentation leading to the FCCM diagnosis, ethnicity, family history (including number of affected family elements and degree of kinship), genotype, presence of other systemic CM (including cutaneous, retinal, or within solid organs) or any combined features of Greig cephalopolysyndactyly in the setting of a 7p deletion syndrome [240] were obtained from medical records. Age at first and last available spine MR, spinal signs and symptoms prior to the detection of SCCM (as classified per Ogilvy *et al*) [287], symptomatic neurological events attributable to SCCM during follow-up, as well as any performed brain or spinal surgery and final neurological outcomes (graded as normal, mild, moderate or severe impairment) were also recorded.

Statistical analysis

Quantitative data were presented as median and interquartile range, and categorical data as frequencies and percentages. Comparisons between SCCM+ and SCCM- patients were performed using student-t/Mann-Whitney or Fisher exact tests, as appropriate. Statistical analyses were performed by using SPSS Statistics software, v24.0 (IBM, Armonk, NY). The significance level was set at P=0.05.

Results

Clinical and genetic results

Fifty patients from 47 different families fulfilled the diagnostic criteria of FCCM. Thirty-one (62%) patients from 29 different families (55% male) had $\geq$1 whole spine MR for review and were

therefore included.

Clinical and genetic data are summarized in **Table 3.1**. Eighty-seven per cent of the cases (26/31) were Caucasian. No child had Hispanic ethnicity. There was a positive family history in 22/31 (71.0%) of patients, with multiple kindred involved in 10 (32.3%). Pathogenic variants in *CCM1, CCM2* and *CCM3* were respectively identified in 17 (54.8%), 6 (19.4%), and 6 (19.4%) cases or in a known first-degree relative. Four of the six (75%) of the *CCM2* patients were confirmed to have a 7p deletion, of which two had features of Greig cephalopolysyndactyly and neurodevelopmental delay.

The mean age at first clinical presentation leading to subsequent FCCM diagnosis was 6.9 years (SD=5.0; range 0.7-16.0 years), typically occurring in the context of a symptomatic hemorrhage associated with a CM located elsewhere in the CNS (17/31, 54.8%). Fifteen (48.4%) patients underwent ≥1 brain surgery (total=21 procedures, range: 0-3), before or after the first available spine MR. No subjects in our cohort underwent spinal surgery. All patients were alive at clinical follow-up (median=24.0 months; range: 15-57) and 20/31 (64.5%) remained neurologically intact at their last clinical visit. However, mild to severe neurologic impairment was present in the remainder, due to intracranial hemorrhagic complications and/or refractory epilepsy, either due to the coexistent cerebral CM or in the context of 7p deletion-associated developmental delay.

Spine MRI findings

A total of 54 spine MR were reviewed, of which 9 (16.7%) performed on a 3.0T. T2 TSE, T1 TSE and/or GRE sequences were included in 47/54 (87%), 46/54 (85%) and 24/54 (44%) of all spine MR examinations, respectively. Overall, 45% of the subjects had at least one available spine MR with a GRE sequence for review. Gadolinium was injected in 3/54 (6%) spine MR studies.

Mean age at first available spine MR was 9.7 years (SD=5.1; range 0.8-18.9 years). Baseline spine imaging was performed due to acute medullary symptoms (Ogilvy type C) in one case (3%), representing the clinical presentation that eventually led to the diagnosis of FCCM in that patient. In the remainder cases (30/31;97%), spine MR was initially performed as a screening strategy in patients that had no related symptoms (corresponding to Ogilvy type E) when FCCM was already confirmed or suspected.

Retrospective longitudinal spine MR was additionally available in 12/31 patients (38.7% of cases, 2 SCCM+ and 10 SCCM- patients, respectively), with a mean follow-up spine MR time of 54.9 months (range: 3-129.6). In all of them, additional spine MR studies were performed as routine examinations as no new neurological events attributable to SCCM developed subsequently during clinical follow-up time.

A total of n=6 SCCM were detected in five different patients (16.2%) of our cohort at a mean age of 13.5 years (range: 10.9-16.3). Lesions were localized in the cervico-medullary junction (n=1), cervical (n=3) and high thoracic (n=2) segments, one of them appearing *de novo* 40 months after the initial spine MR. Four out of five SCCM+ patients had both T2 TSE and GRE sequences available for review, and the SCCM could be depicted in each of these sequences individually. The remainder SCCM+ patient underwent only one spine MR without GRE, and two small SCCM were depicted on sagittal T2 TSE. All five SCCM+ patients had at least one T1 TSE sequence available for review, but the SCCM could be detected in this sequence in only two of them. Further details on the SCCM neuroimaging features are presented in the **Supplemental Table 3.1**. At baseline spine MR SCCM were classified as Zabramski type I, II, and IV in 1, 1 and 2 cases, respectively. The Zabramski type I SCCM changed towards a type II lesion at follow-up **(Figure 3.2)**. In addition, two SCCM were initially considered unclassifiable, one of them subsequently changing towards a Zabramski type III **(Supplemental Figures 3.1 and 3.2)**. Focal spinal cord expansion and presence of an exophytic component were each detected in 3/6 SCCM **(Figure 3.3)**, while a complete hemosiderin ring was detected in one case **(Figure 3.2)**. The single symptomatic SCCM presented initially with adjacent spinal cord edema that resolved at follow-up imaging **(Figure 3.2)**. Finally, intramedullary, flame-like hemorrhage was detected adjacent to one SCCM at diagnosis and developed into the acute hemorrhagic SCCM case at follow-up MR **(Figure 3.2 and Supplemental Figures 3.1 and 3.2).**

None of our children demonstrated an ISVM (either typical or atypical) at initial spinal MR evaluation nor during follow-up. Other spinal neuroimaging findings depicted in our cohort included mild dorsal levoscoliosis (n=4) **(Figure 3.2)**, congenital narrowing of the spinal canal (n=1), osteochondrosis (n=1), and mild dilatation of the central ependymal canal (n=1).

Brain MR findings

All included patients had multiple cerebral CM (median=10; range: 2-80) depicted on T2* GRE and/or SWI sequences at the time of the first available brain MR, performed at the time of,

or more commonly before, the first spinal MR. Sixty-five percent (20/31) of them had ≥1 lesion located in the posterior fossa (median 1; range: 0-10 CM). Two out of the 31 patients (6.5%) demonstrated ≥1 systemic CM (corresponding to a total of 3 of such lesions), both detected in SCCM+ patients with subjacent *CCM1* mutations. More precisely, one child had one CM located in the soft tissues of the right knee and the other had one CM in the soft tissues of the left elbow and another in the left skull base/masticator space.

Group comparisons

When compared with the SCCM- group, SCCM+ patients showed a tendency towards an older age at first spine MR (P=0.14) and ≥1 cerebral CM located in the posterior fossa (P=0.13), although without reaching statistical significance **(Table 3.2)**. Otherwise, there were no statistically significant differences between groups regarding demographic, clinical, and brain imaging features, including total number of intracranial CM at first available brain MR.

Discussion

In this study including 31 children from three tertiary pediatric centers with a confirmed diagnosis of FCCM, we identified five subjects with SCCM, for a total of n=6 SCCM, one of these appearing *de novo* during follow-up spine MR. This corresponds to a detection rate of SCCM in a pediatric-only cohort of FCCM of 16%, confirming a high prevalence of SCCM in the setting of FCCM [274], and showing that these lesions are frequently already present in affected individuals during childhood. Therefore, our results highlight the necessity of dedicated spine MR imaging in patients with suspected or confirmed FCCM starting during the pediatric age.

Although our detection rate of SCCM was relatively high, it was lower than has been reported in other case series, including the prospective component of the study by Mabray *et al* [173, 320, 448], where SCCM were identified in approximately 70% of cases. However, the latter study included children and adults, while our cohort is only pediatric. Indeed, *de novo* formation of CM in multiple sites is a well described phenomenon in FCCM, probably due to a second-site somatic mutation leading to molecular homozygosity at the CCM gene locus ("second-hit hypothesis") [173]. In turn, this dynamic activity increases the chances of spinal cord lesion development with age, as demonstrated in one of our subjects. Correspondingly, our SCCM+

subjects tended to be older at the first available spine MR, although statistical significance was not reached, likely due to the small sample size.

The disparities may also be explained, at least in part, by methodological differences between the two studies. Unlike the Mabray *et al* study [198, 199], not all of our subjects were imaged at 3.0T or had at least one GRE sequence available. As GRE-type sequences (particularly 3D MEDIC) have been shown to have the highest sensitivity for SCCM detection [173], small SCCM may be underreported in this analysis, and prospective studies in this age group should include standardized spine MR sequences.

Finally, differences between studies may also be related to differences in patient populations characteristics as Mabray *et al* included only patients with *CCM1* abnormalities with the pathogenic variant most common in Hispanic patients [173], while we included all types of *CCM1-3* pathogenic variants, none with Hispanic ancestry. Although genetics played no significant role in distinguishing between our SCCM subgroups (P=0.34), the *CCM1*-common Hispanic variant may confer a higher risk for the development of SCCM than other genetic causes. A few FCCM genotype-phenotype correlations already show *CCM3* variants being more frequently associated with spontaneous mutations and a more aggressive disease course compared to other genotypes [173]. Accordingly, *CCM3* pathogenic variants were present in a higher proportion of our cohort than described in most mixed-age studies (20% vs 10-15%), and affected individuals showed a significantly higher mean number of cerebral CM in their first available brain MR (mean=43.2 lesions; range: 6-80; P=0.039) compared with other genotypes [271, 282, 300].

We have not found a statistically significant difference between SCCM+ and SCCM- groups concerning the number of cerebral CM. However, SCCM+ patients showed a tendency towards presence of at least one such lesion in the posterior fossa, although not reaching statistical significance possibly due to the limited sample size. In addition, the only two patients with $\geq$1 extraneural CM were also SCCM+, raising the suspicion that presence of systemic CM may be associated with SCCM. Subsequent prospective studies including a higher number of subjects may further explore these potential associations.

Concerning the imaging features of SCCM, a recent paper by Panda et al [173, 282, 300] has shown that these differ slightly from their intracranial counterparts. In line with the prior report, our study confirms that popcorn morphology, internal blood-fluid levels, and complete T2WI hypointense rims are often absent. The same study also reported that a flame-like

intramedullary hemorrhage can be frequently depicted adjacent to SCCM, and indeed this feature was eventually detected in 2/6 cases, being eccentric and bidirectional in both [317].

The coexistence of SCCMs and cerebral CM has been linked to a more aggressive course and unfavorable outcome [317]**.** In addition, it has been suggested that pediatric SCCM have a less favorable natural clinical history than their adult counterparts, with significantly higher overt hemorrhage and re-hemorrhage rates [318]. However, only one of our pediatric SCCM+ cases presented with acute neurological signs and symptoms attributed to the spinal cord lesion, and no subsequent SCCM-related events were detected in this patient or the remainder SCCM+ cohort during clinical follow-up. Therefore, identification of SCCM in children before they become symptomatic through screening spinal MR is feasible and may help to inform a risk-analysis assessment concerning the best individualized management strategy in each case.

Surgical treatment has been advocated as the preferred therapeutic option in both children and adults with accessible, symptomatic SCCM, while a conservative approach may be considered in asymptomatic cases [276, 277]. After individual assessment, all our SCCM+ patients (including the child with an overt SCCM-related hemorrhage) were managed conservatively, and none of them developed new symptoms nor SCCM-related neurological deficits at last follow-up. Although current management of FCCM is centered on symptom control, novel disease-modifying therapeutic options including statins and propanolol have demonstrated promising results in cerebral CM in preclinical studies and/or case reports, and are already being tested in clinical trials including adults; they might also be beneficial in SCCM [273, 276, 277].

Contrary to other series, we have not identified lesions compatible with IVMS in any of our pediatric cases [27, 29, 435], suggesting they form later in life. Indeed, previous studies have described a positive correlation of IVMS with age, and most published cases were detected in adults [173, 322].

Our study has some limitations, including its retrospective design and tertiary center referral bias. In addition, as guidelines for spine and brain imaging in pediatric FCCM are currently not well defined [173, 322], patients were imaged at inconsistent time points and without standard spine MR technique (including variations in the scanner field strength and/or the protocol), and only a small subset had serial spine MR. This heterogeneity likely resulted in an underestimation of the rate of SCCM. Nevertheless, this research work is a result of an international multicenter collaboration including three tertiary pediatric centers and represents the largest pediatric-only cohort focusing on spinal imaging data of FCCM patients.

In conclusion, our data confirms a relatively high prevalence of SCCM in children with FCCM due to heterogeneous genetic background, and this percentage may represent an underestimation. On the other hand, ISVM were absent in our pediatric-only cohort. An optimized devoted whole-spine screening MR protocol including GRE sequences should be routinely performed at baseline in all pediatric cases with clinical-radiological suspicion of this disorder and serial spinal MR studies should be considered in confirmed cases, even with negative initial imaging studies.

Tables and Legends

Table 3.1. Demographic, genetic and clinical data.

Variables	**N=31**
Male, n (%)	17 (54.8)
Age at initial clinical presentation in yrs, mean (SD)	6.9 (5.0)
Age at first spinal MR in yrs, mean (SD)	9.7 (5.0)
Genotype, n (%)	
C*CM1*	17 (54.8)
CCM2[a]	6 (19.4)
C*CM3*	6 (19.4)
CCM1-3 testing negative	1 (3.2)
CCM1-3 testing not performed	1 (3.2)
Positive family history, n (%)	22 (71.0)
Ethnic origin, n (%)	
Caucasian	26 (87.0)
Asian	2 (6.5)
Arabic	2 (6.5)
African	1 (3.2)
Hispanic	0 (0.0)
Presentation mode, n (%)	
symptomatic hemorrhage of the CNS[b]	17 (54.8)
non-hemorrhagic seizures	4 (12.9)
incidental diagnosis	4 (12.9)
imaging screening	3 (9.7)
headaches	3 (9.7)
Nº cerebral CM at first available brain MR, median (IQR)	10 (17.0)
$\geq$ 1 extra-CNS CM, n (%)	2 (6.5)
$\geq$ 1 SCCM, n (%)	5 (16.1)
$\geq$ 1 brain surgery, n (%)	15 (48.4)
$\geq$ 1 ISVM, n (%)	0 (0.0)
$\geq$ 1 spine surgery, n (%)	0 (0.0)
Neurological outcome at last clinical follow-up, n (%)	
Normal	20 (64.5)
Mild impairment	3 (9.7)
Moderate impairment	6 (19.4)
Severe impairment	2 (6.5)

Legend: CM- cavernous malformation, CNS- central nervous system, IQR- interquartile range, ISVM- intravertebral venous malformation, SCCM- spinal cord cavernous malformation, SD- standard deviation, yrs- years

a includes 4 cases with a 7p deletion; b 1 case due to a SCCM-related hemorrhage

Table 3.2. Comparison between patients with (SCCM+) and without (SCCM-) spinal cord cavernous malformations.

	SCCM+ patients N=5 (16%)	**SCCM- patients N= 26 (84%)**	**P value**
Male, n (%)	3 (60)	14 (54)	0.59
Age at initial clinical presentation in yrs, mean (SD)	8.4 (6.0)	6.6 (4.9)	0.47
Age at first spine MRI in yr, mean (SD)	12.8 (3.4)	9.1 (5.2)	0.14
C*CM1* mutations, n (%)	4 (80)	13 (50)	0.34
Positive family history, n (%)	4 (80)	18 (69)	0.54
Caucasian, n (%)	4 (80)	23 (89)	0.52
Presentation with symptomatic CNS hemorrhage, n (%)	4 (80)	13 (50)	0.34
Nº intracranial brain CM at first available MRI, median (IQR)	12.2 (20)	18.4 (18)	0.35
Presence of >=1 CM in the posterior fossa at first available brain MR, n (%)	5 (100)	15 (58)	0.13
Number of CM in the posterior fossa at first available brain MR, median (IQR)	2(2.0)	1.0 (3.0)	0.35

Legend: CM- cavernous malformations, CNS- Central nervous system, IQR- Interquartile range, SCCM+ - patients with, SCCM- - patients without SCCM, SD- standard deviation, yrs- years

Supplemental Table 3.1. Imaging features of spinal cord cavernous malformations.

	Patient #1	**Patient #2**	**Patient #3**	**Patient #4**	**Patient #5**	
	SCCM1	SCCM2	SCCM3	SCCM4	SCCM5	SCCM6
***de novo* appearance**	Yes	No	No	No	No	No
Sagittal location	High thoracic (D1)	High thoracic (D6)	Cervico-medullary transition (C0)	Cervical (C2)	Cervical (C2-C3)	Cervical (C5-C6)
Axial location	Dorsal + right lateral	Ventral + right lateral	Dorsal	Dorsal	NA	NA
Axial depth	Superficial	Superficial	Superficial	Superficial	NA	NA
T1WI signal **T2WI signal**	Iso Hyper	Iso Hyper	Hypo Hypo + Hyper	Hyper Iso-Hyper	Iso Hypo	Iso Hypo
Zabramski type	Unclassi	Unclass.	II	I	IV	IV
Exophytic	No	Yes	Yes	Yes	No	No
Internal blood-fluid levels	No	No	No	No	No	No
Adjacent intramedullary hemorrhage	Yes bidirectiona, eccentric	No	No	No	No	No
Spinal Cord edema	No	No	No	Yes	No	No
Spinal Cord expansion	No	Yes	Yes	Yes	No	No
Complete hemosiderin rim	No	No	Yes	No	No	No
Available Follow-up spine MRI studies	Yes	No	No	Yes	No	No
Follow-up spine MRI time	36 months	-	-	10 months	-	-
Longitudinal imaging evaluation	Initial lesion growth and then reduction in size and transformation into type III Zabramski type	-	-	Reduction in size/edema Bi-directional, eccentric intra-medullary hemorrhage	-	-

Legend: MR- Magnetic resonance imaging; NA- Non applicable (absence of axial images), SCCM- Spinal cord cavernous malformation; WI- Weighted-imaging.

Figures and Legends

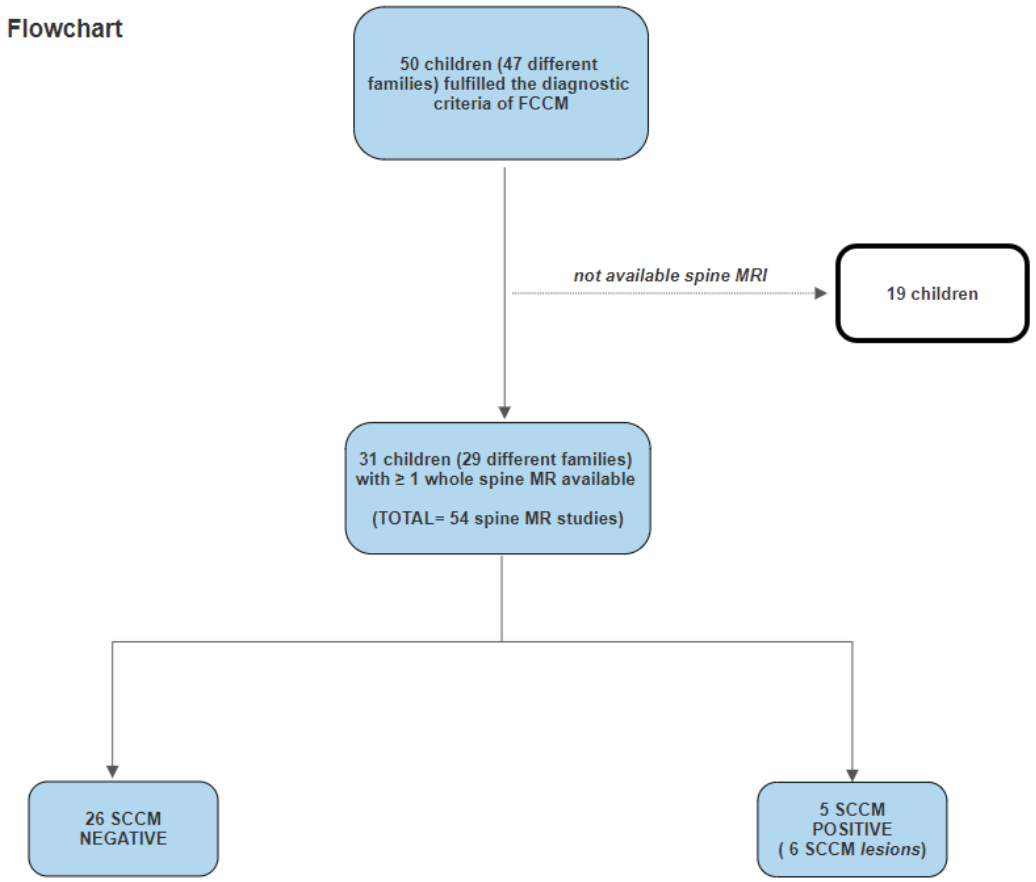

Figure 3.1. Flow chart of the study. Legend: FCCM- Familial cavernous malformation syndrome, SCCM- Spinal cord cavernous malformation.

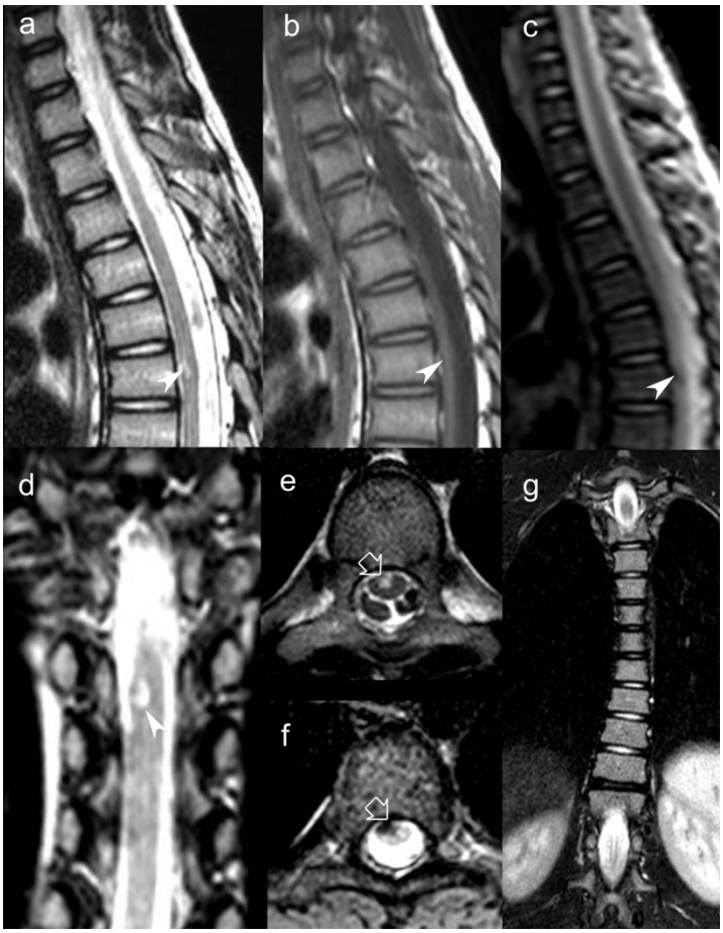

Figure 3.2. Spine MR performed in a 12-year-old boy with familial cerebral cavernous malformation syndrome due to a proven *CCM3* mutation (SCCM patient #2) including sagittal T2FSE (a), T1TSE (b) and GRE (c) as well as coronal T2TSE (d,g) and axial T2 TSE (e) and GRE (f) depicts an intramedullary cavernous malformation located anteriorly at the level of D6 and lateralized to the right (*white arrowheads* and *white empty arrows*). There is a mild focal exophytic component, but no hemosiderin ring nor intramedullary edema. Also note mild dorsal levoscoliosis.

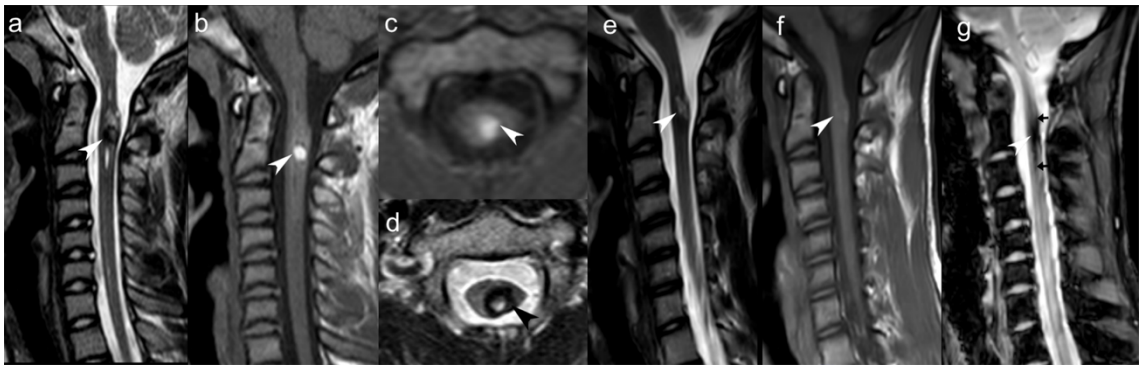

Figure 3.3. Spine MR (a-d) performed in a 15-year-old boy with familial cerebral cavernous malformation syndrome due to a proven *CCM1* mutation (SCCM patient #4) including sagittal T2 TSE(a) and T1 TSE (b) as well as axial T1 TSE (c) and GRE (D), shows an early subacute hemorrhagic intramedullary cavernous malformation located posteriorly at the level of C2 and lateralized to the left (*white and black arrowheads*). There is a nearly complete hemosiderin rim, as well as surrounding edema and focal spinal cord expansion. Follow-up spine MR performed 10 months after (e-g) including sagittal T2 TSE (e), T1TSE (f) and GRE (g) demonstrates interval size reduction of the lesion, expected temporal evolution of the associated blood products, as well as regression of the perilesional edema and associated **reduction of the spinal cord caliber** (white arrowheads). Also note development of a subtle adjacent intramedullary *flame-like* hemorrhage (*thin black arrows*).

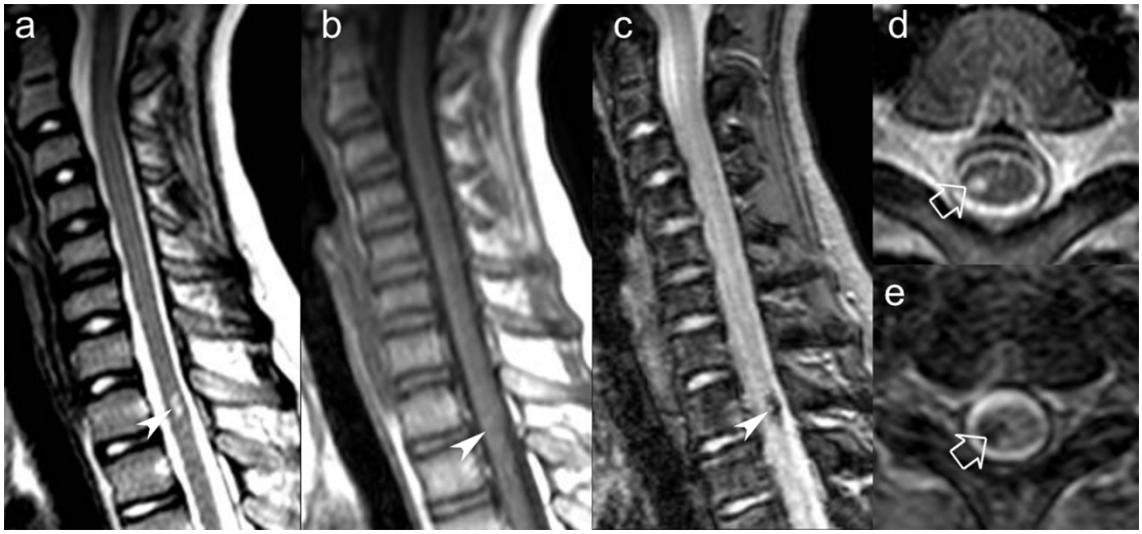

Supplemental Figure 3.1. Spine MR (a-e) performed in a 10-year-old boy with familial cerebral cavernous malformation syndrome due to a proven *CCM1* mutation (SCCM patient #1) including sagittal T2 TSE (a), T1 TSE (b) and GRE (c) as well as axial T2 TSE (d) and GRE (e) demonstrates an intramedullary cavernous malformation located posteriorly and lateralized to the right at the level of T1-T2 (*white arrowheads* and *empty white arrows*). Note absence of hypointense T2 rim, spinal cord expansion or edema.

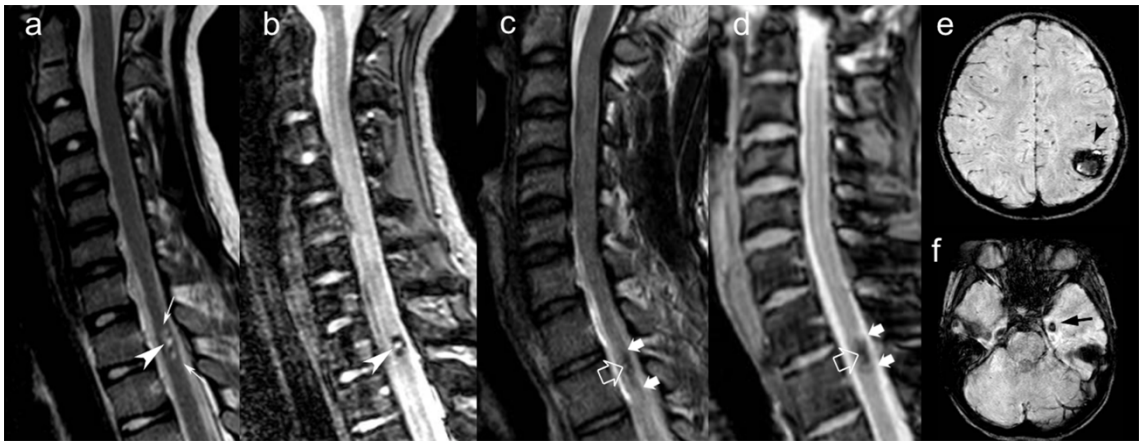

Supplemental Figure 3.2. Follow-up spine MR studies of the same patient presented in Supplemental Figure 1 (SCCM patient #1) performed 7 (a,b) and 36 (c,d) months after including sagittal T2 TSE (a,c) and GRE (b,d) reveal initial subtle growth of the spinal cord cavernous malformation (*white arrowheads* and *empty white arrows*) and mild perilesional edema (*white thin arrows*) followed by size reduction and development of adjacent intramedullary *flame-like* hemorrhage (*thick white arrows*). Brain MR obtained at the time of the initial diagnosis including axial SWI (e,f) images reveals two intracranial cavernous malformations, one in the left parietal lobe (*black arrowhead*) and another in the ipsilateral mesial-temporal region (*thin black arrow*).

PART IV- NATURAL HISTORY OF FAMILIAL CEREBRAL CAVERNOUS MALFORMATION SYNDROME IN CHILDREN: A MULTICENTER COHORT STUDY

Ana Filipa Geraldo[1,2], Cesar Augusto P. F. Alves[3], Aysha Luis[4,5], Domenico Tortora[6], Joana Guimarães[7,8], Daisy Abreu[9], Sofia Reimão[2,10], Marco Pavanello[11], Patrizia de Marco[12], Marcello Scala[13,14], Valeria Capra[12], Rui Vaz[8,15], Andrea Rossi[6,16], Erin Simon Schwartz[3], Kshitij Mankad[4], Mariasavina Severino[6]

[1] Diagnostic Neuroradiology Unit, Department of Radiology, Centro Hospitalar Vila Nova de Gaia/Espinho (CHVNG/E), Vila Nova de Gaia, Portugal

[2] Clínica Universitária de Imagiologia, Faculty of Medicine of the University of Lisbon, Portugal

[3] Department of Radiology, Children's Hospital of Philadelphia, Philadelphia, PA, USA

[4] Department of Radiology, Great Ormond Street Hospital for Children NHS Foundation Trust, London, UK

[5] Department of Radiology, King´s College London, London, UK

[6] Neuroradiology Unit, IRCCS Istituto Giannina Gaslini, Genova, Italy

[7] Department of Neurology, Centro Hospitalar Universitário de São João, Porto, Portugal

[8] Department of Clinical Neurosciences and Mental Health, Faculty of Medicine of the University of Porto, Portugal

[9] Instituto de Medicina Molecular João Lobo Antunes, Lisbon, Portugal

[10] Neurological Imaging Department, Hospital de Santa Maria, Lisbon, Portugal

[11] Neurosurgery Unit, IRCCS Istituto Giannina Gaslini, Genova, Italy

[12] Medical Genetics Unit, IRCCS Istituto Giannina Gaslini, Genova, Italy

[13] Department of Neurosciences, Rehabilitation, Ophthalmology, Genetics, Maternal and Child Health, Università Degli Studi di Genova, Genoa, Italy.

[14] Pediatric Neurology and Muscular Diseases Unit, IRCCS Istituto Giannina Gaslini, Genoa, Italy

[15] Neurosurgical Department, Centro Hospitalar Universitário de São João, Porto, Portugal

[16] Department of Health Sciences (DISSAL), University of Genoa, Genoa, Italy

Abstract

Purpose: There is limited data concerning neuroimaging findings and longitudinal evaluation of familial cerebral cavernous malformations (FCCM) in children. Our aim was to study the natural history of pediatric FCCM, with an emphasis on symptomatic hemorrhagic events and associated clinical and imaging risk factors.

Methods: We retrospectively reviewed all children diagnosed with FCCM in four tertiary pediatric hospitals between January 2010 and March 2022. Subjects with first available brain MRI and ≥3 months of clinical follow-up were included. Neuroimaging studies were reviewed, and clinical data collected. Annual symptomatic hemorrhage risk rates and cumulative risks were

calculated using survival analysis and predictors of symptomatic hemorrhagic identified using regression analysis.

Results: Forty-one children (53.7% males) were included, of whom 15 (36.3%) presenting with symptomatic hemorrhage. Seven symptomatic hemorrhages occurred during 140.5 person-years of follow-up, yielding a 5-year annual hemorrhage rate of 5.0% per person-year. The 1-, 2, and 5-year cumulative risks of symptomatic hemorrhage were 7.3%, 14.6%, and 17.1%, respectively. The latter was higher in children with prior symptomatic hemorrhage (33.3%), *CCM2* genotype (33.3%) and positive family history (20.7%). Number of brainstem (adjusted hazard ratio [HR]=1.37, P=0.005) and posterior fossa (adjusted HR=1.64, P=0.004) CCM at first brain MRI were significant independent predictors of prospective symptomatic hemorrhage.

Conclusion: The 5-year annual and cumulative symptomatic hemorrhagic risk in our pediatric FCCM cohort equals the overall risk described in children and adults with all types of CCM. Imaging features at first brain MRI may help to predict potential symptomatic hemorrhage at 5-years follow-up.

Abbreviations: CASH- cavernous angioma with symptomatic hemorrhage, CCM- cerebral cavernous malformation, CM- cavernous malformation, DVA- developmental venous anomaly, FCCM- familial cerebral cavernous malformation, SWI- susceptibility-weighted image

Introduction

Cerebral cavernous malformations (CCM) are low-flow venous-capillary parenchymal brain lesions composed of enlarged, multilobulated and leaky blood-filled sinusoidal spaces devoid of mature vascular walls and without intervening brain parenchyma [234]. Clinical manifestations of CCM may occur at any age, and include epileptic seizures, impaired consciousness, focal neurologic deficits, and headaches. In addition, asymptomatic presentation in the context of imaging screening or incidental detection of CCM may also occur. Overall, up to 25% of all CCM manifest in childhood [185], and these vascular lesions represent one of the major causes of non-traumatic acute intracranial hemorrhage in this age group [185, 234].

CCM are usually classified as familial (FCCM) or sporadic [449]. Although histopathologically indistinguishable, these conditions usually have distinct genetic signatures. Indeed, FCCM (accounting for up to 20% of all CCM) is an autosomal dominant inherited disease with incomplete penetrance caused by inherited heterozygous germline loss-of-function pathogenic variants in *CCM1-3 genes* [185, 234]. Sporadic CCM are instead mainly due to activating somatic mutations in genes involved in the PI3K-AKT-mTOR pathway, especially *PIK3CA* and *MAP3K3* [201]. Also, unlike sporadic CCM, familial forms often have a positive family history and the disease manifestations tend to present at an earlier age, usually in the form of multiple, scattered CCM [194–196] as well as other systemic CM [185, 242].

Although the natural history of CCM in the general population has been relatively well studied [173, 176], there are limited knowledge and conflicting results concerning the longitudinal evolution of pediatric FCCM. Indeed, most papers focusing on the natural history of CCM in familial cases include mixed-adult and pediatric populations and were published before 2008 [233, 242, 244], year when a consensus statement regarding definitions and reporting standards of CCM-related hemorrhage was issued [305, 450–453]. In addition, prior to 2008, gradient recovery echo-related sequences including T2* and SWI (considered the gold standard for *in vivo* assessment of CCM) were uncommonly used in clinical practice and frequently excluded from analysis [240]. Moreover, the few available studies focusing on younger subjects with CCM are often based on cohorts including both children and young adults and/or all subtypes of CCM [305, 450–453]. Indeed, familial cases only tend account for a small proportion of the complete pediatric patients, with limited data available concerning their clinical features and imaging findings and underlying genotype [15, 16, 18, 184, 252]. All these limitations introduce sample heterogeneity and raise concerns about the appropriateness of extrapolating results to the pediatric FCCM population.

Characterization of pediatric FCCM is relevant for the prognostic assessment of affected children and the development of a more personalized risk-benefit assessment in this population in terms of treatment options, especially regarding potential new disease-modifying pharmacologic agents currently under investigation [15, 16, 18, 184, 252].

Our aim was to study the natural history of pediatric FCCM, with an emphasis on symptomatic hemorrhagic events and associated clinical, genetic, and imaging risk factors.

Material and Methods

Population

We performed a multicenter retrospective cohort study involving four tertiary pediatric institutions including all consecutive subjects with a diagnosis of FCCM during childhood (≤ 18 years) evaluated at least once in the participating hospitals between January 2010 and September 2021, and with an initial brain MRI available for review at least including axial T1WI, T2WI and GRE-type sequences (T2* and/or SWI). The diagnosis of FCCM was based on: 1) presence of ≥1 CCM associated with either a positive family history (defined as ≥1 known first or second-degree relative with a proven CM) and/or 2) a confirmed pathogenic variant in the *CCM1-3* genes in the affected patient or in a first-degree relative [27, 29, 423]. Exclusion criteria included: 1) history of: prior radiation, severe head trauma requiring hospitalization, extracorporeal membrane oxygenation support, intensive care unit stay and/or anticoagulation therapy and 2) poor-quality or incomplete brain MR.

Genetic analysis

DNA extraction: Genomic DNA was isolated from 1 ml of peripheral blood using QIAamp® DNA Blood Midi kit (Qiagen), according to manufacturers instructions. DNA was quantified using a Qubit™ dsDNA BR Assay Kit on a Qubit 2.0 Fluorometer (Life Technologies). **NGS Assay Design:** A next generation sequencing (NGS) custom-designed panel was created using the Ion AmpliSeq™ Designer v6.13 algorithm provided by Thermo Fisher Scientific (Carlsbad, CA, USA) in order to target the entire coding sequence (CDS) and 10 bases of the adjacent intronic regions of KRIT1/CCM1 (NM_194456; 19 exons), CCM2 (NM_031443; 10 exons), and CCM3/PDCD10 (NM_007217; 10 exons). The primers pools were composed by 44 amplicons showing the following features: 100% of total coverage, 0% missed regions, an amplicons range of 125- 275 bp and an exon padding of 10 bp. **Libraries preparation:** Multiplex PCR were performed

manually using 10 ng of genomic DNA with a premixed primer pool and Ion AmpliSeq HiFi master mix (Ion AmpliSeq Library Kit 2.0). The amplicons were treated with 2µl FuPa reagent to partially digest the primer sequences and phosphorylate the amplicons. Amplicons were ligated to adapters with the diluted barcodes of Ion Xpress Barcode Adapters kit (Thermo Fisher Scientific, Inc.). The libraries were purified using the Agencourt AMPure XP Reagent (Beckmann Coulter, CA, USA). The concentration of the final libraries was determined by fluorescent measurement on Qubit 2.0 instrument (Life Technologies). **Template preparation, chip loading and sequencing:** The libraries were diluted to ~100 pM. The clonal amplification of barcoded DNA libraries onto ion spheres was performed on an Ion Chef™ Instrument using Ion 520™ Kit-Chef, according to the manufacturer's instructions (Thermo Fisher Scientific, Inc.). Template-positive spheres from barcoded libraries were loaded onto Ion 510™ Chips following the manufacturer's protocol, and sequencing was run on the Ion Gene Studio S5 system (Thermo Fisher Scientific, Inc.). **Data analysis:** DNA sequence reads were analyzed using both the Ion Reporter Software v.5.6 (Thermo Fisher Scientific, Inc.) and the CLC Genomics Workbanch 6.5.1 software (Qiagen). High-quality Single Nucleotide Variants (SNV) and insertion/deletion variants were strictly defined as: i) FILTER=PASS, ii) QUAL ≥100, iii) depth coverage ≥20X, and iv) variant fraction ≥20%. Bioinformatics tools were used to predict the effect of missense variants: Polyphen-2 (http://genetics.bwh.harvard.edu/pph2/index.shtml), SIFT (http://sift.bii.astar.edu.sg/www/SIFT_seq_submit2.html), MutPred (http://mutpred.mutdb.org/) and Mutation Taster (http://www.mutationtaster.org/). Splicing variants were studied using Human Splicing Finder, vs. 3.0 (http://www.umd.be/HSF3/HSF.html). **Variants validations:** The variants called by both softwares and having a predicted functional effect were validated by Sanger sequencing using High-Fidelity Platinum Master Mix (Invitrogen) for PCR and BigDye Terminator v1.1 kit (Life Technologies). Multiplex Ligation-Dependent Probe Amplification (MLPA) Assay MLPA was performed on those patients who were negative for mutations in CCM1, CCM2 and CCM3 genes using two MLPA probemix, P130 and P131, according to the standard MLPA protocol (MRC-Holland, Amsterdam, The Netherlands). Coffalyser software was used for analysis of peak values obtained from capillary electrophoresis on ABI 3100 Genetic Analyzer (Applied Biosystems). Mean cut-off for normalized peak height ratio of patient to the control sample was less than 0.7 in case of exon deletions and more than 1.30 in case of exon duplications.

MR technique and image analysis

Images were acquired with a 1.5 or a 3.0 Tesla MR scanner, using local protocols, in some subjects including administration of gadolinium-based contrast agents. For each subject, lesion

counts were performed on the first brain MRI based on hemosiderin sensitive sequences (T2* and/or SWI) and the anatomical location. They were assessed for Zabramski type as modified by Nikoubashman [177] and size (corresponding to the largest diameter measured on axial T2WI) [252, 305]. Lesions larger than 40 mm were classified as giant CCM, according to previous definitions [252]. Longitudinal studies were assessed whenever available and correlated with clinical indications, focusing on appearance of new CCM (*de novo* lesions) and evidence of symptomatic hemorrhage, when present. CCM were labeled as *de novo* lesions if their new appearance could be shown on comparable or technically inferior consecutive studies while acute symptomatic hemorrhagic CCM (CASH) at either presentation and/or follow-up were identified according to previous published consensus guidelines [310]. These lesions were further evaluated in relation to their general morphology (uni/multilocular), as well as presence of hemosiderin ring, perilesional vasogenic edema, T1 hyperintense perilesional sign [240], fluid-fluid levels, and/or accompanying developmental venous anomalies (DVA). In cases with clinical symptoms and more than one CCM with signs of recent hemorrhage, the lesion located in the anatomical region corresponding to the neurological manifestations was considered. If the clinico-radiological correlation was uncertain or dubious, the largest hemorrhagic lesion was considered for evaluation.

At each center, images were first analyzed by one rater, blinded to the clinical and genetic information. One of the raters evaluated two sites, corresponding to a total of 3 readers (with 1, 7 and 7 years of experience in pediatric neuroradiology, respectively). Anonymized brain MR studies of all potentially CASH and of other CCM with questionable evaluation were decided by consensus.

Clinical data

Data on demographics, age at clinical presentation leading to the FCCM diagnosis and mode of presentation, ethnicity, family history (including number of affected family elements and degree of kinship), genotype, presence of other systemic CM (including cutaneous, retinal, or within solid organs) or any combined systemic feature (including Greig cephalopolysyndactyly in the setting of a 7p deletion syndrome [307]) were obtained from medical records. Mode of presentation was classified according to previously published reporting standards of CCM [287]. More specifically, symptomatic CCM hemorrhage was defined by presence of acute or subacute onset symptoms (any of headache, epileptic seizure, impaired consciousness, or new/worsened focal neurological deficit referable to the anatomic location of the CM) accompanied by radiological evidence of recent extra- or intralesional hemorrhage. Other types of presentation included non-hemorrhagic epilepsy, non-hemorrhagic focal neurological deficit, non-

hemorrhagic unspecific headaches or asymptomatic forms (such as incidental finding or detection in the context of imaging screening due to family history of CCM). Follow-up data were obtained through routine visits in specialized outpatient clinics and by presentation in the emergency departments, including symptomatic events attributable to CCM according to current guidelines [240] after confirmation by multidisciplinary assessment. In addition, any neurosurgical interventions and final neurological outcomes (graded as normal, mild, moderate, or severe impairment) were also recorded.

Statistical analysis

Quantitative data were presented as median and interquartile range, and categorical data as frequencies and percentages. Fisher exact test or Pearson $\chi 2$ test and student t-test or Mann-Whitney test were used to compare categorical and continuous variables, respectively.

The prospective annual risk of hemorrhage was calculated as the number of hemorrhages during considered follow-up divided by person-years of follow-up during that time. Cumulative rates of symptomatic hemorrhage for the whole sample and stratified by baseline variables were calculated as the ratio between the number of symptomatic hemorrhagic events during follow-up and the number of patients initially at risk. Cumulative rates of symptomatic hemorrhage were also illustrated using the Kaplan–Meier method, and the curves were compared by the log-rank test. Survival analysis was applied to estimate the 1-year risk, 2-year risk, and 5-year risk of symptomatic hemorrhage with corresponding 95% confidence intervals (95CI). Univariable and multivariable Cox regression survival analyses were used to identify risk factors of longitudinal symptomatic hemorrhage during the follow-up period.

Data were excluded if subjects experienced bleeding or were lost to follow-up. Surgical removal of a lesion did not lead to exclusion if the patient had additional CCM(s) amenable to follow-up.

Statistical analyses were performed by using Stata, v14.0 (StataCorp, College Station, Texas). The significance level was set at P=0.05 (2-sided).

Results

Clinical and genetic data

Fifty-three children with FCCM from 49 families were identified, from which 12 patients (22.6%)

were excluded due to non-available first brain MRI. Forty-one children from 38 unrelated families fulfilled the eligibility criteria and were therefore included. Clinical and genetic data are summarized in **Table 4.1**. Twenty-two individuals (53.7%) were male and 30 (73.2%) Caucasian. There was a family history in 29 (70.7%) children, with multiple kindred involved in 18 (63.1%). A genetic diagnosis in the affected individual or in a known first degree relative was available in 30 (73.2%) children, with *CCM1*, *CCM2 and CCM3* loss-of-function variants identified in 17 (56.7%), 6 (20.0%) and 7 (23.3%), respectively. Out of the six subjects with *CCM2* abnormalities, five (83.3%) had a 7p deletion, including two cases with features of Greig cephalopolysyndactyly.

The median age at clinical presentation leading to subsequent FCCM diagnosis was 7.7 years (IQR=9.2; range:0.4-17.3). Fifteen (36.6%) individuals suffered a symptomatic CCM-related hemorrhage of the CNS at presentation, intracranial in 14 (93.3%) cases and involving the spinal cord in one (6.7%).

The median observational period was 54.3 months (IQR:65.0; range:4.0-205.4). All subjects except one (n=40, 97.6%) had more than 6 months of clinical follow-up. During extended, retrospective longitudinal evaluation, 19 (46.3%) subjects underwent at least one CCM-related brain surgery (total of 21 CCM-excisional procedures), with complete removal in 17 (81.0%) and subtotal removal in 4 (19.1%) lesions. Eighteen (94.7%) surgeries were within the first five years after diagnosis. No spinal surgeries were performed. The mean age at first surgery was 9.1 (SD=5.2; range:0.9-17.2). Overall, 11 out of 19 (52.4%) procedures were performed due to a CCM-related symptomatic hemorrhage. Other surgical indications included progressive CCM growth with or without asymptomatic hemorrhage (n=3, 14.3%), medically refractory seizures related to a surgically accessible lesion (n=5, 23.8%) and a giant CCM (n=2, 9.5%). Children undergoing more than 1 surgical CCM removal had a significantly higher rate of symptomatic hemorrhage at presentation (P=0.047) and a significantly lower number of CCM on the first brain MRI (P=0.0204) when compared to those receiving conservative treatment. Otherwise, there were no statistically significant differences between groups regarding other studied demographic, clinical, and brain imaging variables **(Supplemental Table 4.1).**

At their last clinical visit, 29 (70.7%) children remained neurologically intact, while 11 (26.8%) demonstrated some type of neurological impairment. One (2.4%) child died during the follow-up due to sudden-unexpected death in the context of severe medically refractory epilepsy. Within the subgroup with mild to severe neurological impairment, n=5 (45.5%) subjects had $\geq$1 previous symptomatic hemorrhagic event, n=1 (9%) presented refractory epileptic encephalopathy and n=2 (18.2%) showed Greig cephalopolysyndactyly-related developmental

delay.

Brain MR and CCM

A total of 199 brain MRI studies were available for review (median number per patient=4.0; range:1-16), 51 (25.6%) performed on a 1.5T magnet and 148 (74.4%) on a 3.0T magnet. A T2* and/or SWI sequence was respectively available in 80 (40.2%) and 136 (68.3%) studies, while both sequences obtained in 27 (13.9%) examinations. Contrast material was injected in 39 (19.6%) occasions.

At first brain MRI, a total of n=587 CCM were identified on T2* and/or SWI sequences and their neuroimaging features are reported in **Table 4.2**. All children except one (97.6%) demonstrated multiple CCM (median number per child=10.0; IQR=12; range:1-80) at diagnosis. CCM3-affected individuals tended to show a higher median total number of CCM (12.0 vs 7.0, P=0.147) as well as a higher median number of CCM in the posterior fossa (2.4 vs 1.5, P=0.980) and brainstem (1.0 vs 0.7, P=0.800) in their first available brain MRI when compared with subjects with other known genotypes, although not statistically significant.

Longitudinal brain MRs were available in 38 (92.7%) subjects, either performed as a scheduled examination or in the emergency setting due to new neurological events, with a median follow-up brain MRI time of 49.6 months (IQR=68.6; range:3.6-129.1). Fifteen (39.5%) developed at least 1 *de novo* CCM (median lesions per patient=4.5; range:1-16), for a total of 86 new lesions identified in 180.36 person-years of brain MRI follow-up, yielding an annual new lesion rate of 47.7%.

Spine MR and CM

Twenty-three (56.1 %) of the subjects had at least one available whole spine MR for review (total= 44 studies performed). Mean age at first available spine MR was 8.0 years (IQR = 5.0; range: 0.8–16.8 years). Retrospective longitudinal spine MR was additionally available in 11/23 (47.8%) of the cases (range:2-7), with a with a median follow-up spine MR time of 39.5 months (range: 3–123.8). A total of n= 4 spinal CM were detected in three different patients (13%), one of them appearing *de novo*. Except for the single case presenting with a spine-related CASH that was previously described, the remaining spinal CM were asymptomatic.

CASH lesions

Imaging details of CASH lesions (n=23), identified either at clinical presentation (n=15) or during follow-up (n=8), are also presented in **Table 4.2** and some examples are illustrated in **Figure 1**. Briefly, CASH were more commonly cerebral (n=14, 61.0%), multilocular (n=12, 52.2%), and had fluid-fluid levels (n= 13, 56.5%), hemosiderin ring (n=15, 65.2%), perilesional edema (n=17, 73.9%), and/or the T1-hyperintensity sign (n=15, 65.2%). In no case an associated DVA was found. Out of the eight CASH identified during retrospective longitudinal evaluation, 3 were caused by re-hemorrhage of a previous CASH, another 3 corresponded to a first symptomatic hemorrhagic event in known CCM, and 2 were in *de novo* CCM.

Annual prospective symptomatic cerebral hemorrhage rates

In the 5-year follow-up, seven symptomatic hemorrhagic events occurred during 140.5 person-years, corresponding to a 5-year annual prospective symptomatic hemorrhagic rate of 5.0% (95%CI:2.4-10.5). Other stratified hemorrhage risks per year per patient within this period are presented in **Table 4.3**.

In the maximum available follow-up time, one additional symptomatic event occurred, leading to a total of eight of such events occurring during 200.2 person-years and yielding an overall annual symptomatic hemorrhage rate of 4.0% (95%CI:2.0-8.0) per person-year. Median time until the first prospective symptomatic hemorrhagic event during extended follow-up was 18.5 months (IQR=31.3; range:0.03-97.9).

Cumulative risks of prospective hemorrhage

The cumulative risk of symptomatic hemorrhage was 7.3% (1.5-20.0) at 1 year, 14.6% (5.6-29.2) at 2 years, and 17.1% (7.1-31.2) at 5 years. The 5-year cumulative risk was higher in subjects with symptomatic hemorrhage at presentation (33.3%), *CCM2* genotype (33.3%), presence of at least one CCM in the brainstem at first brain MRI (26.7%) and positive family history (20.7%). Other stratified cumulative risks of hemorrhage at 5-years of follow-up are summarized in **Table 4.4.**

A tendency towards a higher cumulative risk of symptomatic hemorrhage at 5-years of follow-up was observed in children presenting with prior symptomatic hemorrhage, with a borderline statistical significance (P=0.0559) (**Figure 4.1)**.

Predictors of symptomatic hemorrhage at presentation

In both uni- and multivariable analysis, none of the studied variables resulted a significant independent predictor of symptomatic hemorrhagic presentation **(Supplemental Table 4.2).**

Predictors of symptomatic hemorrhage at follow-up

In univariable analysis, the total number of CCM located in the brainstem (hazard ratio [HR]=1.63, P=0.003) and total number of CCM located in the posterior fossa (HR=1.37, P=0.005) at the first brain MRI were significant risk factors of subsequent symptomatic hemorrhage at 5 years of follow-up. Multivariable analysis after adjusting for age at presentation and sex confirmed these variables as independent predictors of future symptomatic hemorrhage during that period (adjusted HR=1.64 and 1.39 with P=0.004 and 0.005, respectively). Symptomatic hemorrhagic presentation also showed a trend towards increased risk for subsequent symptomatic hemorrhagic events when compared to other forms of presentation in both univariable and multivariable analysis, although without reaching statistical significance (adjusted HR=4.33 and HR=4.35, P=0.008 and 0.08, respectively) **(Table 4.5).**

Discussion

In this multicenter study evaluating the natural history of pediatric FCCM in 41 children with a confirmed diagnosis of FCCM and incorporating standard definitions of symptomatic hemorrhage, we found that the 1-, 2-, and 5-year cumulative risks of hemorrhage were 7.3%, 14.6%, and 17.1%, respectively.

It has been previously described for the general population that the probability of symptomatic hemorrhage in CCM increases over time in the general population, especially during the first two years after hemorrhagic presentation, a phenomenon known as “temporal clustering” [240]. This finding was also demonstrated in a pediatric cohort study involving children with different CCM subtypes [233, 242, 244, 248] and confirmed in our cohort, including a homogeneous sample of children with FCCM. Indeed, our results show that although the cumulative risks of symptomatic hemorrhage increase over time in affected patients, they grow

much faster in the first two years after presentation of the disease (14.6% at 2 years vs 17.1% at 5 years after presentation). The transversality of temporal clustering suggests that it occurs irrespectively of age at presentation or CCM subtype.

We have also demonstrated that the annual symptomatic hemorrhage rate for our entire cohort at 5-year follow-up after diagnosis was 5.0% per person-year. When compared to the cumulative risk value previously presented, the annual symptomatic hemorrhage rate is a more robust measure, as it takes into account losses to follow-up and when events occur, although its interpretation is less intuitive. The influence of age at presentation and familial subtype in the natural history of subjects with one or multiple CCM remains unclear. Indeed, some authors have reported an increased symptomatic bleeding rate in children with CCM when compared to adults [16], while others have not [18]. Moreover, familial disease has also been linked to an increased symptomatic hemorrhagic risk [15, 16] in the majority of, but not all [452], published studies. These divergent results are justified, at least in part, by methodological differences between the studies, including distinct sample sizes and eligibility criteria, variable proportions of CCM subtypes (familial vs sporadic), modes of presentation (hemorrhagic vs non-hemorrhagic), inconsistent methods of risk calculation (lifetime vs prospective approaches), and heterogenous definitions of hemorrhage [252]. Our results support similar 5-year annual and cumulative symptomatic hemorrhagic risks in pediatric FCCM subjects treated surgically based on clinical judgement in tertiary centers, compared to children and adults with all types of CCM. These findings are in line with the most recent studies on this topic [177, 252]. However, the comparison of results between adult and pediatric cohorts should be made with caution. Indeed, mild symptomatic CCM-related neurologic events may be more commonly missed at young ages, especially if neurological manifestations were transient, insidious, or non-specific, as more frequently occurs in this age group [16, 250]. Additionally, the threshold for a given CCM to become clinically symptomatic in pediatric patients may be higher than for adults, due to pediatric immaturity and/or increased cerebral plasticity of children [454]. This theory can be supported by the fact that the median size of CCM at presentation in children tends to be larger than in adults [455]. In addition, giant CCM are also more commonly found in children [310] and both findings are corroborated by our results. Although giant CCM have primarily been described in sporadic patients, they can also occur in FCCM, as seen in five of our cases and previously reported by Ozgen *et al* [310, 312].

Another factor that may have influenced our results is the overall high rate of surgical treatment in our cohort (46%) when compared with other familial and/or pediatric CCM studies (up to

37.2%) [310]. There are currently no standard treatment guidelines specific for pediatric FCCM and indications for surgical treatment of accessible lesions remain personalized and dependent upon multiple factors, including the individual surgeon's practice standards, patient's insurance, family preference, presentation mode and type, and severity of clinical manifestations at follow-up. The more aggressive approach followed in our referral tertiary pediatric hospitals likely reflects the high surgical training, volume, and expertise available in our centers, and likely contributed to fewer prospective symptomatic hemorrhagic events during follow-up. Planned surgical removal of CCM suspected of high-hemorrhagic risk (namely lesions with dynamic asymptomatic progressive changes detected on routine follow-up imaging or large size) was performed in some of our cases and likely positively modified the natural history of this disease.

The percentage of children in our cohort presenting with symptomatic hemorrhage is lower than reported in most previously published series including subjects with variable ages [15, 16, 18, 250].This is probably due to the high rate of known positive family history of CCM in our cohort, leading to a higher index of suspicion in cases of mild or nonspecific complaints, such as headaches, and/or screening brain MRIs in asymptomatic subjects. As prior symptomatic hemorrhage has been described by most authors as an independent risk factor for future symptomatic hemorrhagic events [15, 16, 184, 250, 451, 452], the intrinsic baseline characteristics of our subjects may have led to our underestimation of the prospective hemorrhagic rates/cumulative risks. We also found that symptomatic hemorrhage at presentation rises the annual hemorrhagic rate and the 5- year cumulative risk of symptomatic hemorrhagic events of affected subjects when compared with other forms of presentation, although not reaching statistical significance as a predictor variable, most likely due to sample size.

In our study, children with pathogenic loss-of-function variants in the *CCM2* gene also demonstrated higher annual hemorrhagic rates and 5-year cumulative risk of symptomatic hemorrhage when compared with subjects with *CCM1* or *CCM3* genetic variants. This association lacked statistical significance and therefore we cannot exclude that these results are due to chance, especially in the setting of the small number of subjects in our cohort harboring CCM2 genetic variants. All three *CCM1-3* genes encode components of a heterotrimeric CCM protein complex involved in endothelial stabilization but each of them has additional cellular functions. More specifically, CCM2 encodes malcavernin, that acts as bridge allowing interaction between the other two CCM proteins and also influences β-Catenin and Wnt signaling, causing MEKK3 inhibition and promotion of RhoA degradation [16, 184, 233, 242, 244]. Although few

studies have specifically focused on *CCM2*-related disease, this genetic form has been so far considered a milder form of FCCM [201]. Instead, previous case series have described a more aggressive clinical course in patients who were carriers of *CCM3* variants [268] when compared with patients with other FCCM genotypes, although this feature has not been confirmed by all authors [268, 271, 282, 300]. In our cohort, although the total number of CCM, posterior fossa CCM, and brainstem CCM was indeed higher in patients with CCM3 variants, differences did not reach statistical significance. In addition, the proportion of our subjects with symptomatic hemorrhagic presentation and moderate to severe neurological deficit at last follow-up or death was lower in CCM3 than in other FCCM disease-causing genes, however also without statistical significance. To the best of our knowledge, no natural history study of FCCM comparing different genotypes has been previously published. Notably, 5/6 cases with variants of CCM2 had no single nucleotide variants but deletions of variable size that can also encompass additional flanking genes, including *GLI3*, leading in two cases Greig cephalopolysyndactyly syndrome [269]. This might have contributed to the disease phenotype and eventually influenced the longitudinal evolution of CCM in our cohort. The role of each gene in the natural history and long-term outcome of subjects with FCCM should be therefore further investigated in larger samples.

Our results also show that the first brain MRI can provide important information that can aid in the prognostication of future symptomatic hemorrhagic events in children with pediatric FCCM. Indeed, both the number of brainstem CCM and posterior fossa CCM at first brain MRI were significant independent predictors of prospective symptomatic hemorrhage events in our study. In contrast, total number of CCM and total number of Zabramsky type II lesions (either as continuous or dichotomized variables) played no significant role. These findings are in line with previous studies (including a meta-analysis) indicating that brainstem CCM location has an increased risk of symptomatic hemorrhage [283, 287]. However, it remains unclear whether brainstem CCM are intrinsically more prone to bleed or if there is an overestimation of the real hemorrhagic rate of CCM in this eloquent region [233, 242, 244, 252]. Aiming to clarify this question, we believe that current reporting standards of hemorrhage from CCM [252] should be reviewed, recommending individualized reporting of both symptomatic and asymptomatic hemorrhage rates per patient and per lesion in future studies.

Differently from previous reports [240], we could not find significant independent predictors of symptomatic hemorrhagic presentation in our cohort, most likely due to sample size.

As expected in FCCM, the vast majority of our subjects had multiple CCM lesions at first brain

MRI, even when the exam was performed during early infancy. A recent report has shown that CCM may even be detected *in utero* in familial cases using fetal MRI [16, 83]. However, it is important to bear in mind that even isolated CCM lesions in children may be familial, as seen in one of our cases. In line with previous studies [292], we have also detected imaging appearance of new CCM over time (reaching 8.3% annual rate per patient-year) and some of these *de novo* CCM were responsible for symptomatic hemorrhagic events. This dynamic activity is consistently higher in familial cases when compared to sporadic ones [177, 251, 452, 453]. Nevertheless, direct comparison between studies concerning the rate of development of new lesions is hampered by methodological differences, as reviewed in a recent meta-analysis by Taslimi *et al* [177, 251, 452, 453].

CASH lesions in our cohort were overall more commonly located supratentorially (probably due to the high supratentorial/infratentorial ratio of lesion counts) and their median size was larger than the median size of all CCM (excluding type IV lesions). These usually demonstrated a hemosiderin ring, extracapsular hemorrhagic extension with associated vasogenic edema, as well as imaging features commonly described in large-size/giant CCM, namely multilobulated morphology and internal fluid levels [177]. In addition, the majority but not all CASH exhibited the T1 hyperintense perilesional signal, an imaging feature with moderate sensitivity and high sensitivity for the diagnosis of hemorrhagic CCM [310]. Nevertheless, it is important to be aware that this imaging sign may also be evident in other lesions, such as melanoma and other hemorrhagic metastasis [307].

Based on the results of this study as well as other recently published papers focusing on FCCM in children, adults and/or mixed populations, we suggest that patients with suspected and/or confirmed FCCM should be imaged at the best available MR scanner (ideally in a 3.0 Tesla unit) with standard imaging technique [308]. The brain MR protocol should include a T1 3D sequence, axial and coronal T2WI, axial or 3D FLAIR and at least one GRE-sequence, preferably SWI [173, 296, 456, 457]. Whole spine MR should be additionally performed at diagnosis regardless of the presentation age as a screening modality, including a T1 TSE, a T2 TSE and at least one GRE sequence, ideally a 3D T2 Multi-Echo Data Image Combination (MEDIC) [296, 456]. Serial spine MR imaging with a similar protocol should be also considered even in patients with initially negative spine MR studies.

Our study has some limitations, including its retrospective design and tertiary center referral bias. In addition, our cohort was also predominantly composed of Caucasian subjects, which may limit generalizability to subjects with other ethnic backgrounds, including the commonly

reported Hispanic FCCM population. As guidelines for brain imaging in pediatric FCCM are currently not well defined [173, 457], subjects were imaged over time at inconsistent time points and without standard MR techniques (including variations in the MR scanner magnetic field strength and/or the protocol). This may have limited the imaging assessment, since identification of CCM is strongly dependent of technical parameters. Moreover, due to the retrospective nature of the study, we have not evaluated advanced imaging techniques such as perfusion and permeability MR that have been recently described as biomarkers of CCM activity and predictors of lesional growth and hemorrhage [234]. Another possible limitation of our results includes the 39% rate of loss to follow-up at 5 years, that occurred mainly due to adult care transferal. Finally, the number of bleeding events was rather low during follow-up, limiting the number of possible variables and increasing the 95% CI in the Cox proportion regression analysis model. Nevertheless, to the best of our knowledge, this is a natural history study conducted in the largest pediatric FCCM cohort reported to date, including a comprehensive clinical, genetic, and imaging evaluation. More especifically, when compared with the recent paper by Santos *et al* [365, 367, 370], our study includes a larger number of patients with pediatric FCCM (41 vs 35) and provides better clinical characterization of the cohort as well detailed neuroimaging assessment of their CCM, with special emphasis on *de novo* CCM and symptomatic hemorrhagic lesions. In addition, and contrarily to the paper by Santos *et al* [16], we specify the pathogenic variants of all subjects with genetic FCCM confirmation and evaluate the relationship between the genetic subtypes of FCCM and the prospective symptomatic hemorrhagic events.

Conclusion

Pediatric FCCM seem to have an overall similar 5-year annual and cumulative symptomatic hemorrhagic risks in subjects treated according to clinical judgement (including medical and/or surgical approach) compared to children with sporadic CCM and adults with either familial or sporadic disease. In addition, children with FCCM can be stratified to predict longitudinal symptomatic hemorrhage risks according to baseline clinical and imaging features, allowing a differentiated treatment strategy. Future prospective multicenter studies in pediatric FCCM using standardized MR performed at fixed time-points and including advanced neuroimaging techniques and genetic investigation would be advisable to increase our current knowledge and test new predictors of both symptomatic and asymptomatic hemorrhagic events as well as overall neurological outcome.

Tables and Legends

Table 4.1. Demographic, genetic, clinical and imaging data

	N=41
Male, n (%)	22 (53.7)
Age at initial clinical presentation in years, median (IQR)	7.7 (3.47-12.67) Range:0.4-17.3
Genotype, n (%)	
C*CM1*	17 (41.5)
CCM2[a]	6 (14.6)
C*CM3*	7 (17.1)
CCM1-3 testing negative/not performed/pending	11 (26.8)
Positive family history, n (%)	29 (70.7)
Nº of affected family members	
n=1	11 (37.9)
n=2	11 (37.9)
≥ 3	7 (24.1)
Ethnic origin, n (%)	
Caucasian	30 (73.2)
African	5 (12.2)
Asian	2 (4.9)
Hispanic	1 (2.4)
Other	3 (7.2)
Presentation mode, n (%)	
Symptomatic hemorrhage of the CNS[b]	15 (36.6)
Non-hemorrhagic seizures	10 (24.4)
Incidental diagnosis	6 (14.6)
Imaging screening	4 (17.1)
Headache	3 (7.2)
≥ 1 extra-CNS CM, n (%)	2 (4.9)
≥ 1 spinal cord CM, n (%)	3 (13.6) [c]
≥ 1 brain surgery, n (%)	19 (46.3)
Number of neurosurgical procedures	
n=1	17 (89.5)
n=2	2 (10.5)
Neurological assessment at last clinical FU, n (%)	
Normal	29 (70.7)
Mild impairment	3 (73)
Moderate impairment	6 (14.6)
Severe impairment	2 (4.9)
Death	1 (2.4)
Seizures at last clinical FU, n (%)	12 (29.3)
Medically controlled	10 (83.3)
Medically refractory	2 (16.7)

Legend: CM, cavernous malformation; CNS, central nervous system; FU- follow-up; IQR, interquartile range; SD, standard deviation

[a] includes 4 cases with a 7p deletion; [b] 1 case due to a SCCM-related hemorrhage, [c] 22/41 subjects (53.7%) underwent at least one whole-spine MR

Table 4.2. Imaging features of CCM detected at first brain MRI and with symptomatic hemorrhage identified at diagnosis and follow-up.

CCM identified at first brain MRI n= 587	
Location, n (%)	
Cerebral lobes	492 (83.8)
Nucleocapsular/Thalamic	23 (3.9)
Brainstem	27 (4.6)
Cerebellum	39 (6.6)
Intra-ventricular	6 (1.0)
Modified Zabramski type, n (%)	
I	20 (3.4)
II	116 (19.8)
III	79 (13.5)
IV	362 (61.7)
V	10 (1.7)
Size in mm (except type IV CCM), median (IQR)	7.0 (1-52)
Giant lesions	5 (0.9)
CASH identified at diagnosis and follow-up n=23	
Location, n (%)	
Cerebral lobes	14 (61.0)
Nucleocapsular/Thalamic	1 (4.4)
Brainstem	5 (21.7)
Cerebellum	2 (8.7)
Spinal cord	1 (4.4)
Modified Zabramski type, n (%)	
I	6 (26.1)
V	17 (73.9)
Size in mm, median (IQR; range)	27 (25;8-52)
Multilocular morphology, n (%)	12 (52.2)
Hemossiderin ring, n (%)	15 (65.2)
Fluid-fluid levels, n (%)	13 (56.5)
T1 hyperintense perilesional sign, n (%)	15 (65.2)
Perilesional edema, n (%)	16 (69.6)
Associated DVA	0 (0.0)

Legend: CASH, Cavernous angioma with symptomatic hemorrhage; DVA, developmental venous anomaly, FU, follow-up; IQR, interquartile range

Table 4.3. Hemorrhage risk per year per patient during 5-year follow-up.

Variable	Total person-years	Nº of symptomatic hemorrhagic events	Incidence rate (95% CI)
Gender			
Male	82.7	4	4.8 (1.8-14.5)
Female	57.9	3	5.2 (1.7-16.1)
Ethic origin			
Caucasian	108.9	6	5.5 (2.5-12.3)
Non-caucasian	31.6	1	3.2 (0.5-22.5)
Age at presentation			
< 6 years	53.1	2	3.8 (1.0-15.1)
≥ 7 years	87.4	5	5.7 (2.4-13.7)
Positive family history			
Yes	93.1	6	6.4 (2.9-15.8)
No	47.4	1	2.1 (0.3-14.3)
Genotype			
CCM1	53.1	3	5.7 (1.8-17.5)
CCM2	16.3	2	12.3 (3.1-49.0)
CCM3	25.8	1	3.9 (0.6-27.5)
Presentation Mode			
Symptomatic hemorrhage	49.2	5	10.2 (4.2-24.4)
Other types of presentation	91.3	2	2.2 (0.6-8.8)
≥ 1 Extra-CNS CM			
Yes	9.2	1	10.9 (1.5-77.4)
No	131.4	6	5.0 (2.4-10.5)
≥ 10 CCM in first brain MRI			
Yes	73.99	3	4.06 (1.31-12.57)
No	66.53	4	6.01 (2.26-16.02)
≥ 1 CCM in the brainstem			
Yes	44.36	4	9.02 (3.39-24.03)
No	96.17	3	3.12 (1.01-9.6)
≥ 1 CCM in the posterior fossa in the first brain MRI			
Yes	86.33	6	6.95 (3.12-15.47)
No	54.19	1	1.8 (0.26-13.10)
≥ 1 Zabramski type II CCM in the first brain MRI			
Yes	105.95	5	5.79 (1.45-23.13)
No	34.57	2	4.72 (1.96-11.34)

Legend: CM, cavernous malformation; CCM, cerebral cavernous malformation; CNS, central nervous system; CI- confidence interval

Table 4.4. Cumulative risk of symptomatic hemorrhage at 5-years of follow-up of the 41 subjects stratified by clinical and genetic characteristics.

Variable	n	Nº symptomatic hemorrhagic events during 5-year follow-up	5-year risk (95% CI)
Gender			
Male	22	4	18.2 (5.2-40.3)
Female	19	3	15.8 (3.4-39.6)
Ethnic origin			
Caucasian	30	6	20.0 (7.7-38.6)
Other	11	1	10.0 (2.3-41.3)
Age at presentation			
< 6 years	27	2	14.3 (1.8-42.8)
≥ 7 years	14	5	18.5 (7.8-39.7)
Positive family history			
Yes	29	6	20.7 (8.0-39.7)
No	12	1	8.3 (2.1-38.5)
Genotype			
CCM1	17	3	17.6 (3.8-43.4)
CCM2	6	2	33.3 (4.3-77.7)
CCM3	6	1	14.3 (0.4-64.1)
Presentation Mode			
Symptomatic Hemorrhage	15	5	33.3 (11.8-61.7)
No hemorrhage	26	2	7.7 (1.0-25.1)
≥ 1 Extra-CNS CM			
Yes	2	1	50.0 (1.3-98.7)
No	39	6	15.4 (5.9-30.5)
≥ 10 CCM at first brain MRI			
Yes	21	3	14.29 (3.05-36.34)
No	20	4	20.00 (5.73-43.66)
≥ 1 CCM in the brainstem at first brain MRI			
Yes	15	4	26.66 (7.79-55.1)
No	26	3	11.54 (2.45-30.15)
≥ 1 CCM in the posterior fossa at first brain MRI			
Yes	26	6	23.08 (8.97-43.65)
No	15	1	6.67 (1.68-31.95)
≥ 1 Zabramski type II CCM at first brain MRI			
Yes	31	5	16.13 (5.45-33.73)
No	10	2	20.0 (2.52-55.61)

Legend: CM, cavernous malformation; CCM, cerebral cavernous malformation; CNS, central nervous system; CI- confidence interval

Table 4.5. Demographic and radiological risk factors of subsequent symptomatic hemorrhage at 5-years follow-up after initial diagnosis.

	Univariable analysis		**Multivariable analysis**[a]	
Variable	**Unadjusted HR (95% CI)**	**P value**	**Adjusted HR (95% CI)**	**P value**
Male gender	1.00 (0.223-4.494)	1.00	0.99 (0.22-4.47)	0.99
Age at presentation, in years	1.02 (0.879-1.1)	0.82	1.02 (0.88-1.18)	0.82
Symptomatic hemorrhagic presentation	4.33 (0.84-22.3)	0.08	4.35 (0.84-22.50)	0.08
Positive family history	2.87 (0.35-23.880)	0.28	2.93 (0.35-24.50)	0.32
Genotype CCM1 CCM2 CCM3	 Reference 2.25 (0.375-3.93) 0.734 (0.076-7.07)	 0.38 0.79	 2.97 (0.42-20.87) 0.67 (0.07-6.71)	 0.27 0.73
Presence of extra-CNS CM	2.51 (0.30-20.99)	0.40	2.70 (0.25-29.68)	
Caucasian ethnicity	1.92 (0.23-15.00)	0.55	1.93 (0.23-16.28)	0.54
Nº intracranial CCM at first MRI	1.02 (0.98-1.06)	0.29	1.02 (0.98-1.06)	0.26
≥ 10 CCM at first brain MRI	0.489 (1.12-1.78)	0.28	0.98 (0.35-2.77)	0.97
Nº of CCM in the post fossa at first brain MRI	1.37 (1.10-1.71)	0.005*	1.39 (1.10-1.76)	0.005*
≥ 1 CCM in the posterior fossa at first brain MRI	3.59 (0.33-4.74)	0.74	4.05 (0.45-36.37)	0.21
Nº of brainstem CCM at first brain MRI	1.63 (1.18-2.26)	0.003*	1.64 (1.18-2.31)	0.004*
≥ 1 CCM in the brainstem at first brain MRI	2.67 (0.60-11.97)	1.00	2.77 (5.91-12.98)	0.20
Nº of Zabramski type II CCM at first brain MRI	1.06 (0.99-1.14)	0.12	1.07 (0.98-1.16)	0.12
≥ 1 Zabramski type II CCM at first brain MRI	0.81 (0.16-4.18)	0.80	0.76 (0.14-4.16)	0.75
≥ 1 *de novo* CCM at follow-up brain MRI	1.00 (0.22-4.48)	0.99	1.02 (0.87.1.19)	0.82
Nº *de novo* CCM at follow-up brain MRI	0.95 (0.76-1.19)	0.67	0.95 (0.75-1.20)	0.66

Legend: CM, cavernous malformation; CCM, cerebral cavernous malformation; CI, confidence interval; CNS, central nervous system; FU- follow-up; HR, Hazard ratio; IQR, interquartile range

[a] adjusted for age at presentation and gender

* statistically significant value

Supplemental Table 4.1. Comparison between subjects surgically and conservatively treated.

	Surgically treated subjects N=19 (46.3%)	**Conservatively treated subjects N= 22 (53.7%)**	**P-value**
Male, n (%)	8 (42.1)	14 (63.6)	0.167
Age at initial clinical presentation in years, median (IQR)	7.8 (4.5-12.8) Range: 0.4-15.8	6.8 (3.0-12.3) Range: 0.8-17.3	0.657
Genotype, n (%) C*CM1* CCM2[a] C*CM3* *CCM1-3* testing negative/not performed/pending	 8 (42.1) 3 (15.8) 3 (15.8) 5 (26.3)	 9 (40.9) 3 (13.6) 4 (18.2) 6 (27.3)	1.0
Positive family history, n (%)	24 (73.7)	15 (68.2)	0.699
Ethnic origin, n (%) Caucasian Other	 15 (79.0) 4 (21.1)	 15 (68.2) 7 (31.8)	0.499
Presentation mode, n (%) Symptomatic hemorrhage of the CNS[b] Other type of clinical presentation	 10 (52.6) 9 (47.4)	 5 (22.7) 17 (77.3)	0.047*
$\geq$ 1 extra-CNS CM, n (%)	1 (5.3)	1 (4.6)	1.0
Neurological assessment at last clinical FU, n (%) Normal/mild Moderate/severe impairment or death	 13 (68.4) 6 (31.6)	 19 (86.4) 3 (13.6)	0.166
Seizures at last clinical FU, n (%)	8 (42.1)	4 (18.2)	0.167
Clinical FU time in months, median (IQR)	46.8 (22.3-97.9) Range:8.9-143.4	58.9 (37.1-92.3) Range: 4.0-205.4	0.548
Nº CCM at first brain MRI, median (IQR)	6 (2-12; 1-80)	12 (8-23; 2-67)	0.0204*
Presence of >=1 CCM in the posterior fossa at first brain MRI, n (%)	10 (52.6)	16 (72.7)	0.183

Legend: CM, cavernous malformation; CCM, cerebral cavernous malformation; CNS, central nervous system; FU- follow-up; IQR, interquartile range

[a] includes 4 cases with a 7p deletion; [b] 1 case due to a SCCM-related hemorrhage

* statistically significant value

Supplemental Table 4.2. Clinical risk of CCM-related symptomatic hemorrhage as mode of presentation.

	Univariable analysis		**Multivariable analysis** [a]	
Variable	**Unadjusted OR (95% CI)**	**P value**	**Adjusted OR (95% CI)**	**P value**
Male gender	1.0 (0.3-3.5)	0.975	0.99 (0.27-3.54)	0.982
Age at presentation in years	1.0 (0.9-1.1)	0.130	0.99 (0.88-1.13)	0.910
Positive family history	2.1 (0.5-9.5)	0.275	2.12 (0.47-9.54)	0.329
Genotype CCM1 CCM2 CCM3	 Reference 0.56 (0.08-3.93) 0.45 (0.068-3.00)	 Reference 0.890 0.246	 Reference 0.56 (0.08-3.98) 0.43 (0.64-3.02)	 Reference 0.566 0.403
Presence of extra-CNS CM	1.8 (0.1-30.8)	0.690	1.97 (0.10-38.86)	0.656
Caucasian ethnicity	0.0 (0.2-4.3)	0.749	1.00 (0.23-3.77)	0.998

Legend: CM, cavernous malformation; CCM, cerebral cavernous malformation; CI, confidence interval; CNS, central nervous system; FU- follow-up; IQR, interquartile range; OR, Odds ratio
[a] adjusted for age at presentation and gender

Figures and Legends

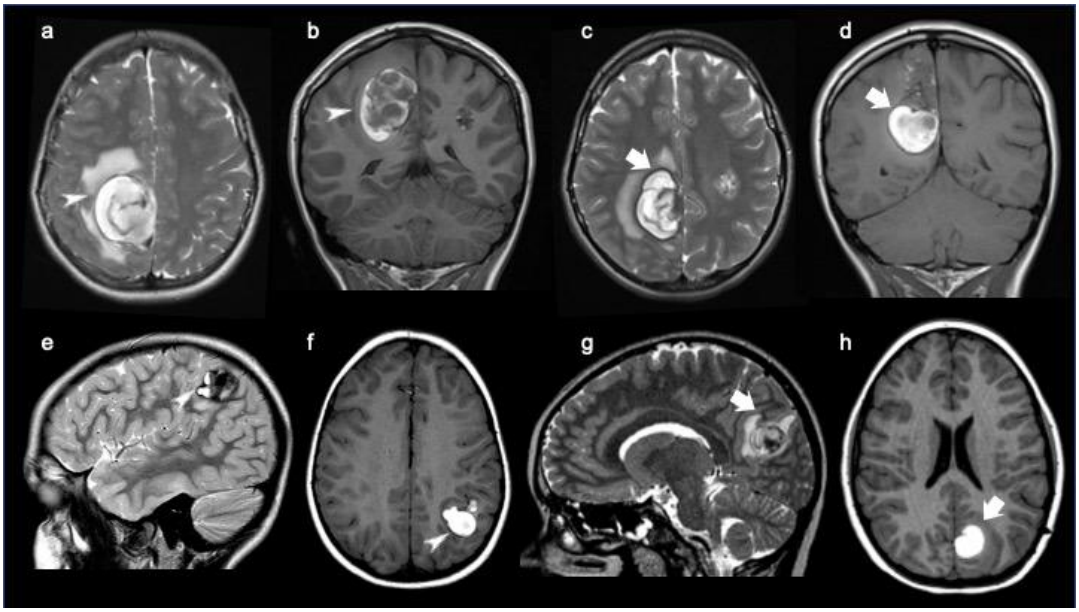

Figure 4.1. Examples of symptomatic hemorrhagic brain cavernous malformations.
Brain MR (a,b) performed in the emergency setting in a 15-year-old girl with familial cerebral cavernous malformation syndrome due to a proven CCM1 mutation including axial T2 TSE (a) and coronal T1 SE (b) demonstrates an acute right parietal symptomatic hemorrhagic cerebral cavernous malformation (*white arrowheads*) with multiloculate appearance, complete hemosiderin ring as well as surrounding edema. No surgical treatment was performed. Follow-up brain MR of the same patient (d, e) performed after 22 months due to development of new acute neurological symptoms, including axial T2 TSE (c) and coronal T1SE (f), reveals symptomatic re-hemorrhage of the same cavernous malformation (*white arrows*), that was subsequently resected. Brain MR (e,f) performed in the emergency setting in a 7-year-old boy with familial cerebral cavernous malformation syndrome due to a proven CCM1 mutation including sagittal T2 TSE (e) and axial T1 SE (f) demonstrates an acute left parietal symptomatic hemorrhagic cerebral cavernous malformation (*white arrowheads*) with multiloculate appearance, complete hemosiderin ring, fluid-fluid levels and a small component of surrounding edema. This lesion was surgically removed with complete resection. Follow-up brain MR (d, e) performed after 50 months due to development of new acute neurological symptoms, including axial T2 TSE (c) and coronal T1SE (f), shows a *de novo* cavernous malformation with signs of acute hemorrhage (*white arrows*), that was also subsequently resected.

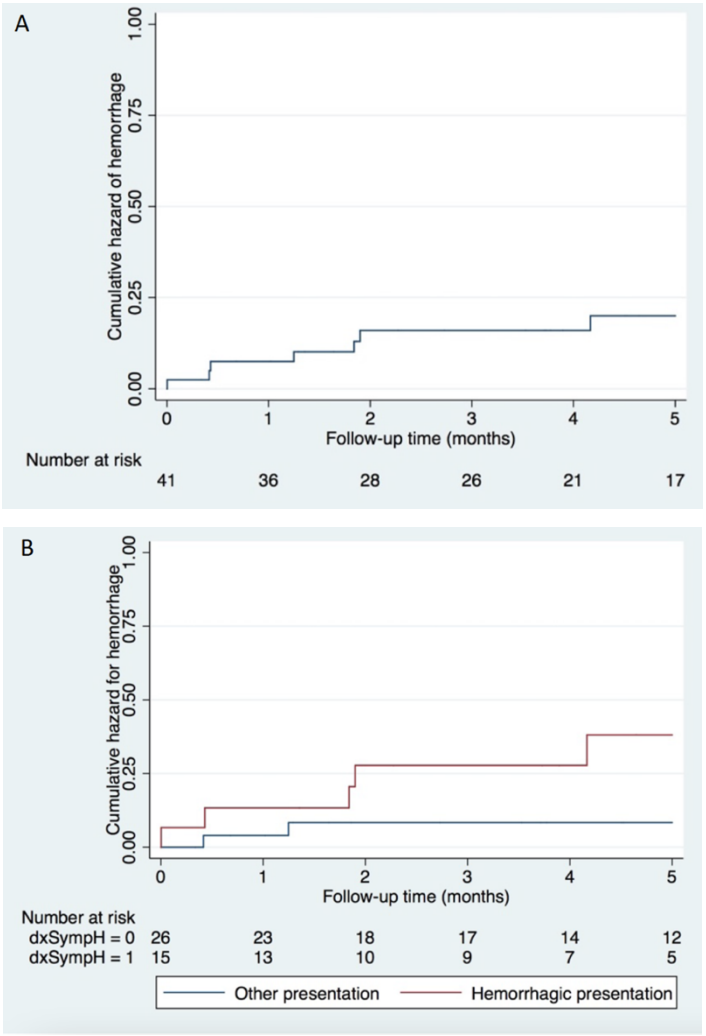

Figure 4.2. Cumulative hazard curves of hemorrhage of 41 children during 5-years follow-up for the entire cohort (A) and stratified by initial presentation with intracranial hemorrhage or other type of presentation (B).

DISCUSSION

We started our work with a narrative literature review on the topic of pediatric CVM, mainly focusing on the neuroimaging findings of the two most common subtypes: DVA, CM and their associated syndromes. This structured state of the art enabled the construction of a solid and deep overall understanding of the field, including current knowledge gaps. In this context, we have also published a case report in the form of a *Letter to the Editor* reporting the imaging features of a DVA detected *in utero* using fetal MRI and subsequently confirmed with postnatal MRI.

Thereafter, we conducted three different retrospective clinical studies divided in two main areas of the scientific topic of interest (namely neonatal DVA and pediatric FCCM), all of them published in peer-reviewed journals.

The **first line of our research** was devoted to the topic of DVA in neonates and we found in our monocenter retrospective study that:

1. Real-world detection rate of DVA using brain MRI in one tertiary pediatric hospital was 1.9%;
2. Retrospective *in utero* detection of DVA was possible in approximately one-quarter (27.3%) of the neonates with a confirmed postnatal DVA and at least one fetal MRI available for review;
3. Greater than one-third (36.6%) of neonates presented with at least one type of neuroimaging complication directly linked to DVA. More specifically, WM signal abnormalities were present in 17.1% of the DVA-positive neonates while associated hemorrhages and/or ischemic changes were identified in our sample in 19.5% and 9.8% of cases, respectively. In addition, CCM and/or polymicrogyria were detected in their vicinity in 4.9% of cases each and obstructive hydrocephalus in 3.2%;
4. Multiple DVA were significantly more frequent in individuals of the c-DVA group ($P = 0.002$); in addition, complicated DVA were significantly associated with presence of multiple and larger collectors ($P = 0.008$ and $P < 0.001$, respectively);
5. Neuroimaging follow-up at a median time = 39.1 months showed signs of improvement in the majority (n= 80%) of children, with no new DVA detected in any case;

6. Neurological outcomes of DVA-positive neonates at a median time = 27.5 months were normal in 64.2% of subjects, while minor or moderate impairment were detected in 28.5% and 7.1% of cases, respectively;
7. No new DVA could be identified in follow-up MRI in any of the cases.

DVA have come a long way from being considered *normal anatomic variants* [31] into being recognized as lesions potentially causing neuroimaging complications, that in turn may be asymptomatic or symptomatic [38–40].

Nevertheless, numerous questions regarding this subtype of CVM remain unanswered, namely the timing of their origin. Indeed, results arising from one published study revealed a significant positive association between age and DVA detection using brain MRI, thereby suggesting that DVA may actually form in post-natal life instead of being congenital lesions [54]. Importantly, this study needs to be interpreted with caution due to its retrospective design, dependence on reporting text, absence of information regarding the clinical indication of the exams (except in case of tumor or epilepsy), significant differences regarding the number of patients included in each age group, absence of healthy control group, and image review by a single neuroradiologist. In our investigation, we have identified DVA already *in utero* in more than one quarter of our neonatal DVA cases with an available fetal MRI, confirming a congenital origin at least in those cases. As fetal MRI has an overall lower image resolution and is more prone to artifacts than postnatal brain MRI with anesthesia and/or *feed and wrap* technique [13, 14] and not all available fetal MRI examinations included a T2*WI sequence as part of the imaging protocol, we believe that the remainder DVA cases were already prenatally present but could not be detected due to their small size and/or technical limitations. Supporting our theory, no new DVA was detected in any case during neuroimaging follow-up.

Interestingly, our real-world MRI-detection of DVA in neonates was 1.9%, lower than generally described for older children and adults [17, 36, 54]. However, DVA are probably more difficult to detect in neonates than in other age groups due to their small head size and incomplete myelination, short imaging protocols with lower rate of gadolinium injection as well as the common occurrence of motion artifacts [9].

More than one third of all our neonatal DVA were complicated by parenchymal abnormalities, most commonly WM signal changes. A high percentage of complications has also been reported in another neonatal cohort of DVA including a smaller number of patients [19]. Therefore, available data suggest that there is a higher risk of flow-related complications in DVA during the

neonatal period than in other phases of life. Putative neonatal risk factors of hemodynamic decompensation of DVA in the neonatal phase include mechanical distortion during vaginal birth and immaturity of the venous, immune, and hemostatic systems as well as hypercoagulability, which may be potentiated by maternal factors or inflammation [82, 441, 442].

Moreover, complications were significantly more common in patients with multiple DVA and in lesions drained by multiple and larger collectors, suggesting that more severe and widespread venous pathology may correspond to a more fragile venous outflow system and/or a higher propensity for thrombotic DVA events. Therefore, in the setting of a specific DVA depicted in a neonate, analysis of these factors as well as identification of coexistent lesions can help predict the occurrence of associated complications.

Finally, during follow-up of neonates with DVA, neuroimaging and neurologic outcomes were favorable in most cases, and this information can be used in clinical practice by referral clinicians to reassure the parents of affected subjects.

In what concerns the **second line of our research**, it focused on the clinical and neuroimaging assessment of pediatric FCCM, including evaluation of SCCM, ISVM and/or CCM in two partially overlapping cohorts with a diagnosis of this rare disorder according to clinical and/or genetic criteria.

More specifically, we found in our multicenter retrospective study concerning the spinal MRI features of pediatric FCCM patients that:

1. Real-world detection rate of SCCM was 16% using diverse spine MRI protocols in three different tertiary pediatric hospitals (for a total of n=6 SCCM, one of them appearing *de novo*);
2. IVMS were not present;
3. There were no statistically significant differences between SCCM+ and SCCM- groups concerning the number of CCM. However, SCCM+ patients showed a tendency towards presence of at least one CCM in the posterior fossa. In addition, the only two patients with ≥1 extraneural CM were also SCCM+.

On the other side, our results concerning the multicenter retrospective study focusing on the natural history of pediatric FCCM patients reveal that:

1. The 1-, 2-, and 5-year cumulative risks of hemorrhage in a cohort of children with a confirmed diagnosis of FCCM and the first brain MRI available for review were 7.3%, 14.6%, and 17.1%, respectively;
2. The annual symptomatic hemorrhage rate for the same cohort at 5-year follow-up after diagnosis was 5.0% per person-year;
3. The 5-year cumulative risk was higher in subjects with prior symptomatic hemorrhage at presentation (33.3%), CCM2 genotype (33.3%) and positive family history (20.7%), nevertheless without reaching statistically significance;
4. In uni and multivariate analysis, no significant independent predictors of presentation with acute symptomatic hemorrhage were identified;
5. Number of brainstem (adjusted HR = 1.37, P = 0.005) and posterior fossa (adjusted HR = 1.64, P = 0.004) CCM at first brain MRI were significant independent predictors of prospective symptomatic hemorrhage.

CM have been the subject of intense collaborative research in the last decades, leading to a dramatic increase in the body of knowledge concerning these entities. Indeed, according to a recent bibliometric analysis, > 800 articles were published between 1974 and 2022 on the topic of CCM [458]. Nevertheless, there is also a clear population gap in the scientific literature concerning CM, as children are not adequately represented and/or under-researched in prior research and especially in clinical trials [459]. In addition, the field of CM is still in need of specific biomarkers which would assist in diagnosis, risk stratification, management, prognostication and treatment monitorization, namely in clinical trials evaluating future innovative therapeutics [228].

Neuroimaging remains an essential component of the investigation of both CCM and SCCM. Indeed, in a recent paper presenting the top 10 research priorities for CM selected by a partnership including a multidisciplinary steering group, two of them concerned radiological-related questions about these entities [460].

Our findings support the increasingly recognized concept of FCCM as a multisystem, progressive disorder in which multiple CM are usually present in many different locations already during the pediatric age, requiring multidisciplinary evaluation and follow-up [173, 185]. Importantly, pharmacological agents are particularly appealing for children with FCCM as preliminary data of preclinical studies suggest that these compounds not only stabilize CM but also prevent their formation [421, 423, 434, 435], which is known to be age-dependent [173, 185, 326]. Indeed, as

the number of CM and associated complications increase over time, it is beneficial to make the diagnosis of this rare disorder as early as possible (ideally in the pediatric age), to identify all CM already present at that time (in the brain but also in the spinal cord) and allow early inclusion of affected patients in ongoing clinical trials. This approach aims to reduce the overall CM load and avoid the installation of neurological deficits, ultimately leading to better clinical outcomes. Diagnosis of FCCM in one child, can also prompt genetic and/or MRI screening of the remainder family members, thereby allowing potential anticipation of the diagnosis in affected relatives, and potentially allowing their inclusion in clinical trials while they are still asymptomatic.

According to our findings, and in line with most recent studies on the topic [16, 246, 250], children with FCCM treated in tertiary pediatric centers seem to have an overall similar 5-year cumulative symptomatic hemorrhage rate when compared with children with sporadic CM disease and adults with either familial and sporadic disease, and this information can help provide more accurate prognostic information to affected children and their parents. Interestingly, besides presentation with symptomatic hemorrhage, also *CCM2* genotype was associated with a higher 5-year cumulative risk of symptomatic hemorrhage when compared with other genotypes, although without reaching statistical significance. This result was unexpected, as *CCM3* genotype has been associated with a more aggressive phenotype and therefore may be due to chance alone [268–271]. Therefore, these results need to be validated in prospective studies including larger sample sizes of children diagnosed with FCCM and with genetic characterization.

On the other side, our data also suggests that neuroimaging features at first brain MRI (namely total number of brainstem and cerebellar CM) in children with FCCM may help to predict symptomatic hemorrhage at 5-year follow-up, thereby having the potential to guide a more individualized management plan. In the meanwhile, another study in a mixed age cohort of FCCM patients showed that total CCM lesion burden is significantly associated with increased risk of subsequent symptomatic ICH [246]. Further study of potential neuroimaging predictors of outcome at first brain MRI in FCCM patients is warranted as they may help establish a more individualized patient risk stratification and treatment approach.

Based on the throughout literature review, in the personal experience of our research group and in the obtained results, we propose a clinical and neuroimaging management protocol, that is presented below as **Figure 5.1 to 5.4**. Specifically, we endorse that these patients should be imaged with the best available MR scanner (ideally in a 3.0-T unit) using a standard imaging technique/protocol. The brain MRI protocol should include a T1 3D sequence, axial and coronal

T2WI, axial 2D or 3D FLAIR, and at least one GRE sequence, preferably SWI. In addition, we recommend an optimized whole-spine MRI at diagnosis in all pediatric cases with clinical-radiological suspicion or a definitive diagnosis of this disorder regardless of the presentation age as a screening modality. This spine MR study should include a T1 TSE, a T2 TSE, and at least one GRE sequence, ideally a 3D T2 MEDIC. On the other side, serial spine MRI with a similar protocol should be also considered in confirmed cases even with negative initial spine MRI studies, ideally performed in the same time slot of the control brain MRI.

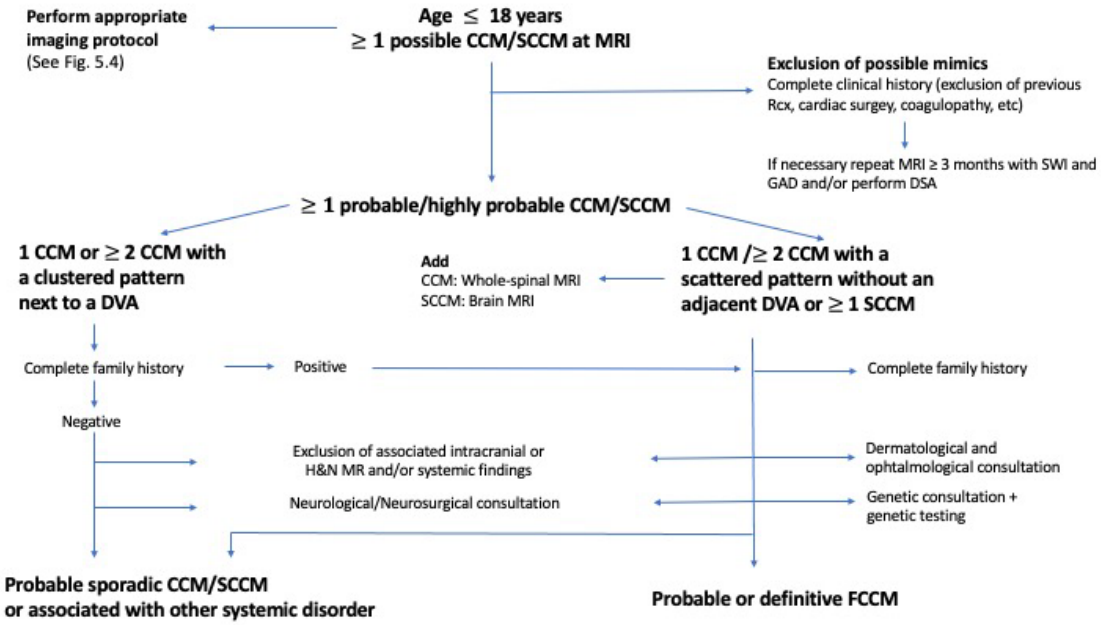

Fig. 5.1. Proposed management algorithm of pediatric patients with at least one possible cerebral or spinal cord cavernous malformation. Legend: CCM- Cerebral cavernous malformation, DSA- Digital subtraction angiography, DVA- Developmental venous anomaly, FCCM- Familial cerebral cavernous malformation syndrome, H&N- Head and neck, MRI- Magnetic resonance imaging, Rcx- Radiosurgery, SCCM- Spinal cord cavernous malformations.

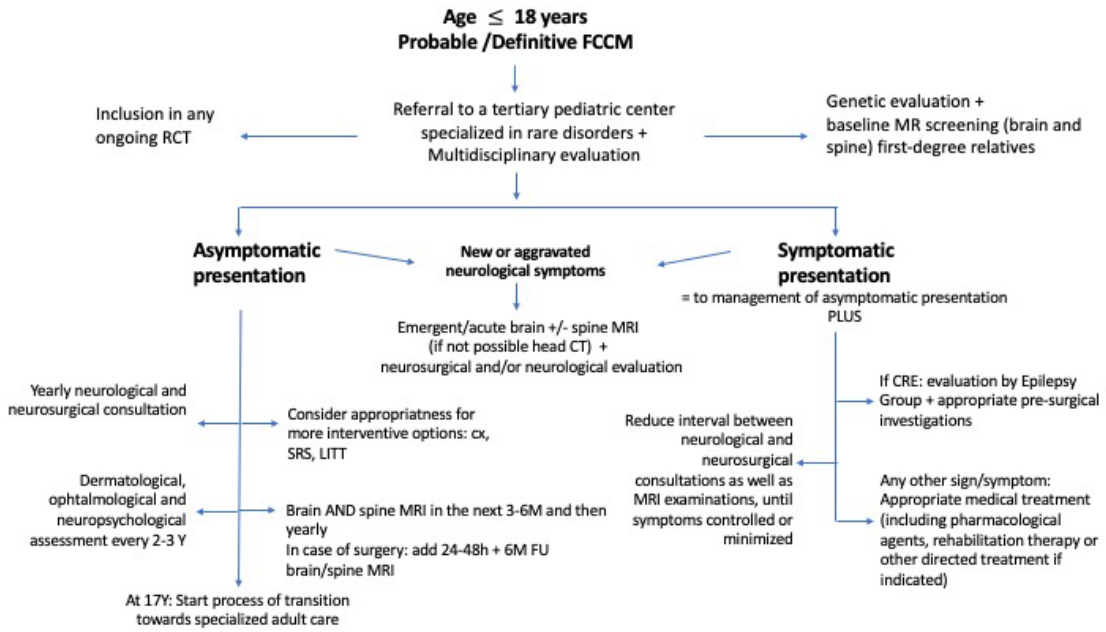

Fig. 5.2. Proposed management algorithm of pediatric patients with probable or definitive familial cerebral cavernous malformation syndrome. Legend: CRE- Cavernoma related epilepsy, CT- Computed tomography, cx- Surgery, FU- Follow-up, LITT- Laser interstitial thermal therapy, MRI- Magnetic resonance imaging, RCT- Randomized clinical trial, SRS- Stereotactic radiosurgery, Y- years.

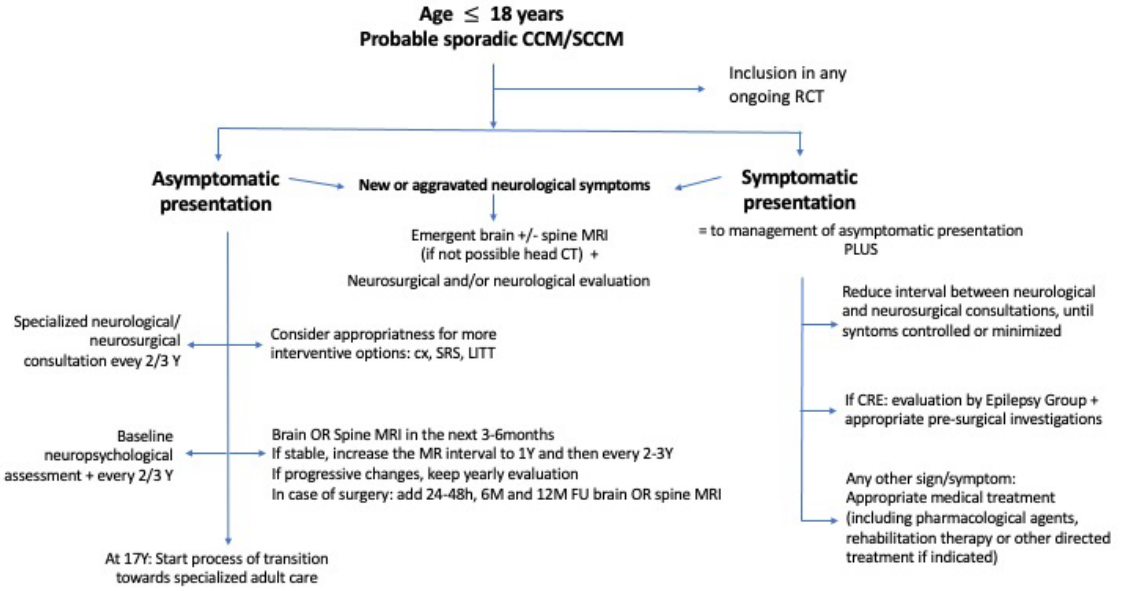

Fig. 5.3. Proposed management algorithm of pediatric patients with probable sporadic cerebral or spinal cord cavernous malformation. Legend: CRE- Cavernoma related epilepsy, CT- Computed tomography, cx- Surgery, FU- Follow-up, LITT- Laser interstitial thermal therapy, MRI- Magnetic resonance imaging, RCT- Randomized clinical trial, SRS- Stereotactic radiosurgery, Y- years.

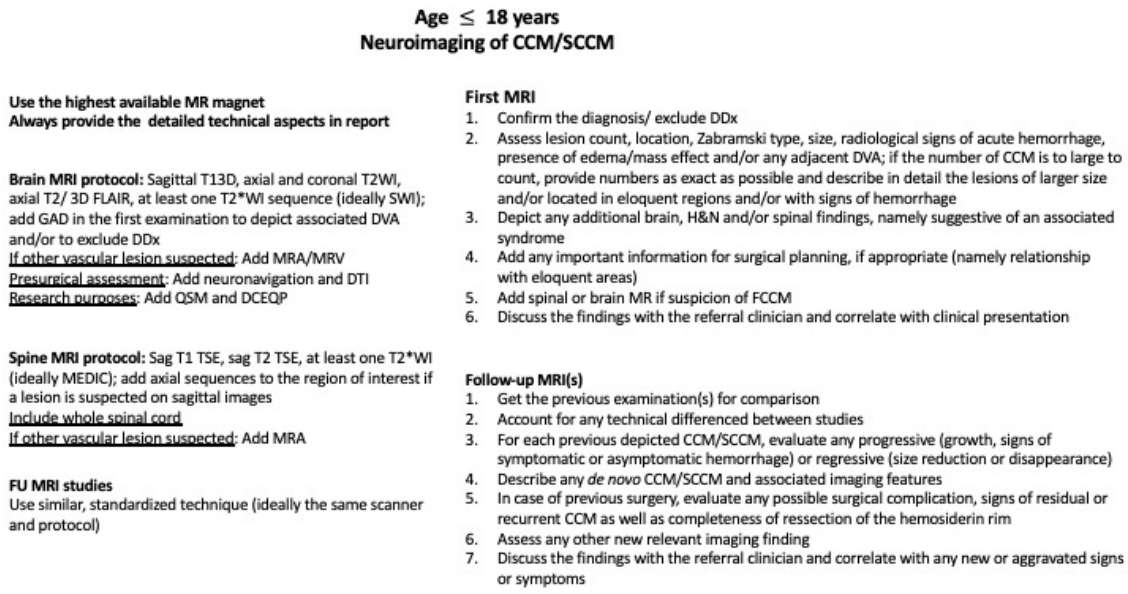

Fig. 5.4. Proposed neuroimaging approach to cerebral and/or spinal cord cavernous malformations. Legend: 2D- Two-dimensional, 3D- Three-dimensional, CCM- Cerebral cavernous malformation, DCEQP- Dynamic contrast-enhanced quantitative perfusion, DDx- Differential diagnosis, DTI- Diffusion tensor imaging, DVA- Developmental venous anomaly, FCCM- Familial cerebral cavernous malformation syndrome, FLAIR- Fluid attenuated inversion recovery, GAD- Gadolinium, MEDIC- T2 multi-echo data image combination, MRA- Magnetic resonance angiography, MRI- Magnetic resonance imaging, MRV- Magnetic resonance venography, QSM- Quantitative susceptibility mapping, SCCM- Spinal cord cavernous malformations, SWI- Susceptibility-weighted imaging, WI- Weighted-imaging.

Strengths and limitations of our results

Looking at the global work developed in this dissertation, emerges as particularly relevant to the concretization of our work the establishment of an international collaborative multidisciplinary research network devoted to this area of investigation. Research networks are critically important tools for research concretization in all medical fields, but even more pivotal in the setting of rare diseases that, by definition, affect an exceedingly small number of patients (usually < 40-50/100,000 persons) [461, 462]. Indeed, as the type and power of statistical analysis goes hand in hand with sample size, investigations in these disorders strongly rely on multicenter (often international) collaboration and corresponding pooled efforts and resources including data sharing. Eligibility of patients for studies focusing on rare disorders remains even more limited if only specific age groups are studied, such as in our research topic.

Resulting from this collaboration, and as far as we are concerned, we have published the neuroimaging-related study that included the largest cohort of neonates with ≥ 1 MRI-confirmed DVA. In addition, both our published studies concerning the neuroimaging findings of CM also included the larger sample size of pediatric only cohorts of FCCM patients available in the English

scientific literature, allowing more accurate and reliable results. The group interactions that were built also open new possibilities and are the basis for a long-term path that we hope may bring a major contribution to the imaging study of CVM.

Finally, based on the results of our two studies including children with FCCM and on the extensive literature review on the topic we propose a new management protocol for children in which this disorder is suspected or confirmed. Indeed, as current consensus guidelines are lacking, this algorithm can be easily applied to the routine clinical setting and may be used to guide clinicians and standardize the current medical practice.

There are some overall limitations to our investigation, the major being its retrospective design, that is intrinsically prone to multiple biases and presents inferior level of evidence compared with prospective studies.

Additionally, all studies were performed in tertiary pediatric institutions, leading to potential selection bias towards more severe and/or complex cases. Moreover, our cohorts were predominantly composed of Caucasian subjects, which may limit generalizability to subjects with other ethnic backgrounds, including the commonly reported Hispanic FCCM population.

It is also important to note that subjects were imaged at inconsistent time points and without standard brain and/or spine MRI technique, including variations in the scanner field strength (1.5 vs 3.0-T) and/or the protocol (namely acquisition of different MR sequences and planes, occasional usage of gadolinium-based contrast media and variable sedation strategies). This may have limited the imaging assessment and likely resulted in an underestimation of the detection of DVA, CCM and SCCM, as their identification is strongly dependent on technical parameters. We have neither evaluated advanced MRI techniques such as QSM and DCEPQ that have been recently described as biomarkers of CCM activity and predictors of lesional growth and hemorrhage [365, 369–371]. Indeed, although these techniques are usually not performed routinely in the clinical setting, they are already being incorporated in clinical trials in adults with CM [375–377] and we believe that future studies should evaluate their role in children as well.
Another limitation of our research is the fact that follow-up clinical and imaging data were missing in some patients, limiting longitudinal assessment. In particular, we had a 39% rate of loss to follow-up at 5 years in the research study evaluating the natural history of CCM in FCCM, which occurred mainly due to adult care transferal, potentially interfering with the accuracy of our results. Finally, the number of symptomatic bleeding events in the latter study was rather

low during follow-up, limiting the number of potential variables to be included and increasing the 95% CI in the Cox proportion regression analysis model.

Future directions/perspectives

Future endeavors directly related to this thesis include collaborative work with the recently founded national association of CM, the "*Cavernoma Portugal*". Similar networks including patients, relatives, care givers, healthcare workers, representatives of patient support associations and medical societies as well as academics already exist abroad, such as the *Brain Vascular Malformation Consortium* from the *Rare Diseases Clinical Research Network* and the *Alliance to Cure Cavernous Malformations (alliancetocure.org)*. Nevertheless, none of them includes a strong Force Task dedicated to the specificities of the pediatric population living with CM and/or other CVM and such effort should be initiated as soon as possible. Progressive growth of such an organized and formal patient organization in Portugal in collaboration with its international counterparts as well as related skateholders and medical societies would facilitate establishment in a near future of a standardized national rare disease registry of children with CCM/FCCM and other CVM as well as cooperation of Portugal in formal European research networks including hospitals and institutions dedicated to pediatric CVM, namely as part of joint programs and calls supported by the European Union. In addition, it could facilitate the initiation of a systematic collection and storage of biological samples and imaging of affected patients including children in dedicated national BioBanks as well as promote bridges between clinicians and basic scientists aiming for future translational research in this topic. Finally, joint efforts should be made in order to advocate for the inclusion of Portuguese centers in future pediatric clinical trials in CVM, namely in FCCM, thereby contributing for early and free access to innovative pharmacological therapies in Portugal.

In the short-term period, it would also be important to obtain national and international endorsement of the proposed imaging protocol for diagnosis and follow-up of pediatric patients with CM/FCCM.

Despite answering some questions, the present works opens many others, that may be undertaken that we hope to pursue. Indeed, our findings open a path for ongoing and future research in the topics of DVA and FCCM in children at all ages.

More specifically, we believe that joint efforts should be made aiming to confirm the genetic origin of DVA associated with CM [60] as well as to study the genetic origin of isolated DVA. As

surgical resection and/or biopsy of DVA in the setting of complicated lesions is in general contra-indicated [38, 39], it is difficult to obtain biological material of these lesions, thereby complicating this task. Nevertheless, material from autopsies and/or hemispherectomies may be used instead. In addition, it would also be important for a better comprehension of the origin of DVA to conduct more fetopathology and postmortem MRI studies of the fetal and stillborn CNS focused on these vascular malformations and to correlate obtained data with available prenatal US and fetal MRI.

On the other side, case-control studies comparing the prevalence of DVA between children diagnosed with MS and age and sex-matched controls should be performed, aiming do further explore the potential association between DVA and MS that is still unclear in adults [128–133].

In what concerns to future investigations within the field of CM, and given the recently published positive results of the Treat_CCM clinical trial regarding safety and efficacy of treatment with oral propranolol plus standard of care vs standard care alone in a cohort of adults with FCCM [28], a subsequent clinical trial with a similar design but including only pediatric patients with this rare disease should be launched soon. In addition, response assessment of SCCM and systemic CM to propranolol and other novel medical treatments in pediatric FCCM nd effects of the subjacent genotype in potential differences of the treatment effect should also be addressed in future clinical trials.

Moreover, the role of asymptomatic prospective radiologic changes in both SCCM and CCM (especially asymptomatic hemorrhage), should be further investigated in prospective neuroimaging studies at fixed time-points during the pediatric age using standard technique. Accordingly, we believe that in the meanwhile current reporting standards of hemorrhage from CCM should be reviewed [240], and individualized reporting of both symptomatic and asymptomatic hemorrhage rates *per patient* and *per lesion* in future studies should be recommended instead [177, 252, 325]. This approach can also help understanding if brainstem CCM are indeed intrinsically more aggressive or if hemorrhages in this location although occurring at the same rate as in other locations tend to cause more often associated symptoms.

On the other side, as application of advanced neuroimaging techniques such as QSM and DCPEQ in children with CM either familial or sporadic is lagging behind with regards to adult populations [365, 369–371], joint international efforts should be made in order to correct this asymmetry.

In addition, novel integrative approaches, namely including information arising from both conventional and advanced neuroimaging techniques with blood circulating candidate

biomarkers are already being investigated in adults with sporadic and/or familial CCM [224–231] and should be translated as soon as possible to pediatric populations. In particular, blood level differences of CM-related microRNA and/or angiogenic and inflammatory molecules between affected children and adults as well as between different phases of the normal development during childhood should be explored in the near future.

Combination of data obtained from analysis of the *microbiotia* and application of multimodal neuroimaging techniques in children with CM is another possible line of research, that may allow a better understanding of the role of the *brain-gut axis* in the pathogenesis and natural history of these entities [218–221]. More specifically, it would be of interest to investigate differences in human gut microbiomes with variable CCM disease presentation and severity as well as between sporadic/familial subtypes and in the latter case, between specific genotypes and ultimately to correlate the findings with the corresponding MR phenotype.

Finally, in both pediatric DVA and CM, development of clinically meaningful patient-reported outcomes and their incorporation in clinical studies and correlation with neuroimaging findings should be pursued.

The ultimate goal of CVM research focused on pediatric cohorts with either DVA and CM is to place the child and its parents/family at the center of the investigation and care, thereby taking into account their special needs, providing a more individualized approach and ultimately improving their health outcomes, including quality of life.

Given their essential role in the diagnosis, classification and monitoring of CVM as well as the potential contribute of advanced MRI techniques as related biomarkers, radiologists with differentiation in pediatric neuroradiology should be actively involved in clinical and research teams focusing on children with CM and DVA.

CONCLUSION

The present doctoral dissertation is the culminate result of an investigation project using brain and/or spine MRI to study CVM, and focusing on neonatal DVA and pediatric FCCM.

Our research was able to demonstrate a real-world MRI-detection rate of DVA in neonates of 1.9%, with 36.6% of cases being complicated by parenchymal abnormalities, especially in the setting of multiple of DVA and specific angioarchitectural features.

The current thesis also reveals that SCCM can be detected in up to 16% of cases of a pediatric cohort of FCCM patients using diverse spine MRI protocols and may appear *de novo*, while ISVM are absent instead. In addition, our investigation establishes that the 5-year annual and cumulative symptomatic hemorrhagic risk in our pediatric FCCM cohort equals the overall risk described in children and adults with all types of CCM and that imaging features at first brain MRI may help to predict symptomatic hemorrhage at 5-year follow-up.

Importantly, the conducted work has allowed the establishment of an informal international multi-disciplinary team focused on the area of pediatric CVM, including tertiary pediatric centers from Portugal, Italy, United Kingdom and United States of America, with subsequent development and publication in peer-reviewed journals of three related studies focusing on the corresponding clinico-radiological features, each of them including the largest cohort of patients published to date harboring the respective pathology of interest in the specific age group.

Based on the narrative review of the scientific literature and the results from the research work, we also provide a clinico-radiological algorithm for management of pediatric patients with CM, including those in the setting of FCCM.

Our investigation supports the central role of neuroimaging in the evaluation of neonatal DVA and pediatric FCCM, and the presented results can be used by radiologists and clinicians alike in everyday clinical practice, namely for improving individual prognostication and more precise parental counselling. Gathered data may also be used by skateholders, including development of health policies and/or application in future clinical trials as surrogate endpoints and/or for sample size calculation.

Finally, the conducted work addresses the current population gap in CVM publications, acknowledging the uniqueness of children and placing them at the center of medical care and research. Therefore, we believe that it opens new paths for research in pediatric CVM, with potential impact in clinical practice and management of affected children.

REFERENCES

1. Krings T, Geibprasert S, TerBrugge K (2010) Classification and Endovascular Management of Pediatric Cerebral Vascular Malformations. Neuroimaging Clin N Am 21:463–482
2. Wassef M, Blei F, Adams D, et al (2015) Vascular anomalies classification: Recommendations from the international society for the study of vascular anomalies. Pediatrics 136:e203–e214
3. Mankad K, Biswas A, Espagnet MCR, et al (2020) Venous pathologies in paediatric neuroradiology: from foetal to adolescent life. Neuroradiology 62:15–37
4. Martinez-Lopez A, Salvador-Rodriguez L, Montero-Vilchez T, et al (2019) Vascular malformations syndromes: An update. Curr Opin Pediatr 31:747–753
5. Borst AJ, Nakano TA, Blei F, et al (2020) A Primer on a Comprehensive Genetic Approach to Vascular Anomalies. Front Pediatr 8:579591
6. Wang MX, Kamel S, Elsayes KM, et al (2022) Vascular Anomaly Syndromes in the ISSVA Classification System: Imaging Findings and Role of Interventional Radiology in Management. RadioGraphics 42:1598–1620
7. Huisman TAGM, Singhi S, Pinto PS (2010) Non-invasive imaging of intracranial pediatric vascular lesions. Childs Nerv Syst 26:1275–1295
8. Chang W, Huang M, Chien A (2015) Emerging techniques for evaluation of the hemodynamics of intracranial vascular pathology. Neuroradiol J 28:19–27
9. Rossi A, Argyropoulou M, Zlatareva D, et al (2022) European recommendations on practices in pediatric neuroradiology: consensus document from the European Society of Neuroradiology (ESNR), European Society of Paediatric Radiology (ESPR) and European Union of Medical Specialists Division of Neuroradiology. Pediatr Radiol 53:159–168
10. Zafar A, Fiani B, Hadi H, et al (2020) Cerebral vascular malformations and their imaging modalities. Neurol Sci 41:2407–2421
11. Tong KA, Ashwal S, Obenaus A, et al (2008) Susceptibility-weighted MR imaging: a review of clinical applications in children. AJNR Am J Neuroradiol 29:9–17
12. Ho ML, Campeau NG, Ngo TD, et al (2017) Pediatric brain MRI, Part 2: Advanced techniques. Pediatr Radiol 47:544–555
13. Prayer D, Malinger G, Brugger PC, et al (2017) ISUOG Practice Guidelines: performance of fetal magnetic resonance imaging. Ultrasound Obs Gynecol 49:671–680
14. Aertsen M, Diogo M, Dymarkowski S, et al (2020) Fetal MRI for dummies: what the fetal medicine specialist should know about acquisitions and sequences. Prenat Diagn 40:6–17
15. Al-Holou WN, O'Lynnger TM, Pandey AS, et al (2012) Natural history and imaging prevalence of cavernous malformations in children and young adults. Clinical article. J Neurosurg Pediatr 9:198–205
16. Santos AN, Rauschenbach L, Saban D, et al (2022) Natural Course of Cerebral Cavernous Malformations in Children: A Five-Year Follow-Up Study. Stroke 53:817–824
17. Silva AHD, Wijesinghe H, Lo WB, et al (2020) Paediatric developmental venous anomalies

(DVAs): how often do they bleed and where? Childs Nerv Syst 36:1435–1443

18. Acciarri N, Galassi E, Giulioni M, et al (2009) Cavernous malformations of the central nervous system in the pediatric age group. Pediatr Neurosurg 45:81–104

19. Horsch S, Govaert P, Cowan FM, et al (2014) Developmental venous anomaly in the newborn brain. Neuroradiology 56:579–588

20. Linscott LL, Leach JL, Zhang B, Jones B V (2014) Brain parenchymal signal abnormalities associated with developmental venous anomalies in children and young adults. AJNR Am J Neuroradiol 35:1600–1607

21. Okudera T, Huang YP, Ohta T, et al (1994) Development of posterior fossa dural sinuses, emissary veins, and jugular bulb: Morphological and radiologic study. AJNR Am J Neuroradiol 15:1871–1883

22. Raybaud C (2010) Normal and abnormal embryology and development of the intracranial vascular system. Neurosurg Clin N Am 21:399–426

23. Larson AS, Lanzino G, Brinjikji W (2020) Variations of Intracranial Dural Venous Sinus Diameters from Birth to 20 Years of Age: An MRV-Based Study. AJNR Am J Neuroradiol 41:2351–2357

24. Pauls E, Gulko E, Sadowsky D, et al (2020) Anatomic Variations of the Dural Venous Sinuses: A Primer for the Practicing Neuroradiologist. Neurographics 10:223–227

25. Barkovich MJ, Li Y, Desikan RS, et al (2019) Challenges in pediatric neuroimaging. Neuroimage 185:793–801

26. Dong SZ, Zhu M, Bulas D (2019) Techniques for minimizing sedation in pediatric MRI. J Magn Reson Imaging 50:1047–1054

27. Lanfranconi S, Scola E, Bertani GA, et al (2020) Propranolol for familial cerebral cavernous malformation (Treat_CCM): Study protocol for a randomized controlled pilot trial. Trials 21:401

28. Lanfranconi S, Scola E, Meessen JMTA, et al (2023) Safety and efficacy of propranolol for treatment of familial cerebral cavernous malformations (Treat _ CCM): a randomised , open-label blinded-endpoint phase 2 pilot trial. Lancet Neurol 22:35–44

29. Polster SP, Stadnik A, Akers AL, et al (2019) Atorvastatin Treatment of Cavernous Angiomas with Symptomatic Hemorrhage Exploratory Proof of Concept (AT CASH EPOC) Trial. Neurosurgery 85:843–853

30. Burch EA, Orbach DB (2015) Pediatric central nervous system vascular malformations. Pediatr Radiol 45 Suppl 3:S463-72

31. Lasjaunias P, Burrows P, Planet C (1986) Developmental venous anomalies (DVA): the so-called venous angioma. Neurosurg Rev 9:233–242

32. Barbosa M, Mahadevan J, Weon YC, et al (2003) Dural sinus malformation (DSM) with giant lakes, in neonates and infants. Review of 30 consecutive cases. Interv Neuroradiol 9:407–424

33. Lee C, Pennington MA, Kenney CM 3rd (1996) MR evaluation of developmental venous anomalies: Medullary venous anatomy of venous angiomas. AJNR Am J Neuroradiol 17:61–70

34. Linscott LL, Leach JL, Jones B V, Abruzzo TA (2016) Developmental venous anomalies of

the brain in children — imaging spectrum and update. Pediatr Radiol 46:394–406

35. Hon JML, Bhattacharya JJ, Counsell CE, et al (2009) The presentation and clinical course of intracranial developmental venous anomalies in adults: A systematic review and prospective, population-based study. Stroke 40:1980–1985

36. Gökçe E, Acu B, Beyhan M, et al (2014) Magnetic resonance imaging findings of developmental venous anomalies. Clin Neuroradiol 24:135–143

37. Brzegowy K, Kowalska N, Solewski B, et al (2021) Prevalence and anatomical characteristics of developmental venous anomalies: an MRI study. Neuroradiology 63:1001–1008

38. Pereira VM, Geibprasert S, Krings T, et al (2008) Pathomechanisms of symptomatic developmental venous anomalies. Stroke 39:3201–3215

39. Rinaldo L, Lanzino G, Flemming KD, et al (2020) Symptomatic developmental venous anomalies. Acta Neurochir 162:1115–1125

40. Hsu CC, Krings T (2023) Symptomatic Developmental Venous Anomaly: State-of-the- Art Review on Genetics, Pathophysiology and Imaging. AJNR Am J Neuroradiol 44:498–504

41. Kim SJ (2000) Blue rubber bleb nevus syndrome with central nervous system involvement. Pediatr Neurol 22:410–2

42. Ballieux F, Boon LM, Vikkula M (2015) Blue bleb rubber nevus syndrome. Handb Clin Neurol 132:223–230

43. Chung J, Alvarez H, Lasjaunias P (2003) Multifocal cerebral venous malformations and associated developmental venous anomalies in a case of blue rubber bleb nevus syndrome. Interv Neuroradiol 9:169–176

44. Gabikian P, Clatterbuck RE, Gailloud P, Rigamonti D (2003) Developmental venous anomalies and sinus pericranii in the blue rubber-bleb nevus syndrome. Case report. J Neurosurg 99:409–411

45. Park CO, Park J, Chung KY (2006) Blue rubber bleb nevus syndrome with central nervous system involvement. J Dermatol 33:649–651

46. Tan WH, Baris HN, Burrows PE, et al (2007) The spectrum of vascular anomalies in patients with PTEN mutations: implications for diagnosis and management. J Med Genet 44:594–602

47. Dhamija R, Weindling SM, Porter AB, et al (2018) Neuroimaging abnormalities in patients with Cowden syndrome: retrospective single-center study. Neurol Clin Pr 8:207–213

48. Dhamija R, Hoxworth JM (2020) Imaging of PTEN-related abnormalities in the central nervous system. Clin Imaging 60:180–185

49. Shiran SI, Ben-Sira L, Elhasid R, et al (2018) Multiple brain developmental venous anomalies as a marker for constitutional mismatch repair deficiency syndrome. AJNR Am J Neuroradiol 39:1943–1946

50. Kerpel A, Yalon M, Soudack M, et al (2020) Neuroimaging findings in children with constitutional mismatch repair deficiency syndrome. AJNR Am J Neuroradiol 41:904–910

51. Chhabda S, Sudhakar S, Mankad K, et al (2021) Constitutional mismatch repair deficiency (CMMRD) presenting with high-grade glioma, multiple developmental venous anomalies and malformations of cortical development—a multidisciplinary/multicentre approach

and neuroimaging clues to clinching the diagnos. Childs Nerv Syst 37:2375–2379

52. Al-Shahi R, Bhattacharya JJ, Currie DG, et al (2003) Prospective, population-based detection of intracranial vascular malformations in adults: The Scottish Intracranial Vascular Malformation Study (SIVMS). Stroke 34:1163–1169

53. Lee M, Kim MS (2012) Image findings in brain developmental venous anomalies. J Cerebrovasc Endovasc Neurosurg 14:37–43

54. Brinjikji W, El-Masri AE, Wald JT, Lanzino G (2017) Prevalence of Developmental Venous Anomalies Increases with Age. Stroke 48:1997–1999

55. McCormick WF (1966) The pathology of vascular ("arteriovenous") malformations. J Neurosurg 24:807–816

56. Töpper R, Jürgens E, Reul J, Thron A (1999) Clinical significance of intracranial developmental venous anomalies. Neurol Neurosurg Psychiatry 67:234–238

57. Abe M, Hagihara N, Tabuchi K, et al (2003) Histologically classified venous angiomas of the brain: a controversy. Neurol Med Chir 43:1–10; discussion 11

58. Ruíz DS, Yilmaz H, Gailloud P (2009) Cerebral developmental venous anomalies: Current concepts. Ann Neurol 66:271–283

59. Aoki R, Srivatanakul K (2016) Developmental venous anomaly: Benign or not benign. Neurol Med Chir 56:534–543

60. Snellings DA, Girard R, Lightle R, et al (2022) Developmental Venous Anomalies are a Genetic Primer for Cerebral Cavernous Malformations. Nat Cardiovasc Res 1:246–252

61. San Millán Ruíz D, Gailloud P (2010) Cerebral developmental venous anomalies. Childs Nerv Syst 26:1395–1406

62. Thompson JE, Castillo M, Thomas D, et al (1997) Radiologic-pathologic correlation polymicrogyria. AJNR Am J Neuroradiol 18:307–312

63. Riel-Romero RM, Mattingly M (2005) Developmental venous anomaly in association with neuromigrational anomalies. Pediatr Neurol 32:53–55

64. Arita H, Kishima H, Hosomi K, et al (2012) Hemifacial spasm caused by intra-axial brainstem cavernous angioma with venous angiomas. Br J Neurosurg 26:281–283

65. Chiaramonte R, Bonfiglio M, D'Amore A, Chiaramonte I (2013) Developmental venous anomaly responsible for hemifacial spasm. Neuroradiol J 26:201–207

66. Samadian M, Bakhtevari MH, Nosari MA, et al (2015) Trigeminal Neuralgia Caused by Venous Angioma: A Case Report and Review of the Literature. World Neurosurg 84:860–864

67. Blackmore CC, Mamourian AC (1996) Aqueduct compression from venous angioma: MR findings. AJNR Am J Neuroradiol 17:458–460

68. Yagmurlu B, Fitoz S, Atasoy C, et al (2005) An unusual cause of hydrocephalus: Aqueductal developmental venous anomaly. Eur Radiol 15:1159–1162

69. Inoue K, Yoshioka F, Nakahara Y, et al (2013) Obstructive hydrocephalus following aqueductal stenosis caused by supra- and infratentorial developmental venous anomaly: Case report. Childs Nerv Syst 29:329–334

70. Higa N, Dwiutomo R, Oyoshi T, et al (2020) A case of developing obstructive hydrocephalus following aqueductal stenosis caused by developmental venous anomalies. Childs Nerv Syst 36:1549–1555

71. De Maria L, Lanzino G, Flemming KD, Brinjikji W (2019) Transitional venous anomalies and DVAs draining brain AVMs: A single-institution case series and review of the literature. J Clin Neurosci 66:165–177

72. Falconer RA, Shah T, Giles A, et al (2019) Unilateral Hyperkinetic Choreiform Movements due to Calcification of the Putamen and Caudate from an Underlying Developmental Venous Anomaly. Cureus 11:e3990

73. Oran I, Kiroglu Y, Yurt A, et al (2009) Developmental venous anomaly (DVA) with arterial component: A rare cause of intracranial haemorrhage. Neuroradiology 51:25–32

74. Roccatagliata L, van den Berg R, Soderman M, et al (2012) Developmental venous anomalies with capillary stain: A subgroup of symptomatic DVAs? Neuroradiology 54:475–480

75. Zhang M, Telischak NA, Fischbein NJ, et al (2018) Clinical and Arterial Spin Labeling Brain MRI Features of Transitional Venous Anomalies. J Neuroimaging 28:289–300

76. Idiculla PS, Gurala D, Philipose J, et al (2020) Cerebral Cavernous Malformations, Developmental Venous Anomaly, and Its Coexistence: A Review. Eur Neurol 83:360–368

77. Meng G, Bai C, Yu T, et al (2014) The association between cerebral developmental venous anomaly and concomitant cavernous malformation: an observational study using magnetic resonance imaging. BMC Neurol 14:50

78. Cakirer S (2003) De novo formation of a cavernous malformation of the brain in the presence of a developmental venous anomaly. Clin Radiol 58:251–256

79. Campeau NG, Lane JI (2005) De novo development of a lesion with the appearance of a cavernous malformation adjacent to an existing developmental venous anomaly. AJNR Am J Neuroradiol 26:156–159

80. Su IC, Krishnan P, Rawal S, Krings T (2013) Magnetic resonance evolution of de novo formation of a cavernoma in a thrombosed developmental venous anomaly: a case report. Neurosurgery 73:E739-744; discussion E745

81. Brinjikji W, El-Masri AE, Wald JT, et al (2017) Prevalence of cerebral cavernous malformations associated with developmental venous anomalies increases with age. Childs Nerv Syst 33:1539–1543

82. Kumar S, Lanzino G, Brinjikji W, et al (2019) Infratentorial Developmental Venous Abnormalities and Inflammation Increase Odds of Sporadic Cavernous Malformation. J Stroke Cerebrovasc Dis 28:1662–1667

83. Kashefiolasl S, Bruder M, Brawanski N, et al (2018) A benchmark approach to hemorrhage risk management of cavernous malformations. Neurology 90:e856–e863

84. Chen B, Herten A, Saban D, et al (2020) Hemorrhage from cerebral cavernous malformations: The role of associated developmental venous anomalies. Neurology 95:e89–e96

85. Lee RR, Becher MW, Benson ML, Rigamonti D (1997) Brain capillary telangiectasia: MR imaging appearance and clinicohistopathologic findings. Radiology 205:797–805

86. Castillo M, Morrison T, Shaw JA, Bouldin TW (2001) MR imaging and histologic features of capillary telangiectasia of the basal ganglia. AJNR Am J Neuroradiol 22:1553–1555

87. Sayama CM, Osborn AG, Chin SS, Couldwell WT (2010) Capillary telangiectasias: Clinical, radiographic, and histopathological features. Clinical article. J Neurosurg 113:709–714

88. Chaudhry U, De Bruin DE, Policeni BA (2014) Susceptibility-Weighted MR Imaging: A Better Technique in the Detection of Capillary Telangiectasia compared with T2* gradient-echo. AJNR Am J Neuroradiol 35:2302–2305

89. Clatterbuck RE, Elmací I, Rigamonti D (2001) The juxtaposition of a capillary telangiectasia, cavernous malformation, and developmental venous anomaly in the brainstem of a single patient: case report. Neurosurgery 49:1246–1250

90. Pozzati E, Marliani AF, Zucchelli M, et al (2007) The neurovascular triad: Mixed cavernous, capillary, and venous malformations of the brainstem. J Neurosurg 107:1113–1119

91. Abla A, Wait SD, Uschold T, et al (2008) Developmental venous anomaly, cavernous malformation, and capillary telangiectasia: Spectrum of a single disease. Acta Neurochir 150:487–489; discussion 489

92. Gaztanaga W, Luther E, McCarthy D, et al (2022) Giant, symptomatic mixed vascular malformation containing a cavernoma, developmental venous anomaly, and capillary telangiectasia in a 19-month-old infant. Childs Nerv Syst 38:1005–1009

93. Naik S, Bhoi SK (2019) Association of venous varix and developmental venous anomaly: report of a case and review of literature. BMJ Case Rep 12:e228067

94. Brandt AH, Dahl RH, Hauerberg J, Benndorf G (2022) Improved Characterization of a Developmental Venous Anomaly with a Varix-like Lesion and a Venous Malformation by Venous 3D-DSA. Clin Neuroradiol 32:1135–1140

95. Brinjikji W, Nicholson P, Hilditch CA, et al (2020) Cerebrofacial venous metameric syndrome — spectrum of imaging findings. Neuroradiology 62:417–425

96. Brinjikji W, Hilditch CA, Tsang AC, et al (2018) Facial venous malformations are associated with cerebral developmental venous anomalies. AJNR Am J Neuroradiol 39:2103–2107

97. Brinjikji W, Mark IT, Silvera VM, Guerin JB (2020) Cervicofacial venous malformations are associated with intracranial developmental venous anomalies and dural venous sinus abnormalities. AJNR Am J Neuroradiol 41:1209–1214

98. Soblet J, Kangas J, Nätynki M, et al (2017) Blue Rubber Bleb Nevus (BRBN) Syndrome Is Caused by Somatic TEK (TIE2) Mutations. J Invest Dermatol 137:207–216

99. Isoldi S, Belsha D, Yeop I, et al (2019) Diagnosis and management of children with Blue Rubber Bleb Nevus Syndrome: A multi-center case series. Dig Liver Dis 51:1537–1546

100. Shams PN, Cugati S, Wells T, et al (2015) Orbital Varix Thrombosis and Review of Orbital Vascular Anomalies in Blue Rubber Bleb Nevus Syndrome. Ophthalmic Plast Reconstr Surg 31:e82-86

101. De Loecker K, Labarque V, Seynaeve H, Casteels I (2021) Subconjunctival Hemorrhage in a Child with the Blue Rubber Bleb Nevus Syndrome on Treatment with Oral Propranolol. Case Rep Ophthalmol 12:451–456

102. Wimmer K, Kratz CP, Vasen HFA, et al (2014) Diagnostic criteria for constitutional mismatch repair deficiency syndrome: Suggestions of the European consortium “Care for

CMMRD" (C4CMMRD). J Med Genet 51:355–365

103. Tabori U, Hansford JR, Achatz MI, et al (2017) Clinical management and tumor surveillance recommendations of inherited mismatch repair deficiency in childhood. Clin Cancer Res 23:e32–e37

104. Suerink M, Ripperger T, Messiaen L, et al (2019) Constitutional mismatch repair deficiency as a differential diagnosis of neurofibromatosis type 1: Consensus guidelines for testing a child without malignancy. J Med Genet 56:53–62

105. Aronson M, Colas C, Shuen A, et al (2022) Diagnostic criteria for constitutional mismatch repair deficiency (CMMRD): recommendations from the international consensus working group. J Med Genet 59:318–327

106. Kehrer-Sawatzki H, Cooper DN (2022) Challenges in the diagnosis of neurofibromatosis type 1 (NF1) in young children facilitated by means of revised diagnostic criteria including genetic testing for pathogenic NF1 gene variants. Hum Genet 141:177–191

107. Keppler-Noreuil KM, Sapp JC, Lindhurst MJ, et al (2014) Clinical delineation and natural history of the PIK3CA-related overgrowth spectrum. Am J Med Genet A 164A:1713–1733

108. Keppler-Noreuil KM, Rios JJ, Parker VE, et al (2015) PIK3CA-related overgrowth spectrum (PROS): diagnostic and testing eligibility criteria, differential diagnosis, and evaluation. Am J Med Genet A 167A:287–295

109. Kuentz P, St-Onge J, Duffourd Y, et al (2017) Molecular diagnosis of PIK3CA-related overgrowth spectrum (PROS) in 162 patients and recommendations for genetic testing. Genet Med 19:989–997

110. Yeung KS, Ip JJ, Chow CP, et al (2017) Somatic PIK3CA mutations in seven patients with PIK3CA-related overgrowth spectrum. Am J Med Genet A 173:978–984

111. Sheppard SE, Sanders VR, Srinivasan A, et al (2021) Cerebrofacial vascular metameric syndrome is caused by somatic pathogenic variants in PIK3CA. Cold Spring Harb Mol Case Stud 7:a006147

112. Boutarbouch M, Ben Salem D, Giré L, et al (2010) Multiple cerebral and spinal cord cavernomas in Klippel-Trenaunay-Weber syndrome. J Clin Neurosci 17:1073–1075

113. Larson A, Covington T, Anderson K, et al (2021) Spinal Neurovascular Malformations in Klippel-Trenaunay Syndrome: A Single Center Study. Neurosurgery 88:515–522

114. Pilarski R, Burt R, Kohlman W, et al (2013) Cowden syndrome and the PTEN Hamartoma tumor syndrome: systematic review and revised diagnostic criteria. J Natl Cancer Inst 105:1607–1616

115. Mester J, Charis E (2015) PTEN hamartoma tumor syndrome. Handb Clin Neurol 132:129–137

116. Pilarski R (2019) PTEN hamartoma tumor syndrome: a clinical overview. Cancers (Basel) 11:844

117. Moon K, Ducruet AF, Crowley RW, et al (2013) Complex dural arteriovenous fistula in Bannayan-Riley-Ruvalcaba syndrome. J Neurosurg Pediatr 12:87–92

118. Bhargava R, Au Yong KJ, Leonard N (2014) Bannayan-Riley-Ruvalcaba syndrome: MRI neuroimaging features in a series of 7 patients. AJNR Am J Neuroradiol 35:402–406

119. Prats-Sánchez LA, Hervás-García J V, Becerra JL, et al (2016) Multiple intracranial

arteriovenous fistulas in Cowden syndrome. J Stroke Cerebrovasc Dis 25:e93-94

120. Barreras P, Gailloud P, Pardo CA (2018) A longitudinally extensive myelopathy associated with multiple spinal arteriovenous fistulas in a patient with Cowden Syndrome: a case report. Spine J 18:e1–e5

121. Ciaccio C, Saletti V, D´Arrigo S, et al (2019) Clinical spectrum of PTEN mutation in pediatric patients. A bicenter experience. Eur J Med Genet 62:103596

122. Roux A, Edjlali M, Porelli S, et al (2020) Developmental venous anomaly in adult patients with diffuse glioma: A clinically relevant coexistence? Neurology 92:e55–e62

123. Jones B V, Linscott L, Koberlein G, et al (2015) Increased prevalence of developmental venous anomalies in children with intracranial neoplasms. AJNR Am J Neuroradiol 36:1782–1785

124. Roux A, Boddaert N, Grill J, et al (2020) High Prevalence of Developmental Venous Anomaly in Diffuse Intrinsic Pontine Gliomas: A Pediatric Control Study. Neurosurgery 86:517–523

125. Roux A, Vikkula M, Pallud J (2020) Letter: Is Developmental Venous Anomaly an Imaging Biomarker of PIK3CA Mutated Gliomas? Neurosurgery 86:E93

126. Rogers DM, Peckham ME, Shah LM, Wiggins RH 3rd (2018) Association of developmental venous anomalies with demyelinating lesions in patients with multiple sclerosis. AJNR Am J Neuroradiol 39:97–101

127. Rogers DM, Shah LM, Wiggins RH 3rd (2018) The central vein: FLAIR signal abnormalities associated with developmental venous anomalies in patients with multiple sclerosis. AJNR Am J Neuroradiol 39:2007–2013

128. Sasani MR, Dehghan AR, Ali Reza N (2017) The relationship of multiple sclerosis and cerebral developmental venous anomaly with an advantageous role in the multiple sclerosis diagnosis. Iran J Neurol 16:168–172

129. Halicioglu S, Turkoglu SA (2019) Role of developmental venous anomalies in etiopathogenesis of demyelinating diseases. Int J Neurosci 129:245–251

130. Grazzini I, Calchetti B, Cuneo GL (2020) Developmental venous anomalies in patients with multiple sclerosis: is that a coincidence or an ancillary finding? Neurol Sci 42:2453–2460

131. Kruczek P, Bellenberg B, Lutz T, et al (2021) Developmental Venous Anomalies are More Common in Patients with Multiple Sclerosis and Clinically Isolated Syndrome: Coincidence or Relevant? Clin Neuroradiol 31:225–234

132. Sagtas E, Guneyli S, Akyilmaz D, et al (2020) Multiparametric MRI Evaluation of Developmental Venous Anomalies in the Brain: Association with Signal Changes on FLAIR in Patients with Multiple Sclerosis. Curr Med Imaging 16:928–935

133. Magyar M, Gattringer T, Enzinger C, et al (2022) Incidence of Developmental Venous Anomalies in Patients With Multiple Sclerosis: A 3 Tesla MRI Study. Front Neurol 13:824347

134. Haacke EM, Ge Y, Sethi SK, et al (2021) An Overview of Venous Abnormalities Related to the Development of Lesions in Multiple Sclerosis. Front Neurol 12:561458

135. Geraldo AF, Melo M, Monteiro D, et al (2018) Developmental venous anomaly depicted incidentally in fetal MRI and confirmed in post-natal MRI. Neuroradiology 60:993–994

136. Krajden Haratz K, Peled A, Weizman B, et al (2018) Unique imaging features enabling the prenatal diagnosis of developmental venous anomalies: A persistent echogenic brain lesion drained by a collecting vein in contrast with normal brain parenchyma on MRI. Fetal Diagn Ther 43:53–60

137. San Millán Ruíz D, Delavelle J, Yilmaz H, et al (2007) Parenchymal abnormalities associated with developmental venous anomalies. Neuroradiology 49:987–995

138. Dehkharghani S, Dillon WP, Bryant SO, Fischbein NJ (2010) Unilateral calcification of the caudate and putamen: Association with underlying developmental venous anomaly. AJNR Am J Neuroradiol 31:1848–1852

139. Young A, Poretti A, Bosemani T, et al (2017) Sensitivity of susceptibility-weighted imaging in detecting developmental venous anomalies and associated cavernomas and microhemorrhages in children. Neuroradiology 59:797–802

140. Fuhler AMG, van Dijk JMC, Koopman K, Luijckx GJ (2010) Teaching NeuroImages: a giant developmental venous anomaly in the absence of a superficial venous drainage system. Neurology 75:2009–2010

141. Casey MA, Lahoti S, Gordhan A (2011) Pediatric holohemispheric developmental venous anomaly: Definitive characterization by 3D susceptibility weighted magnetic resonance angiography. J Radiol Case Rep 5:10–18

142. Jung AK, Henson JW, Susanto D, et al (2013) Holohemispheric developmental venous anomaly. Neurology 80:1718–1719

143. Bosemani T, Poretti A, Huisman TAGM (2014) Susceptibility-weighted imaging in pediatric neuroimaging. J Magn Reson Imaging 40:530–544

144. Fushimi Y, Miki Y, Togashi K, et al (2008) A developmental venous anomaly presenting atypical findings on susceptibility-weighted imaging. AJNR Am J Neuroradiol 29:E56

145. Sedlacik J, Löbel U, Kocak M, et al (2010) Attenuation of cerebral venous contrast in susceptibility-weighted imaging of spontaneously breathing pediatric patients sedated with propofol. AJNR Am J Neuroradiol 31:901–906

146. Dammann P, Barth M, Zhu Y, et al (2010) Susceptibility weighted magnetic resonance imaging of cerebral cavernous malformations: Prospects, drawbacks, and first experience at ultra-high field strength (7-Tesla) magnetic resonance imaging. Neurosurg Focus 29:E5

147. Frischer JM, Göd S, Gruber A, et al (2012) Susceptibility-weighted imaging at 7 T: Improved diagnosis of cerebral cavernous malformations and associated developmental venous anomalies. Neuroimage Clin 1:116–120

148. Flemming KD, Lanzino G (2020) Cerebral Cavernous Malformation: What a Practicing Clinician Should Know. Mayo Clin Proc 95:2005–2020

149. Takasugi M, Fujii S, Shinohara Y, et al (2013) Parenchymal hypointense foci associated with developmental venous anomalies: Evaluation by phase-sensitive MR imaging at 3T. AJNR Am J Neuroradiol 34:1940–1944

150. Santucci GM, Leach JL, Ying J, et al (2008) Brain parenchymal signal abnormalities associated with developmental venous anomalies: Detailed MR imaging assessment. AJNR Am J Neuroradiol 29:1317–1323

151. Umino M, Maeda M, Matsushima N, et al (2014) High-signal-intensity abnormalities evaluated by 3D fluid-attenuated inversion recovery imaging within the drainage

territory of developmental venous anomalies identified by susceptibility-weighted imaging at 3 T. Jpn J Radiol 32:397–404

152. Choi Y, Jang J, Nam Y, et al (2019) Relationship between abnormal hyperintensity on T2-weighted images around developmental venous anomalies and magnetic susceptibility of their collecting veins: In-vivo quantitative susceptibility mapping study. Korean J Radiol 20:662–670

153. Dorn F, Brinker G, Blau T, et al (2013) Spontaneous thrombosis of a DVA with subsequent intracranial hemorrhage. Clin Neuroradiol 23:315–317

154. Leach JL, Howard T, Abruzzo T, et al (2012) Postnatal evolution of a developmental venous anomaly. J Pediatr Neuroradiol 1:305–311

155. Brinjikji W, Cloft HJ, Flemming K, Lanzino G (2020) Evolution of Developmental Venous Anomalies in the Setting of a Torcular Dural Arteriovenous Fistula and Cerebrofacial Venous Metameric Syndrome. World Neurosurg 143:46–50

156. Camacho DL, Smith JK, Grimme JD, et al (2004) Atypical MR imaging perfusion in developmental venous anomalies. AJNR Am J Neuroradiol 25:1549–1552

157. Hanson EH, Roach CJ, Ringdahl EN, et al (2011) Developmental venous anomalies: Appearance on whole-brain CT digital subtraction angiography and CT perfusion. Neuroradiology 53:331–341

158. Sharma A, Zipfel GJ, Hildebolt C, Derdeyn CP (2013) Hemodynamic effects of developmental venous anomalies with and without cavernous malformations. AJNR Am J Neuroradiol 34:1746–1751

159. Noh JH, Cho KR, Yeon JY, et al (2014) Microsurgical treatment and outcome of pediatric supratentorial cerebral cavernous malformation. J Korean Neurosurg Soc 56:237–242

160. Iv M, Fischbein NJ, Zaharchuk G (2015) Association of developmental venous anomalies with perfusion abnormalities on arterial spin labeling and bolus perfusion-weighted imaging. J Neuroimaging 25:243–250

161. Larvie M, Timerman D, Thum JA (2015) Brain metabolic abnormalities associated with developmental venous anomalies. AJNR Am J Neuroradiol 36:475–480

162. Timerman D, Thum JA, Larvie M (2016) Quantitative Analysis of Metabolic Abnormality Associated with Brain Developmental Venous Anomalies. Cureus 8:e799

163. Sundermann B, Pfleiderer B, Minnerup H, Berger K (2018) Interaction of developmental venous anomalies with resting state functional MRI measures. AJNR Am J Neuroradiol 39:2326–2331

164. Patel VJ, Lall RR, Desai S, Mohanty A (2015) Spontaneous Thrombosis and Subsequent Recanalization of a Developmental Venous Anomaly. Cureus 7:e334

165. Kishore K, Bodani V, Olatunji R, et al (2022) Venous outflow stenting for symptomatic developmental venous anomaly. Interv Neuroradiol (In press)

166. Cutsforth-Gregory JK, Lanzino G, Link MJ, et al (2015) Characterization of radiation-induced cavernous malformations and comparison with a nonradiation cavernous malformation cohort. J Neurosurg 122:1214–1222

167. Patet G, Bartoli A, Meling TR (2022) Natural history and treatment options of radiation-induced brain cavernomas: a systematic review. Neurosurg Rev 45:243–251

168. Gross BA, Du R (2017) Hemorrhage from cerebral cavernous malformations: A systematic pooled analysis. J Neurosurg 126:1079–1087

169. Kivelev J, Laakso A, Niemelä M, Hernesniemi J (2011) A proposed grading system of brain and spinal cavernomas. Neurosurgery 69:807–813

170. Cohen-Gadol AA, Jacob JT, Edwards DA, Krauss WE (2006) Coexistence of intracranial and spinal cavernous malformations: A study of prevalence and natural history. J Neurosurg 104:376–381

171. Goyal A, Rinaldo L, Alkhataybeh R, et al (2019) Clinical presentation, natural history and outcomes of intramedullary spinal cord cavernous malformations. J Neurol Neurosurg Psychiatry 90:695–703

172. Asimakidou E, Meszaros LT, Anestis DM, Tsitsopoulos PP (2022) A systematic review on the outcome of intramedullary spinal cord cavernous malformations. Eur Spine J 31:3119–3129

173. Mabray MC, Starcevich J, Hallstrom J, et al (2020) High prevalence of spinal cord cavernous malformations in the familial cerebral cavernous malformations type 1 cohort. AJNR Am J Neuroradiol 41:1126–1130

174. Labauge P, Krivosic V, Denier C, et al (2006) Frequency of retinal cavernomas in 60 patients with familial cerebral cavernomas: a clinical and genetic study. Arch Ophthalmol 124:885–886

175. Strickland CD, Eberhardt SC, Bartlett MR, et al (2017) Familial cerebral cavernous malformations are associated with adrenal calcifications on CT scans: An imaging biomarker for a hereditary cerebrovascular condition. Radiology 284:443–450

176. Manole AK, Forrester VJ, Zlotoff BJ, et al (2020) Cutaneous findings of familial cerebral cavernous malformation syndrome due to the common Hispanic mutation. Am J Med Genet A 182:1066–1072

177. Taslimi S, Ku JC, Modabbernia A, Macdonald RL (2019) Hemorrhage, Seizures, and Dynamic Changes of Familial versus Nonfamilial Cavernous Malformation: Systematic Review and Meta-analysis. World Neurosurg 126:241–246

178. Kurihara N, Suzuki H, Kato Y, et al (2020) Hemorrhage owing to cerebral cavernous malformation: imaging, clinical, and histopathological considerations. Jpn J Radiol 38:613–621

179. Otten P, Pizzolato G, Rilliet B, Berney J (1989) A propos de 131 cas d'angiomes caverneux (cavernomes) du s.n.c., repérés par l'analyse rétrospective de 24 535 autopsies [131 cases of cavernous angioma (cavernomas) of the CNS, discovered by retrospective analysis of 24,535 autopsies. Neurochirurgie 35:82–83, 128–131

180. Flemming KD, Graff-Radford J, Aakre J, et al (2017) Population-based prevalence of cerebral cavernous malformations in older adults: Mayo clinic study of aging. JAMA Neurol 74:801–805

181. Gunel M, Awad IA, Finberg K, et al (1996) A founder mutation as a cause of cerebral cavernous malformation in Hispanic Americans. N Engl J Med 334:946–951

182. Gallione CJ, Solatycki A, Awad IA, Weber JL (2011) A founder mutation in the Ashkenazi Jewish population affecting messenger RNA splicing of the CCM2 gene causes cerebral cavernous malformations. Genet Med 13:662–666

183. Cau M, Loi M, Melis M, et al (2009) C329X in KRIT1 is a founder mutation among CCM patients in Sardinia. Eur J Med Genet 52:344–348

184. Gross BA, Du R, Orbach DB, et al (2016) The natural history of cerebral cavernous malformations in children. J Neurosurg Pediatr 17:123–128

185. Zafar A, Quadri SA, Farooqui M, et al (2019) Familial Cerebral Cavernous Malformations. Stroke 50:1294–1301

186. Steiger H, Markwalder T, Reulen H (1987) Clinicopathological relations of cerebral cavernous angiomas: observations in eleven cases. Neurosurgery 21:879–884

187. Clatterbuck R, Eberhart C, Crain B, Rigamonti D (2001) Ultrastructural and immunocytochemical evidence that an incompetent blood-brain barrier is related to the pathophysiology of cavernous malformations. J Neurol Neurosurg Psychiatry 71:188–192

188. Cox EM, Bambakidis NC, Cohen ML (2017) Pathology of cavernous malformations. Handb Clin Neurol 143:267–277

189. Sure U, Freman S, Bozinov O, et al (2005) Biological activity of adult cavernous malformations: a study of 56 patients. J Neurosurg 102:342–347

190. Shi C, Shenkar R, Kinloch A, et al (2014) Immune complex formation and in situ B-cell clonal expansion in human cerebral cavernous malformations. J Neuroimmunol 272:67–75

191. McDonald DA, Shi C, Shenkar R, et al (2012) Fasudil decreases lesion burden in a murine model of cerebral cavernous malformation disease. Stroke 43:571–574

192. Huo R, Wang J, Sun YF, et al (2022) Simplex cerebral cavernous malformations with MAP3K3 mutation have distinct clinical characteristics. Front Neurol 13:946324

193. Snellings DA, Hong CC, Ren AA, et al (2021) Cerebral Cavernous Malformation: From Mechanism to Therapy. Circ Res 129:195–215

194. Hong T, Xiao X, Ren J, et al (2021) Somatic MAP3K3 and PIK3CA mutations in sporadic cerebral and spinal cord cavernous malformations. Brain 144:2648–2658

195. Peyre M, Miyagishima D, Bielle F, et al (2021) Somatic PIK3CA Mutations in Sporadic Cerebral Cavernous Malformations. N Engl J Med 385:996–1004

196. Ren AA, Snellings DA, Su YS, et al (2021) PIK3CA and CCM mutations fuel cavernomas through a cancer-like mechanism. Nature 594:271–276

197. Weng J, Yang Y, Song D, et al (2021) Somatic MAP3K3 mutation defines a subclass of cerebral cavernous malformation. Am J Hum Genet 108:942–950

198. Akers AL, Johnson E, Steinberg GK, et al (2009) Biallelic somatic and germline mutations in cerebral cavernous malformations (CCMs): evidence for a two-hit mechanism of CCM pathogenesis. Hum Mol Genet 18:919–930

199. Pagenstecher A, Stahl S, Sure U, Felbor U (2009) A two-hit mechanism causes cerebral cavernous malformations: complete inactivation of CCM1, CCM2 or CCM3 in affected endothelial cells. Hum Mol Genet 18:911–918

200. Retta SF, Perrelli A, Trabalzini L, Finetti F (2020) From Genes and Mechanisms to Molecular-Targeted Therapies: The Long Climb to the Cure of Cerebral Cavernous Malformation (CCM) Disease. Methods Mol Biol 2152:3–25

201. Riolo G, Ricci C, Battistini S (2021) Molecular genetic features of cerebral cavernous malformations (CCM) patients: An overall view from genes to endothelial cells. Cells 10:704

202. Chohan MO, Marchiò S, Morrison LA, et al (2019) Emerging Pharmacologic Targets in Cerebral Cavernous Malformation and Potential Strategies to Alter the Natural History of a Difficult Disease: A Review. JAMA Neurol 76:492–500

203. Maddaluno L, Rudini N, Cuttano R, et al (2013) EndMT contributes to the onset and progression of cerebral cavernous malformations. Nature 498:492–496

204. Bravi L, Malinverno M, Pisati F, et al (2016) Endothelial Cells Lining Sporadic Cerebral Cavernous Malformation Cavernomas Undergo Endothelial-to-Mesenchymal Transition. Stroke 47:886–890

205. Wüstehube J, Bartol A, Liebler SS, et al (2010) Cerebral cavernous malformation protein CCM1 inhibits sprouting angiogenesis by activating DELTA-NOTCH signaling. Proc Natl Acad Sci U S A 107:12640–12645

206. Schulz GB, Wieland E, Wüstehube-Lausch J, et al (2015) Cerebral Cavernous Malformation-1 Protein Controls DLL4- Notch3 Signaling Between the Endothelium and Pericytes. Stroke 46:1337–1343

207. You C, Zhao K, Dammann P, et al (2017) EphB4 forward signalling mediates angiogenesis caused by CCM3/PDCD10-ablation. J Cell Mol Med 21:1848–1858

208. Marchi S, Corricelli M, Trapani E, et al (2015) Defective autophagy is a key feature of cerebral cavernous malformations. EMBO Mol Med 7:1403–1417

209. Goitre L, De Luca E, Braggion S, et al (2014) KRIT1 loss of function causes a ROS-dependent upregulation of c-Jun. Free Radic Biol Med 68:134–147

210. Retta SF, Glading AJ (2016) Oxidative stress and inflammation in cerebral cavernous malformation disease pathogenesis: Two sides of the same coin. Int J Biochem Cell Biol 81:254–270

211. Antognelli C, Trapani E, Delle Monache S, et al (2018) KRIT1 loss-of-function induces a chronic Nrf2-mediated adaptive homeostasis that sensitizes cells to oxidative stress: Implication for Cerebral Cavernous Malformation disease. Free Radic Biol Med 115:202–218

212. Jenny Zhou H, Qin L, Zhang H, et al (2016) Endothelial exocytosis of angiopoietin-2 resulting from CCM3 deficiency contributes to cerebral cavernous malformation. Nat Med 22:1033–1042

213. Lai CC, Nelsen B, Frias-Anaya E, et al (2022) Neuroinflammation Plays a Critical Role in Cerebral Cavernous Malformation Disease. Circ Res 131:909–925

214. Tu T, Peng Z, Ren J, Zhang H (2022) Cerebral Cavernous Malformation: Immune and Inflammatory Perspectives. Front Immunol 13:922281

215. Yau ACY, Globisch MA, Onyeogaziri FC, et al (2022) Inflammation and neutrophil extracellular traps in cerebral cavernous malformation. Cell Mol Life Sci 79:206

216. Globisch MA, Onyeogaziri FC, Smith RO, et al (2022) Dysregulated Hemostasis and Immunothrombosis in Cerebral Cavernous Malformations. Int J Mol Sci 23:12575

217. Lopez-Ramirez MA, Lai CC, Soliman SI, et al (2021) Astrocytes propel neurovascular

dysfunction during cerebral cavernous malformation lesion formation. J Clin Invest 131:e139570

218. Tang AT, Choi JP, Kotzin JJ, et al (2017) Endothelial TLR4 and the microbiome drive cerebral cavernous malformations. Nature 545:305–310

219. Tang AT, Sullivan KR, Hong CC, et al (2019) Distinct cellular roles for PDCD10 define a gut-brain axis in cerebral cavernous malformation. Sci Transl Med 11:eaaw3521

220. Wang K, Zhou HJ, Wang M (2019) CCM3 and cerebral cavernous malformation disease. Stroke Vasc Neurol 4:67–70

221. Polster SP, Sharma A, Tanes C, et al (2020) Permissive microbiome characterizes human subjects with a neurovascular disease cavernous angioma. Nat Commun 11:2659

222. Su VL, Calderwood DA (2020) Signalling through cerebral cavernous malformation protein networks: CCM protein signaling. Open Biol 10:200263

223. Grdseloff N, Boulday G, Rödel CJ, et al (2023) Impaired retinoic acid signaling in cerebral cavernous malformations. Sci Rep 13:5572

224. Kar S, Bali KK, Baisantry A, et al (2017) Genome-Wide Sequencing Reveals MicroRNAs Downregulated in Cerebral Cavernous Malformations. J Mol Neurosci 61:178–188

225. Florian IA, Buruiana A, Timis TL, et al (2021) An insight into the microRNAs associated with arteriovenous and cavernous malformations of the brain. Cells 10:1373

226. Lyne SB, Girard R, Koskimäki J, et al (2019) Biomarkers of cavernous angioma with symptomatic hemorrhage. JCI Insight 4:e128577

227. Romanos SG, Srinath A, Li Y, et al (2022) Circulating Plasma miRNA Homologs in Mice and Humans Reflect Familial Cerebral Cavernous Malformation Disease. Transl Stroke Res (In press)

228. Girard R, Li Y, Stadnik A, et al (2021) A Roadmap for Developing Plasma Diagnostic and Prognostic Biomarkers of Cerebral Cavernous Angioma With Symptomatic Hemorrhage (CASH). Neurosurgery 88:686–697

229. Choquet H, Pawlikowska L, Nelson J, et al (2014) Polymorphisms in inflammatory and immune response genes associated with cerebral cavernous malformation type 1 severity. Cerebrovasc Dis 38:433–440

230. Girard R, Zeineddine HA, Fam MD, et al (2018) Plasma Biomarkers of Inflammation Reflect Seizures and Hemorrhagic Activity of Cerebral Cavernous Malformations. Transl Stroke Res 9:34–43

231. Girard R, Zeineddine HA, Koskimäki J, et al (2018) Plasma biomarkers of inflammation and angiogenesis predict cerebral cavernous malformation symptomatic hemorrhage or lesional growth short communication. Circ Res 122:1716–1721

232. Moore SA, Brown RDJ, Christianson TJH, Flemming KD (2014) Long-term natural history of incidentally discovered cavernous malformations in a single-center cohort: Clinical article. J Neurosurg 120:1188–1192

233. Horne MA, Flemming KD, Su IC, et al (2016) Clinical course of untreated cerebral cavernous malformations: a meta-analysis of individual patient data. Lancet Neurol 15:166–173

234. Akers A, Al-Shahi Salman R, Awad IA, et al (2017) Synopsis of guidelines for the clinical

management of cerebral cavernous malformations: Consensus recommendations based on systematic literature review by the angioma alliance scientific advisory board clinical experts panel. Neurosurgery 80:665–680

235. Agrawal A, Cincu R, Joharapurkar SR, et al (2009) Hemorrhage in brain stem cavernoma presenting with torticollis. Pediatr Neurosurg 45:49–52

236. Qiu J, Cui Y, Sun L, et al (2018) Hemichorea associated with cavernous angioma and a small errhysis: A case report and literature review. Med 97:e12889

237. Liu H, Chen C, Liu Y, et al (2022) Trigeminal neuralgia caused by cavernoma: A case report with literature review. Front Neurol 13:982503

238. Villaseñor-Ledezma J, Budke M, Alvarez-Salgado JA, et al (2017) Pediatric cerebellar giant cavernous malformation: case report and review of literature. Childs Nerv Syst 33:2187–2191

239. Gaddi MJS, Pascual JSG, Legaspi EDC, et al (2020) Giant Cerebellar Cavernomas in Pediatric Patients: Systematic Review with Illustrative Case. J Stroke Cerebrovasc Dis 29:105264

240. Al-Shahi Salman R, Berg MJ, Morrison L, et al (2008) Hemorrhage from cavernous malformations of the brain: definition and reporting standards. definition and reporting standards. Angioma Alliance Scientific Advisory Board. Stroke 39:3222–3230

241. Velz J, Özkaratufan S, Krayenbühl N, et al (2022) Pediatric brainstem cavernous malformations: 2-center experience in 40 children. J Neurosurg Pediatr (In press)

242. Taslimi S, Modabbernia A, Amin-Hanjani S, et al (2016) Natural history of cavernous malformation. Neurology 86:1984–1991

243. Flemming KD, Link MJ, Christianson TJH, Brown RDJ (2012) Prospective hemorrhage risk of intracerebral cavernous malformations. Neurology 78:632–636

244. Al-Shahi Salman R, Hall JM, Horne MA, et al (2012) Untreated clinical course of cerebral cavernous malformations: A prospective, population-based cohort study. Lancet Neurol 11:217–224

245. Dammann P, Jabbarli R, Wittek P, et al (2016) Solitary Sporadic Cerebral Cavernous Malformations: Risk Factors of First or Recurrent Symptomatic Hemorrhage and Associated Functional Impairment. World Neurosurg 91:73–80

246. Weinsheimer S, Nelson J, Abla AA, et al (2023) Intracranial Hemorrhage Rate and Lesion Burden in Patients With Familial Cerebral Cavernous Malformation. J Am Hear Assoc 12:e027572

247. Jeon JS, Kim JE, Chung YS, et al (2014) A risk factor analysis of prospective symptomatic haemorrhage in adult patients with cerebral cavernous malformation. J Neurol Neurosurg Psychiatry 85:1366–1370

248. Barker FG 2nd, Amin-Hanjani S, Butler WE, et al (2001) Temporal clustering of hemorrhages from untreated cavernous malformations of the central nervous system. Neurosurgery 49:5–24; discussion 24-5

249. Shim Y, Phi JH, Wang KC, et al (2022) Clinical outcomes of pediatric cerebral cavernous malformation: an analysis of 124 consecutive cases. J Neurosurg Pediatr (In press)

250. Santos AN, Rauschenbach L, Saban D, et al (2022) Multiple cerebral cavernous

malformations: Clinical course of confirmed, assumed and non-familial disease. Eur J Neurol 29:1427–1434

251. Nikoubashman O, Wiesmann M, Tournier-Lasserve E, et al (2013) Natural history of cerebral dot-like cavernomas. Clin Radiol 68:e453-459

252. Nikoubashman O, Di Rocco F, Davagnanam I, et al (2015) Prospective hemorrhage rates of cerebral cavernous malformations in children and adolescents based on MRI appearance. AJNR Am J Neuroradiol 36:2177–2183

253. Abdulrauf SI, Kaynar MY, Awad IA (1999) A comparison of the clinical profile of cavernous malformations with and without associated venous malformations. Neurosurgery 41:41–46; discussion 46-47

254. Prolo LM, Jin MC, Loven T, et al (2020) Recurrence of cavernous malformations after surgery in childhood. J Neurosurg Pediatr 26:179–188

255. Choquet H, Nelson J, Pawlikowska L, et al (2014) Association of cardiovascular risk factors with disease severity in cerebral cavernous malformation type 1 subjects with the common hispanic mutation. Cerebrovasc Dis 37:57–63

256. Chen B, Saban D, Rauscher S, et al (2021) Modifiable Cardiovascular Risk Factors in Patients with Sporadic Cerebral Cavernous Malformations: Obesity Matters. Stroke 52:1259–1264

257. Ma L, Zhang S, Li Z, et al (2020) Morbidity After Symptomatic Hemorrhage of Cerebral Cavernous Malformation: A Nomogram Approach to Risk Assessment. Stroke 51:2997–3006

258. Awad I, Jabbour P (2006) Cerebral cavernous malformations and epilepsy. Neurosurg Focus 21:e7

259. Cappabianca P, Alfieri A, Maiuri F, et al (1997) Supratentorial cavernous malformations and epilepsy: Seizure outcome after lesionectomy on a series of 35 patients. Clin Neurol Neurosurg 99:179–183

260. Josephson CB, Leach JP, Duncan R, et al (2011) Seizure risk from cavernous or arteriovenous malformations: prospective population-based study. Neurology 76:1548–1554

261. Leone MA, Ivashynka A V, Tonini MC, et al (2011) Risk factors for a first epileptic seizure symptomatic of brain tumour or brain vascular malformation. A case control study. Swiss Med Wkly 141:w13155

262. Rosenow F, Alonso-Vanegas MA, Baumgartner C, et al (2013) Cavernoma-related epilepsy: Review and recommendations for management - Report of the Surgical Task Force of the ILAE Commission on Therapeutic Strategies. Epilepsia 54:2025–2035

263. Lin Q, Yang PF, Jia YZ, et al (2018) Surgical Treatment and Long-Term Outcome of Cerebral Cavernous Malformations-Related Epilepsy in Pediatric Patients. Neuropediatrics 49:173–179

264. Menzler K, Chen X, Thiel P, et al (2010) Epileptogenicity of cavernomas depends on (archi-) cortical localization. Neurosurgery 67:12–15

265. Agosti E, Flemming KD, Lanzino G (2019) Symptomatic Cavernous Malformation Presenting with Seizure without Hemorrhage: Analysis of Factors Influencing Clinical Presentation. World Neurosurg 129:e387–e392

266. Shih YC, Chou CC, Peng SJ, et al (2022) Clinical characteristics and long-term outcome of cerebral cavernous malformations-related epilepsy. Epilepsia 63:2056–2067

267. Fox CK, Nelson J, McCulloch CE, et al (2021) Seizure Incidence Rates in Children and Adults With Familial Cerebral Cavernous Malformations. Neurology 97:e1210–e1216

268. Denier C, Labauge P, Bergametti F, et al (2006) Genotype-phenotype correlations in cerebral cavernous malformations patients. Ann Neurol 60:550–556

269. Cigoli MS, Avemaria F, De Benedetti S, et al (2014) PDCD10 gene mutations in multiple cerebral cavernous malformations. PLoS One 9:e110438

270. Spiegler S, Najm J, Liu J, et al (2014) High mutation detection rates in cerebral cavernous malformation upon stringent inclusion criteria: one-third of probands are minors. Mol Genet Genomic Med 2:176–185

271. Shenkar R, Shi C, Rebeiz T, et al (2015) Exceptional aggressiveness of cerebral cavernous malformation disease associated with PDCD10 mutations. Genet Med 17:188–196

272. Orlev A, Feghali J, Kimchi G, et al (2022) Neurological event prediction for patients with symptomatic cerebral cavernous malformation: the BLED2 score. J Neurosurg (In press)

273. Badhiwala JH, Farrokhyar F, Alhazzani W, et al (2014) Surgical outcomes and natural history of intramedullary spinal cord cavernous malformations: a single-center series and meta-analysis of individual patient data: Clinical article. J Neurosurg Spine 21:662–676

274. Ogilvy CS, Louis DN, Ojemann RG (1992) Intramedullary cavernous angiomas of the spinal cord: Clinical presentation, pathological features, and surgical management. Neurosurgery 31:219–229; discussion 229-30

275. Ren J, Jiang N, Bian L, et al (2022) Natural History of Spinal Cord Cavernous Malformations: A Multicenter Cohort Study. Neurosurgery 90:390–398

276. Ren J, Hong T, Zeng G, et al (2020) Characteristics and Long-Term Outcome of 20 Children with Intramedullary Spinal Cord Cavernous Malformations. Neurosurgery 86:817–824

277. Zhang L, Qiao G, Yang W, et al (2021) Clinical features and long-term outcomes of pediatric spinal cord cavernous malformation-a report of 18 cases and literature review. Childs Nerv Syst 37:235–242

278. Rauschenbach L, Santos AN, Gull HH, et al (2023) Functional impact of multiple bleeding events in patients with conservatively treated spinal cavernous malformations. J Neurosurg Spine 38:405–411

279. Liu T, Li K, Wang Y, et al (2021) Treatment strategies and prognostic factors for spinal cavernous malformation: a single-center retrospective cohort study. J Neurosurg Spine 35:824–833

280. Spiegler S, Rath M, Paperlein C, Felbor U (2018) Cerebral Cavernous Malformations: An Update on Prevalence, Molecular Genetic Analyses, and Genetic C ounselling. Mol Syndr 9:60–69

281. Mespreuve M, Vanhoenacker F, Lemmerling M (2016) Familial multiple cavernous malformation syndrome: MR features in this uncommon but silent threat. J Belg Soc Radiol 100:51

282. Merello E, Pavanello M, Consales A, et al (2016) Genetic Screening of Pediatric Cavernous Malformations. J Mol Neurosci 60:232–238

283. Liquori CL, Berg MJ, Squitieri F, et al (2007) Deletions in CCM2 are a common cause of cerebral cavernous malformations. Am J Hum Genet 80:69–75

284. Spiegler S, Rath M, Hoffjan S, et al (2018) First large genomic inversion in familial cerebral cavernous malformation identified by whole genome sequencing. Neurogenetics 19:55–59

285. Pilz RA, Schwefel K, Weise A, et al (2020) First interchromosomal insertion in a patient with cerebral and spinal cavernous malformations. Sci Rep 10:6306

286. Sirvente J, Enjolras O, Wassef M, et al (2009) Frequency and phenotypes of cutaneous vascular malformations in a consecutive series of 417 patients with familial cerebral cavernous malformations. J Eur Acad Dermatol Venereol 23:1066–1072

287. Bilguvar K, Bydon M, Bayrakli F, et al (2007) A novel syndrome of cerebral cavernous malformation and Greig cephalopolysyndactyly. Laboratory investigation. J Neurosurg 107:495–499

288. Henrich W, Stupin JH, Bühling KJ, et al (2002) Prenatal sonographic findings of thalamic cavernous angioma. Ultrasound Obs Gynecol 19:518–522

289. Hayashi S, Kondoh T, Morishita A, et al (2004) Congenital cavernous angioma exhibits a progressive decrease in size after birth. Childs Nerv Syst 20:199–203

290. Lerner A, Gilboa Y, Gerad L, et al (2006) Sonographic detection of fetal cerebellar cavernous hemangioma with in-utero hemorrhage leading to cerebellar hemihypoplasia. Ultrasound Obs Gynecol 28:968–971

291. Sarnat HB, Wei XC, Flores-Sarnat L, et al (2012) Fetal opercular cavernous angioma causing cerebral cleft: Contralateral primitive vascular anomaly and subicular dysgenesis. J Child Neurol 27:478–484

292. Cheng D, Shang X, Gao W, et al (2021) Fetal Familial Cerebral Cavernous Malformation With a Novel Heterozygous KRIT1 Variation. Neurology 97:986–988

293. Campbell PG, Jabbour P, Yadla S, Awad IA (2010) Emerging clinical imaging techniques for cerebral cavernous malformations: A systematic review. Neurosurg Focus 29:E6

294. Schlamann M, Maderwald S, Becker W, et al (2010) Cerebral Cavernous Hemangiomas at 7 Tesla. Initial Experience. Acad Radiol 17:3–6

295. Cooper AD, Campeau NG, Meissner I (2008) Susceptibility-weighted imaging in familial cerebral cavernous malformations. Neurology 71:382

296. de Souza JM, Domingues RC, Cruz LCHJ, et al (2008) Susceptibility-weighted imaging for the evaluation of patients with familial cerebral cavernous malformations: A comparison with T2-weighted fast spin-echo and gradient-echo sequences. AJNR Am J Neuroradiol 29:154–158

297. de Champfleur NM, Langlois C, Ankenbrandt WJ, et al (2011) Magnetic resonance imaging evaluation of cerebral cavernous malformations with susceptibility-weighted imaging. Neurosurgery 68:641–647

298. Kuroedov D, Cunha B, Pamplona J, et al (2023) Cerebral cavernous malformations: Typical and atypical imaging characteristics. J Neuroimaging 33:202–217

299. Kumar S, Brinjikji W, Lanzino G, Flemming KD (2020) Distinguishing mimics from true hemorrhagic cavernous malformations. J Clin Neurosci 74:11–17

300. Riant F, Bergametti F, Fournier HD, et al (2013) CCM3 mutations are associated with early-onset cerebral hemorrhage and multiple meningiomas. Mol Syndr 4:165–172

301. Ponrartana S, Moore MM, Chan SS, et al (2021) Safety issues related to intravenous contrast agent use in magnetic resonance imaging. Pediatr Radiol 51:736–747

302. Noda SM, Oztek MA, Stanescu AL, et al (2022) Gadolinium retention: should pediatric radiologists be concerned, and how to frame conversations with families. Pediatr Radiol 52:345–353

303. Petersen TA, Morrison LA, Schrader RM, Hart BL (2010) Familial versus sporadic cavernous malformations: Differences in developmental venous anomaly association and lesion phenotype. AJNR Am J Neuroradiol 31:377–382

304. Dammann P, Wrede K, Zhu Y, et al (2017) Correlation of the venous angioarchitecture of multiple cerebral cavernous malformations with familial or sporadic disease: A susceptibility-weighted imaging study with 7-Tesla MRI. J Neurosurg 126:570–577

305. Zabramski JM, Wascher TM, Spetzler RF, et al (1994) The natural history of familial cavernous malformations: results of an ongoing study. J Neurosurg 80:422–432

306. Flemming KD, Kumar S, Lanzino G, Brinjikji W (2019) Baseline and Evolutionary Radiologic Features in Sporadic, Hemorrhagic Brain Cavernous Malformations. AJNR Am J Neuroradiol 40:967–972

307. Yun TJ, Na DG, Kwon BJ, et al (2008) A T1 hyperintense perilesional signal aids in the differentiation of a cavernous angioma from other hemorrhagic masses. AJNR Am J Neuroradiol 29:494–500

308. Nabavizadeh SA, Pechersky D, Schmitt JE, et al (2017) Perilesional Hyperintensity on T1-Weighted Images in Intra-Axial Brain Masses other than Cavernous Malformations. J Neuroimaging 27:531–538

309. Kan P, Tubay M, Osborn A, et al (2008) Radiographic features of tumefactive giant cavernous angiomas. Acta Neurochir 150:49–55

310. Ozgen B, Senocak E, Oguz KK, et al (2011) Radiological features of childhood giant cavernous malformations. Neuroradiology 53:283–289

311. Knerlich-Lukoschus F, Steinbok P, Dunham C, Cochrane DD (2015) Cerebellar cavernous malformation in pediatric patients: defining clinical, neuroimaging, and therapeutic characteristics. J Neurosurg Pediatr 16:256–266

312. Wang C, Zhao W, Wang J, et al (2018) Giant cavernous malformations: A single center experience and literature review. J Clin Neurosci 56:108–113

313. Lim SC, Hong R, Kim YS, Jang SJ (2006) Large cystic cavernous angioma of the cerebellum mimicking pilocytic astrocytoma. J Neurooncol 79:169–170

314. Lu VM, Daniels DJ (2019) Large Cystic Cavernous Malformation in Infant with Novel KRIT1 Gene Abnormality. World Neurosurg 130:304–305

315. Bradley WGJ (1993) MR appearance of hemorrhage in the brain. Radiology 189:15–26

316. Jeon I, Jung WS, Suh SH, et al (2016) MR imaging features that distinguish spinal cavernous angioma from hemorrhagic ependymoma and serial MRI changes in cavernous angioma. J Neurooncol 130:229–236

317. Panda A, Diehn FE, Kim DK, et al (2020) Spinal Cord Cavernous Malformations: MRI

Commonly Shows Adjacent Intramedullary Hemorrhage. J Neuroimaging 30:690–696

318. Ren J, Hong T, He C, et al (2019) Coexistence of intracranial and spinal cord cavernous malformations predict aggressive clinical presentation. Front Neurol 10:618

319. Clatterbuck RE, Cohen B, Gailloud P, et al (2002) Vertebral hemangiomas associated with familial cerebral cavernous malformation: segmental disease expression. Case report. J Neurosurg 97:227–230

320. Toldo I, Drigo P, Mammi I, et al (2009) Vertebral and spinal cavernous angiomas associated with familial cerebral cavernous malformation. Surg Neurol 71:167–171

321. Lanfranconi S, Ronchi D, Ahmed N, et al (2014) A novel CCM1 mutation associated with multiple cerebral and vertebral cavernous malformations. BMC Neurol 14:158

322. Tandberg SR, Bocklage T, Bartlett MR, et al (2020) Vertebral Intraosseous Vascular Malformations in a Familial Cerebral Cavernous Malformation Population: Prevalence, Histologic Features, and Associations With CNS Disease. AJR Am J Roentgenol 214:428–436

323. Velz J, Vasella F, Yang Y, et al (2020) Limited Impact of Serial Follow-Up Imaging in Clinically Stable Patients With Brainstem Cavernous Malformations. Front Neurol 11:789

324. Velz J, Stienen MN, Neidert MC, et al (2018) Routinely performed serial follow-up imaging in asymptomatic patients with multiple cerebral cavernous malformations has no influence on surgical decision making. Front Neurol 9:848

325. Carrión-Penagos J, Zeineddine HA, Polster SP, et al (2020) Subclinical imaging changes in cerebral cavernous angiomas during prospective surveillance. J Neurosurg 134:1147–1154

326. Kim S, Moon J, Jung KH, et al (2023) Clinicoradiologic data of familial cerebral cavernous malformation with age-related disease burden. Ann Clin Transl Neurol 10:373–383

327. Zou X, Hart BL, Mabray M, et al (2017) Automated algorithm for counting microbleeds in patients with familial cerebral cavernous malformations. Neuroradiology 59:685–690

328. Fontanella MM, Bacigaluppi S, Doglietto F, et al (2021) An international call for a new grading system for cerebral and cerebellar cavernomas. J Neurosurg Sci 65:239–246

329. Fontanella MM, Zanin L, Panciani P, et al (2022) Preliminary Validation of FoRCaSco: A New Grading System for Cerebral and Cerebellar Cavernomas. World Neurosurg 162:e597–e604

330. Kikuta K, Nozaki K, Takahashi JA, et al (2004) Postoperative evaluation of microsurgical resection for cavernous malformations of the brainstem. J Neurosurg 101:607–612

331. Garcia RM, Oh T, Cole TS, et al (2020) Recurrent brainstem cavernous malformations following primary resection: Blind spots, fine lines, and the right-angle method. J Neurosurg 135:671–682

332. Chen B, Göricke S, Wrede K, et al (2017) Reliable? The Value of Early Postoperative Magnetic Resonance Imaging after Cerebral Cavernous Malformation Surgery. World Neurosurg 103:138–144

333. Dammann P, Schaller C, Sure U (2017) Should we resect peri-lesional hemosiderin deposits when performing lesionectomy in patients with cavernoma-related epilepsy (CRE)? Neurosurg Rev 40:39–43

334. Cenzato M, Stefini R, Ambrosi C, Giovanelli M (2008) Post-operative remnants of brainstem cavernomas: Incidence, risk factors and management. Acta Neurochir 150:879–886; discussion 887

335. Abla AA, Lekovic GP, Garrett M, et al (2010) Cavernous malformations of the brainstem presenting in childhood: surgical experience in 40 patients. Neurosurgery 67:1589–1598; discussion 1598-1599

336. Li D, Hao SY, Tang J, et al (2014) Surgical management of pediatric brainstem cavernous malformations. J Neurosurg Pediatr 13:484–502

337. Rollins NK (2007) Clinical applications of diffusion tensor imaging and tractography in children. Ped Radiol 37:769–780

338. Vorona GA, Berman JI (2015) Review of diffusion tensor imaging and its application in children. Pediatr Radiol 45 Suppl 3:S375-381

339. Tae WS, Ham BJ, Pyun SB, et al (2018) Current Clinical Applications of Diffusion-Tensor Imaging in Neurological Disorders. J Clin Neurol 14:129–140

340. Rogalska M, Antkowiak L, Mandera M (2022) Clinical application of diffusion tensor imaging and fiber tractography in the management of brainstem cavernous malformations: a systematic review. Neurosurg Rev 45:2027–2040

341. Abhinav K, Pathak S, Richardson RM, et al (2014) Application of high-definition fiber tractography in the management of supratentorial cavernous malformations: A combined qualitative and quantitative approach. Neurosurgery 74:668–680

342. Lin Y, Lin F, Kang D, et al (2018) Supratentorial cavernous malformations adjacent to the corticospinal tract: Surgical outcomes and predictive value of diffusion tensor imaging findings. J Neurosurg 128:541–552

343. Abhinav K, Nielsen TH, Singh R, et al (2020) Utility of a Quantitative Approach Using Diffusion Tensor Imaging for Prognostication Regarding Motor and Functional Outcomes in Patients with Surgically Resected Deep Intracranial Cavernous Malformations. Neurosurgery 86:665–675

344. Colasurdo M, Chen H, Navarra R, et al (2023) Reliability of Functional and Diffusion MR Imaging near Cerebral Cavernous Malformations. AJNR Am J Neuroradiol 44:150–156

345. Ulrich NH, Ahmadli U, Woernle CM, et al (2014) Diffusion tensor imaging for anatomical localization of cranial nerves and cranial nerve nuclei in pontine lesions: Initial experiences with 3T-MRI. J Clin Neurosci 21:1924–1927

346. Faraji AH, Abhinav K, Jarbo K, et al (2015) Longitudinal evaluation of corticospinal tract in patients with resected brainstem cavernous malformations using high-definition fiber tractography and diffusion connectometry analysis: preliminary experience. J Neurosurg 123:1133–1144

347. Ordóñez-Rubiano EG, Johnson JM, Younus I, et al (2019) Recovery of consciousness after a brainstem cavernous malformation hemorrhage: A descriptive study of preserved reticular activating system with tractography. J Clin Neurosci 59:372–377

348. Zdunczyk A, Roth F, Picht T, Vajkoczy P (2021) Functional DTI tractography in brainstem cavernoma surgery. J Neurosurg 135:712–721

349. Topcuoglu OM, Yaltirik K, Firat Z, et al (2021) Limited positive predictive value of diffusion tensor tractography in determining clinically relevant white matter damage in brain stem

cavernous malformations: A retrospective study in a single center surgical cohort. J Neuroradiol 48:432–437

350. Kovanlikaya I, Firat Z, Kovanlikaya A, et al (2011) Assessment of the corticospinal tract alterations before and after resection of brainstem lesions using Diffusion Tensor Imaging (DTI) and tractography at 3 T. Eur J Radiol 77:383–391

351. Ulrich NH, Kockro RA, Bellut D, et al (2014) Brainstem cavernoma surgery with the support of pre- and postoperative diffusion tensor imaging: initial experiences and clinical course of 23 patients. Neurosurg Rev 37:481–492

352. Flores BC, Whittemore AR, Samson DS, Barnett SL (2015) The utility of preoperative diffusion tensor imaging in the surgical management of brainstem cavernous malformations. J Neurosurg 122:653–662

353. Yao Y, Ulrich NH, Guggenberger R, et al (2015) Quantification of Corticospinal Tracts with Diffusion Tensor Imaging in Brainstem Surgery: Prognostic Value in 14 Consecutive Cases at 3T Magnetic Resonance Imaging. World Neurosurg 83:1006–1014

354. Li D, Jiao YM, Wang L, et al (2019) Surgical outcome of motor deficits and neurological status in brainstem cavernous malformations based on preoperative diffusion tensor imaging: A prospective randomized clinical trial. J Neurosurg 130:286–301

355. Schlosser MJ, McCarthy G, Fulbright RK, et al (1997) Cerebral vascular malformations adjacent to sensorimotor and visual cortex. Functional magnetic resonance imaging studies before and after therapeutic intervention. Stroke 28:1130–1137

356. Möller-Hartmann W, Krings T, Coenen VA, et al (2002) Preoperative assessment of motor cortex and pyramidal tracts in central cavernoma employing functional and diffusion-weighted magnetic resonance imaging. Surg Neurol 58:302–307; discussion 308

357. Thickbroom GW, Byrnes ML, Morris IT, et al (2004) Functional MRI near vascular anomalies: comparison of cavernoma and arteriovenous malformation. J Clin Neurosci 11:845–848

358. Zotta D, Di Rienzo A, Scogna A, et al (2005) Supratentorial cavernomas in eloquent brain areas: application of neuronavigation and functional MRI in operative planning. J Neurosurg Sci 49:13–19

359. Deng X, Xu L, Zhang Y, et al (2016) Difference of language cortex reorganization between cerebral arteriovenous malformations, cavernous malformations, and gliomas: a functional MRI study. Neurosurg Rev 39:241–249; discussion 249

360. Maestú F, Saldaña C, Amo C, et al (2004) Can small lesions induce language reorganization as large lesions do? Brain Lang 89:433–438

361. Shenkar R, Venkatasubramanian PN, Zhao J, et al (2008) Cavernous Malformations: part I. High Field Imaging of excised human lesions. Neurosurgery 63:782–789; discussion 789

362. Ferrier MC, Sarin H, Fung SH, et al (2007) Validation of dynamic contrast-enhanced magnetic resonance imaging-derived vascular permeability measurements using quantitative autoradiography in the RG2 rat brain tumor model. Neoplasia 9:546–555

363. Larsson HBW, Courivaud F, Rostrup E, Hansen AE (2009) Measurement of brain perfusion, blood volume, and blood-brain barrier permeability, using dynamic contrast-enhanced T1-weighted MRI at 3 tesla. Magn Reson Med 62:1270–1281

364. Hoffmann A, Bredno J, Wendland MF, et al (2011) Validation of in vivo magnetic

resonance imaging blood-brain barrier permeability measurements by comparison with gold standard histology. Stroke 42:2054–2060

365. Girard R, Fam MD, Zeineddine HA, et al (2017) Vascular permeability and iron deposition biomarkers in longitudinal follow-up of cerebral cavernous malformations. J Neurosurg 127:102–110

366. Sone JY, Li Y, Hobson N, et al (2021) Perfusion and permeability as diagnostic biomarkers of cavernous angioma with symptomatic hemorrhage. J Cereb Blood Flow Metab 41:2944–2956

367. Sone JY, Hobson N, Srinath A, et al (2022) Perfusion and Permeability MRI Predicts Future Cavernous Angioma Hemorrhage and Growth. J Magn Reson Imaging 55:1440–1449

368. Tan H, Liu T, Wu Y, et al (2014) Evaluation of iron content in human cerebral cavernous malformation using quantitative susceptibility mapping. Invest Radiol 49:498–504

369. Tan H, Zhang L, Mikati AG, et al (2016) Quantitative susceptibility mapping in cerebral cavernous malformations: Clinical correlations. AJNR Am J Neuroradiol 37:1209–1215

370. Mikati AG, Tan H, Shenkar R, et al (2014) Dynamic permeability and quantitative susceptibility related imaging biomarkers in cerebral cavernous malformations. Stroke 45:598–601

371. Zeineddine HA, Girard R, Cao Y, et al (2018) Quantitative susceptibility mapping as a monitoring biomarker in cerebral cavernous malformations with recent hemorrhage. J Magn Reson Imaging 47:1133–1138

372. Incerti I, Fusco M, Contarino VE, et al (2023) Magnetic susceptibility as a 1-year predictor of outcome in familial cerebral cavernous malformations: a pilot study. Eur Radiol 33:4158–4166

373. Mikati AG, Khanna O, Zhang L, et al (2015) Vascular permeability in cerebral cavernous malformations. J Cereb Blood Flow Metab 35:1632–1639

374. Hobson N, Polster SP, Cao Y, et al (2020) Phantom validation of quantitative susceptibility and dynamic contrast-enhanced permeability MR sequences across instruments and sites. J Magn Reson Imaging 51:1192–1199

375. Polster SP, Cao Y, Carroll T, et al (2019) Trial readiness in cavernous angiomas with symptomatic hemorrhage (CASH). Neurosurgery 84:954–964

376. Kim H, Flemming KD, Nelson JA, et al (2021) Baseline characteristics of patients with cavernous angiomas with symptomatic hemorrhage in Multisite Trial Readiness Project. Stroke 52:3829–3838

377. Mabray MC, Caprihan A, Nelson J, et al (2020) Effect of Simvastatin on Permeability in Cerebral Cavernous Malformation Type 1 Patients: Results from a Pilot Small Randomized Controlled Clinical Trial. Transl Stroke Res 11:319–321

378. Flemming KD (2017) Clinical Management of Cavernous Malformations. Curr Cardiol Rep 19:122

379. Hirschmann D, Czech T, Roessler K, et al (2022) How can we optimize the long-term outcome in children with intracranial cavernous malformations? A single-center experience of 61 cases. Neurosurg Rev 45:3299–3313

380. Moriarity J, Wetzel M, Clatterbuck R, et al (1999) The natural history of cavernous

malformations: a prospective study of 68 patients. Neurosurgery 44:1166–1171; discussion 1172-1173

381. Lee Y, Cho KH, Kim HI, et al (2017) Clinical outcome following medical treatment of cavernous malformation related epilepsy. Seizure 45:64–69

382. von der Brelie C, Kuczaty S, Von Lehe M (2014) Surgical management and long-term outcome of pediatric patients with different subtypes of epilepsy associated with cerebral cavernous malformations. J Neurosurg Pediatr 13:699–705

383. Gao X, Yue K, Sun J, et al (2020) Treatment of Cerebral Cavernous Malformations Presenting With Seizures: A Systematic Review and Meta-Analysis. Front Neurol 11:590589

384. Rinkel LA, Al Shahi-Salman R, Rinkel GJ, Greving JP (2019) Radiosurgical, neurosurgical, or no intervention for cerebral cavernous malformations: A decision analysis. Int J Stroke 14:939–945

385. Witiw CD, Abou-Hamden A, Kulkarni A V, et al (2012) Cerebral cavernous malformations and pregnancy: Hemorrhage risk and influence on obstetrical management. Neurosurgery 71:626–630

386. Abla AA, Lekovic GP, Turner JD, et al (2011) Advances in the treatment and outcome of brainstem cavernous malformation surgery: A single-center case series of 300 surgically treated patients. Neurosurgery 68:403–414; discussion 414-415

387. Ruan D, Yu XB, Shrestha S, et al (2015) The role of hemosiderin excision in seizure outcome in cerebral cavernous malformation surgery: A systematic review and meta-analysis. PLoS One 10:e0136619

388. Poorthuis MHF, Klijn CJM, Algra A, et al (2014) Treatment of cerebral cavernous malformations: A systematic review and meta-regression analysis. J Neurol Neurosurg Psychiatry 85:1319–1323

389. Moultrie F, Horne MA, Josephson CB, et al (2014) Outcome after surgical or conservative management of cerebral cavernous malformations. Neurology 83:582–589

390. Qiao N, Ma Z, Song J, et al (2015) A systematic review and meta-analysis of surgeries performed for treating deep-seated cerebral cavernous malformations. Br J Neurosurg 29:493–499

391. Kearns KN, Chen CJ, Tvrdik P, et al (2019) Outcomes of surgery for brainstem cavernous malformations a systematic review. Stroke 50:2964–2966

392. Harris L, Poorthuis MHF, Grover P, et al (2022) Surgery for cerebral cavernous malformations: a systematic review and meta-analysis. Neurosurg Rev 45:231–241

393. Cornelius JF, Kürten K, Fischer I, et al (2016) Quality of Life After Surgery for Cerebral Cavernoma: Brainstem Versus Nonbrainstem Location. World Neurosurg 95:315–321

394. Hardian RF, Goto T, Fujii Y, et al (2019) Intraoperative facial motor evoked potential monitoring for pontine cavernous malformation resection. J Neurosurg 132:265–271

395. Jeltema HR, Ohlerth AK, de Wit A, et al (2021) Comparing navigated transcranial magnetic stimulation mapping and “gold standard” direct cortical stimulation mapping in neurosurgery: a systematic review. Neurosurg Rev 44:1903–1920

396. Oertel J, Fischer G, Linsler S, et al (2022) Endoscope-assisted resection of brainstem

cavernous malformations. Neurosurg Rev 45:2823–2836

397. Lin F, Li C, Yan X, et al (2021) Endoscopic Surgery for Supratentorial Deep Cavernous Malformation Adjacent to Cortical Spinal Tract: Preliminary Experience and Technical Note. Front Neurol 12:678413

398. Sommer B, Grummich P, Coras R, et al (2013) Integration of functional neuronavigation and intraoperative MRI in surgery for drug-resistant extratemporal epilepsy close to eloquent brain areas. Neurosurg Focus 34:E4

399. Torné R, Urra X, Topczeswki TE, et al (2021) Intraoperative magnetic resonance imaging for cerebral cavernous malformations: When is it maybe worth it? J Clin Neurosci 89:85–90

400. Hugelshofer M, Acciarri N, Sure U, et al (2011) Effective surgical treatment of cerebral cavernous malformations: A multicenter study of 79 pediatric patients. J Neurosurg Pediatr 8:522–525

401. Gao X, Yue K, Sun J, et al (2022) A systematic review and meta-analysis of surgeries performed for cerebral cavernous malformation-related epilepsy in pediatric patients. Front Pediatr 10:892456

402. Azad TD, Veeravagu A, Li A, et al (2018) Long-term effectiveness of gross-total resection for symptomatic spinal cord cavernous malformations. Neurosurgery 83:1201–1208

403. Niedermeyer S, Szelenyi A, Schichor C, et al (2022) Intramedullary spinal cord cavernous malformations—association between intraoperative neurophysiological monitoring changes and neurological outcome. Acta Neurochir 164:2595–2604

404. Lu XY, Sun H, Xu JG, Li QY (2014) Stereotactic radiosurgery of brainstem cavernous malformations: A systematic review and meta-analysis. J Neurosurg 120:982–987

405. Poorthuis MHF, Rinkel LA, Lammy S, Al-Shahi Salman R (2019) Stereotactic radiosurgery for cerebral cavernous malformations: A systematic review. Neurology 93:e1971–e1979

406. Wen R, Shi Y, Gao Y, et al (2019) The Efficacy of Gamma Knife Radiosurgery for Cavernous Malformations: A Meta-Analysis and Review. World Neurosurg 123:371–377

407. Samanci Y, Ardor GD, Peker S (2022) Management of pediatric cerebral cavernous malformations with gamma knife radiosurgery: a report of 46 cases. Childs Nerv Syst 38:929–938

408. McCracken DJ, Willie JT, Fernald BA, et al (2016) Magnetic Resonance Thermometry-Guided Stereotactic Laser Ablation of Cavernous Malformations in Drug-Resistant Epilepsy: Imaging and Clinical Results. Oper Neurosurg 12:39–48

409. Carminucci A, Parr M, Bitar M, Danish SF (2019) Delayed-Onset Cyst Formation After Laser Interstitial Thermal Therapy: Unreported Long-Term Complication. World Neurosurg 124:219–223

410. Willie JT, Malcolm JG, Stern MA, et al (2019) Safety and effectiveness of stereotactic laser ablation for epileptogenic cerebral cavernous malformations. Epilepsia 60:220–232

411. Gamboa NT, Karsy M, Iyer RR, et al (2020) Stereotactic laser interstitial thermal therapy for brainstem cavernous malformations: two preliminary cases. Acta Neurochir 162:1771–1775

412. Satzer D, Tao JX, Issa NP, et al (2020) Stereotactic laser interstitial thermal therapy for

epilepsy associated with solitary and multiple cerebral cavernous malformations. Neurosurg Focus 48:E12

413. Lawrence JD, Rehman AA, Lee M (2021) Treatment of a Pontine Cavernoma With Laser Interstitial Thermal Therapy: Case Report. Neurol Surg B Skull Base 82:S65–S270

414. Malcolm JG, Douglas JM, Greven A, et al (2021) Feasibility and Morbidity of Magnetic Resonance Imaging-Guided Stereotactic Laser Ablation of Deep Cerebral Cavernous Malformations: A Report of 4 Cases. Neurosurgery 89:635–644

415. Ogasawara C, Watanabe G, Young K, et al (2022) Laser Interstitial Thermal Therapy for Cerebral Cavernous Malformations: A Systematic Review of Indications, Safety, and Outcomes. World Neurosurg 166:279-287.e1

416. Yousefi O, Sabahi M, Malcolm J, et al (2022) Laser Interstitial Thermal Therapy for Cavernous Malformations: A Systematic Review. Front Surg 9:887329

417. Glading A, Han J, Stockton RA, Ginsberg MH (2007) KRIT-1/CCM1 is a Rap1 effector that regulates endothelial cell-cell junctions. J Cell Biol 179:247–254

418. Whitehead KJ, Chan AC, Navankasattusas S, et al (2009) The Cerebral Cavernous Malformation signaling pathway promotes vascular integrity via Rho GTPases. Nat Med 15:177–184

419. Stockton RA, Shenkar R, Awad IA, Ginsberg MH (2010) Cerebral cavernous malformations proteins inhibit Rho kinase to stabilize vascular integrity. J Exp Med 207:881–896

420. McDonald DA, Shenkar R, Shi C, et al (2011) A novel mouse model of cerebral cavernous malformations based on the two-hit mutation hypothesis recapitulates the human disease. Hum Mol Genet 20:211–222

421. Shenkar R, Shi C, Austin C, et al (2017) RhoA kinase inhibition with fasudil versus simvastatin in murine models of cerebral cavernous malformations. Stroke 48:187–194

422. Mckerracher L, Shenkar R, Abbinanti M, et al (2021) A Brain Targeted Orally Available ROCK2 Inhibitor Benefits Mild and Aggressive Cavernous Angioma Disease. Transl Stroke Res 11:365–376

423. Shenkar R, Peiper A, Pardo H, et al (2019) Rho kinase inhibition blunts lesion development and hemorrhage in murine models of aggressive Pdcd10/Ccm3 disease. Stroke 50:738–744

424. Gomez-Paz S, Salem MM, Maragkos GA, et al (2020) Role of aspirin and statin therapy in patients with cerebral cavernous malformations. J Clin Neurosci 78:246–251

425. Zuurbier SM, Hickman CR, Rinkel LA, et al (2022) Association between Beta-Blocker or Statin Drug Use and the Risk of Hemorrhage from Cerebral Cavernous Malformations. Stroke 53:2521–2527

426. Santos AN, Rauschenbach L, Saban D, et al (2022) Medication intake and hemorrhage risk in patients with familial cerebral cavernous malformations. J Neurosurg (In press)

427. Léauté-Labrèze C, Hoeger P, Mazereeuw-Hautier J, et al (2015) A Randomized, Controlled Trial of Oral Propranolol in Infantile Hemangioma. N Engl J Med 372:735–746

428. Moschovi M, Alexiou G, Stefanaki K, et al (2010) Propranolol treatment for a giant infantile brain cavernoma. J Child Neurol 25:653–655

429. Zabramski JM, Kalani MYS, Filippidis AS, Spetzler RF (2016) Propranolol Treatment of

Cavernous Malformations with Symptomatic Hemorrhage. World Neurosurg 88:631–639

430. Berti I, Marchetti F, Skabar A, et al (2014) Propranolol for cerebral cavernous angiomatosis: A magic bullet. Clin Pediatr 53:189–190

431. Hoffman JE, Ryan M, Wittenberg B, et al (2020) Successful treatment of hemorrhagic brainstem cavernous malformation with hematoma evacuation and postoperative propranolol. Childs Nerv Syst 36:2109–2112

432. Tiefenbach J, Park JJ, Kaliaperumal C (2023) A 5-year outcome of propranolol for the treatment of paediatric intracranial cavernoma: case report and a review of the literature. Childs Nerv Syst 39:269–272

433. Gibson CC, Zhu W, Davis CT, et al (2015) Strategy for Identifying Repurposed Drugs for the Treatment of Cerebral Cavernous Malformation. Circulation 131:289–299

434. Li W, Shenkar R, Detter MR, et al (2021) Propranolol inhibits cavernous vascular malformations by β1 adrenergic receptor antagonism in animal models. J Clin Invest 131:e144893

435. Oldenburg J, Malinverno M, Globisch MA, et al (2021) Propranolol Reduces the Development of Lesions and Rescues Barrier Function in Cerebral Cavernous Malformations: A Preclinical Study. Stroke 52:1418–1427

436. Goldberg J, Jaeggi C, Schoeni D, et al (2019) Bleeding risk of cerebral cavernous malformations in patients on b-blocker medication: A cohort study. J Neurosurg 1306:1931–1936

437. Lamy S, Lachambre MP, Lord-Dufour S, Béliveau R (2010) Propranolol suppresses angiogenesis in vitro: Inhibition of proliferation, migration, and differentiation of endothelial cells. Vasc Pharmacol 53:200–208

438. Malova M, Rossi A, Severino M, et al (2017) Incidental findings on routine brain MRI scans in preterm infants. Arch Dis Child Fetal Neonatal Ed 102:F73–F78

439. Zhang S, Ma L, Wu C, et al (2020) A rupture risk analysis of cerebral cavernous malformation associated with developmental venous anomaly using susceptibility-weighted imaging. Neuroradiology 61:39–47

440. Okudera T, Huang YP, Fukusumi A, et al (1999) Micro-angiographical studies of the medullary venous system of the cerebral hemisphere. Neuropathology 19:93–111

441. Yang JY, Chan AK, Callen DJ, Paes BA (2010) Neonatal cerebral sinovenous thrombosis: shifting the evidence for a diagnostic plan and treatment strategy. Pediatrics 126:e693–700

442. Ami O, Maran JC, Gabor P, et al (2019) Three-dimensional magnetic resonance imaging of fetal head molding and brain shape changes during the second stage of labor. PLoS One 14:e0215721

443. Hong YJ, Chung TS, Suh SH, et al (2010) The angioarchitectural factors of the cerebral developmental venous anomaly; can they be the causes of concurrent sporadic cavernous malformation? Neuroradiology 52:883–891

444. Cagneaux M, Paoli V, Blanchard G, et al (2013) Pre- and postnatal imaging of early cerebral damage in Sturge-Weber syndrome. Pediatr Radiol 43:1536–1539

445. De Ciantis A, Barkovich AJ, Cosottini M, et al (2015) Ultra-high-field MR imaging in

polymicrogyria and epilepsy. AJNR Am J Neuroradiol 36:309–316

446. Stutterd CA, Leventer RJ (2014) Polymicrogyria: a common and heterogeneous malformation of cortical development. Am J Med Genet C Semin Med Genet 166C:227–239

447. Choquet H, Pawlikowska L, Lawton MT, Kim H (2015) Genetics of cerebral cavernous malformations: current status and future prospects. Neurosurg Sci 59:211–220

448. de Vos IJ, Vreeburg M, Koek GH, van Steensel MAM (2017) Review of familial cerebral cavernous malformations and report of seven additional families. Am J Med Genet A 173:338–351

449. Boulouis G, Blauwblomme T, Hak JF, et al (2019) Nontraumatic pediatric intracerebral hemorrhage. Stroke 50:3654–3661

450. Labauge P, Laberge S, Brunereau L, et al (1998) Hereditary cerebral cavernous angiomas: Clinical and genetic features in 57 French families. Lancet 352:1892–1897

451. Brunereau L, Labauge P, Tournier-Lasserve E, et al (2000) Familial form of intracranial cavernous angioma: MR imaging findings in 51 families. Radiology 214:209–216

452. Labauge P, Brunereau L, Lévy C, et al (2000) The natural history of familial cerebral cavernomas: A retrospective MRI study of 40 patients. Neuroradiology 42:327–332

453. Brunereau L, Levy C, Laberge S, et al (2000) De novo lesions in familial form of cerebral cavernous malformations: Clinical and MR features in 29 non-Hispanic families. Surg Neurol 53:475–483; discussion 482-483

454. Houwing ME, Grohssteiner RL, Dremmen MHG, et al (2022) Silent cerebral infarcts in patients with sickle cell disease: a systematic review and meta-analysis. BMC Med 18:393

455. Bonfanti L, Charvet CJ (2021) Brain Plasticity in Humans and Model Systems: Advances, Challenges, and Future Directions. Int J Mol Sci 22:9358

456. Sparacia G, Speciale C, Banco A, et al (2016) Accuracy of SWI sequences compared to T2∗-weighted gradient echo sequences in the detection of cerebral cavernous malformations in the familial form. Neuroradiol J 29:326–335

457. Geraldo AF, Luis A, Alves CAPF, et al (2022) Spinal involvement in pediatric familial cavernous malformation syndrome. Neuroradiology 64:1671–1679

458. Fry L, Heskett C, De Stefano FA, et al (2023) A Bibliometric Analysis of the Top 100 Most Influential Articles on Cerebral Cavernous Malformations. World Neurosurg 170:138–148

459. Robinson K, Saldanha I, Mckoy N (2011) Development of a framework to identify research gaps from systematic reviews. J Clin Epidemiol 64:1325–30

460. Al-Shahi Salman R, Kitchen N, Thomson J, et al (2016) Top ten research priorities for brain and spine cavernous malformations. Lancet Neurol 15:354–355

461. Rodwell C, Aymé S (2015) Rare disease policies to improve care for patients in Europe. Biochim Biophys Acta 1852:2329–2335

462. Richter T, Nestler-Parr S, Babela R, et al (2015) Rare Disease Terminology and Definitions-A Systematic Global Review: Report of the ISPOR Rare Disease Special Interest Group. Value Heal 18:906–914

FACSIMILE

Neuroradiology
https://doi.org/10.1007/s00234-018-2089-y

LETTER TO THE EDITOR

Developmental venous anomaly depicted incidentally in fetal MRI and confirmed in post-natal MRI

Ana Filipa Geraldo[1] · Mónica Melo[2] · David Monteiro[1] · Francisco Valente[2] · Joana Nunes[1]

Received: 14 August 2018 / Accepted: 21 August 2018

Dear Editor-in-Chief,

Cerebral developmental venous anomalies (DVAs) are the most common subtype of congenital brain vascular malformation. They are widely reported in the adult population and less frequently within the pediatric age group [1, 2]. Interestingly, their depiction and characterization in utero using cerebral ultrasound with Doppler and/or fetal brain MRI has only recently been described in a small case series, although post-natal images were not provided in that paper [3].

We herein report a case of 2 gravida 0 para mother with chronic hypertension referred to our pediatric imaging unit at 33 weeks' gestation following the detection of apparently isolated ventricular enlargement in fetal ultrasound. Fetal brain MRI was performed at the same gestational age, confirming mild left ventriculomegaly. In addition, a linear hypointense signal on T2 HASTE and gradient echo (GRE) images was incidentally depicted in the left parietal region, extending from the enlarged ventricular surface up to the cortex (Fig. 1). No other anomalies in the central nervous system were identified and the diagnosis of cerebral developmental venous anomaly (DVA) was assumed. In light of the above, fetal ultrasound with high definition Doppler was repeated at 34 weeks' gestation showing venous flow in the corresponding area, although no associated changes in the echogenicity of the adjacent parenchyma could still be appreciated. The infant was born prematurely at 35 weeks' gestation by vaginal vacuum delivery. Post-natal MRI was undertaken at 1 month of age (corresponding to 39 weeks' corrected age) due to progressive enlargement of the left lateral ventricle in consecutive transcranial cerebral ultrasounds performed in the neonatal unit. The prenatal diagnosis of a left parietal DVA was then confirmed (Fig. 2). No associated cavernous malformation or signal abnormality in the adjacent parenchyma could be detected.

DVAs consist of dilated venules disposed with a radial configuration between normal neural parenchyma and converging centripetally into a large collector vein; this collector in turn drains into ependymal veins, into cortical veins, or rarely into a combination of both. Complex DVAs may also occur, with multiple collectors draining a single DVA or multiple DVA's draining into the same collector. The etiology of DVAs is not clearly understood, but the most accepted theory states that they represent a compensatory mechanism secondary to any phenomenon disturbing the normal development of the transmedullary veins [1–3]. They have been classically regarded as normal variants, but their ability to become symptomatic either spontaneously or by mechanical/flow-related factors has also been addressed in the literature [4]. Interestingly, in this specific case, the DVA was ipsilateral to the unilaterally enlarged lateral ventricle. This can be regarded as a matter of coincidence, but also allows us to hypothesize that the enlargement could be secondary to a small intraventricular hemorrhagic complication of this lesion. We favor this second theory as a focal area of hypointensity on GRE could be depicted in the ependymal surface of the left occipital horn in the post-natal MRI, although we cannot completely rule out traumatic birth-related hemorrhage. Other possibilities include chronic ischemia secondary to venous hypertension leading to parenchymal volume loss with *ex vacuo* dilatation of the ipsilateral lateral ventricle or a single developmental insult causing both the DVA and the adjacent parenchymal atrophy.

This case report further supports the concept that DVAs are congenital lesions that can actually be diagnosed in utero, as described by Haratz et al. [3]. In addition, it suggests that fetal MRI including GRE sequences has the ability to identify and characterize these lesions in utero even when they are not

✉ Ana Filipa Geraldo
anafilipageraldo@gmail.com

[1] Department of Medical Imaging, Neuroradiology Unit, CHVNG/E-Centro Hospitalar Vila Nova de Gaia/Espinho, Rua Conceição Fernandes, 4434-502 Vila Nova de Gaia, Portugal

[2] Department of Gynecology-Obstetrics, Prenatal Diagnosis Unit, CHVNG/E- Centro Hospitalar Vila Nova de Gaia/Espinho, Vila Nova de Gaia, Portugal

Published online: 28 August 2018

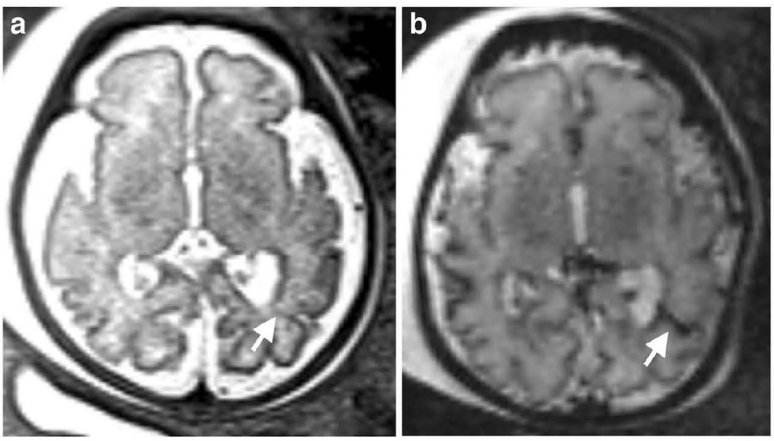

Fig. 1 Pre-natal brain MRI of the child at 33 weeks gestational age. Axial T2 HASTE (**a**) and T2 gradient echo (**b**) showing a linear hypointense image in the left parietal region extending from the atrium of the lateral ventricle up to the cortex (*arrow*), compatible with a developmental venous anomaly. Unilateral mild ventriculomegaly is also present

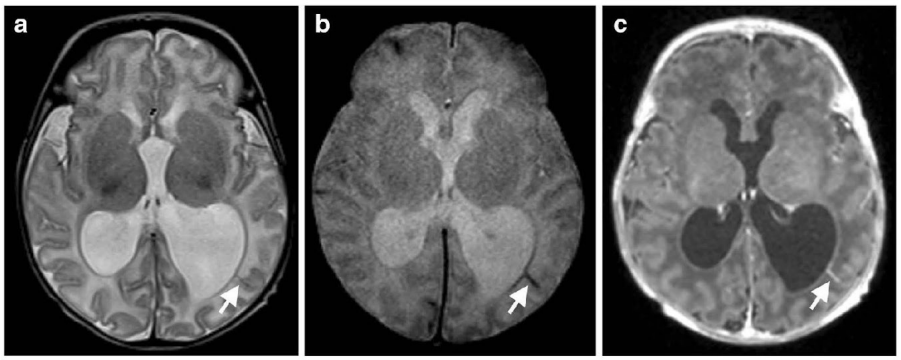

Fig. 2 Post-natal brain MRI of the same child at 4 weeks of age (corresponding to 39 weeks' corrected age). Axial T2-weighted (**a**), gradient echo (**b**), and axial T1 contrast-enhanced (**c**) images showing the linear structure with vascular flow-void and enhancement in the left parietal region compatible with a subpendymal developmental venous anomaly with cortical drainage (white *arrow*)

associated with changes in the normal echogenicity of the cerebral parenchyma in fetal ultrasound.

Compliance with ethical standards

Funding No funding was received for this study.

Conflict of interest The authors declare that they have no conflict of interest.

Ethical approval All procedures performed in studies involving human participants were in accordance with ethical standards of the institutional and/or national research committee and with the 1964 Helsinki declaration and its later amendments or comparable ethical standards. For this type of study formal consent is not required.

Informed consent For this type of retrospective study formal consent is not required.

References

1. Horsch S, Govaert P, Cowan FM, Benders MJ, Groenendaal F, Lequin MH, Saliou G, de Vries LS (2014) Developmental venous anomaly in the newborn brain. Neuroradiology 56(7):579–588
2. Linscott LL, Leach JL, Jones BV, Abruzzo TA (2016) Developmental venous anomalies of the brain in children – imaging spectrum and update. Pediatr Radiol 46(3):394–406
3. Krajden Haratz K, Peled A, Weizman B, Gindes L, Tamarkin M, Lev D, Kidron D, Ben-Sira L, Malinger G, Lerman-Sagie T, Leibovitz Z (2018) Unique imaging features enabling the prenatal diagnosis of developmental venous anomalies: a persistent echogenic brain lesion drained by a collecting vein in contrast with normal brain parenchyma on MRI. Fetal Diagn Ther 43(1):53–60
4. Pereira VM, Geibprasert S, Krings T, Aurboonyawat T, Ozanne A, Toulgoat F, Pongpech S, Lasjaunias PL (2008) Pathomechanisms of symptomatic developmental venous anomalies. Stroke 39(12):3201–3215

Published October 22, 2020 as 10.3174/ajnr.A6829

ORIGINAL RESEARCH
PEDIATRICS

Neonatal Developmental Venous Anomalies: Clinicoradiologic Characterization and Follow-Up

A.F. Geraldo, S.S. Messina, D. Tortora, A. Parodi, M. Malova, G. Morana, C. Gandolfo, A. D'Amico, E. Herkert, P. Govaert, L.A. Ramenghi, A. Rossi, and M. Severino

ABSTRACT

BACKGROUND AND PURPOSE: Although developmental venous anomalies have been frequently studied in adults and occasionally in children, data regarding these entities are scarce in neonates. We aimed to characterize clinical and neuroimaging features of neonatal developmental venous anomalies and to evaluate any association between MR imaging abnormalities in their drainage territory and corresponding angioarchitectural features.

MATERIALS AND METHODS: We reviewed parenchymal abnormalities and angioarchitectural features of 41 neonates with developmental venous anomalies (20 males; mean corrected age, 39.9 weeks) selected through a radiology report text search from 2135 neonates who underwent brain MR imaging between 2008 and 2019. Fetal and longitudinal MR images were also reviewed. Neurologic outcomes were collected. Statistics were performed using χ^2, Fisher exact, Mann-Whitney *U*, or *t* tests corrected for multiple comparisons.

RESULTS: Developmental venous anomalies were detected in 1.9% of neonatal scans. These were complicated by parenchymal/ventricular abnormalities in 15/41 cases (36.6%), improving at last follow-up in 8/10 (80%), with normal neurologic outcome in 9/14 (64.2%). Multiple collectors ($P = .008$) and larger collector caliber ($P < .001$) were significantly more frequent in complicated developmental venous anomalies. At a patient level, multiplicity ($P = .002$) was significantly associated with the presence of ≥1 complicated developmental venous anomaly. Retrospective fetal detection was possible in 3/11 subjects (27.2%).

CONCLUSIONS: One-third of neonatal developmental venous anomalies may be complicated by parenchymal abnormalities, especially with multiple and larger collectors. Neuroimaging and neurologic outcomes were favorable in most cases, suggesting a benign, self-limited nature of these vascular anomalies. A congenital origin could be confirmed in one-quarter of cases with available fetal MR imaging.

ABBREVIATIONS: CCM = cerebral cavernous malformation; c-DVA = complicated developmental venous anomaly; cUS = cerebral ultrasound; CVMS = cerebrofacial venous metameric syndrome; DVA = developmental venous anomaly; u-DVA = uncomplicated developmental venous anomaly

Developmental venous anomalies (DVAs) are the most frequently diagnosed intracranial vascular malformations, often encountered as incidental neuroimaging findings.[1,2] On MR imaging, DVAs are recognized on postcontrast T1WI as radially oriented veins with a "caput medusae" pattern converging into 1 (or rarely more) dilated venous collector.[3,4] These features may be also detected on precontrast MR images,[3-5] especially if T2*-weighted sequences such as high-resolution SWI are included in the protocol.[5] In addition, DVAs may be occasionally recognized in utero using fetal MR imaging.[6]

DVAs are usually considered benign anatomic variants.[7] However, they represent areas of venous fragility that can become symptomatic through diverse pathomechanisms.[8,9] Indeed, DVA-associated brain abnormalities are frequently depicted, including-

Received April 15, 2020; accepted after revision August 6.

From the Neuroradiology Unit (A.F.G.), Centro Hospitalar de Vila Nova de Gaia/Espinho, Vila Nova de Gaia, Portugal; Neuroradiology Unit (A.F.G., D.T., G.M., A.R., M.S.), Neonatal Intensive Care Unit (A.P., M.M., L.A.R.), and Interventional Unit (C.G.), IRCCS Istituto Giannina Gaslini, Genova, Italy; Radiology Unit (S.S.M.), Casa di Cura Regina Pacis, Palermo, Italy; Dipartimento di Scienze Biomediche Avanzate (A.D.), Universita' Federico II, Napoli, Italy; and Division of Neonatology (E.H., P.G.), Department of Paediatrics, Erasmus University Medical Centre, Rotterdam, the Netherlands.

This work was supported by funds from "Ricerca Corrente Disordini Neurologici e Muscolari (Linea 5)" of the Italian Ministry of Health and the Compagnia di San Paolo (ROL 20573).

Paper previously presented, in part, as an oral communication at: Italian Congress of Pediatric Neuroradiology, October 11–13, 2018; Brescia, Italy.

All procedures performed in the studies involving human participants were in accordance with the ethical standards of 1964 Helsinki Declaration and its later amendments or comparable ethical standards. Informed consent was waived by the institutional research committee.

Please address correspondence to Andrea Rossi, MD, Neuroradiology Unit, IRCCS Istituto Giannina Gaslini, Via Gaslini 5, Genova 16148 Italia; e-mail: andrearossi@gaslini.org; @AndreaRossi_NRX; @MSavinaSeverino

Indicates open access to non-subscribers at www.ajnr.org

Indicates article with supplemental on-line appendix and table.

Indicates article with supplemental on-line photos.

http://dx.doi.org/10.3174/ajnr.A6829

but-not limited-to sporadic cerebral cavernous malformations (CCMs).[8-16] Moreover, a higher prevalence of DVAs has been described in patients with different pathologies and/or genetic conditions.[17-21]

Although DVAs are widely described and characterized in adults, they remain under-reported in the pediatric population. Indeed, there are noticeably fewer studies focusing exclusively on DVAs in this age group, especially in the neonatal period.[17,18,21-24] In particular, the largest case series of neonatal DVAs described so far included 14 neonates, mostly detected using ultrasound during routine scanning for other reasons,[22] with limited information on the prevalence and perinatal characteristics of these vascular abnormalities, including complications and longitudinal evolution. Moreover, additional data on neonatal and fetal DVAs would be of great interest because there is an ongoing debate regarding their congenital or postnatal etiology.[25]

In this study, we aimed to describe the pre- and postnatal appearance of DVAs and associated brain anomalies in a relatively large single-center group of neonates, providing information on their imaging and clinical follow-up. In addition, we tested a possible association between parenchymal and ventricular abnormalities in the drainage territory of neonatal DVAs and their angioarchitectural features.

MATERIALS AND METHODS

Population

After institutional review board approval, 1 pediatric neuroradiologist (M.S.) searched in the radiology information system of a tertiary pediatric institution (IRCCS Istituto Giannina Gaslini, Genoa, Italy) for reports of brain MR imaging studies performed in subjects up to 28 days of corrected age containing the term "developmental venous anomaly," during a 12-year period (January 2008 to December 2019). During this period, 2135 neonates underwent brain MR imaging. All procedures performed in the studies involving human participants were in accordance with the ethical standards of 1964 Helsinki Declaration and its later amendments or comparable ethical standards. Informed consent was waived by the institutional research committee.

MR Imaging Technique and Image Analysis

Neonates were scanned on 1.5T or 3T MR imaging units with different imaging protocols, all including at least T1WI, T2WI, DWI, and T2*WI (either gradient recalled-echo or SWI) sequences. Gadolinium-based contrast agents were injected only if clinically indicated. Neonates were fed before the MR imaging examination to achieve spontaneous sleep, with mild oral midazolam sedation (0.1 mg/kg) in case of head movements, and were breathing spontaneously during the examination.

Brain MR imaging studies were reviewed by 2 pediatric neuroradiologists (M.S. and A.F.G. with 10 and 5 years of experience, respectively), who confirmed the diagnosis and evaluated the presence of DVA-related mechanical compression of adjacent structures, draining vein thrombosis, and/or parenchymal abnormalities within the drainage territory. The latter included any of the following: increased T2 signal of surrounding WM, foci of restricted diffusion, hemorrhage, CCM,[26] malformations of cortical development, or calcifications (defined as focal areas of hyperintensity on SWI phase images in right-handed MR imaging systems or hyperdensity on head CT scans). Microhemorrhages were distinguished from type IV CCMs on the basis of their evolution on imaging. Indeed, vessels of CCMs have a tendency to leak and bleed, thus frequently increasing or stabilizing in size with time, while microhemorrhages typically present a regular evolution of hemoglobin degradation with a faster reduction in size and/or complete regression.

Subjects with ≥1 associated abnormality were considered to have complicated DVAs (c-DVA group), and the remainder, uncomplicated DVAs (u-DVA group).

Additionally, we registered the number of DVAs per patient as well as the corresponding angioarchitecture features:[3,11] direction of drainage, number of collector veins, and mean collector caliber (defined as the caliber of the collector vein in case of a single collector or the mean of all collector calibers in case of multiple collectors, measured on axial T2*WI). Multiple collectors were defined as ≥2 draining veins. Fetal MR imaging, neonatal cerebral ultrasound (cUS), DSA, and follow-up MR imaging were reviewed when available.

Imaging findings at last MR imaging follow-up were classified as interval improvement, progression, stability, or mixed evolution.

Discrepancies were resolved by a third pediatric neuroradiologist (A.R. with 25 years of experience).

Clinical Data

Data on sex, pregnancy history, gestational age at birth, cause of prematurity, type of delivery, Apgar scores, corrected age at first MR imaging, and imaging indications were obtained from the electronic clinical records. For neonates with c-DVAs, additional data including treatment, age at last clinical assessment, and neurologic outcome (graded as normal, mild, moderate, or severe impairment) were also registered.

Statistical Analysis

Quantitative data were presented as median and interquartile range, and categoric data, as frequencies and percentages. Fisher exact, χ^2, and independent samples Student t tests were used to compare clinical characteristics between patient groups with c-DVAs and u-DVAs. Fisher exact, χ^2, and Mann-Whitney U tests were used to compare angioarchitectural characteristics and associated parenchymal/ventricular abnormalities between individual complicated and uncomplicated DVAs. All results were corrected for multiple-comparison testing using the Bonferroni correction method. Statistical significance was reached if the P value was $<0.05/k$, where k indicates the number of tests, resulting in thresholds for statistical significance of $P < .0045$ and .0083 for patient and DVA levels of comparison, respectively. Statistical analyses were performed using SPSS Statistics software, Version 24.0 (IBM).

RESULTS

Neonatal Imaging Features

Forty-one neonates with DVAs were retrieved by a report search and confirmed by image review (20 males; mean corrected age at first MR imaging, 39.9 weeks; range, 33–44 weeks), corresponding to a real-world MR imaging DVA detection of 1.9% (41/2135) in a tertiary pediatric center. Neonates were preterm in 46.3% of cases ($n = 19$). Brain MR imaging was obtained on a 3T scanner in 22 cases (53.7%). SWI and postcontrast T1WI were acquired in 38 (92.7%) and 7 cases (17.1%), respectively.

Table 1: Location and angioarchitecture characteristics of developmental venous anomalies

	Total ($n = 58$)	Complicated DVA ($n = 21$) (36.2%)	Uncomplicated DVA ($n = 37$) (63.2%)	P Value[a]
Location (%)				.44
Frontal	24 (41.4)	9 (42.9)	15 (40.5)	
Parieto-occipital	16 (27.7)	6 (28.6)	10 (27)	
Temporal	8 (13.8)	3 (14.3)	5 (13.5)	
Basal ganglia/thalami	5 (8.6)	0 (0)	5 (13.5)	
Brain stem	2 (3.4)	1 (4.8)	1 (2.7)	
Cerebellum	3 (5.2)	2 (9.5)	1 (2.7)	
Infratentorial (%)	5 (8.6)	3 (14.3)	2 (5.4)	.34
Right side (%)	33 (56.9)	13 (61.9)	20 (54.1)	.59
Multiple collectors (%)	9 (15.5)	7 (33.3)	2 (5.4)	.008[b]
Main collector caliber (median) (IQR) (mm)	1.6 (1.18–2.10)	2.1 (1.95–2.30)	1.2 (1–1.6)	<.001[b]
Drainage (%)				.70
Deep	31 (53.4)	11 (52.4)	20 (54.1)	
Superficial	19 (32.8)	6 (28.6)	13 (35.1)	
Both	8 (13.8)	4 (19)	4 (10.8)	

Note:—IQR indicates interquartile range.

[a] P values for group comparisons were determined by χ^2 or Fisher exact tests for categoric variables or by Mann-Whitney U tests for continuous variables, as appropriate.

[b] Value statistically significant (statistical significance was set at $P < .0083$ after Bonferroni correction for multiple comparisons).

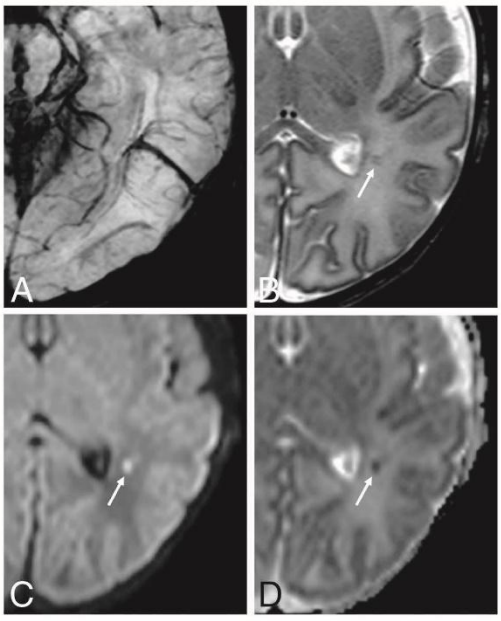

FIG 1. Neonatal developmental venous anomaly complicated by focal areas of venous ischemia. *A*, Axial SWI shows a left parietal developmental venous anomaly with superficial drainage. *B*, Axial T2WI reveals small linear hypointense lesions in the surrounding WM (*arrow*), with corresponding hyperintensity on $b = 1000$ image (*C*, *arrow*) and low ADC values on the ADC map (*D*, *arrow*).

Fifteen patients (36.6%) had at least 1 DVA (range, 1–6) associated with parenchymal abnormalities and/or CSF obstruction (c-DVA group) (Table 1 and Figs 1–3). Two of these neonates were affected by cerebrofacial venous metameric syndrome (CVMS). The On-line Table summarizes clinicoradiologic associations. In particular, at-term birth ($P = .02$), higher gestational age ($P = .05$), and imaging indications other than "preterm screening" ($P = .005$) were significantly more frequent in the c-DVA group but did not reach statistical significance after adjusting for multiple comparisons. Moreover, multiple DVAs as well as additional craniofacial vascular lesions were also more common in patients with c-DVAs ($P = .002$ and $P = .02$, respectively), but only multiplicity remained significant after multiple-comparison correction. Neonatal seizures likely attributable to a symptomatic DVA were detected in 2/15 patients with c-DVAs. One additional patient with a c-DVA developed probable DVA-related seizures at 11 months. A direct causal relationship between the DVA and neonatal seizures was not identified in 2 patients with u-DVA presenting with this symptom.

Overall, 58 DVAs were identified, comprising multiple DVAs in 9 cases. DVA location and angioarchitecture features are presented in Table 1. Multiple collectors and larger collector calibers were significantly more frequent in complicated DVAs ($P = .008$ and $P < .001$, respectively), even after adjusting for multiple comparisons.

DSA was performed in 4 patients with c-DVAs. No signs of arteriovenous shunting through the DVA with or without an associated classic nidus were identified, while a subject with CVMS had an intraorbital AVF.

Fetal MR Imaging and Postnatal cUS

Fetal MR imaging was performed in 11 patients (26.8%), of whom 6 belonged to the c-DVA group (21 examinations in total, 1–4 studies per patient, acquired between 20 and 38 gestational weeks). Retrospective analysis of single-shot FSE, $b = 0$, and/or T2*WI identified a DVA and/or an abnormally enlarged draining pathway in 3 fetuses (27.3%). In another case, a DVA-associated cerebellar hemorrhage was detected but precluded the identification of the subjacent DVA. Of the remaining 7 fetuses in whom the DVA was not visible, 3 presented with craniofacial vascular lesions.

Postnatal cUS was available in 36 neonates: In 3 cases, the DVA was suspected before the MR imaging examination due to the presence of a parenchymal linear hyperechogenic focus.

Management and Clinicoradiologic Outcome of Neonates with c-DVAs

Of 15 neonates with c-DVAs, 13 were conservatively managed, with a wait-and-see approach in 10 cases, anticoagulation treatment in 2, and antiepileptic drugs in 1. Endoscopic third ventriculostomy was performed in 1 neonate with DVA-related obstructive

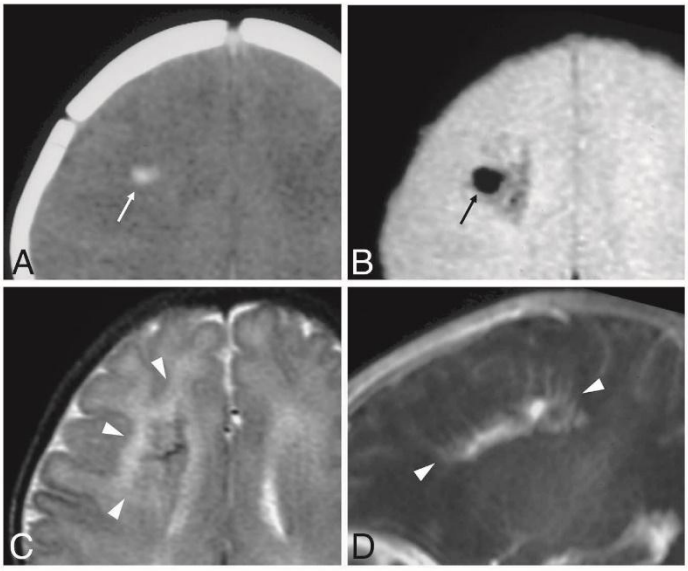

FIG 2. Neonatal developmental venous anomaly complicated by focal hemorrhage and diffuse WM signal abnormalities likely related to venous congestion. *A*, Unenhanced head CT scan demonstrates a focal area of spontaneous hyperdensity (*white arrow*) in the right frontal region, suggestive of recent hemorrhage. Corresponding axial gradient-echo T2*-weighted image (*B*) and T2WI (*C*) show a blooming artifact (*black arrow*) in the region corresponding to the hemorrhage, which subsequently regressed (not shown), and diffuse hyperintensity of the surrounding WM (*arrowheads*), in keeping with venous congestion. *D*, Sagittal contrast-enhanced T1WI reveals a large developmental venous anomaly characterized by several radially-oriented dilated veins with a caput medusae morphology and deep venous drainage (*arrowheads*).

hydrocephalus. Multiple interventional procedures were performed in the child with CVMS and an AVF.

Table 2 reports the clinicoradiologic outcome of subjects with c-DVAs. Longitudinal MR imaging was available in 10/15 patients (median follow-up, 39.1 months; range, 2–97 months; age at last follow-up, 2.5 months–8.2 years). Eight patients (80%) showed imaging signs of improvement, while stability ($n = 1$) or mixed evolution ($n = 1$) was detected in the remaining cases.

Follow-up neurologic evaluation was available in 14 neonates with c-DVAs (median follow-up, 27.5 months; range, 11–97 months), and findings were judged normal in 9 cases (64.2%), while minor or moderate psychomotor impairment was detected in 4 (28.5%) and 1 (7.1%) patient, respectively.

A brief description of a few illustrative cases of neonatal c-DVA is presented in the On-line Appendix.

DISCUSSION

In this study, we identified 41 neonates with DVAs, for a total of 58 DVAs, from a population of 2135 neonates undergoing brain MR imaging for diverse clinical reasons and with different imaging techniques, corresponding to a real-world detection in a tertiary pediatric center of 1.9%. These findings are similar to a recent retrospective study by Brinjikji et al,[25] describing a prevalence of 1.5% in the 0- to 12-month age group. Most interesting, both percentages are lower than those reported in studies including older children, adults, or mixed populations (5%–10%).[4,23,25] Because the pathogenesis of DVAs remains controversial, including their cause and timing of development, some authors have attributed these age-related prevalence differences to a postnatal origin.[25] However, caution is advised due to methodologic discrepancies among studies in terms of selection criteria and imaging protocols. In addition, DVAs may potentially be more difficult to detect in neonates due to small head size, incomplete myelination, short imaging protocols, and motion artifacts. On the other hand, statistically significant associations between DVAs and both primary brain tumors and multiple sclerosis have been previously described.[18,20] Because these disorders are frequent MR imaging indications in adults but very uncommon in the neonatal setting and infancy, the clinical indication itself may act as a confounder in the relationship between age and DVAs. Prospective neuroimaging studies in the healthy population at different ages using standardized imaging protocols are needed to better understand the relationship between age and DVAs. Of note, we retrospectively identified DVAs and/or related enlarged drainage pathways in 27.2% of cases with available fetal MR imaging, confirming a congenital origin of these vascular abnormalities in those patients.[6,27] Conversely, we did not identify new DVAs in follow-up studies, but we considered this a limited population; thus, we cannot exclude some DVAs actually developing de novo postnatally.

In our cohort, greater than one-third of neonates presented with at least 1 type of vascular complication directly linked to DVAs. Similarly, Horsch et al[22] found a high percentage (42.9%) of abnormalities surrounding neonatal DVAs, while variable frequencies have been described in studies including adults and/or older children.[10–13,15] Of note, initial differences regarding the corrected age at first MR imaging, prematurity, and imaging indications between neonates with cDVAs and u-DVAs likely represent a detection bias related to the neuroimaging screening program of preterm neonates with birth weights of <1500 g performed in our institution or even by chance, because these values did not reach statistical significance after multiple-comparison correction.

In detail, associated WM signal abnormalities were present in 17.1% of our neonates and were even more frequent in the series published by Horsch et al[22] (21.4%). Previous studies have suggested that DVA-related WM changes present a bimodal distribution, peaking in younger children and older adults.[11,12] However,

the underlying mechanisms of these signal changes remain poorly understood. In younger children, delayed myelination in the draining territory of the DVA has been proposed as a potential explanation.[12] Alternatively, these signal alterations may represent venous congestion edema in the DVA territory due to an imbalance of the in- and outflow of blood in the DVA system, raising the pressure in the DVA.[8] Of note, the latter mechanisms can also explain the relatively high frequency of associated hemorrhages and/or ischemic changes identified in our sample (19.5% and 9.8% of cases, respectively). In the general population, the risk of DVA-related hemorrhage is considered to be low (<1%/year) and is usually attributed to adjacent CCM bleeding.[2] However, we detected CCMs in only a small percentage of cases (4.9%), in keeping with the theory that nonfamilial CCMs are acquired lesions related to DVAs through the process of hemorrhagic angiogenic proliferation.[28,29]

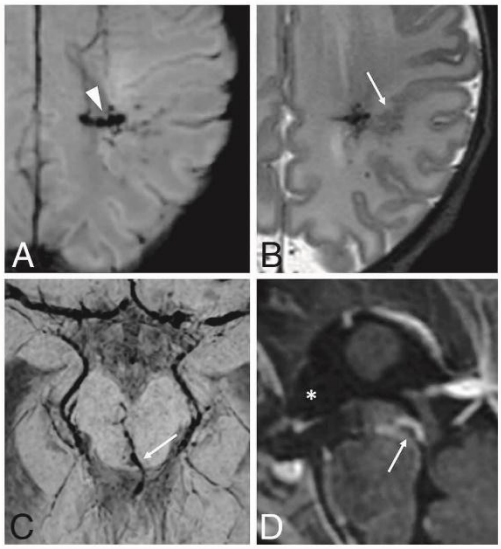

FIG 3. Neonatal developmental venous anomalies associated with focal polymicrogyria (*A* and *B*) and supratentorial hydrocephalus (*C* and *D*) in 2 different patients. Axial SWI (*A*) and T2WI (*B*) depict a developmental venous anomaly with deep venous drainage (*arrowhead*) and an adjacent area of cortical abnormality consistent with focal polymicrogyria (*arrow*). Axial SWI (*C*) and sagittal postgadolinium TIWI (*D*) demonstrate a mesencephalic developmental venous anomaly with the venous collector (*arrows*) causing focal compression of the inferior third of the cerebral aqueduct and consequent dilation of the anterior recesses of the third ventricle (*asterisk*), in keeping with supratentorial obstructive hydrocephalus (see also On-line Fig 8).

Taken together, our findings suggest that in the neonatal period, there is a higher risk of flow-related complications in DVAs, potentially leading to venous hypertension and associated venous congestion, hemorrhage, and/or infarction. Putative neonatal risk factors of hemodynamic decompensation include mechanical distortion during vaginal birth and immaturity of the venous, immune, and hemostatic systems as well as hypercoagulability, which may be potentiated by maternal factors or inflammation.[30-32] Finally, angioarchitectural factors yet unexplored in the neonatal setting, including angulation and stenosis of draining veins or tortuosity of medullary veins, could contribute to the development of ischemic or hemorrhagic complications.[10,33]

Most interesting, the presence of multiple DVAs (ie, multiplicity) was significantly more common in neonates with c-DVAs, even after multiple-comparisons correction, suggesting that more severe and widespread venous pathology may correspond to a more fragile venous outflow system and/or a higher propensity for thrombotic DVA events. Of note, 2 of these neonates presented with clinical-neuroradiologic features consistent with CVMS, a rare craniofacial vascular malformation disorder characterized by a wide spectrum of slow-flow vascular lesions distributed along ≥1 of the 3 craniofacial metameres, further supporting this theory.[19] Remarkably, 1 neonate also presented with a superior orbital fissure AVF, suggesting that this complex disorder may actually be a continuum potentially affecting >1 vessel type.

Our study also revealed focal polymicrogyria in the draining region of a DVA in 2 neonates (4.9%). DVAs or other venous drainage abnormalities or both have already been described adjacent to dysplastic cortical areas using conventional and ultra-high-field MR imaging.[34-37] Because polymicrogyria is frequently associated with in utero disruptive events, coexistence of these 2 lesions suggests a causative effect of the DVA in the formation of this cortical malformation or, more probably, a shared pathomechanism related to early failure, abnormal development, or intrauterine occlusion of normal cerebral vessels.[34,35,38] Finally, in 1 neonate, we observed obstructive hydrocephalus related to another type of DVA complication, ie, mechanical compression of the cerebral aqueduct.[8] As in our patient, CSF diversion techniques usually lead to a good outcome in these rare cases.[39]

Table 2: Neuroimaging abnormalities associated with developmental venous anomalies

MRI Abnormalities	Neonatal Period[a] (*n* = 15)	Last Follow-Up[a] (*n* = 10)
WM T2 signal abnormalities	7	Reduced 2/5 Stable 1/5 Complete regression, 2/5
Restricted diffusion foci	4	Total regression, 2/2
Hemorrhagic foci	8	Gliosis with or without hemosiderin deposits, 3/3
Multiple CCM	2[b]	Stable, 1/2 Growth, 1/2
PMG	2	Stable, 2/2
Calcifications	2	Stable, 2/2
Triventricular hydrocephalus	1	Resolution, 1/1[c]
Draining venous varix thrombosis	1	Recanalization, 1/1

Note:—PMG indicates polymicrogyria.
[a] Some patients presented with ≥1 DVA-related complication.
[b] Includes 1 neonate with cerebrofacial venous metameric syndrome.
[c] Postendoscopic third ventriculostomy.

As previously described, in our neonatal cohort, DVAs were more commonly located supratentorially and in the frontal lobe (41.4%).[10,32] Other common locations included the parieto-occipital (27.7%) and temporal (13.8%) lobes, while the basal ganglia and thalamus were involved in only 8.6% of cases. Of note, different from a previous neonatal case series, in our series, we identified infratentorial DVAs in 8.4% of cases, thus confirming a potential selection bias related to the use of cUS to depict posterior fossa DVAs.[22]

Regarding angioarchitecture features, we noticed a higher prevalence of multiple DVA collectors, which, together with larger caliber collectors, were significantly associated with DVA-related parenchymal abnormalities. These features may be related to the DVA size and, ultimately, to the volume of parenchyma under hemodynamic stress, ie, with reduced venous drainage capacity. Larger collectors may also be theoretically more prone to abnormal venous flow, with increased stasis and thrombosis. However, other studies performed in adults did not show statistically significant differences between parenchymal abnormalities and collecting vein diameters;[11] therefore, the relationship between these neuroimaging features requires more detailed study. Similarly, in the present study, posterior fossa location was not a risk factor for complicated DVAs. Methodologic issues in terms of populations of interest and types of complication may justify this variability,[16,23,32] and further studies are needed to also address this topic.

Serial imaging of a subgroup of neonates with c-DVAs revealed that DVAs and adjacent MR imaging abnormalities frequently present a dynamic evolution during the early years of life. These findings are in line with previous studies and probably reflect progressive brain and vascular maturation during early infancy.[22,40] Indeed, neuroimaging follow-up demonstrated overall improvement in most cases of c-DVAs. More specifically, WM abnormalities were reduced in size or even completely resolved. Furthermore, ischemic and hemorrhagic foci also tended to subside without signs of intracranial re-hemorrhage. Of note, clinical outcomes of patients with c-DVAs was concordant with their favorable MR imaging evolution, with normal neurologic examination findings in most cases. Good clinical and neurologic outcomes were also reported by Horsch et al[22] and are probably related to intrinsic brain plasticity as well as normalization of potential risk factors present in the neonatal phase.

Limitations

This study has some limitations. First, case selection was based on a retrospective single-center search of radiology reports. Therefore, although DVAs are routinely described in our institution by all staff members, the true DVA prevalence might be underestimated. Similarly, a relevant number of neonates was scanned on a 1.5T system, and gadolinium-based contrast media were only occasionally used, potentially leading to lower DVA detection.[34] However, SWI was performed in almost all neonates (92.7%) and has a high diagnostic sensitivity for DVAs in children, especially when sedation is achieved without propofol and sevoflurane.[4] Second, this study was performed in a tertiary pediatric institution, leading to potential selection bias toward inclusion of more severe DVA cases and limiting generalizability toward a different setting. Moreover, DVA collectors were measured on axial T2*WI, and this sequence can be influenced by the level of blood oxygenation and the magnetic field strength. However, none of the neonates were examined under general anesthesia, and complicated DVAs were actually less frequent in the group of subjects scanned using a 3T magnet. Therefore, if there were any bias related to the examination technique in terms of DVA collector size and MR imaging complications, it would actually exert its influence toward the null hypothesis. Finally, longitudinal data were missing in some patients, and clinical evaluation at follow-up was obtained from clinical records, though formal neurologic evaluation was performed in all assessed cases.

CONCLUSIONS

Real-world DVA detection in this population of neonates with clinically-indicated brain MR imaging reached 1.9%, which is lower than percentages of studies including older children and adults and might be an underestimation of the true prevalence. Of all neonates with detected DVAs, around one-third presented with DVA-related complications. The latter group had a significant tendency toward multiplicity and additional vascular malformations but usually had favorable neuroimaging findings and neurologic evolution at follow-up. DVAs could be retrospectively diagnosed in utero in one-quarter of neonates with fetal MR imaging, confirming, at least in these cases, a congenital origin.

Disclosures: Ana F. Geraldo—*UNRELATED: Grants/Grants Pending*: European Society of Neuroradiology, *Comments*: annual research grant. Alessandro Parodi—*UNRELATED*: *Consultancy*: Shire Human Genetic Therapies, *Comments*: 2018–2019 collaboration in the ROPP-2008-01 clinical trial (assessment of cranial ultrasound images of enrolled subjects). Paul Govaert—*UNRELATED*: *Payment for Development of Educational Presentations*: book, Mac Keith Press London. Mariasavina Severino—*RELATED*: *Grant*: "Ricerca Corrente Disordini Neurologici e Muscolari (Linea 5)" of Italian Ministry of Health, Compagnia di San Paolo (ROL 20573)*; *UNRELATED*: *Employment*: neuroradiology consultant, Scientific Institute for Research, Hospitalization and Healthcare Istituto Giannina Gaslini. *Money paid to the institution.

REFERENCES

1. Malova M, Rossi A, Severino M, et al. **Incidental findings on routine brain MRI scans in preterm infants.** *Arch Dis Child Fetal Neonatal Ed* 2017;102:F73–78 CrossRef Medline
2. Hon JM, Bhattacharya JJ, Counsell CE, et al; SIVMS Collaborators. **The presentation and clinical course of intracranial developmental venous anomalies in adults: a systematic review and prospective, population-based study.** *Stroke* 2009;40:1980–85 CrossRef Medline
3. Lee C, Pennington MA, Kenney CM, et al. **MR evaluation of developmental venous anomalies: medullary venous anatomy of venous angiomas.** *AJNR Am J Neuroradiol* 1996;17:61–70 Medline
4. Gökçe E, Acu B, Beyhan M, et al. **Magnetic resonance imaging findings of developmental venous anomalies.** *Clin Neuroradiol* 2014;24:135–43 CrossRef Medline
5. Young A, Poretti A, Bosemani T, et al. **Sensitivity of susceptibility-weighted imaging in detecting developmental venous anomalies and associated cavernomas and microhemorrhages in children.** *Neuroradiology* 2017;59:797–802 CrossRef Medline
6. Geraldo AF, Melo M, Monteiro D, et al. **Developmental venous anomaly depicted incidentally in fetal MRI and confirmed in postnatal MRI.** *Neuroradiology* 2018;60:993–94 CrossRef Medline
7. Lasjaunias P, Burrows P, Planet C. **Developmental venous anomalies (DVA): the so-called venous angioma.** *Neurosurg Rev* 1986;9:233–42 CrossRef Medline

8. Pereira VM, Geibprasert S, Krings T, et al. **Pathomechanisms of symptomatic developmental venous anomalies.** *Stroke* 2008;39:3201–15 CrossRef Medline
9. Rinaldo L, Lanzino G, Flemming KD, et al. **Symptomatic developmental venous anomalies.** *Acta Neurochir (Wien)* 2020;162:1115–25 CrossRef Medline
10. San Millán Ruíz D, Delavelle J, Yilmaz H, et al. **Parenchymal abnormalities associated with developmental venous anomalies.** *Neuroradiology* 2007;49:987–95 CrossRef Medline
11. Santucci GM, Leach JL, Ying J, et al. **Brain parenchymal signal abnormalities associated with developmental venous anomalies: detailed MR imaging assessment.** *AJNR Am J Neuroradiol* 2008;29:1317–23 CrossRef Medline
12. Linscott LL, Leach JL, Zhang B, et al. **Brain parenchymal signal abnormalities associated with developmental venous anomalies in children and young adults.** *AJNR Am J Neuroradiol* 2014;35:1600–07 CrossRef Medline
13. Takasugi M, Fujii S, Shinohara Y, et al. **Parenchymal hypointense foci associated with developmental venous anomalies: evaluation by phase-sensitive MR imaging at 3T.** *AJNR Am J Neuroradiol* 2013;34:1940–44 CrossRef Medline
14. Sharma A, Zipfel GJ, Hildebolt C, et al. **Hemodynamic effects of developmental venous anomalies with and without cavernous malformations.** *AJNR Am J Neuroradiol* 2013;34:1746–51 CrossRef Medline
15. Umino M, Maeda M, Matsushima N, et al. **High-signal-intensity abnormalities evaluated by 3D fluid-attenuated inversion recovery imaging within the drainage territory of developmental venous anomalies identified by susceptibility-weighted imaging at 3 T.** *Jpn J Radiol* 2014;32:397–404 CrossRef Medline
16. Zhang S, Ma L, Wu C, et al. **A rupture risk analysis of cerebral cavernous malformation associated with developmental venous anomaly using susceptibility-weighted imaging.** *Neuroradiology* 2020;62:39–47 CrossRef Medline
17. Jones BV, Linscott L, Koberlein G, et al. **Increased prevalence of developmental venous anomalies in children with intracranial neoplasms.** *AJNR Am J Neuroradiol* 2015;36:1782–85 CrossRef Medline
18. Roux A, Edjlali M, Porelli S, et al. **Developmental venous anomaly in adult patients with diffuse glioma: a clinically relevant coexistence?** *Neurology* 2019;92:e55–62 CrossRef Medline
19. Brinjikji W, Nicholson P, Hilditch CA, et al. **Cerebrofacial venous metameric syndrome: spectrum of imaging findings.** *Neuroradiology* 2020;62:417–25 CrossRef Medline
20. Halicioglu S, Turkoglu SA. **Role of developmental venous anomalies in etiopathogenesis of demyelinating diseases.** *Int J Neurosci* 2019;129:245–51 CrossRef Medline
21. Shiran SI, Ben-Sira L, Elhasid R, et al. **Multiple brain developmental venous anomalies as a marker for constitutional mismatch repair deficiency syndrome.** *AJNR Am J Neuroradiol* 2018;39:1943–46 CrossRef Medline
22. Horsch S, Govaert P, Cowan FM, et al. **Developmental venous anomaly in the newborn brain.** *Neuroradiology* 2014;56:579–88 CrossRef Medline
23. Silva AH, Wijesinghe H, Lo WB, et al. **Paediatric developmental venous anomalies (DVAs): how often do they bleed and where?** *Childs Nerv Syst* 2020;36:1435–43 CrossRef Medline
24. Linscott LL, Leach JL, Jones BV, et al. **Developmental venous anomalies of the brain in children: imaging spectrum and update.** *Pediatr Radiol* 2016;46:394–406 CrossRef Medline
25. Brinjikji W, El-Masri AE, Wald JT, et al. **Prevalence of developmental venous anomalies increases with age.** *Stroke* 2017;48:1997–99 CrossRef Medline
26. Zabramski JM, Wascher TM, Spetzler RF, et al. **The natural history of familial cavernous malformations: results of an ongoing study.** *J Neurosurg* 1994;80:422–32 CrossRef Medline
27. Okudera T, Huang YP, Fukusumi A, et al. **Micro-angiographical studies of the medullary venous system of the cerebral hemisphere.** *Neuropathology* 1999;19:93–118 CrossRef Medline
28. Dammann P, Wrede K, Zhu Y, et al. **Correlation of the venous angioarchitecture of multiple cerebral cavernous malformations with familial or sporadic disease: a susceptibility-weighted imaging study with 7-Tesla MRI.** *J Neurosurg* 2017;126:570–77 CrossRef Medline
29. Brinjikji W, El-Masri AE, Wald JT, et al. **Prevalence of cerebral cavernous malformations associated with developmental venous anomalies increases with age.** *Childs Nerv Syst* 2017;33:1539–43 CrossRef Medline
30. Yang JY, Chan AK, Callen DJ, et al. **Neonatal cerebral sinovenous thrombosis: shifting the evidence for a diagnostic plan and treatment strategy.** *Pediatrics* 2010;126:e693–e700 CrossRef Medline
31. Ami O, Maran JC, Gabor P, et al. **Three-dimensional magnetic resonance imaging of fetal head molding and brain shape changes during the second stage of labor.** *PLoS One* 2019;14:e0215721 CrossRef Medline
32. Kumar S, Lanzino G, Brinjikji W, et al. **Infratentorial developmental venous abnormalities and inflammation increase odds of sporadic cavernous malformation.** *J Stroke Cerebrovasc Dis* 2019;28:1662–67 CrossRef Medline
33. Hong YJ, Chung TS, Suh SH, et al. **The angioarchitectural factors of the cerebral developmental venous anomaly: can they be the causes of concurrent sporadic cavernous malformation?** *Neuroradiology* 2010;52:883–91 CrossRef Medline
34. Thompson JE, Castillo M, Thomas D, et al. **Radiologic-pathologic correlation polymicrogyria.** *AJNR Am J Neuroradiol* 1997;18:307–12 Medline
35. Cagneaux M, Paoli V, Blanchard G, et al. **Pre- and postnatal imaging of early cerebral damage in Sturge-Weber syndrome.** *Pediatr Radiol* 2013;43:1536–39 CrossRef Medline
36. De Ciantis A, Barkovich AJ, Cosottini M, et al. **Ultra-high-field MR imaging in polymicrogyria and epilepsy.** *AJNR Am J Neuroradiol* 2015;36:309–16 CrossRef Medline
37. Mankad K, Biswas A, Espagnet MCR, et al. **Venous pathologies in paediatric neuroradiology: from foetal to adolescent life.** *Neuroradiology* 2020;62:15–37 CrossRef Medline
38. Stutterd CA, Leventer RJ. **Polymicrogyria: a common and heterogeneous malformation of cortical development.** *Am J Med Genet C Semin Med Genet* 2014;166C:227–39 CrossRef Medline
39. Higa N, Dwiutomo R, Oyoshi T, et al. **A case of developing obstructive hydrocephalus following aqueductal stenosis caused by developmental venous anomalies.** *Childs Nerv Syst* 2020;36:1549–55 CrossRef Medline
40. Howard T, Abruzzo T, Jones B, et al. **Postnatal evolution of a developmental venous anomaly.** *J Pediatr Neuroradiol* 2015;01:305–11 CrossRef

Neuroradiology
https://doi.org/10.1007/s00234-022-02958-1

PAEDIATRIC NEURORADIOLOGY

Spinal involvement in pediatric familial cavernous malformation syndrome

Ana Filipa Geraldo[1,2] · Aysha Luis[3,4] · Cesar Augusto P. F. Alves[5] · Domenico Tortora[6] · Joana Guimarães[7,8] · Sofia Reimão[2,9] · Marco Pavanello[10] · Patrizia de Marco[11] · Marcello Scala[12,13] · Valeria Capra[11] · Andrea Rossi[6,14] · Erin Simon Schwartz[5] · Kshitij Mankad[3] · Mariasavina Severino[6]

Received: 13 March 2022 / Accepted: 10 April 2022

Abstract

Purpose The aim of the study was to assess the prevalence and characteristics of spinal cord cavernous malformations (SCCM) and intraosseous spinal vascular malformations (ISVM) in a pediatric familial cerebral cavernous malformation (FCCM) cohort and evaluate clinico-radiological differences between children with (SCCM +) and without (SCCM-) SCCM.

Methods All patients with a pediatric diagnosis of FCCM evaluated at three tertiary pediatric hospitals between January 2010 and August 2021 with ≥ 1 whole spine MR available were included. Brain and spine MR studies were retrospectively evaluated, and clinical and genetic data collected. Comparisons between SCCM + and SCCM- groups were performed using student-t/Mann–Whitney or Fisher exact tests, as appropriate.

Results Thirty-one children (55% boys) were included. Baseline spine MR was performed (mean age = 9.7 years) following clinical manifestations in one subject (3%) and as a screening strategy in the remainder. Six SCCM were detected in five patients (16%), in the cervico-medullary junction ($n=1$), cervical ($n=3$), and high thoracic ($n=2$) regions, with one appearing during follow-up. A tendency towards an older age at first spine MR ($P=0.14$) and ≥ 1 posterior fossa lesion ($P=0.13$) was observed in SCCM + patients, lacking statistical significance. No subject demonstrated ISVM.

Conclusion Although rarely symptomatic, SCCM can be detected in up to 16% of pediatric FCCM patients using diverse spine MR protocols and may appear de novo. ISVM were instead absent in our cohort. Given the relative commonality of asymptomatic SCCM, serial screening spine MR should be considered in FCCM starting in childhood.

Keywords Cavernous malformation · Familial cavernous malformation syndrome · Magnetic resonance imaging · Spinal imaging

✉ Andrea Rossi
andrearossi@ospedale-gaslini.ge.it

1 Diagnostic Neuroradiology Unit, Department of Radiology, Centro Hospitalar Vila Nova de Gaia/Espinho (CHVNG/E), Vila Nova de Gaia, Portugal

2 Clínica Universitária de Imagiologia, Faculty of Medicine of the University of Lisbon, Lisbon, Portugal

3 Department of Radiology, Great Ormond Street Hospital for Children NHS Foundation Trust, London, UK

4 Department of Radiology, King's College London, London, UK

5 Department of Radiology, Children's Hospital of Philadelphia, Philadelphia, PA, USA

6 Neuroradiology Unit, IRCCS Istituto Giannina Gaslini, Genoa, Italy

7 Department of Neurology, Centro Hospitalar Universitário de São João, Porto, Portugal

8 Department of Clinical Neurosciences and Mental Health, Faculty of Medicine of the University of Porto, Porto, Portugal

9 Neuroimaging department, Hospital de Santa Maria, Lisbon, Portugal

10 Neurosurgery Unit, IRCCS Istituto Giannina Gaslini, Genoa, Italy

11 Medical Genetics Unit, IRCCS Istituto Giannina Gaslini, Genoa, Italy

12 Department of Neurosciences, Rehabilitation, Ophthalmology, Genetics, Maternal and Child Health, University of Genoa, Genoa, Italy

13 Pediatric Neurology and Muscular Diseases Unit, IRCCS Istituto Giannina Gaslini, Genoa, Italy

14 Department of Health Sciences (DISSAL), University of Genoa, Genoa, Italy

Published online: 22 April 2022

Abbreviations

CM	Cavernous malformation
FCCM	Familial cerebral cavernous malformation syndrome
ISVM	Intraosseous spinal vascular malformations
SCCM	Spinal cord cavernous malformation

Introduction

Familial cerebral cavernous malformation syndrome (FCCM) is an autosomal dominant inherited disorder with incomplete penetrance and high intra- and inter-familial phenotypical variability, caused by heterozygous germline loss-of-function pathogenic variants in either one of three gene complexes involved in the maintenance of endothelial integrity: *CCM1* (*KRIT1,* OMIM * 604214), *CCM2* (Malcavernin, OMIM * 607929), and *CCM3* (*PDCD10,* OMIM * 609118) [1, 2]. Although this entity has been classically defined by the association of multiple cerebral cavernous malformations (CM) and a positive family history, it is now increasingly recognized as a multisystem, progressive disorder, with development of CM in multiple locations over time [1, 3, 4]. In particular, spinal cord cavernous malformations (SCCM) are being increasingly reported in the setting of FCCM [5–7], most likely due to the combination of increasingly widespread MR availability, improved imaging techniques, and a higher awareness of their possible occurrence. Similarly, it has been shown that a high percentage of patients of all ages (15–40%) presenting with a SCCM may harbor at least one similar intracranial lesion, supporting their association [8–10]. The spinal vascular lesions are histologically identical to their intracranial counterparts and also have a propensity to enlarge and/or hemorrhage over time. However, their clinical and imaging features have been less thoroughly established in the literature, likely due to their rarity [10].

In addition to SCCM, vertebral intraosseous spinal vascular malformations (ISVM) have also been associated with FCCM in case reports and small case series [5, 11, 12] and recently in case–control and prospective studies [7, 13].

Studies focusing on SCCM and other spinal abnormalities including ISVM in cohorts of pediatric-only FCCM patients are currently lacking, and previous evidence suggests that pediatric presentation and familiarity have the potential to influence the natural history of both cerebral CM and SCCM [14–16]. Additional clinical and imaging data on these lesions would thus be valuable for the assessment of the prognosis of affected individuals and the development of potential imaging screening programs and imaging endpoints in future clinical trials, since medical therapies are already being investigated for CM [17–19]. Pharmacological agents are particularly appealing for children with FCCM, as preliminary data suggest that these compounds not only stabilize CM but also prevent their formation, which is known to be age-dependent [17–19].

The aim of our study was to assess the prevalence and characteristics of SCCM and ISVM in a pediatric cohort of FCCM and to evaluate any clinico-radiological differences between patients with (SCCM +) and without (SCCM-) SCCM. We hypothesized that SCCM are common and already present during the pediatric age in FCCM and that SCCM + patients have a higher number of intracranial and extra-CNS CM.

Material and methods

Population

We performed a multicenter retrospective study involving three tertiary pediatric centers. All consecutive patients with a diagnosis of FCCM during the childhood (< 19 years) evaluated at least once in the participating hospitals between January 2010 and August 2021 and with at least one complete spine MRI available were identified. The diagnosis of FCCM was based on (1) the presence of ≥ 1 cerebral CM or SCCM associated with a positive family history (defined as presence of ≥ 1 known first or second-degree relative with a proven CM) and/or (2) a confirmed pathogenic variant in *CCM1-3* in the affected patient or in a first-degree relative [7, 20]. Exclusion criteria included (1) history of prior radiation and (2) poor-quality spine MR images. IRB approval was obtained, and written informed consent was waived because of the retrospective nature of the study. An overall outline of the study is displayed in Fig. 1.

MR technique and image analysis

We retrospectively reviewed all available spine MR of the included subjects. Images were acquired at either 1.5 or 3.0 Tesla using local imaging protocols, including some with images following administration of gadolinium-based contrast agents.

A structured list of SCCM imaging features (including size, location, and signal intensity with subsequent Zabramski type classification [21], along with adjacent intramedullary hemorrhage, blood-fluid levels and spinal cord edema) was scored according to previously published criteria [22] in the first spine MR available for each subject. Presence, location, and size of potential lesions compatible with ISVM were also searched as part of our methodologic strategy [13].

Evaluation of available longitudinal spine MR was retrospectively performed to analyze for changes in any previously identified lesions as well as for development of new lesions. Lesions were regarded as de novo only if their new

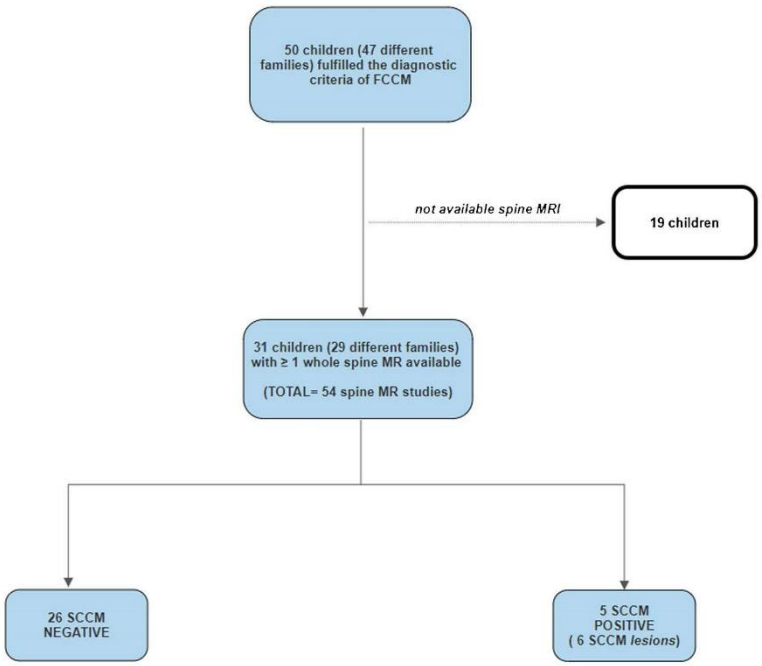

Fig. 1 Flow chart of the study. FCCM, familial cavernous malformation syndrome; SCCM, spinal cord cavernous malformation

appearance could be demonstrated employing magnets of similar or lower field strength and with identical protocols.

The first available brain MR for each patient was also reviewed (assessing total number and location of cerebral CM on GRE T2* or SWI images) as well as any available body MR and/or CT scans. Symptomatic cerebral CM hemorrhage was defined according to previous guidelines [23], and a similar approach was used for SCCM.

At each of the three involved hospitals, imaging studies were initially analyzed by one rater (for a total of three raters with 1, 7 and 7 years of experience in pediatric neuroradiology, respectively), blinded to the clinical and genetic information. Subsequently, anonymized MR studies with questionable evaluation and spine MR images of SCCM + patients were decided by final consensus of all three readers during scheduled monthly meetings.

Clinical data

Data on demographics, method, and age at clinical presentation leading to the FCCM diagnosis, ethnicity, family history (including number of affected family elements and degree of kinship), genotype, presence of other systemic CM (including cutaneous, retinal, or within solid organs), or any combined features of Greig cephalopolysyndactyly in the setting of a 7p deletion syndrome [24] were obtained from medical records. Age at first and last available spine MR, spinal signs and symptoms prior to the detection of SCCM (as classified per Ogilvy et al.) [25], symptomatic neurological events attributable to SCCM during follow-up, as well as any performed brain or spinal surgery and final neurological outcomes (graded as normal, mild, moderate or severe impairment) were also recorded.

Statistical analysis

Quantitative data were presented as median and interquartile range and categorical data as frequencies and percentages. Comparisons between SCCM + and SCCM- patients were performed using student-t/Mann–Whitney or Fisher exact tests, as appropriate. Statistical analyses were performed by using SPSS Statistics software, v24.0 (IBM, Armonk, NY). The significance level was set at $P = 0.05$.

Results

Clinical and genetic results

Fifty patients from 47 different families fulfilled the diagnostic criteria of FCCM. Thirty-one (62%) patients from 29

different families (55% male) had ≥ 1 whole spine MR for review and were therefore included.

Clinical and genetic data are summarized in Table 1. Eighty-seven percent of the cases (26/31) were Caucasian. No child had Hispanic ethnicity. There was a positive family history in 22/31 (71.0%) of patients, with multiple kindred involved in 10 (32.3%). Pathogenic variants in *CCM1, CCM2*, and *CCM3* were respectively identified in 17 (54.8%), 6 (19.4%), and 6 (19.4%) cases or in a known first-degree relative. Four of the six (75%) of the *CCM2* patients were confirmed to have a 7p deletion, of which two had features of Greig cephalopolysyndactyly and neurodevelopmental delay.

Table 1 Demographic, genetic and clinical data

	N = 31
Male, n (%)	17 (54.8)
Age at initial clinical presentation in yrs, mean (SD)	6.9 (5.0)
Age at first spinal MR in yrs, mean (SD)	9.7 (5.0)
Genotype, n (%)	
CCM1	17 (54.8)
CCM2[a]	6 (19.4)
CCM3	6 (19.4)
CCM1-3 testing negative	1 (3.2)
CCM1-3 testing not performed	1 (3.2)
Positive family history, n (%)	22 (71.0)
Ethnic origin, n (%)	
Caucasian	26 (87.0)
Asian	2 (6.5)
Arabic	2 (6.5)
African	1 (3.2)
Hispanic	0 (0.0)
Presentation mode, n (%)	
Symptomatic hemorrhage of the CNS[b]	17 (54.8)
Non-hemorrhagic seizures	4 (12.9)
Incidental diagnosis	4 (12.9)
Imaging screening	3 (9.7)
Headaches	3 (9.7)
N° cerebral CM at first available brain MR, median (IQR)	10 (17.0)
≥ 1 extra-CNS CM, *n* (%)	2 (6.5)
≥ 1 SCCM, *n* (%)	5 (16.1)
≥ 1 brain surgery, *n* (%)	15 (48.4)
≥ 1 ISVM, *n* (%)	0 (0.0)
≥ 1 spine surgery, *n* (%)	0 (0.0)
Neurological outcome at last clinical follow-up, *n* (%)	
Normal	20 (64.5)
Mild impairment	3 (9.7)
Moderate impairment	6 (19.4)
Severe impairment	2 (6.5)

Legend: *CM* cavernous malformation, *CNS* central nervous system, *IQR* interquartile range, *ISVM* intraosseous spinal venous malformation, *SCCM* spinal cord cavernous malformation, *SD* standard deviation, *yrs* years

[a]Includes 4 cases with a 7p deletion; [b] Includes 1 case due to a SCCM-related hemorrhage

The mean age at first clinical presentation leading to subsequent FCCM diagnosis was 6.9 years (SD = 5.0; range 0.7–16.0 years), typically occurring in the context of a symptomatic hemorrhage associated with a CM located elsewhere in the CNS (17/31, 54.8%). Fifteen (48.4%) patients underwent ≥ 1 brain surgery (total = 21 procedures, range: 0–3), before or after the first available spine MR. No subjects in our cohort underwent spinal surgery. All patients were alive at clinical follow-up (median = 24.0 months; range: 15–57) and 20/31 (64.5%) remained neurologically intact at their last clinical visit. However, mild to severe neurologic impairment was present in the remainder, due to intracranial hemorrhagic complications and/or refractory epilepsy, either due to the coexistent cerebral CM or in the context of 7p deletion-associated developmental delay.

Spine MR findings

A total of 54 spine MR were reviewed, of which 9 (16.7%) performed on a 3.0 T. T2 TSE, T1 TSE, and/or GRE sequences were included in 47/54 (87%), 46/54 (85%), and 24/54 (44%) of all spine MR examinations, respectively. Overall, 45% of the subjects had at least one available spine MR with a GRE sequence for review. Gadolinium was injected in 3/54 (6%) spine MR studies.

Mean age at first available spine MR was 9.7 years (SD = 5.1; range 0.8–18.9 years). Baseline spine imaging was performed due to acute medullary symptoms (Ogilvy type C) in one case (3%), representing the clinical presentation that eventually led to the diagnosis of FCCM in that patient. In the remainder cases (30/31;97%), spine MR was initially performed as a screening strategy in patients that had no related symptoms (corresponding to Ogilvy type E) when FCCM was already confirmed or suspected.

Retrospective longitudinal spine MR was additionally available in 12/31 patients (38.7% of cases, 2 SCCM + and 10 SCCM- patients, respectively), with a mean follow-up spine MR time of 54.9 months (range: 3–129.6). In all of them, additional spine MR studies were performed as routine examinations as no new neurological events attributable to SCCM developed subsequently during clinical follow-up time.

A total of *n* = 6 SCCM were detected in five different patients (16.2%) of our cohort at a mean age of 13.5 years (range: 10.9–16.3). Lesions were localized in the cervicomedullary junction (*n* = 1), cervical (*n* = 3), and high thoracic (*n* = 2) segments, one of them appearing de novo 40 months after the initial spine MR. Four out of five SCCM + patients had both T2 TSE and GRE sequences available for review, and the SCCM could be depicted

in each of these sequences individually. The remainder SCCM + patient underwent only one spine MR without GRE, and two small SCCM were depicted on sagittal T2 TSE. All five SCCM + patients had at least one T1 TSE sequence available for review, but the SCCM could be detected in this sequence in only two of them. Further details on the SCCM neuroimaging features are presented in the Supplemental Table 1. At baseline spine MR SCCM were classified as Zabramski types I, II, and IV in 1, 1, and 2 cases, respectively. The Zabramski type I SCCM changed towards a type II lesion at follow-up (Fig. 2). In addition, two SCCM were initially considered unclassifiable, one of them subsequently changing towards a Zabramski type III (Supplemental Figs. 1 and 2). Focal spinal cord expansion and presence of an exophytic component were each detected in 3/6 SCCM (Fig. 3), while a complete hemosiderin ring was detected in one case (Fig. 2). The single symptomatic SCCM presented initially with adjacent spinal cord edema that resolved at follow-up imaging (Fig. 2). Finally, intramedullary, flame-like hemorrhage was detected adjacent to one SCCM at diagnosis and developed into the acute hemorrhagic SCCM case at follow-up spine MR (Fig. 2 and Supplemental Figs. 1 and 2).

None of our children demonstrated an ISVM (either typical or atypical) at initial spine MR evaluation nor during follow-up. Other spinal neuroimaging findings depicted in our cohort included mild dorsal levoscoliosis ($n = 4$) (Fig. 2), congenital narrowing of the spinal canal ($n = 1$),

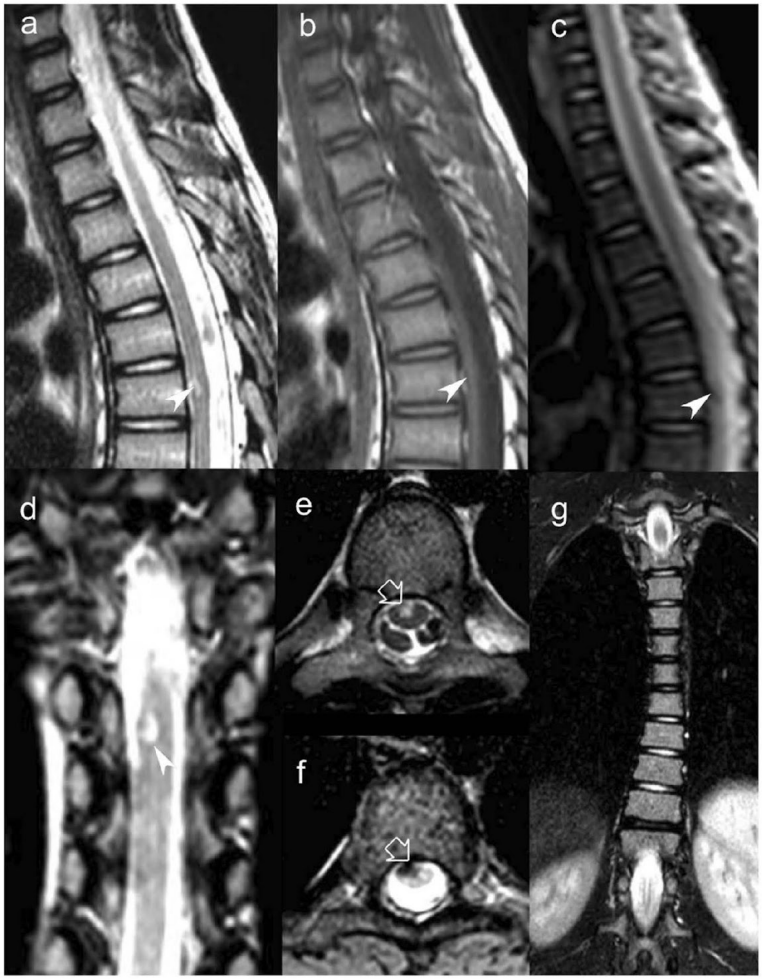

Fig. 2 Spine MR performed in a 12-year-old boy with familial cerebral cavernous malformation syndrome due to a proven *CCM3* mutation (SCCM patient #2) including sagittal T2FSE (**a**), T1TSE (**b**), and GRE (**c**) as well as coronal T2TSE (**d**, **g**) and axial T2 TSE (**e**) and GRE (**f**) depicts an intramedullary cavernous malformation located anteriorly at the level of D6 and lateralized to the right (white arrowheads and white empty arrows). There is a mild focal exophytic component, but no hemosiderin ring nor intramedullary edema. Also note mild dorsal levoscoliosis

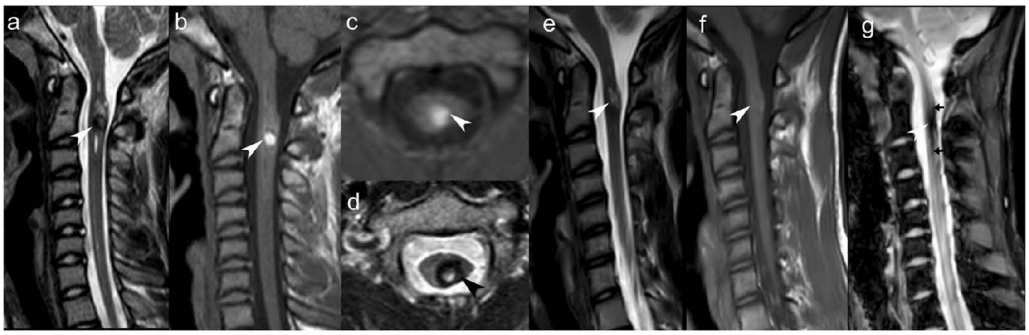

Fig. 3 Spine MR (**a-d**) performed in a 15-year-old boy with familial cerebral cavernous malformation syndrome due to a proven *CCM1* mutation (SCCM patient #4) including sagittal T2 TSE(**a**) and T1 TSE (**b**) as well as axial T1 TSE (**c**) and GRE (**d**) shows an early subacute hemorrhagic intramedullary cavernous malformation located posteriorly at the level of C2 and lateralized to the left (white and black arrowheads). There is a nearly complete hemosiderin rim, as well as surrounding edema and focal spinal cord expansion. Follow-up spine MR performed 10 months after (**e–g**) including sagittal T2 TSE (**e**), T1TSE (**f**), and GRE (**g**) demonstrates interval size reduction of the lesion, expected temporal evolution of the associated blood products, as well as regression of the perilesional edema and associated reduction of the spinal cord caliber (white arrowheads). Also note development of a subtle adjacent intramedullary flame-like hemorrhage (thin black arrows)

osteochondrosis ($n=1$), and mild dilatation of the central ependymal canal ($n=1$).

Brain MR findings

All included patients had multiple cerebral CM (median = 10; range: 2–80) depicted on T2* GRE and/or SWI sequences at the time of the first available brain MR, performed at the time of, or more commonly before, the first spine MR. Sixty-five percent (20/31) of them had ≥ 1 lesion located in the posterior fossa (median 1; range: 0–10 CM). Two out of the 31 patients (6.5%) demonstrated ≥ 1 systemic CM (corresponding to a total of 3 of such lesions), both detected in SCCM + patients with subjacent *CCM1* mutations. More precisely, one child had one CM located in the soft tissues of the right knee and the other had one CM in the soft tissues of the left elbow and another in the left skull base/masticator space.

Group comparisons

When compared with the SCCM- group, SCCM + patients showed a tendency towards an older age at first spine MR ($P=0.14$) and ≥ 1 cerebral CM located in the posterior fossa ($P=0.13$), although without reaching statistical significance (Table 2). Otherwise, there were no statistically significant

Table 2 Comparison between patients with (SCCM +) and without (SCCM-) spinal cavernous malformations

	SCCM + patients $N=5$ (16%)	SCCM- patients $N=26$ (84%)	*P* value
Male, n (%)	3 (60)	14 (54)	0.59
Age at initial clinical presentation in yrs, mean (SD)	8.4 (6.0)	6.6 (4.9)	0.47
Age at first spine MRI in yrs, mean (SD)	12.8 (3.4)	9.1 (5.2)	0.14
CCM1 mutations, *n* (%)	4 (80)	13 (50)	0.34
Positive family history, *n* (%)	4 (80)	18 (69)	0.54
Caucasian, *n* (%)	4 (80)	23 (89)	0.52
Presentation with symptomatic CNS hemorrhage, *n* (%)	4 (80)	13 (50)	0.34
N° intracranial brain CM at first available MR, median (IQR)	12.2 (20)	18.4 (18)	0.35
Presence of > = 1 CM in the posterior fossa at first available brain MR, *n* (%)	5 (100)	15 (58)	0.13
Number of CM in the posterior fossa at first available brain MR, median (IQR)	2.0 (2.0)	1.0 (3.0)	0.35

Legend: *CM* cavernous malformations, *CNS* central nervous system, *IQR* interquartile range, *SCCM* spinal cord cavernous malformation-, *SCCM-* patients without SCCM, *SCCM+* patients with SCCM, *SD* standard deviation, *yrs* years

differences between groups regarding demographic, clinical, and brain imaging features, including total number of intracranial CM at first available brain MR.

Discussion

In this study including 31 children from three tertiary pediatric centers with a confirmed diagnosis of FCCM, we identified five subjects with SCCM, for a total of $n=6$ SCCM, one of these appearing de novo during follow-up spine MR. This corresponds to a detection rate of SCCM in a pediatric-only cohort of FCCM of 16%, confirming a high prevalence of SCCM in the setting of FCCM [5–7] and showing that these lesions are frequently already present in affected individuals during childhood. Therefore, our results highlight the necessity of dedicated spine MR imaging in patients with suspected or confirmed FCCM starting during the pediatric age.

Although our detection rate of SCCM was relatively high, it was lower than has been reported in other published papers, including the prospective component of the study by Mabray et al. [7], where SCCM were identified in approximately 70% of cases. However, the latter study included children and adults, while our cohort is only pediatric. Indeed, de novo formation of CM in multiple sites is a well described phenomenon in FCCM, probably due to a second-site somatic mutation leading to molecular homozygosity at the CCM gene locus ("second-hit hypothesis") [26, 27]. In turn, this dynamic activity increases the chances of spinal cord lesion development with age, as demonstrated in one of our subjects. Correspondingly, our SCCM + subjects tended to be older at the first available spine MR, although statistical significance was not reached, likely due to the small sample size.

The disparities may also be explained, at least in part, by methodological differences between the two studies. Unlike the Mabray et al. study [7], not all of our subjects were imaged at 3.0 T or had at least one GRE sequence available. As GRE-type sequences (particularly 3D MEDIC) have been shown to have the highest sensitivity for SCCM detection [7], small SCCM may be underreported in this analysis, and prospective studies in this age group should include standardized spine MR sequences.

Finally, differences between studies may also be related to differences in patient populations characteristics as Mabray et al. included only patients with *CCM1* abnormalities with the pathogenic variant most common in Hispanic patients [7], while we included all types of *CCM1-3* pathogenic variants, none with Hispanic ancestry. Although genetics played no significant role in distinguishing between our SCCM subgroups ($P=0.34$), the *CCM1*-common Hispanic variant may confer a higher risk for the development of SCCM than other genetic causes. A few FCCM genotype–phenotype correlations have already been published, showing that *CCM3* variants are more frequently associated with spontaneous mutations and a more aggressive disease course compared to other genotypes [16, 28, 29]. Accordingly, *CCM3* pathogenic variants were present in a higher proportion of our cohort than described in most mixed-age studies (20% vs 10–15%) and affected individuals showed a significantly higher mean number of cerebral CM in their first available brain MR (mean = 43.2 lesions; range: 6–80; $P=0.039$) compared with other genotypes [7, 16, 28].

We have not found a statistically significant difference between SCCM + and SCCM- groups concerning the number of cerebral CM. However, SCCM + patients showed a tendency towards presence of at least one such lesion in the posterior fossa, although not reaching statistical significance possibly due to the limited sample size. In addition, the only two patients with ≥ 1 extraneural CM were also SCCM +, raising the suspicion that presence of systemic CM may be associated with SCCM. Subsequent prospective studies including a higher number of subjects may further explore these potential associations.

Concerning the imaging features of SCCM, a recent paper by Panda et al. [22] has shown that these differ slightly from their intracranial counterparts. In line with the prior report, our study confirms that popcorn morphology, internal blood-fluid levels, and complete T2WI hypointense rims are often absent. The same study also reported that a flame-like intramedullary hemorrhage can be frequently depicted adjacent to SCCM, and indeed this feature was eventually detected in 2/6 cases, being eccentric and bidirectional in both [22].

The coexistence of SCCMs and cerebral CM has been linked to a more aggressive course and unfavorable outcome [10]. In addition, it has been suggested that pediatric SCCM have a less favorable natural clinical history than their adult counterparts, with significantly higher overt hemorrhage and re-hemorrhage rates [14, 15]. However, only one of our pediatric SCCM + cases presented with acute neurological signs and symptoms attributed to the spinal cord lesion, and no subsequent SCCM-related events were detected in this patient or the remainder SCCM + cohort during clinical follow-up. Therefore, identification of SCCM in children before they become symptomatic through screening spinal MR is feasible and may help to inform a risk-analysis assessment concerning the best individualized management strategy in each case.

Surgical treatment has been advocated as the preferred therapeutic option in both children and adults with accessible, symptomatic SCCM, while a conservative approach may be considered in asymptomatic cases [9, 14, 15]. After individual assessment, all of our SCCM + patients (including the child with an overt SCCM-related hemorrhage) were managed conservatively, and none of them developed new

symptoms nor SCCM-related neurological deficits at last follow-up as previously mentioned. Although current management of FCCM is centered on symptom control, novel disease-modifying therapeutic options including statins and propanolol have demonstrated promising results in cerebral CM in preclinical studies and/or case reports and are already being tested in clinical trials including adults; they might also be beneficial in SCCM [17–19].

Contrary to other series, we have not identified lesions compatible with IVMS in any of our pediatric cases [7, 13], suggesting they form later in life. Indeed, previous studies have described a positive correlation of IVMS with age, and most published cases were detected in adults [7, 13].

Our study has some limitations, including its retrospective design and tertiary center referral bias. In addition, as guidelines for spine and brain imaging in pediatric FCCM are currently not well defined [30], patients were imaged at inconsistent time points and without standard spine MR technique (including variations in the scanner field strength and/or the protocol), and only a small subset had serial spine MR. This heterogeneity likely resulted in an underestimation of the rate of SCCM. Nevertheless, this research work is a result of an international multicenter collaboration including three tertiary pediatric centers and represents the largest pediatric-only cohort focusing on spinal imaging data of FCCM patients.

In conclusion, our data confirms a relatively high prevalence of SCCM in children with FCCM due to heterogeneous genetic background, and this percentage may represent an underestimation. On the other hand, ISVM were absent in our pediatric-only cohort. An optimized devoted whole-spine screening MR protocol including GRE sequences should be routinely performed at baseline in all pediatric cases with clinical-radiological suspicion of this disorder, and serial spinal MR studies should be considered in confirmed cases, even with negative initial imaging studies.

Supplementary Information The online version contains supplementary material available at https://doi.org/10.1007/s00234-022-02958-1.

Author contribution AF Geraldo, S Reimao, Severino M: study concept and design. AF Geraldo, A Luis, CAPF Alves, D Tortora, E S Shwartz, K Mankad, A Rossi, M Severino: analysis and interpretation of imaging data. AF Geraldo: statistical analysis. AF Geraldo: drafting the manuscript. AF Geraldo, A Luis, CAPFAlves, D Tortora, J Guimarães, S Reimão, A Rossi, M Pavanello, P De Marco, M Scala, V Capra, Rossi A, E S Shwartz, K Mankad, M Severino: revising the manuscript.

Funding Twelve months research fellowship in diagnostic neuroradiology, European Society of Neuroradiology (AF Geraldo).

Declarations

Ethics approval All procedures performed in studies involving human participants were in accordance with ethical standards of the institutional and/or national research committee and with the 1964 Helsinki declaration and its later amendments or comparable ethical standards.

Informed consent For this type of study, formal consent is not required.

Conflict of interest The authors declare no competing interests.

References

1. Zafar A, Quadri SA, Farooqui M et al (2019) Familial cerebral cavernous malformations. Stroke 50:1294–1301
2. Choquet H, Pawlikowska L, Lawton MT, Kim H (2015) Genetics of cerebral cavernous malformations: current status and future prospects. Neurosurg Sci 59:211–220
3. Strickland CD, Eberhardt SC, Bartlett MR et al (2017) Familial cerebral cavernous malformations are associated with adrenal calcifications on CT scans: an imaging biomarker for a hereditary cerebrovascular condition. Radiology 284:443–450
4. Manole AK, Forrester VJ, Zlotoff BJ et al (2020) Cutaneous findings of familial cerebral cavernous malformation syndrome due to the common Hispanic mutation. Am J Med Genet A 182:1066–1072
5. Toldo I, Drigo P, Mammi I et al (2009) Vertebral and spinal cavernous angiomas associated with familial cerebral cavernous malformation. Surg Neurol 71:167–171
6. de Vos IJHM, Vreeburg M, Koek GH, van Steensel MAM (2017) Review of familial cerebral cavernous malformations and report of seven additional families. Am J Med Genet A 173:338–351
7. Mabray MC, Starcevich J, Hallstrom J et al (2020) High prevalence of spinal cord cavernous malformations in the familial cerebral cavernous malformations type 1 cohort. AJNR Am J Neuroradiol 41:1126–1130
8. Cohen-Gadol AA, Jacob JT, Edwards DA, Krauss WE (2006) Coexistence of intracranial and spinal cavernous malformations: a study of prevalence and natural history. J Neurosurg 104:376–381
9. Badhiwala JH, Farrokhyar F, Alhazzani W et al (2014) Surgical outcomes and natural history of intramedullary spinal cord cavernous malformations: a single-center series and meta-analysis of individual patient data. J Neurosurg Spine 21:662–676
10. Ren J, Hong T, He C, et al (2019) Coexistence of intracranial and spinal cord cavernous malformations predict aggressive clinical presentation. Front Neurol 10:
11. Clatterbuck RE, Cohen B, Gailloud P et al (2002) Vertebral hemangiomas associated with familial cerebral cavernous malformation: segmental disease expression. Case report J Neurosurg 97:227–230
12. Lanfranconi S, Ronchi D, Ahmed N, et al (2014) A novel CCM1 mutation associated with multiple cerebral and vertebral cavernous malformations. BMC Neurol 14:
13. Tandberg SR, Bocklage T, Bartlett MR et al (2020) Vertebral intraosseous vascular malformations in a familial cerebral cavernous malformation population: prevalence, histologic features, and associations with CNS disease. AJR Am J Roentgenol 214:428–436
14. Ren J, Hong T, Zeng G et al (2020) Characteristics and long-term outcome of 20 children with intramedullary spinal cord cavernous malformations. Neurosurgery 86:817–824
15. Zhang L, Qiao G, Yang W et al (2021) Clinical features and long-term outcomes of pediatric spinal cord cavernous malformation-a report of 18 cases and literature review. Childs Nerv Syst 37:235–242

16. Merello E, Pavanello M, Consales A et al (2016) Genetic Screening of pediatric cavernous malformations. J Mol Neurosci 60:232–238
17. Lanfranconi S, Scola E, Bertani GA et al (2020) Propranolol for familial cerebral cavernous malformation (Treat_CCM): Study protocol for a randomized controlled pilot trial. Trials 21:401
18. Oldenburg J, Malinverno M, Globisch MA et al (2021) Propranolol reduces the development of lesions and rescues barrier function in cerebral cavernous malformations: a preclinical study. Stroke 52:1418–1427
19. Polster SP, Stadnik A, Akers AL et al (2019) Atorvastatin treatment of cavernous angiomas with symptomatic hemorrhage exploratory proof of concept (AT CASH EPOC) trial. Neurosurgery 85:843–853
20. Mespreuve M, Vanhoenacker F, Lemmerling M (2016) Familial multiple cavernous malformation syndrome: MR features in this uncommon but silent threat. J Belg Soc Radiol 100:51
21. Zabramski JM, Wascher TM, Spetzler RF et al (1994) The natural history of familial cavernous malformations: results of an ongoing study. J Neurosurg 80:422–432
22. Panda A, Diehn FE, Kim DK et al (2020) Spinal cord cavernous malformations: MRI commonly Shows adjacent intramedullary hemorrhage. J Neuroimaging 30:690–696
23. Al-Shahi Salman R, Berg MJ, Morrison L et al (2008) Hemorrhage from cavernous malformations of the brain: definition and reporting standards. Stroke 39:3222–3230
24. Bilguvar K, Bydon M, Bayrakli F et al (2007) A novel syndrome of cerebral cavernous malformation and Greig cephalopolysyndactyly: Laboratory investigation. J Neurosurg 107:495–499
25. Ogilvy CS, Louis DN, Ojemann RG (1992) Intramedullary cavernous angiomas of the spinal cord: clinical presentation, pathological features, and surgical management. Neurosurgery 31:219–230
26. Akers AL, Johnson E, Steinberg GK et al (2009) Biallelic somatic and germline mutations in cerebral cavernous malformations (CCMs): evidence for a two-hit mechanism of CCM pathogenesis. Hum Mol Genet 18:919–930
27. Pagenstecher A, Stahl S, Sure U, Felbor U (2009) A two-hit mechanism causes cerebral cavernous malformations: complete inactivation of CCM1, CCM2 or CCM3 in affected endothelial cells. Hum Mol Genet 18:911–918
28. Riant F, Bergametti F, Fournier HD et al (2013) CCM3 mutations are associated with early-onset cerebral hemorrhage and multiple meningiomas. Mol Syndr 4:165–172
29. Shenkar R, Shi C, Rebeiz T et al (2015) Exceptional aggressiveness of cerebral cavernous malformation disease associated with PDCD10 mutations. Genet Med 17:188–196
30. Akers A, Al-Shahi Salman R, Awad IA et al (2017) Synopsis of guidelines for the clinical management of cerebral cavernous malformations: consensus recommendations based on systematic literature review by the angioma alliance scientific advisory board clinical experts panel. Neurosurgery 80:665–680

Neuroradiology
https://doi.org/10.1007/s00234-022-03056-y

DIAGNOSTIC NEURORADIOLOGY

Natural history of familial cerebral cavernous malformation syndrome in children: a multicenter cohort study

Ana Filipa Geraldo[1,2] · Cesar Augusto P. F. Alves[3] · Aysha Luis[4,5] · Domenico Tortora[6] · Joana Guimarães[7,8] · Daisy Abreu[9] · Sofia Reimão[2,10] · Marco Pavanello[11] · Patrizia de Marco[12] · Marcello Scala[13,14] · Valeria Capra[12] · Rui Vaz[8,15] · Andrea Rossi[6,16] · Erin Simon Schwartz[3] · Kshitij Mankad[4] · Mariasavina Severino[6]

Received: 26 July 2022 / Accepted: 17 September 2022

Abstract

Purpose There is limited data concerning neuroimaging findings and longitudinal evaluation of familial cerebral cavernous malformations (FCCM) in children. Our aim was to study the natural history of pediatric FCCM, with an emphasis on symptomatic hemorrhagic events and associated clinical and imaging risk factors.

Methods We retrospectively reviewed all children diagnosed with FCCM in four tertiary pediatric hospitals between January 2010 and March 2022. Subjects with first available brain MRI and ≥ 3 months of clinical follow-up were included. Neuroimaging studies were reviewed, and clinical data collected. Annual symptomatic hemorrhage risk rates and cumulative risks were calculated using survival analysis and predictors of symptomatic hemorrhagic identified using regression analysis.

Results Forty-one children (53.7% males) were included, of whom 15 (36.3%) presenting with symptomatic hemorrhage. Seven symptomatic hemorrhages occurred during 140.5 person-years of follow-up, yielding a 5-year annual hemorrhage rate of 5.0% per person-year. The 1-, 2-, and 5-year cumulative risks of symptomatic hemorrhage were 7.3%, 14.6%, and 17.1%, respectively. The latter was higher in children with prior symptomatic hemorrhage (33.3%), *CCM2* genotype (33.3%), and positive family history (20.7%). Number of brainstem (adjusted hazard ratio [HR] = 1.37, $P = 0.005$) and posterior fossa (adjusted HR = 1.64, $P = 0.004$) CCM at first brain MRI were significant independent predictors of prospective symptomatic hemorrhage.

Conclusion The 5-year annual and cumulative symptomatic hemorrhagic risk in our pediatric FCCM cohort equals the overall risk described in children and adults with all types of CCM. Imaging features at first brain MRI may help to predict potential symptomatic hemorrhage at 5-year follow-up.

Keywords Cavernous malformation · Familial cavernous malformation syndrome, Magnetic resonance imaging · Brain imaging

Abbreviations

CASH	Cavernous angioma with symptomatic hemorrhage
CCM	Cerebral cavernous malformation
CM	Cavernous malformation
DVA	Developmental venous anomaly
FCCM	Familial cerebral cavernous malformation
SWI	Susceptibility-weighted image

Introduction

Cerebral cavernous malformations (CCM) are low-flow venous-capillary parenchymal brain lesions composed of enlarged, multilobulated, and leaky blood-filled sinusoidal spaces devoid of mature vascular walls and without intervening brain parenchyma [1]. Clinical manifestations of CCM may occur at any age, and include epileptic seizures, impaired consciousness, focal neurologic deficits, and headaches. In addition, asymptomatic presentation in the context of imaging screening or incidental detection of CCM may also occur. Overall, up to 25% of all CCM manifest in childhood [1, 2], and these vascular lesions represent one of the

✉ Andrea Rossi
andrearossi@gaslini.org

Extended author information available on the last page of the article

Published online: 06 October 2022

major causes of non-traumatic acute intracranial hemorrhage in this age group [3].

CCM are usually classified as familial (FCCM) or sporadic [1, 2]. Although histopathologically indistinguishable, these conditions usually have distinct genetic signatures. Indeed, FCCM (accounting for up to 20% of all CCM) is an autosomal dominant inherited disease with incomplete penetrance caused by inherited heterozygous germline loss-of-function pathogenic variants in *CCM1-3 genes* [4]. Sporadic CCM are instead mainly due to activating somatic mutations in genes involved in the PI3K-AKT-mTOR pathway, especially *PIK3CA* and *MAP3K3* [5–7]. Also, unlike sporadic CCM, familial forms often have a positive family history and the disease manifestations tend to present at an earlier age, usually in the form of multiple, scattered CCM [1, 8] as well as other systemic CM [9, 10].

Although the natural history of CCM in the general population has been relatively well studied [8, 11, 12], there are limited knowledge and conflicting results concerning the longitudinal evolution of pediatric FCCM. Indeed, most papers focusing on the natural history of CCM in familial cases include mixed-adult and pediatric populations and were published before 2008 [13–17], the year when a consensus statement regarding definitions and reporting standards of CCM-related hemorrhage was issued [18]. In addition, prior to 2008, gradient recovery echo-related sequences including T2* and SWI (considered the gold standard for in vivo assessment of CCM) were uncommonly used in clinical practice and frequently excluded from the analysis [13–17]. Moreover, the few available studies focusing on younger subjects with CCM are often based on cohorts including both children and young adults and/or all subtypes of CCM [19–23]. Indeed, familial cases only tend to account for a small proportion of the complete pediatric patients, with limited data available concerning their clinical features and imaging findings and underlying genotype [19–23]. All these limitations introduce sample heterogeneity and raise concerns about the appropriateness of extrapolating results to the pediatric FCCM population.

Characterization of pediatric FCCM is relevant for the prognostic assessment of affected children and the development of a more personalized risk–benefit assessment in this population in terms of treatment options, especially regarding potential new disease-modifying pharmacologic agents currently under investigation [24–26].

Our aim was to study the natural history of pediatric FCCM, with an emphasis on symptomatic hemorrhagic events and associated clinical, genetic, and imaging risk factors.

Material and methods

Population

We performed a multicenter retrospective cohort study involving four tertiary pediatric institutions including all consecutive subjects with a diagnosis of FCCM during childhood (≤ 18 years) evaluated at least once in the participating hospitals between January 2010 and September 2021, and with an initial brain MRI available for review at least including axial T1WI, T2WI, and GRE-type sequences (T2* and/or SWI). The diagnosis of FCCM was based on (1) the presence of ≥ 1 CCM associated with either a positive family history (defined as ≥ 1 known first or second-degree relative with a proven CM) and/or (2) a confirmed pathogenic variant in the *CCM1-3* genes in the affected patient or in a first-degree relative [27]. Exclusion criteria included (1) history of prior radiation, severe head trauma requiring hospitalization, extracorporeal membrane oxygenation support, intensive care unit stay, and/or anticoagulation therapy and (2) poor-quality or incomplete brain MR.

Genetic analysis

Details on genetic analysis are presented in the Online Supplemental Data.

MR technique and image analysis

Images were acquired with a 1.5 or a 3.0 Tesla MR scanner, using local protocols, in some subjects including administration of gadolinium-based contrast agents. For each subject, lesion counts were performed on the first brain MRI based on hemosiderin-sensitive sequences (T2* and/or SWI) and the anatomical location. They were assessed for Zabramski type as modified by Nikoubashman [13, 21] and size (corresponding to the largest diameter measured on axial T2WI) [21]. Lesions larger than 40 mm were classified as giant CCM, according to previous definitions [28]. Longitudinal studies were assessed whenever available and correlated with clinical indications, focusing on the appearance of new CCM (de novo lesions) and evidence of symptomatic hemorrhage, when present. CCM were labeled as de novo lesions if their new appearance could be shown on comparable or technically inferior consecutive studies while acute symptomatic hemorrhagic CCM (CASH) at either presentation and/or follow-up were identified according to previously published consensus guidelines [18]. These lesions were further evaluated in relation to their general morphology (uni/multilocular), as well as the presence of hemosiderin ring, perilesional vasogenic edema, T1 hyperintense perilesional sign

[29], fluid–fluid levels, and/or accompanying developmental venous anomalies (DVA). In cases with clinical symptoms and more than one CCM with signs of recent hemorrhage, the lesion located in the anatomical region corresponding to the neurological manifestations was considered. If the clinico-radiological correlation was uncertain or dubious, the largest hemorrhagic lesion was considered for evaluation.

At each center, images were first analyzed by one rater, blinded to the clinical and genetic information. One of the raters evaluated two sites, corresponding to a total of 3 readers (with 1, 7, and 7 years of experience in pediatric neuroradiology, respectively). Anonymized brain MR studies of all potentially CASH and of other CCM with questionable evaluation were decided by consensus.

Clinical data

Data on demographics, age at clinical presentation leading to the FCCM diagnosis and mode of presentation, ethnicity, family history (including the number of affected family elements and degree of kinship), genotype, presence of other systemic CM (including cutaneous, retinal, or within solid organs), or any combined systemic feature (including Greig cephalopolysyndactyly in the setting of a 7p deletion syndrome [30]) were obtained from medical records. The mode of the presentation was classified according to previously published reporting standards of CCM [18]. More specifically, symptomatic CCM hemorrhage was defined by the presence of acute or subacute onset symptoms (any of headache, epileptic seizure, impaired consciousness, or new/worsened focal neurological deficit referable to the anatomic location of the CM) accompanied by radiological evidence of recent extra- or intralesional hemorrhage. Other types of presentation included non-hemorrhagic epilepsy, non-hemorrhagic focal neurological deficit, non-hemorrhagic unspecific headaches, or asymptomatic forms (such as incidental finding or detection in the context of imaging screening due to family history of CCM). Follow-up data were obtained through routine visits in specialized outpatient clinics and by presentation in the emergency departments, including symptomatic events attributable to CCM according to current guidelines [18] after confirmation by multidisciplinary assessment. In addition, any neurosurgical interventions and final neurological outcomes (graded as normal, mild, moderate, or severe impairment) were also recorded.

Statistical analysis

Quantitative data were presented as median and interquartile range, and categorical data as frequencies and percentages. Fisher's exact test or Pearson's χ^2 test and Student's t-test or the Mann–Whitney test were used to compare categorical and continuous variables, respectively.

The prospective annual risk of hemorrhage was calculated as the number of hemorrhages during considered follow-up divided by person-years of follow-up during that time. Cumulative rates of symptomatic hemorrhage for the whole sample and stratified by baseline variables were calculated as the ratio between the number of symptomatic hemorrhagic events during follow-up and the number of patients initially at risk. Cumulative rates of symptomatic hemorrhage were also illustrated using the Kaplan–Meier method, and the curves were compared by the log-rank test. Survival analysis was applied to estimate the 1-year risk, 2-year risk, and 5-year risk of symptomatic hemorrhage with corresponding 95% confidence intervals (95CI). Univariable and multivariable Cox regression survival analyses were used to identify risk factors of longitudinal symptomatic hemorrhage during the follow-up period.

Data were excluded if subjects experienced bleeding or were lost to follow-up. Surgical removal of a lesion did not lead to exclusion if the patient had additional CCM(s) amenable to follow-up.

Statistical analyses were performed by using Stata, v14.0 (StataCorp, College Station, Texas). The significance level was set at $P = 0.05$ (2-sided).

Data availability statement

Any data not published within the article will be shared, in anonymized form, by request from any qualified investigator.

Results

Clinical and genetic data

Fifty-three children with FCCM from 49 families were identified, from which 12 patients (22.6%) were excluded due to non-available first brain MRI. Forty-one children from 38 unrelated families fulfilled the eligibility criteria and were therefore included. Clinical and genetic data are summarized in Table 1. Twenty-two individuals (53.7%) were male and 30 (73.2%) Caucasian. There was a family history in 29 (70.7%) children, with multiple kindred involved in 18 (63.1%). A genetic diagnosis in the affected individual or in a known first-degree relative was available in 30 (73.2%) children, with *CCM1*, *CCM2*, and *CCM3* loss-of-function variants identified in 17 (56.7%), 6 (20.0%), and 7 (23.3%), respectively. Out of the six subjects with *CCM2* abnormalities, five (83.3%) had a 7p deletion, including two cases with features of Greig cephalopolysyndactyly.

The median age at clinical presentation leading to subsequent FCCM diagnosis was 7.7 years (IQR = 9.2; range: 0.4–17.3). Fifteen (36.6%) individuals suffered a symptomatic CCM-related hemorrhage of the central nervous

Table 1 Demographic, genetic, clinical, and spine imaging data

	N=41
Male, *n* (%)	22 (53.7)
Age at initial clinical presentation in years, median (IQR)	7.7 (3.47–12.67) Range: 0.4–17.3
Genotype, *n* (%)	
CCM1	17 (41.5)
CCM2[a]	6 (14.6)
CCM3	7 (17.1)
CCM1-3 testing negative/not performed/pending	11 (26.8)
Positive family history, *n* (%)	29 (70.7)
No. of affected family members	
n=1	11 (37.9)
n=2	11 (37.9)
≥3	7 (24.1)
Ethnic origin, *n* (%)	
Caucasian	30 (73.2)
African	5 (12.2)
Asian	2 (4.9)
Hispanic	1 (2.4)
Other	3 (7.2)
Presentation mode, *n* (%)	
Symptomatic hemorrhage of the CNS[b]	15 (36.6)
Non-hemorrhagic seizures	10 (24.4)
Incidental diagnosis	6 (14.6)
Imaging screening	4 (17.1)
Headache	3 (7.2)
≥1 extra-CNS CM, *n* (%)	2 (4.9)
≥1 spinal cord CM, *n* (%)	3 (13.6) [c]
≥1 brain surgery, *n* (%)	19 (46.3)
Number of neurosurgical procedures	
n=1	17 (89.5)
n=2	2 (10.5)
Neurological assessment at last clinical FU, *n* (%)	
Normal	29 (70.7)
Mild impairment	3 (73)
Moderate impairment	6 (14.6)
Severe impairment	2 (4.9)
Death	1 (2.4)
Seizures at last clinical FU, *n* (%)	12 (29.3)
Medically controlled	10 (83.3)
Medically refractory	2 (16.7)

Legend: *CM*, cavernous malformation; *CNS*, central nervous system; *FU*, follow-up; *IQR*, interquartile range; *SD*, standard deviation

[a]Includes 4 cases with a 7p deletion; [b]1 case due to a SCCM-related hemorrhage, [c]22/41 subjects (53.7%) underwent at least one whole-spine MR

system at presentation, intracranial in 14 (93.3%) cases, and involving the spinal cord in one (6.7%).

The median observational period was 54.3 months (IQR: 65.0; range: 4.0–205.4). All subjects except one ($n=40$, 97.6%) had more than 6 months of clinical follow-up. During extended, retrospective longitudinal evaluation, 19 (46.3%) subjects underwent at least one CCM-related brain surgery (total of 21 CCM-excisional procedures), with complete removal in 17 (81.0%) and subtotal removal in 4 (19.1%) lesions. Eighteen (94.7%) surgeries were within the first 5 years after diagnosis. No spinal surgeries were performed. The mean age at first

surgery was 9.1 (SD = 5.2; range: 0.9–17.2). Overall, 11 out of 19 (52.4%) procedures were performed due to a CCM-related symptomatic hemorrhage. Other surgical indications included progressive CCM growth with or without asymptomatic hemorrhage ($n = 3$, 14.3%), medically refractory seizures related to a surgically accessible lesion ($n = 5$, 23.8%), and a giant CCM ($n = 2$, 9.5%). Children undergoing more than 1 surgical CCM removal had a significantly higher rate of symptomatic hemorrhage at presentation ($P = 0.047$) and a significantly lower number of CCM on the first brain MRI ($P = 0.0204$) when compared to those receiving conservative treatment. Otherwise, there were no statistically significant differences between groups regarding other studied demographic, clinical, and brain imaging variables (Supplemental Table 1).

At their last clinical visit, 29 (70.7%) children remained neurologically intact, while 11 (26.8%) demonstrated some type of neurological impairment. One (2.4%) child died during the follow-up due to sudden-unexpected death in the context of severe medically refractory epilepsy. Within the subgroup with mild to severe neurological impairment, $n = 5$ (45.5%) subjects had ≥ 1 previous symptomatic hemorrhagic event, $n = 1$ (9%) presented refractory epileptic encephalopathy, and $n = 2$ (18.2%) showed Greig cephalopolysyndactyly–related developmental delay.

Brain MR and CCM

Details on neuroimaging studies and protocols are presented in the Online Supplemental Data. At first brain MRI, a total of $n = 587$ CCM were identified on T2* and/or SWI sequences and their neuroimaging features are reported in Table 2. All children except one (97.6%) demonstrated multiple CCM (median number per child = 10.0; IQR = 12; range: 1–80) at diagnosis. CCM3-affected individuals tended to show a higher median total number of CCM (12.0 vs 7.0, $P = 0.147$) as well as a higher median number of CCM in the posterior fossa (2.4 vs 1.5, $P = 0.980$) and brainstem (1.0 vs 0.7, $P = 0.800$) in their first available brain MRI when compared with subjects with other known genotypes, although not statistically significant.

Longitudinal brain MRs were available in 38 (92.7%) subjects, either performed as a scheduled examination or in the emergency setting due to new neurological events, with a median follow-up brain MRI time of 49.6 months (IQR = 68.6; range: 3.6–129.1). Fifteen (39.5%) developed at least 1 de novo CCM (median lesions per patient = 4.5; range: 1–16), for a total of 86 new lesions identified in 180.36 person-years of brain MRI follow-up, yielding an annual new lesion rate of 47.7%.

Table 2 Imaging features of CCM detected at first brain MRI and with symptomatic hemorrhage identified at diagnosis and follow-up

CCM identified at first brain MRI $n = 587$	
Location, *n* (%)	
Cerebral lobes	492 (83.8)
Nucleocapsular/Thalamic	23 (3.9)
Brainstem	27 (4.6)
Cerebellum	39 (6.6)
Intra-ventricular	6 (1.0)
Modified Zabramski type, *n* (%)	
I	20 (3.4)
II	116 (19.8)
III	79 (13.5)
IV	362 (61.7)
V	10 (1.7)
Size in mm (except type IV CCM), median (IQR)	7.0 (1–52)
Giant lesions	5 (0.9)
CASH identified at diagnosis and follow-up $n = 23$	
Location, *n* (%)	
Cerebral lobes	14 (61.0)
Nucleocapsular/thalamic	1 (4.4)
Brainstem	5 (21.7)
Cerebellum	2 (8.7)
Spinal cord	1 (4.4)
Modified Zabramski type, *n* (%)	
I	6 (26.1)
V	17 (73.9)
Size in mm, median (IQR; range)	27 (25;8–52)
Multilocular morphology, *n* (%)	12 (52.2)
Hemossiderin ring, *n* (%)	15 (65.2)
Fluid–fluid levels, *n* (%)	13 (56.5)
T1 hyperintense perilesional sign, *n* (%)	15 (65.2)
Perilesional edema, *n* (%)	16 (69.6)
Associated DVA	0 (0.0)

Legend: *CASH*, cavernous angioma with symptomatic hemorrhage; *DVA*, developmental venous anomaly; *FU*, follow-up; *IQR*, interquartile range

Spine MR and CM

Twenty-three (56.1%) of the subjects had at least one available whole-spine MR for review (total = 44 studies performed). The mean age at the first available spine MR was 8.0 years (IQR = 5.0; range: 0.8–16.8 years). Retrospective longitudinal spine MR was additionally available in 11/23 (47.8%) of the cases (range: 2–7), with a median follow-up spine MR time of 39.5 months (range: 3–123.8). A total of $n = 4$ spinal CM were detected in three different patients (13%), one of them appearing de novo. Except for the single case presenting with a spine-related CASH that

was previously described, the remaining spinal CM were asymptomatic.

CASH lesions

Imaging details of CASH lesions ($n=23$), identified either at clinical presentation ($n=15$) or during follow-up ($n=8$), are also presented in Table 2 and some examples are illustrated in Fig. 1. Briefly, CASH were more commonly cerebral ($n=14$, 61.0%), multilocular ($n=12$, 52.2%), and had fluid–fluid levels ($n=13$, 56.5%), hemosiderin ring ($n=15$, 65.2%), perilesional edema ($n=17$, 73.9%), and/or the T1-hyperintensity sign ($n=15$, 65.2%). In no case, an associated DVA was found. Out of the eight CASH identified during retrospective longitudinal evaluation, 3 were caused by re-hemorrhage of a previous CASH, another 3 corresponded to a first symptomatic hemorrhagic event in known CCM, and 2 were in de novo CCM.

Annual prospective symptomatic cerebral hemorrhage rates

In the 5-year follow-up, seven symptomatic hemorrhagic events occurred during 140.5 person-years, corresponding to a 5-year annual prospective symptomatic hemorrhagic rate of 5.0% (95% CI: 2.4–10.5). Other stratified hemorrhage risks per year per patient within this period are presented in Table 3.

In the maximum available follow-up time, one additional symptomatic event occurred, leading to a total of eight of such events occurring during 200.2 person-years and yielding an overall annual symptomatic hemorrhage rate of 4.0% (95% CI: 2.0–8.0) per person-year. The median time until

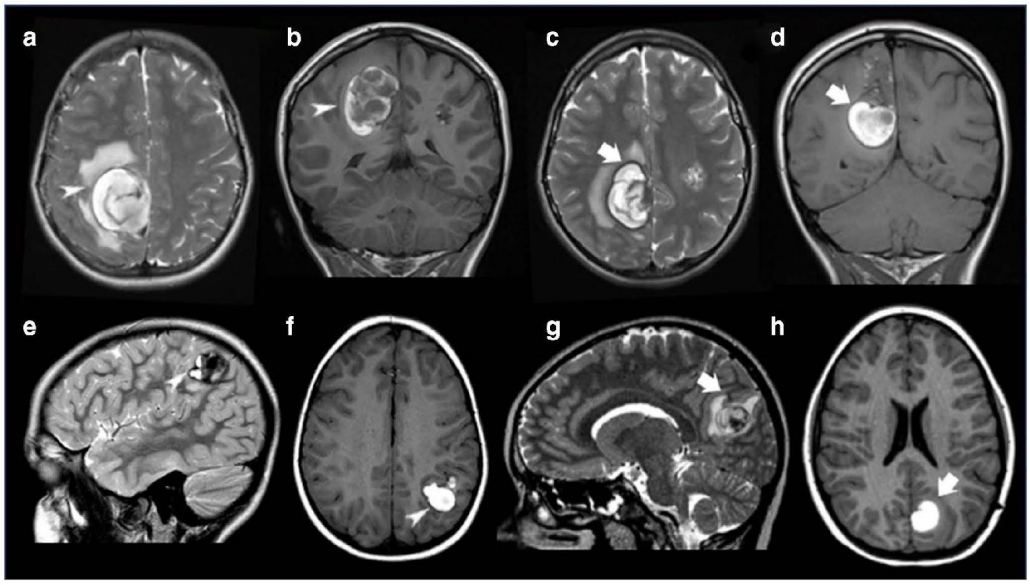

Fig. 1 Examples of symptomatic hemorrhagic brain cavernous malformations. Brain MR (**a**, **b**) performed in the emergency setting in a 15-year-old girl with familial cerebral cavernous malformation syndrome due to a proven CCM1 mutation including axial T2 TSE (**a**) and coronal T1 SE (**b**) demonstrates an acute right parietal symptomatic hemorrhagic cerebral cavernous malformation (white arrowheads) with multiloculate appearance and complete hemosiderin ring as well as surrounding edema. No surgical treatment was performed. Follow-up brain MR of the same patient (**c**, **d**) performed after 22 months due to development of new acute neurological symptoms, including axial T2 TSE (**c**) and coronal T1SE (**d**), reveals symptomatic re-hemorrhage of the same cavernous malformation (white arrows), that was subsequently resected. Brain MR (**e**, **f**) performed in the emergency setting in a 7-year-old boy with familial cerebral cavernous malformation syndrome due to a proven CCM1 mutation including sagittal T2 TSE (**e**) and axial T1 SE (**f**) demonstrates an acute left parietal symptomatic hemorrhagic cerebral cavernous malformation (white arrowheads) with multiloculate appearance, complete hemosiderin ring, fluid–fluid levels and a small component of surrounding edema. This lesion was surgically removed with complete resection. Follow-up brain MR (**g**, **h**) performed after 50 months due to development of new acute neurological symptoms, including change to sagittal T2 TSE (**g**) and axial T1SE (**h**), shows a de novo cavernous malformation with signs of acute hemorrhage (white arrows), that was also subsequently resected

Table 3 Hemorrhage risk per year per patient during 5-year follow-up

Variable	Total person-years	No. of symptomatic hemorrhagic events	Incidence rate (95% CI)
Gender			
Male	82.7	4	4.8 (1.8–14.5)
Female	57.9	3	5.2 (1.7–16.1)
Ethnic origin			
Caucasian	108.9	6	5.5 (2.5–12.3)
Non-Caucasian	31.6	1	3.2 (0.5–22.5)
Age at presentation			
< 6 years	53.1	2	3.8 (1.0–15.1)
≥ 7 years	87.4	5	5.7 (2.4–13.7)
Positive family history			
Yes	93.1	6	6.4 (2.9–15.8)
No	47.4	1	2.1 (0.3–14.3)
Genotype			
CCM1	53.1	3	5.7 (1.8–17.5)
CCM2	16.3	2	12.3 (3.1–49.0)
CCM3	25.8	1	3.9 (0.6–27.5)
Presentation mode			
Symptomatic hemorrhage	49.2	5	10.2 (4.2–24.4)
Other types of presentation	91.3	2	2.2 (0.6–8.8)
≥ 1 extra-CNS CM			
Yes	9.2	1	10.9 (1.5–77.4)
No	131.4	6	5.0 (2.4–10.5)
≥ 10 CCM in the first brain MRI			
Yes	73.99	3	4.06 (1.31–12.57)
No	66.53	4	6.01 (2.26–16.02)
≥ 1 CCM in the brainstem			
Yes	44.36	4	9.02 (3.39–24.03)
No	96.17	3	3.12 (1.01–9.6)
≥ 1 CCM in the posterior fossa in the first brain MRI			
Yes	86.33	6	6.95 (3.12–15.47)
No	54.19	1	1.8 (0.26–13.10)
≥ 1 Zabramski type II CCM in the first brain MRI			
Yes	105.95	5	5.79 (1.45–23.13)
No	34.57	2	4.72 (1.96–11.34)

Legend: *CM*, cavernous malformation; *CCM*, cerebral cavernous malformation; *CNS*, central nervous system; *CI*, confidence interval

the first prospective symptomatic hemorrhagic event during extended follow-up was 18.5 months (IQR = 31.3; range: 0.03–97.9).

Cumulative risks of prospective hemorrhage

The cumulative risk of symptomatic hemorrhage was 7.3% (1.5–20.0) at 1 year, 14.6% (5.6–29.2) at 2 years, and 17.1% (7.1–31.2) at 5 years. The 5-year cumulative risk was higher in subjects with symptomatic hemorrhage at presentation (33.3%), *CCM2* genotype (33.3%), presence of at least one CCM in the brainstem at first brain MRI (26.7%), and positive family history (20.7%). Other stratified cumulative risks of hemorrhage at 5 years of follow-up are summarized in Table 4.

A tendency towards a higher cumulative risk of symptomatic hemorrhage at 5 years of follow-up was observed in children presenting with prior symptomatic hemorrhage, with a borderline statistical significance ($P = 0.0559$) (Fig. 2).

Predictors of symptomatic hemorrhage at presentation

In both uni- and multivariable analysis, none of the studied variables resulted in a significant independent predictor

Table 4 Cumulative risk of symptomatic hemorrhage at 5 year follow-up of the 41 subjects stratified by clinical and genetic characteristics

Variable	*n*	No. of symptomatic hemorrhagic events during 5-year follow-up	5-year risk (95% CI)
Gender			
Male	22	4	18.2 (5.2–40.3)
Female	19	3	15.8 (3.4–39.6)
Ethnic origin			
Caucasian	30	6	20.0 (7.7–38.6)
Other	11	1	10.0 (2.3–41.3)
Age at presentation			
< 6 years	27	2	14.3 (1.8–42.8)
≥ 7 years	14	5	18.5 (7.8–39.7)
Positive family history			
Yes	29	6	20.7 (8.0–39.7)
No	12	1	8.3 (2.1–38.5)
Genotype			
CCM1	17	3	17.6 (3.8–43.4)
CCM2	6	2	33.3 (4.3–77.7)
CCM3	6	1	14.3 (0.4–64.1)
Presentation mode			
Symptomatic hemorrhage	15	5	33.3 (11.8–61.7)
No hemorrhage	26	2	7.7 (1.0–25.1)
≥ 1 extra-CNS CM			
Yes	2	1	50.0 (1.3–98.7)
No	39	6	15.4 (5.9–30.5)
≥ 10 CCM at first brain MRI			
Yes	21	3	14.29 (3.05– 36.34)
No	20	4	20.00 (5.73–43.66)
≥ 1 CCM in the brainstem at first brain MRI			
Yes	15	4	26.66 (7.79–55.1)
No	26	3	11.54 (2.45–30.15)
≥ 1 CCM in the posterior fossa at first brain MRI			
Yes	26	6	23.08 (8.97–43.65)
No	15	1	6.67 (1.68–31.95)
≥ 1 Zabramski type II CCM at first brain MRI			
Yes	31	5	16.13 (5.45–33.73)
No	10	2	20.0 (2.52–55.61)

Legend: *CM*, cavernous malformation; *CCM*, cerebral cavernous malformation; *CNS*, central nervous system; *CI*, confidence interval

of symptomatic hemorrhagic presentation (Supplemental Table 2).

Predictors of symptomatic hemorrhage at follow-up

In univariable analysis, the total number of CCM located in the brainstem (hazard ratio [HR] = 1.63, $P = 0.003$) and the total number of CCM located in the posterior fossa (HR = 1.37, $P = 0.005$) at the first brain MRI were significant risk factors of subsequent symptomatic hemorrhage at 5 years of follow-up. Multivariable analysis after adjusting for age at presentation and sex confirmed these variables as independent predictors of future symptomatic hemorrhage during that period (adjusted HR = 1.64 and 1.39 with $P = 0.004$ and 0.005, respectively). The symptomatic hemorrhagic presentation also showed a trend towards an increased risk for subsequent symptomatic hemorrhagic events when compared to other forms of presentation in both univariable and multivariable analysis, although without reaching statistical significance (adjusted HR = 4.33 and HR = 4.35, $P = 0.008$ and 0.08, respectively) (Table 5).

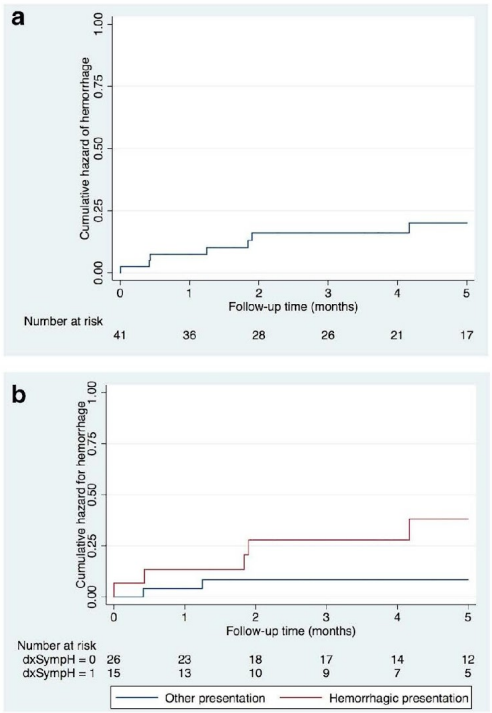

Fig. 2 Cumulative hazard curves of hemorrhage of 41 children during 5-year follow-up for the entire cohort (**A**) and stratified by initial presentation of hemorrhage or other type of presentation (**B**)

Discussion

In this multicenter study evaluating the natural history of pediatric FCCM in 41 children with a confirmed diagnosis of FCCM and incorporating standard definitions of symptomatic hemorrhage, we found that the 1-, 2-, and 5-year cumulative risks of hemorrhage were 7.3%, 14.6%, and 17.1%, respectively.

It has been previously described for the general population that the probability of symptomatic hemorrhage in CCM increases over time in the general population, especially during the first 2 years after hemorrhagic presentation, a phenomenon known as "temporal clustering" [8, 11, 12, 31]. This finding was also demonstrated in a pediatric cohort study involving children with different CCM subtypes [23] and confirmed in our cohort, including a homogeneous sample of children with FCCM. Indeed, our results show that although the cumulative risks of symptomatic hemorrhage increase over time in affected patients, they grow much faster in the first 2 years after the presentation of the disease (14.6% at 2 years vs 17.1% at 5 years after presentation). The transversality of temporal clustering suggests that it occurs irrespectively of age at presentation or CCM subtype.

We have also demonstrated that the annual symptomatic hemorrhage rate for our entire cohort at 5-year follow-up after diagnosis was 5.0% per person-year. When compared to the cumulative risk value previously presented, the annual symptomatic hemorrhage rate is a more robust measure, as it takes into account losses to follow-up and when events occur, although its interpretation is less intuitive. The influence of age at presentation and familial subtype in the natural history of subjects with one or multiple CCM remains unclear. Indeed, some authors have reported an increased symptomatic bleeding rate in children with CCM when compared to adults [19], while others have not [20, 23]. Moreover, the familial disease has also been linked to an increased symptomatic hemorrhagic risk [16] in the majority of, but not all [21], published studies. These divergent results are justified, at least in part, by methodological differences between the studies, including distinct sample sizes and eligibility criteria, variable proportions of CCM subtypes (familial vs sporadic), modes of presentation (hemorrhagic vs non-hemorrhagic), inconsistent methods of risk calculation (lifetime vs prospective approaches), and heterogenous definitions of hemorrhage [21, 27]. Our results support similar 5-year annual and cumulative symptomatic hemorrhagic risks in pediatric FCCM subjects treated surgically based on clinical judgement in tertiary centers, compared to children and adults with all types of CCM. These findings are in line with the most recent studies on this topic [23, 32]. However, the comparison of results between adult and pediatric cohorts should be made with caution. Indeed, mild symptomatic CCM-related neurologic events may be more commonly missed at young ages, especially if neurological manifestations were transient, insidious, or non-specific, as more frequently occurs in this age group [33]. Additionally, the threshold for a given CCM to become clinically symptomatic in pediatric patients may be higher than for adults, due to pediatric immaturity and/or increased cerebral plasticity of children [34]. This theory can be supported by the fact that the median size of CCM at presentation in children tends to be larger than in adults [28]. In addition, giant CCM are also more commonly found in children [28, 35] and both findings are corroborated by our results. Although giant CCM have primarily been described in sporadic patients, they can also occur in FCCM, as seen in five of our cases and previously reported by Ozgen et al. [28].

Another factor that may have influenced our results is the overall high rate of surgical treatment in our cohort (46%) when compared with other familial and/or pediatric CCM studies (up to 37.2%) [19, 20, 23, 32]. There are currently no

Table 5 Demographic and radiological risk factors of subsequent symptomatic hemorrhage at 5-year follow-up after initial diagnosis

Variable	Univariable analysis		Multivariable analysis[a]	
	Unadjusted HR (95% CI)	*P* value	Adjusted HR (95% CI)	*P* value
Male gender	1.00 (0.22–4.49)	1.00	0.99 (0.22–4.47)	0.99
Age at presentation, in years	1.02 (0.88–1.10)	0.82	1.02 (0.88–1.18)	0.82
Symptomatic hemorrhagic presentation	4.33 (0.84–22.3)	0.08	4.35 (0.84–22.50)	0.08
Positive family history	2.87 (0.35–23.88)	0.28	2.93 (0.35–24.50)	0.32
Genotype				
CCM1	Reference			
CCM2	2.25 (0.38–3.93)	0.38	2.97 (0.42–20.87)	0.27
CCM3	0.734 (0.08–7.07)	0.79	0.67 (0.07–6.71)	0.73
Presence of extra-CNS CM	2.51 (0.30–20.99)	0.40	2.70 (0.25–29.68)	0.84
Caucasian ethnicity	1.92 (0.23–15.00)	0.55	1.93 (0.23–16.28)	0.54
No. of CCM at first brain MRI	1.02 (0.98–1.06)	0.29	1.02 (0.98–1.06)	0.26
≥ 10 CCM at first brain MRI	0.489 (1.12–1.78)	0.28	0.98 (0.35–2.77)	0.97
No. of CCM in the post fossa at first brain MRI	1.37 (1.10–1.71)	0.005*	1.39 (1.10–1.76)	0.005*
≥ 1 CCM in the posterior fossa at first brain MRI	3.59 (0.33–4.74)	0.74	4.05 (0.45–36.37)	0.21
No. of brainstem CCM at first brain MRI	1.63 (1.18–2.26)	0.003*	1.64 (1.18–2.31)	0.004*
≥ 1 CCM in the brainstem at first brain MRI	2.67 (0.60–11.97)	1.00	2.77 (5.91–12.98)	0.20
No. of Zabramski type II CCM at first brain MRI	1.06 (0.99–1.14)	0.12	1.07 (0.98–1.16)	0.12
≥ 1 Zabramski type II CCM at first brain MRI	0.81 (0.16–4.18)	0.80	0.76 (0.14–4.16)	0.75
≥ 1 de novo CCM at follow-up brain MRI	1.00 (0.22–4.48)	0.99	1.02 (0.87.1.19)	0.82
No. of de novo CCM at follow-up brain MRI	0.95 (0.76–1.19)	0.67	0.95 (0.75–1.20)	0.66

Legend: *CM*, cavernous malformation; *CCM*, cerebral cavernous malformation; *CI*, confidence interval; *CNS*, central nervous system; *FU*, follow-up; *HR*, hazard ratio; *IQR*, interquartile range

[a]Adjusted for age at presentation and gender

*Statistically significant value

standard treatment guidelines specific for pediatric FCCM and indications for surgical treatment of accessible lesions remain personalized and dependent upon multiple factors, including the individual surgeon's practice standards, patient's insurance, family preference, presentation mode and type, and severity of clinical manifestations at follow-up. The more aggressive approach followed in our referral tertiary pediatric hospitals likely reflects the high surgical training, volume, and expertise available in our centers, and likely contributed to fewer prospective symptomatic hemorrhagic events during follow-up. Planned surgical removal of CCM suspected of high-hemorrhagic risk (namely lesions with dynamic asymptomatic progressive changes detected on routine follow-up imaging or large size) was performed in some of our cases and likely positively modified the natural history of this disease.

The percentage of children in our cohort presenting with symptomatic hemorrhage is lower than reported in most previously published series including subjects with variable ages [15, 16, 20, 22, 23, 32]. This is probably due to the high rate of known positive family history of CCM in our cohort, leading to a higher index of suspicion in cases of mild or non-specific complaints, such as headaches, and/or screening brain MRIs in asymptomatic subjects. As prior symptomatic hemorrhage has been described by most authors as an independent risk factor for future symptomatic hemorrhagic events [8, 11, 12, 22, 23], the intrinsic baseline characteristics of our subjects may have led to our underestimation of the prospective hemorrhagic rates/cumulative risks. We also found that symptomatic hemorrhage at presentation rises the annual hemorrhagic rate and the 5-year cumulative risk of symptomatic hemorrhagic events of affected subjects when compared with other forms of presentation, although not reaching statistical significance as a predictor variable, most likely due to the sample size.

In our study, children with pathogenic loss-of-function variants in the *CCM2* gene also demonstrated higher annual hemorrhagic rates and 5-year cumulative risk of symptomatic hemorrhage when compared with subjects with *CCM1* or *CCM3* genetic variants. This association lacked statistical significance and therefore we cannot exclude that these results are due to chance, especially in the setting of the small number of subjects in our cohort harboring CCM2 genetic variants. All three *CCM1-3* genes encode components of a heterotrimeric CCM protein complex involved in endothelial stabilization but each of

them has additional cellular functions. More specifically, CCM2 encodes malcavernin that acts as bridge allowing interaction between the other two CCM proteins and also influences β-catenin and Wnt signaling, causing MEKK3 inhibition and promotion of RhoA degradation [4]. Although few studies have specifically focused on *CCM2*-related disease, this genetic form has been so far considered a milder form of FCCM [36]. Instead, previous case series have described a more aggressive clinical course in patients who were carriers of *CCM3* variants [36–39] when compared with patients with other FCCM genotypes, although this feature has not been confirmed by all authors [40]. In our cohort, although the total number of CCM, posterior fossa CCM, and brainstem CCM was indeed higher in patients with CCM3 variants, differences did not reach statistical significance. In addition, the proportion of our subjects with symptomatic hemorrhagic presentation and moderate to severe neurological deficit at last follow-up or death was lower in CCM3 than in other FCCM disease-causing genes; however, also without statistical significance. To the best of our knowledge, no natural history study of FCCM comparing different genotypes has been previously published. Notably, 5/6 cases with variants of CCM2 had no single nucleotide variants but deletions of variable size that can also encompass additional flanking genes, including *GLI3*, leading to two cases of Greig cephalopolysyndactyly syndrome [30, 41]. This might have contributed to the disease phenotype and eventually influenced the longitudinal evolution of CCM in our cohort. The role of each gene in the natural history and long-term outcome of subjects with FCCM should be therefore further investigated in larger samples.

Our results also show that the first brain MRI can provide important information that can aid in the prognostication of future symptomatic hemorrhagic events in children with pediatric FCCM. Indeed, both the number of brainstem CCM and posterior fossa CCM at first brain MRI were significant independent predictors of prospective symptomatic hemorrhage events in our study. In contrast, the total number of CCM and the total number of Zabramsky type II lesions (either as continuous or dichotomized variables) played no significant role. These findings are in line with previous studies (including a meta-analysis) indicating that brainstem CCM location has an increased risk of symptomatic hemorrhage [8, 11, 12, 21]. However, it remains unclear whether brainstem CCM are intrinsically more prone to bleed or if there is an overestimation of the real hemorrhagic rate of CCM in this eloquent region [21]. Aiming to clarify this question, we believe that current reporting standards of hemorrhage from CCM [18] should be reviewed, recommending individualized reporting of both symptomatic and asymptomatic hemorrhage rates per patient and per lesion in future studies.

Differently from previous reports [23, 42], we could not find significant independent predictors of symptomatic hemorrhagic presentation in our cohort, most likely due to the sample size.

As expected in FCCM, the vast majority of our subjects had multiple CCM lesions at first brain MRI, even when the exam was performed during early infancy. A recent report has shown that CCM may even be detected in utero in familial cases using fetal MRI [43]. However, it is important to bear in mind that even isolated CCM lesions in children may be familial, as seen in one of our cases. In line with previous studies [16, 17, 27, 44], we have also detected the imaging appearance of new CCM over time (reaching an 8.3% annual rate per patient-year) and some of these de novo CCM were responsible for symptomatic hemorrhagic events. This dynamic activity is consistently higher in familial cases when compared to sporadic ones [16, 17, 27, 44]. Nevertheless, direct comparison between studies concerning the rate of development of new lesions is hampered by methodological differences, as reviewed in a recent meta-analysis by Taslimi et al. [27].

CASH lesions in our cohort were overall more commonly located supratentorially (probably due to the high supratentorial/infratentorial ratio of lesion counts) and their median size was larger than the median size of all CCM (excluding type IV lesions). These usually demonstrated a hemosiderin ring and extracapsular hemorrhagic extension with associated vasogenic edema as well as imaging features commonly described in large-size/giant CCM, namely multilobulated morphology and internal fluid levels [28]. In addition, the majority but not all CASH exhibited the T1 hyperintense perilesional signal, an imaging feature with moderate sensitivity and high sensitivity for the diagnosis of hemorrhagic CCM [29]. Nevertheless, it is important to be aware that this imaging sign may also be evident in other lesions, such as melanoma and other hemorrhagic metastasis [45].

Based on the results of this study as well as other recently published papers focusing on FCCM in children, adults, and/or mixed populations, we suggest that patients with suspected and/or confirmed FCCM should be imaged at the best available MR scanner (ideally in a 3.0 Tesla unit) with standard imaging technique [9, 46–48]. The brain MR protocol should include a T1 3D sequence, axial and coronal T2WI, axial or 3D FLAIR, and at least one GRE sequence, preferably SWI [46, 47] Whole-spine MR should be additionally performed at diagnosis regardless of the presentation age as a screening modality, including a T1 TSE, a T2 TSE, and at least one GRE sequence, ideally a 3D T2 Multi-Echo Data Image Combination (MEDIC) [9, 48] Serial spine MR imaging with a similar protocol should be also considered even in patients with initially negative spine MR studies.

Our study has some limitations, including its retrospective design and tertiary center referral bias. In addition, our cohort was also predominantly composed of Caucasian subjects, which may limit generalizability to subjects with other ethnic

backgrounds, including the commonly reported Hispanic FCCM population. As guidelines for brain imaging in pediatric FCCM are currently not well defined [2], subjects were imaged over time at inconsistent time points and without standard MR techniques (including variations in the MR scanner magnetic field strength and/or the protocol). This may have limited the imaging assessment, since the identification of CCM is strongly dependent on technical parameters. Moreover, due to the retrospective nature of the study, we have not evaluated advanced imaging techniques such as perfusion and permeability MR that have been recently described as biomarkers of CCM activity and predictors of lesional growth and hemorrhage [49–51]. Another possible limitation of our results includes the 39% rate of loss to follow-up at 5 years that occurred mainly due to adult care transferal. Finally, the number of bleeding events was rather low during follow-up, limiting the number of possible variables and increasing the 95% CI in the Cox proportion regression analysis model. Nevertheless, to the best of our knowledge, this is a natural history study conducted in the largest pediatric FCCM cohort reported to date, including a comprehensive clinical, genetic, and imaging evaluation. More specifically, when compared with the recent paper by Santos et al. [23], our study includes a larger number of patients with pediatric FCCM (41 vs 35) and provides a better clinical characterization of the cohort as well detailed neuroimaging assessment of their CCM, with special emphasis on de novo CCM and symptomatic hemorrhagic lesions. In addition, and contrarily to the paper by Santos et al. [23], we specify the pathogenic variants of all subjects with genetic FCCM confirmation and evaluate the relationship between the genetic subtypes of FCCM and the prospective symptomatic hemorrhagic events.

Conclusions

Pediatric FCCM seem to have an overall similar 5-year annual and cumulative symptomatic hemorrhagic risks in subjects treated according to clinical judgement (including medical and/or surgical approach) compared to children with sporadic CCM and adults with either familial or sporadic disease. In addition, children with FCCM can be stratified to predict longitudinal symptomatic hemorrhage risks according to baseline clinical and imaging features, allowing a differentiated treatment strategy. Future prospective multicenter studies in pediatric FCCM using standardized MR performed at fixed time points and including advanced neuroimaging techniques and genetic investigation would be advisable to increase our current knowledge and test new predictors of both symptomatic and asymptomatic hemorrhagic events as well as the overall neurological outcome.

Supplementary Information The online version contains supplementary material available at https://doi.org/10.1007/s00234-022-03056-y.

Author contribution Study concept and design: AFG, SR, MSS; acquisition of data: AFG, CAPFA, AL, DT, MP, PM, MS, VC, AR, ESS, KM; drafting of the manuscript: AFG; statistical analysis: AFG, DA; critical revision of the manuscript for important intellectual content: CAPFA, AL, DT, JG, SR, MP, PM, MS, VC, AR, ESS, KM, RV; study supervision: SR, MSS. All authors read and approved the final manuscript.

Funding Open access funding provided by Università degli Studi di Genova within the CRUI-CARE Agreement. Twelve-month research fellowship in diagnostic neuroradiology, European Society of Neuroradiology (AF Geraldo).

Declarations

Conflict of interest The authors declare no competing interests.

Ethics approval This study was conducted according to the 1964 Declaration of Helsinki and its amendments and approved by the local Ethical Committee that waived written informed consent due to the retrospective nature.

Informed consent Written informed consent was waived due to the retrospective nature of the study.

References

1. Zafar A, Quadri SA, Farooqui M et al (2019) Familial cerebral cavernous malformations. Stroke 50:1294–1301
2. Akers A, Al-Shahi Salman R, Awad IA et al (2017) Synopsis of guidelines for the clinical management of cerebral cavernous malformations: consensus recommendations based on systematic literature review by the angioma alliance scientific advisory board clinical experts panel. Neurosurgery 80:665–680
3. Boulouis G, Blauwblomme T, Hak JF et al (2019) Nontraumatic pediatric intracerebral hemorrhage. Stroke 50:3654–3661
4. Riolo G, Ricci C, Battistini S (2021) Molecular genetic features of cerebral cavernous malformations (CCM) patients: an overall view from genes to endothelial cells. Cells 10:704
5. Ren AA, Snellings DA, Su YS et al (2021) PIK3CA and CCM mutations fuel cavernomas through a cancer-like mechanism. Nature 594:271–276
6. Hong T, Xiao X, Ren J et al (2021) Somatic MAP3K3 and PIK3CA mutations in sporadic cerebral and spinal cord cavernous malformations. Brain 144:2648–2658
7. Peyre M, Miyagishima D, Bielle F et al (2021) Somatic PIK3CA mutations in sporadic cerebral cavernous malformations. N Engl J Med 385:996–1004
8. Taslimi S, Modabbernia A, Amin-Hanjani S et al (2016) Natural history of cavernous malformation. Neurology 86:1984–1991

9. Mabray MC, Starcevich J, Hallstrom J et al (2020) High prevalence of spinal cord cavernous malformations in the familial cerebral cavernous malformations type 1 cohort. AJNR Am J Neuroradiol 41:1126–1130
10. Manole AK, Forrester VJ, Zlotoff BJ et al (2020) Cutaneous findings of familial cerebral cavernous malformation syndrome due to the common Hispanic mutation. Am J Med Genet A 182:1066–1072
11. Al-Shahi Salman R, Hall JM, Horne MA et al (2012) Untreated clinical course of cerebral cavernous malformations: a prospective, population-based cohort study. Lancet Neurol 11:217–224
12. Horne MA, Flemming KD, Su IC et al (2016) Clinical course of untreated cerebral cavernous malformations: a meta-analysis of individual patient data. Lancet Neurol 15:166–173
13. Zabramski JM, Wascher TM, Spetzler RF et al (1994) The natural history of familial cavernous malformations: results of an ongoing study. J Neurosurg 80:422–432
14. Labauge P, Laberge S, Brunereau L et al (1998) Hereditary cerebral cavernous angiomas: clinical and genetic features in 57 French families. Lancet 352:1892–1897
15. Brunereau L, Labauge P, Tournier-Lasserve E et al (2000) Familial form of intracranial cavernous angioma: MR imaging findings in 51 families. Radiology 214:209–216
16. Labauge P, Brunereau L, Lévy C et al (2000) The natural history of familial cerebral cavernomas: a retrospective MRI study of 40 patients. Neuroradiology 42:327–332
17. Brunereau L, Levy C, Laberge S et al (2000) De novo lesions in familial form of cerebral cavernous malformations: clinical and MR features in 29 non-Hispanic families. Surg Neurol 53:475–483
18. Al-Shahi Salman R, Berg MJ, Morrison L et al (2008) Hemorrhage from cavernous malformations of the brain: definition and reporting standards. Stroke 39:3222–3230
19. Acciarri N, Galassi E, Giulioni M et al (2009) Cavernous malformations of the central nervous system in the pediatric age group. Pediatr Neurosurg 45:81–104
20. Al-Holou WN, O'Lynnger TM, Pandey AS et al (2012) Natural history and imaging prevalence of cavernous malformations in children and young adults. Clinical article. J Neurosurg Pediatr 9:198–205
21. Nikoubashman O, Di Rocco F, Davagnanam I et al (2015) Prospective hemorrhage rates of cerebral cavernous malformations in children and adolescents based on MRI appearance. AJNR Am J Neuroradiol 36:2177–2183
22. Gross BA, Du R, Orbach DB et al (2016) The natural history of cerebral cavernous malformations in children. J Neurosurg Pediatr 17:123–128
23. Santos AN, Rauschenbach L, Saban D et al (2022) Natural course of cerebral cavernous malformations in children: a five-year follow-up study. Stroke 53:817–824
24. Polster SP, Stadnik A, Akers AL et al (2019) Atorvastatin treatment of cavernous angiomas with symptomatic hemorrhage exploratory proof of concept (AT CASH EPOC) Trial. Neurosurgery 85:843–853
25. Shenkar R, Peiper A, Pardo H et al (2019) Rho kinase inhibition blunts lesion development and hemorrhage in murine models of aggressive Pdcd10/Ccm3 disease. Stroke 50:738–744
26. Lanfranconi S, Scola E, Bertani GA et al (2020) Propranolol for familial cerebral cavernous malformation (Treat_CCM): study protocol for a randomized controlled pilot trial. Trials 21:401
27. Taslimi S, Ku JC, Modabbernia A, Macdonald RL (2019) Hemorrhage, seizures, and dynamic changes of familial versus nonfamilial cavernous malformation: systematic review and meta-analysis. World Neurosurg 126:241–246
28. Ozgen B, Senocak E, Oguz KK et al (2011) Radiological features of childhood giant cavernous malformations. Neuroradiology 53:283–289
29. Yun TJ, Na DG, Kwon BJ et al (2008) A T1 hyperintense perilesional signal aids in the differentiation of a cavernous angioma from other hemorrhagic masses. AJNR Am J Neuroradiol 29:494–500
30. Bilguvar K, Bydon M, Bayrakli F et al (2007) A novel syndrome of cerebral cavernous malformation and Greig cephalopolysyndactyly: Laboratory investigation. J Neurosurg 107:495–499
31. Barker FG 2nd, Amin-Hanjani S, Butler WE et al (2001) Temporal clustering of hemorrhages from untreated cavernous malformations of the central nervous system. Neurosurgery 49:5–24
32. Santos AN, Rauschenbach L, Saban D et al (2022) Multiple cerebral cavernous malformations: clinical course of confirmed, assumed and non-familial disease. Eur J Neurol 29:1427–1434
33. Houwing ME, Grohssteiner RL, Dremmen M et al (2022) Silent cerebral infarcts in patients with sickle cell disease: a systematic review and meta-analysis. BMC Med 18:393
34. Bonfanti L, Charvet CJ (2021) Brain plasticity in humans and model systems: advances, challenges, and future directions. Int J Mol Sci 22:9358
35. Wang C, Zhao M, Wang J et al (2018) Giant cavernous malformations: a single center experience and literature review. J Clin Neurosci 56:108–113
36. Denier C, Labauge P, Bergametti F et al (2006) Genotype-phenotype correlations in cerebral cavernous malformations patients. Ann Neurol 60:550–556
37. Riant F, Bergametti F, Fournier HD et al (2013) CCM3 mutations are associated with early-onset cerebral hemorrhage and multiple meningiomas. Mol Syndr 4:165–172
38. Shenkar R, Shi C, Rebeiz T et al (2015) Exceptional aggressiveness of cerebral cavernous malformation disease associated with PDCD10 mutations. Genet Med 17:188–196
39. Merello E, Pavanello M, Consales A et al (2016) Genetic screening of pediatric cavernous malformations. J Mol Neurosci 60:232–238
40. Cigoli MS, Avemaria F, De Benedetti S et al (2014) PDCD10 gene mutations in multiple cerebral cavernous malformations. PLoS One 9:18–26
41. Liquori CL, Berg MJ, Squitieri F et al (2007) Deletions in CCM2 are a common cause of cerebral cavernous malformations. Am J Hum Genet 80:69–75
42. Kashefiolasl S, Bruder M, Brawanski N et al (2018) A benchmark approach to hemorrhage risk management of cavernous malformations. Neurology 90:e856–e863
43. Cheng D, Shang X, Gao W et al (2021) Fetal familial cerebral cavernous malformation with a novel heterozygous KRIT1 variation. Neurology 97:986–988
44. Nikoubashman O, Wiesmann M, Tournier-Lasserve E et al (2013) Natural history of cerebral dot-like cavernomas. Clin Radiol 68:e453–e459
45. Nabavizadeh SA, Pechersky D, Schmitt JE et al (2017) Perilesional hyperintensity on T1-weighted images in intra-axial brain masses other than cavernous malformations. J Neuroimaging 27:531–538
46. de Souza JM, Domingues RC, Cruz LCHJ et al (2008) Susceptibility-weighted imaging for the evaluation of patients with familial cerebral cavernous malformations: a comparison with T2-weighted fast spin-echo and gradient-echo sequences. AJNR Am J Neuroradiol 29:154–158
47. Sparacia G, Speciale C, Banco A et al (2016) Accuracy of SWI sequences compared to T2*-weighted gradient echo sequences in the detection of cerebral cavernous malformations in the familial form. Neuroradiol J 29:326–335
48. Geraldo AF, Luis A, Alves CAPF et al (2022) Spinal involvement in pediatric familial cavernous malformation syndrome. Neuroradiology 64:1671–1679

49. Mikati AG, Tan H, Shenkar R et al (2014) Dynamic permeability and quantitative susceptibility related imaging biomarkers in cerebral cavernous malformations. Stroke 45:598–601
50. Girard R, Fam MD, Zeineddine HA et al (2017) Vascular permeability and iron deposition biomarkers in longitudinal follow-up of cerebral cavernous malformations. J Neurosurg 127:102–110
51. Sone JY, Hobson N, Srinath A et al (2022) Perfusion and permeability MRI predicts future cavernous angioma hemorrhage and growth. J Magn Reson Imaging 55:1440–1449

Authors and Affiliations

Ana Filipa Geraldo[1,2] · Cesar Augusto P. F. Alves[3] · Aysha Luis[4,5] · Domenico Tortora[6] · Joana Guimarães[7,8] · Daisy Abreu[9] · Sofia Reimão[2,10] · Marco Pavanello[11] · Patrizia de Marco[12] · Marcello Scala[13,14] · Valeria Capra[12] · Rui Vaz[8,15] · Andrea Rossi[6,16] · Erin Simon Schwartz[3] · Kshitij Mankad[4] · Mariasavina Severino[6]

1 Diagnostic Neuroradiology Unit, Department of Radiology, Centro Hospitalar Vila Nova de Gaia/Espinho (CHVNG/E), Vila Nova de Gaia, Portugal

2 Clínica Universitária de Imagiologia, Faculty of Medicine of the University of Lisbon, Lisbon, Portugal

3 Department of Radiology, Children's Hospital of Philadelphia, Philadelphia, PA, USA

4 Department of Radiology, Great Ormond Street Hospital for Children, NHS Foundation Trust, London, UK

5 Department of Radiology, King's College London, London, UK

6 Neuroradiology Unit, IRCCS Istituto Giannina Gaslini, Genova, Italia

7 Department of Neurology, Centro Hospitalar Universitário de São João, Porto, Portugal

8 Department of Clinical Neurosciences and Mental Health, Faculty of Medicine of the University of Porto, Porto, Portugal

9 Instituto de Medicina Molecular João Lobo Antunes, Lisbon, Portugal

10 Neurological Imaging Department, Hospital de Santa Maria, Lisbon, Portugal

11 Neurosurgery Unit, IRCCS Istituto Giannina Gaslini, Genoa, Italy

12 Medical Genetics Unit, IRCCS Istituto Giannina Gaslini, Genoa, Italy

13 Department of Neurosciences, Rehabilitation, Ophthalmology, Genetics, Maternal and Child Health, Università Degli Studi Di Genova, Genoa, Italy

14 Pediatric Neurology and Muscular Diseases Unit, IRCCS Istituto Giannina Gaslini, Genoa, Italy

15 Neurosurgical Department, Centro Hospitalar Universitário de São João, Porto, Portugal

16 Department of Health Sciences (DISSAL), University of Genoa, Genoa, Italy